ROLE OF BRAIN-DERIVED NEUROTROPHIC FACTOR AND MITOCHONDRIAL FUNCTION IN HUNTINGTON´S DISEASE

Ana Cristina Rosa da Silva

Dissertation submitted to Faculty of Sciences and Technology of the University of Coimbra in partial fulfillment of the requirements for the Degree of Doctor of Philosophy in Biochemistry

Dissertação apresentada à Faculdade de Ciências e Tecnologia da Universidade de Coimbra para obtenção do Grau de Doutor em Bioquímica.

Coimbra, 2012

Life Sciences Department
Faculty of Sciences and Technology
University of Coimbra

This work was performed at Center for Neuroscience and Cell Biology of Coimbra, University of Coimbra, Portugal, under the supervision of Professor Ana Cristina Carvalho Rego and co-supervision of Professor Luis Pereira d'Almeida and institutional supervision of Professor Carlos Duarte from Life Sciences Department of the University of Coimbra.

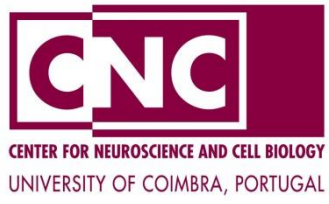

Supported by a Doctoral fellowship granted by FCT (*Fundação para a Ciência e a Tecnologia*), BD/30147/2006, and financed by POPH-QREN and FSE.

Thesis Cover:

Confocal microscopy image of neuronal-like cells derived from mice SVZ and differentiated *in vitro*. The cells were stained for microtubule associated protein (MAP)-2 (in red) and synaptophysin (in green).

To those who carry more that they can bear

Acknowledgements

This is a hard task, to give a proper acknowledgement to ALL the people who have passed through my life, and in some cases, still remain in it, and which in their particular way contributed to this work. For sure that I did not accomplish it without their help because we are made of pieces that, in every other moment, someone help to build. To the people I will probably forget I apologize and I thank you.

I want to thank Professor Catarina Resende de Oliveira, for accepting me at the Center and allow my investigation work.
To Luísa Ferreira for her help in the lab and care.
To Luísa Cortes and Isabel Nunes for their experimental help, friendship and always be available, THANK YOU!
To my co-supervisor, Professor Luis Almeida, for support and availability.

My special “thank you” with all my heart to my supervisor, Professor Ana Cristina Carvalho Rego, who taught and guided me throughout all my scientific way since ever. For her patience, her friendship and care and for being a person with a true and big heart, I am grateful.

To Professor Teresa Cruz, that I found late in this process but to whom I am truly indebted. There are moments in life that we thank for meeting such good persons, not just because they help us but because they give us the opportunity to know them and to believe in Good. You are one of such persons. Thank You Teresa!

To 'Mitochondrial Dysfunction and Signaling in Neurodegeneration' group and ‘Cellular Immunology and Oncobiology’ group, thank you for your support!

To my friends Rita, Catarina, Mário, Tatiana, Inês, Sandra and Bruno, I cannot say it would be impossible to do this without them, because there are no such things as impossible, but it would be much, much harder than it was. The real friendship and care, the laughs, the sad moments that would soon turn into laughs, the lazy moments, the work supporting moments (especially in the “cutting heads off” moments, right Sandra and Tati?!)…and I could go on indefinitely because there are not enough good words that

could say it all. Thank you Rita for being my friend since the beginning of times…of my Coimbra times, and everything else I hope to say to you along our lives.

To my long time friends, that even far never forgets and expresses their friendship in so many different, warm and cozy ways. For your HONEST CARE, thank you Ana, Carla and Sandra. We can go on through life in so many different ways but there will always be that special place for us.

To my friend and cousin Artur. For being in my life since EVER. Another chapter that I close in my life and where you took part, as always. Love you!

To Ananda, my Yoga master, who taught me into Yoga philosophy. Your help and friendship are some of the things that I treasure the most. Thank you for be at my life!

To D. Eunira, for their presence even far away. For her friendship that passes the barriers of time.

And least but not last, to all my family. Their support is one of the most important things in my life.
To Tia Cristina and Paula, thank you for your comforting and open arms.

To my Father, thank you for you Love and care. It was in a very happy state of mind that I wrote down these words.

And to whom I dedicate this work, my Mother, the person to whom I always did and always will dedicate my important closures. Without her I dare to say it would be quite impossible to achieve this goal. For all she taught me, for being the marvelous person she is, for her unconditional Love and every kind of support she gave and gives me, for being my Mother…I Love You. Thank you!!!

To the Supreme and all the good *Purusas* I know THANK YOU for everything.

TABLE OF CONTENTS

ABREVIATIONS LIST

3-NP, 3-Nitropropionic acid
7-AAD, 7-Aminoactinomycin D
A2A, A2 adenosine receptor
aa, amino acid
Ac-DEVD-AFC, N-acetyl-Asp-Glu-Val-Asp-AFC substrate
ADP, Adenosine diphosphate
AIF, apoptosis-inducing factor
AKT, *see PKB*
AMP, Adenosine monophosphate
AMPK, AMP-activated protein kinase
ANOVA, Analysis of variance
Apaf1, Apoptotic protease-activating factor-1
Asp, aspartyl protease
Atg, Autophagy-related protein
ATP, Adenosine triphosphate
BAC, Bacterial artificial chromosome
BACHD, BAC transgenic mouse model of HD
BAX, Bcl2-associated X protein
Bcl2, B-cell lymphoma-2
Bid, BH3 interacting-domain death agonist
BDNF, Brain-derived neurotrophic factor
BSA, Bovine serum albumin
CAD, Caspase-activated DNase
CAG, Cytosine-Adenine-Guanine
Calp, Calpains
cAMP, cyclic AMP
Casp, Caspases
Caspases, Cysteinyl aspartate-specific proteinases
CB, Cannabinoid
CBP, CREB-binding protein
CdK5, Cyclin-dependent kinase 5
CMV, Cytomegalovirus

CNS, Central nervous system

CNTF, Ciliary neurotrophic factor

CRE, cAMP response element

CREB, CRE-binding protein

CtBP, Transcriptional co-repressor C-terminal binding protein

CTR, Control

Cx, (mitochondrial) Complex

D1 or 2, Dopamine receptor 1 or 2

DAG, Diacylglycerol

DARPP-32, Dopamine and cAMP regulated phosphoprotein

DCPIP, 6,6-dichlorophenolindophenol

DG, Dentate gyrus

DMEM, Dulbecco's Modified Eagle Media

DNA, Desoxyribonucleic acid

DOC, Deoxycholate

DRPLA, Dentatorubral and pallidoluysian atrophy

DTT, Dithiothreitol

ECF, Enhanced chemifluorescence reagent

ECM, Extracellular matrix

EDTA, Ethylenediamine tetraacetic acid

EdU, 5-ethynyl-2’-deoxyuridine

EGF, Epidermal growth factor

eGFP, enhanced Green fluorescent protein

EGTA, Ethylene glycol tetraacetic acid

ERK, Extracellular-signal-regulated kinase

ESC, Embryonic stem cells

ETS, Electron transport system

FACS fluorescence-activated cell sorter

FBS, Fetal bovine serum

FCS, Foetal calf serum

FCCP, carbonylcyanide-p-trifluoromethoxyphenylhydrazone

FGF-2, basic fibroblast growth factor

FL, Full-length

FN, fibronectin

FoxO, forkhead box transcription factors classe O

Fura-2/AM, Fura-2-acetoxymethyl ester

GABA, γ (Gamma)-aminobutyric acid

GDNF, Glial cell-derived neurotrophic factor

GFAP, Glial fibrillary acidic protein

GPe, external segment of the Globus pallidus

GPi, internal segment of the Globus pallidus

H1R, Histamine receptor 1

HAP-1, Htt-associated protein-1

HAP1A, HAP-1 isoform A

HAT, Histone acetyl transferase

HD, Huntington's disease

HDACs, Histone deacetylases

Hdh, mouse Huntington's disease gene homolog

HDL, Huntington's disease-like

HEAT, Huntingtin, elongation factor 3 (EF3), protein phosphatase 2A (PP2A), yeast PI3K TOR-1

HIP, Htt-interacting protein

HIPPI, HIP-1 Protein interactor

HP, Hippocampus

HSP, Heat shock protein

Htt or *htt*, Huntingtin protein or human *huntingtin* gene

IAP, Inhibitor of apoptosis

IGF-1, Insulin-like growth factor 1

IP_3, inositol 1,4,5-trisphosphate

IP_3R1, IP_3 type 1 receptor

iPSCs, induced Pluripotent stem cells

IT15, Interesting Transcript 15

JNK, c-Jun N-terminal kinase

JPH3, junctophilin 3 gene

KA, Kainic acid

KCl, Potassium chloride

KI, Knock-in

KO, Knock-out

LV, Lateral ventricle

MAP2, Microtubule-associated protein 2

MAPK, Mitogen-activated protein kinase

mHtt, mutant Huntingtin

mo, month-old

MPT, mitochondrial permeability transition

mRNA, messenger RNA

MSN, Medium size spiny neurons

mt-, mitochondrial encoded

mTOR, mammalian TOR

n-, nuclear encoded

NADH, Nicotinamide adenine dinucleotide

NADPH, Nicotinamide adenine dinucleotide phosphate

N-CoR, nuclear receptor co-repressor

NES, Nuclear export signal

NF-kB, nuclear factor kappa-light-chain-enhancer of activated B cells

NGF, Nerve growth factor

NIIs, Neuronal intranuclear inclusions

NLS, Nuclear localization signal

NMDA, *N*-methyl-D-aspartate

NMDAR, NMDA receptor

NPC, Neural progenitor cells

NRSE, Neuron restrictive silencer element

NRSF, Neuron restrictive silencer factor

NS, Neurospheres

NSC, Neural stem cells

NT, Neurotrophin

OB, Olfactory bulb

Omi/HtrA2, Omi stress-regulated endoprotease/high temperature requirement protein A2

PBS, Phosphate buffered saline

PCR, Polymerase chain reaction

PET, Positron emission tomography

PGC-1α, Proliferator-activated receptor gamma co-activator 1-alpha

PI, Propidium iodide

PI3K, PhosphatidyIinositol 3-kinase

PKB, protein kinase B (*AKT*)

PLC-γ1, Phospholipase C-gamma1

PLL, poly-L-lysine

PMSF, Phenylmethylsufonyl fluoride

PolyProl, polyproline rich domain

PolyQ, Polyglutamine

PRNP, prion protein gene

PRP, Platelet rich plasm

PSA-NCAM*,* Polysialylated neural cell adhesion molecule

PSD-95, Postsynaptic density-95

PTP, permeability transition pore

PUMA, p53-upregulated modulator of apoptosis

PVDF, Polyvinylidene difluoride

QA, Quinolinic acid

RE, Repressor element-1

REST, RE1-silencing transcription factor

RFU, Relative fluorescence units

Rh123, Rhodamine-123

rhBDNF, recombinant human BDNF

RIPA, Radio-immunoprecipitation assay

RMS, Rostral migratory stream

RNA, Ribonucleic acid

RT, Room temperature

RV, Retroviral

SBMA, Spinobulbar muscular atrophy

SCA, Spinocerebellar ataxia

SDS, Sodium dodecyl dulfate

SDS-PAGE, SDS-polyacrylamide gel

SGZ, Subgranular zone

SMAC/DIABLO, second mitochondria-derived activator of caspase/direct IAP binding protein with a low pI

SNpc, *Substantia nigra pars compacta*

SNpr, *Substantia nigra pars reticulata*

STN, Subthalamic nucleus

STS, Staurosporine

SVZ, Subventricular zone

T, Truncated

tBID, truncated BID

TBP, TATA box protein

TBS(-T), Tris-buffered saline (-Tween 20)

TGF, Transforming growth factor

TNF, Tumor necrosis factor

TOR, Target of rapamycin

TPR, Translocated promoter region

Trk, Tropomyosin-receptor-kinase

TTFA, Thenoyltrifluoroacetone

UHDRS, Unified Huntington's Disease Rating Scale

UPS, Ubiquitin-Proteasome system

VSCC, Voltage sensitive calcium channels

VSV-G, Vesicular somatitis virus-glycoprotein

wk, week

WT, Wild type

YAC, Yeast artificial chromosome

LIST OF FIGURES

LIST OF TABLES

ABSTRACT

Huntington's disease (HD) is a fatal and inherited autosomal dominant neurodegenerative disorder caused by a single mutation, an expansion of unstable CAG repeats in the coding region of the *HD* gene, leading to a polyglutamine expansion at the *N*-terminus of the huntingtin (Htt) protein. HD is primarily considered a hyperkinetic disorder characterized by motor dysfunction, behavioral and psychiatric disturbances, cognitive impairment and, at the cellular level, by a selective loss of striatal neurons. Deficient neurotrophic support and mitochondrial dysfunction have been reported as possible mechanisms underlying HD pathogenesis. In this thesis we aimed to determine the role of brain-derived neurotrophic factor (BDNF) and BDNF-mediated TrkB receptor signaling, and the involvement of mitochondrial dysfunction in neural differentiation and cell survival pathways in HD affected cells.

In *Chapter 2* we studied the influence of BDNF and TrkB receptor-overexpression in striatal cell lines derived from homozygous HD knock-in and wild-type mice. AKT activation was observed in BDNF and TrkB-overexpressing HD cells and in TrkB-overexpressed HD cells exposed to recombinant human BDNF. Increased phosphorylation of ERK was detected in HD BDNF/TrkB co-cultures and in both HD non-transduced and TrkB-overexpressing cells incubated with BDNF. The benefits of TrkB overexpression were further confirmed after the observation of reduced apoptotic cell death features (evaluated through analysis of caspase-3 activation and fragmented DNA) in mutant cells, suggesting that TrkB receptor-mediated AKT signaling may trigger survival mechanisms in HD striatal cells.

Considering that adult neurogenesis appears to be inefficient in eliciting endogenous functional neuronal replacement in HD, in *Chapter 3* we characterized the formation of new neurons derived from subventricular zone (SVZ) neurospheres. Thus, we described how undifferentiated cells derived from the SVZ of transgenic YAC128 mice, bearing full-length human mutant Htt, responded to neuronal differentiation induced by BDNF. In an undifferentiated state (as neurospheres), YAC128 and wild-type SVZ cells derived from animals with 6 or 10 months, at different stages of HD pathology, displayed similar proliferation and cell cycle phases. Nevertheless, at a mild HD stage (at 6 months of age) YAC128 cells exhibited higher migratory capacity, compared to WT cells, a difference not

observed at a late HD symptomatic stage (at 10 months of age). Moreover, 6 month-old YAC128 cells exhibited a higher number of microtubule-associated protein 2 (MAP2)+ and synaptophysin+ cells than WT cells, suggesting that HD cells possess increased capacity to differentiate into mature neurons, capable of forming synapses. Importantly, differences observed between HD and wild-type cells at a mild symptomatic stage of HD were lost with the progression of the disease (at 10 months of age). 6 month-old YAC128 SVZ-derived cells also showed increased intracellular Ca^{2+} levels in response to KCl, which was promoted by BDNF, evidencing the presence of mature neurons; interestingly, these features were diminished in 10 month-old YAC128 cells. Late symptomatic YAC128 cells also displayed lower mitochondrial membrane potential and increased mitochondrial Ca^{2+} accumulation, compared to mild symptomatic YAC128 cells. These data evidence reduced migration and neuronal differentiation potential, along with decreased mitochondrial function in YAC128 mice SVZ-derived cells in advanced HD symptomatic phases.

In the last chapter of this work (*Chapter 4*) we defined mitochondrial dysfunction at different symptomatological stages of HD in mitochondria isolated from human peripheral platelets. We determined mitochondrial complexes (I-IV) activities, nuclear- and mitochondrial-encoded subunit protein expression levels and mitochondrial energy levels in mitochondrial platelets from non-medicated pre-symptomatic and medicated symptomatic HD patients *versus* aged-matched controls. Data herein provide evidence for decreased activity of citrate synthase and mitochondrial complex I in mitochondrial platelets from pre-symptomatic individuals and increased complex IV activity in mitochondrial platelets from symptomatic HD patients. Significant and positive correlations were observed between complex I activity and 20 kDa mitochondrial-encoded subunit, as well as between complex II activity and 30 kDa nuclear-encoded subunit in HD symptomatic samples only. In addition, AMP levels were significantly increased in pre-symptomatic HD carriers. Taken together, these data suggest the hypothesis that dysfunction of mitochondrial complexes may occur very early during HD progression. Moreover, biochemical analysis of peripheral cells derived from HD carriers might be relevant in deciphering HD markers.

Overall, the results presented in this thesis support the importance of deregulated neurotrophic signaling and dysfunctional mitochondria in HD pathogenesis. In particular,

these data highlight the importance of BDNF in promoting the survival of striatal cells, the most affected cell population in HD brain, and reveal modified age-dependent responses of HD affected cells to this neurotrophin. Indeed, BDNF and TrkB receptor may be considered strong HD therapeutic candidates. The results herein presented suggest increased mitochondrial membrane potential during neuronal differentiation *in vitro*, at a mild stage of the disease in HD mice, possibly reflecting a compensatory response to the effects caused by mutant Htt. Moreover, data show that mitochondrial deficits are early events in HD pathogenesis, occurring in pre-symptomatic stages of the disease in peripheral human cells, which might be relevant when considering the use of mitochondrial-based therapeutic interventions.

RESUMO

A doença de Huntington (HD, do inglês *Huntington's disease*) é uma doença fatal hereditária, autossómica dominante, resultante de uma única mutação, uma expansão de repetições do tripleto instável CAGCAG na região codificante do gene da *huntingtina*, conduzindo à expansão de poliglutaminas no terminal amínico da proteína huntingtina (Htt). A HD é caracterizada por hipercinésia, disfunção motora, distúrbios comportamentais e psiquiátricos, défice cognitivo e, a nível celular, pela perda seletiva de neurónios estriatais. Um défice do suporte neurotrófico e disfunção mitocondrial têm sido descritos como mecanismos associados à patogenia da HD. Neste trabalho determinámos o papel do fator neurotrófico derivado do cérebro (BDNF, do inglês *brain-derived neurotrophic factor*) e da sinalização do recetor TrkB mediada por BDNF, e o envolvimento da disfunção mitocondrial na diferenciação neuronal e nas vias de sobrevivência celular em células afetadas pela HD.

No *Capítulo 2* analisámos a influência da sobrexpressão de BDNF e TrkB em células estriatais derivadas de murganhos homozigóticos *knock-in* para a HD e murganhos *wild-type*. Observámos a ativação da AKT em células HD que sobre-expressam BDNF e TrkB e em células HD que sobre-expressam TrkB expostas à forma recombinante humana de BDNF. Detetámos ainda um aumento da fosforilação da ERK em co-culturas de células HD que sobre-expressam BDNF ou TrkB e em células controlo (não infetadas) e células que sobre-expressam TrkB expostas a BDNF. Os benefícios da sobre-expressão do recetor TrkB foram confirmados após observação da redução da morte celular por apoptose (avaliada através da análise da ativação da caspase-3 e da fragmentação do DNA) em células mutantes, sugerindo que a sinalização da AKT mediada pelo recetor TrkB pode desencadear mecanismos de sobrevivência em células estriatais HD.

Considerando que a neurogénese adulta parece ser ineficiente no processo de substituição endógena de neurónios funcionais na HD, no *Capítulo 3* caracterizámos a formação de novos neurónios derivados de neurosferas da zona subventricular (SVZ, do inglês *subventricular zone*). Assim, observámos o processo de diferenciação neuronal em resposta a BDNF, a partir de células indiferenciadas derivadas da SVZ de murganhos transgénicos YAC128, que expressam a Htt mutante humana completa, em diferentes estadios da doença. Num estadio indiferenciado (como neurosferas), as células

derivadas da SVZ obtidas de murganhos YAC128 e *wild-type* apresentaram um perfil de proliferação e ciclo celular semelhantes. No entanto, num estadio moderado da HD (aos 6 meses de idade) as células YAC128 exibiram uma capacidade migratória superior, comparativamente às células derivadas de murganhos *wild-type*; contudo esta diferença não foi observada num estadio mais avançado da doença, aos 10 meses de idade. Além disso, as células derivadas de murganhos YAC128 com 6 meses de idade apresentaram um maior número de células positivas para a proteína associada aos microtúbulos 2 (MAP2, do inglês *microtubule-associated protein 2*) e sinaptofisina, comparativamente às células *wild-type*, sugerindo que as células HD possuem uma maior capacidade de diferenciação em neurónios maduros, capazes de formar sinapses. De forma interessante, os resultados obtidos nas células YAC128 num estadio moderado da HD desapareceram numa fase mais avançada da progressão da doença, i.e., aos 10 meses de idade. As células derivadas da SVZ de murganhos YAC128 com 6 meses de idade também demonstraram um aumento dos níveis de Ca^{2+} intracelular em resposta à despolarização por KCl, que foi incrementado na presença de BDNF, evidenciando a presença de neurónios maduros; contudo, estas características apresentaram-se diminuídas nas células YAC128 aos 10 meses de idade. Num estadio mais avançado da doença, as células YAC128 apresentaram um menor potencial mitocondrial transmembranar e um aumento da acumulação de Ca^{2+} mitocondrial, comparativamente às células YAC128 num estadio moderado da doença. Estes dados demonstram uma redução da capacidade migratória e do potencial de diferenciação neuronal, e uma diminuição da função mitocondrial em células derivadas da SVZ de murganhos HD YAC128 em fases sintomáticas e avançadas da HD.

No último capítulo deste trabalho (*Capítulo 4*) avaliámos a disfunção mitocondrial em diferentes fases sintomáticas da HD, em mitocôndrias isoladas a partir de plaquetas periféricas humanas. Neste estudo determinámos a atividade dos complexos mitocondriais (I-IV), os níveis proteicos de subunidades codificadas pelo núcleo e pela mitocôndria, e os níveis energéticos em mitocôndrias de plaquetas derivadas de doentes pré-sintomáticos (não medicados) e doentes HD (medicados), *versus* controlos com idade semelhante. Os resultados evidenciaram um decréscimo da atividade da enzima citrato sintetase e do complexo I mitocondrial em mitocôndrias de plaquetas de indivíduos pré-sintomáticos e um aumento da atividade do complexo IV em mitocôndrias de plaquetas derivadas de doentes HD. Observaram-se correlações positivas e

significativas entre a atividade do complexo I e a subunidade de 20 kDa codificada pela mitocôndria, assim como entre a atividade do complexo II e a subunidade de 30 kDa codificada pelo núcleo, apenas nas amostras derivadas de doentes com HD. Para além disso, os níveis de AMP apresentaram-se significativamente aumentados em indivíduos pré-sintomáticos, portadores da mutação. Em conjunto, os resultados do *Capítulo 4* levantam a hipótese de que a disfunção dos complexos mitocondriais possa ocorrer muito cedo durante a progressão da doença. Desta forma, a análise bioquímica de células periféricas derivadas de portadores da mutação poderá ser relevante na 'descodificação' de marcadores periféricos para a HD.

Globalmente, os resultados apresentados nesta tese realçam o défice da sinalização neurotrófica e a disfunção mitocondrial como fatores importantes para a patogenicidade que ocorre na HD. Em particular, os dados demonstram a importância do BDNF na promoção da sobrevivência de neurónios estriatais, a população cerebral mais afetada na HD, e na aquisição de um fenótipo neuronal maduro; contudo, dependendo da idade e estadio da HD (definida no modelo transgénico YAC128), as células revelam respostas divergentes a BDNF relativamente ao processo de diferenciação neuronal. Nesta perspetiva, o BDNF e o recetor TrkB poderão ser considerados fortes candidatos para o tratamento da doença. Numa fase moderada da doença no modelo transgénico da HD, o processo de diferenciação neuronal *in vitro* evidenciou um aumento do potencial mitocondrial transmembranar, que poderá resultar de um efeito compensatório relativamente aos efeitos causados pela mHtt. Para além disso, demonstramos que os défices mitocondriais ocorrem precocemente na HD, em fases pré-sintomáticas da doença, tal como observado em células periféricas humanas, o que pode ser relevante se considerarmos o uso de intervenções terapêuticas baseadas na mitocôndria.

CHAPTER 1

GENERAL INTRODUCTION

1.1. POLYGLUTAMINE-EXPANSION DISORDERS

Polyglutamine (polyQ) expansion disorders are a group of hereditary neurodegenerative diseases that have in common the expression of proteins with an expanded stretch of glutamines, as a result of abnormal expansion of cytosine-adenine-guanine (CAG) trinucleotide repeats in the gene coding region. Nine CAG polyQ diseases have been described so far (Table 1.1).

Table 1.1 – Characteristics of CAG expansion related disorders

Disease	Locus	Protein	polyQ expansion		Affected Brain Regions
			Normal	Pathological	
DRPLA	12p13	Atrophin-1	3-38	49-88	Cerebellum, cerebral cortex, basal ganglia, Luys body
HD	4p16.3	Huntingtin	6-35	36-121	Striatum (caudate and putamen), cerebral córtex, hypothalamus
SBMA (Kennedy disease)	Xq11-q12	Androgen Receptor	6-36	38-62	Anterior horn and bulbar neurons, dorsal root ganglia
SCA1	6p23	Ataxin-1	6-44	39-82	Cerebellar Purkinje cells, dentate nucleus, brain stem
SCA2	12q24	Ataxin-2	15-24	32-200	Cerebellar Purkinje cells, fronto-temporal lobes, brain stem
SCA3 (Machado-Joseph disease)	14q24.3-q31	Ataxin-3	13-36	61-84	Cerebellar dentate neurons, basal ganglia, brain stem, spinal cord
SCA6	19p13	α1A-voltage dependent Ca^{2+} channel	4-19	10-33	Cerebellar Purkinje cells, dentate nucleus, inferior olive
SCA7	3p21.1-p12	Ataxin-7	4-35	37-306	Cerebellum, brain stem, macula, visual cortex
SCA17 (HDL4)	6q27	TBP	25-42	47-63	Cerebellum, caudate nucleus, putamen, thalamus, frontal and temporal cortex

(adapted from Zoghbi and Orr (2000) and Bauer and Nukina (2009), for review).

CAG triplet repeat disease family comprise dentatorubral and pallidoluysian atrophy (DRPLA), Huntington's disease (HD), spinobulbar muscular atrophy (SBMA or Kennedy disease) and spinocerebellar ataxias (SCA) type 1, 2, 3 (or Machado-Joseph disease), 6, 7 and 17 (reviewed by Bauer and Nukina, 2009). SBMA, which is linked to progressive motor neurodegeneration, was the first CAG repeat expansion disease to be described in 1991 (La Spada *et al.* 1991). Among polyQ diseases, the most prevalent worldwide is HD. Interestingly, in rare cases, some patients who exhibit a syndrome similar to HD do not express the trinucleotide repeat expansion in the HD gene. These genetic disorders are therefore referred to as 'Huntington's disease-like' (HDL) syndromes and the associated genes have been previously identified (e.g. prion protein (*PRNP*) gene in

HDL1, junctophilin 3 (*JPH3*) gene in HDL2; TATA box-binding protein (*TBP*) gene in HDL4 or SCA17; reviewed in Schneider *et al*., 2007).

In general, the first symptoms in polyQ expansion diseases appear in midlife and death of the patients occurs a few years later. However, trinucleotide CAG repeats are unstable and tend to expand from generation to generation, resulting in an earlier age of onset and a more severe symptomatology and disease course in the following generations (Bauer and Nukina, 2009, for review). In fact, large expansions lead to drastic juvenile-onset cases.

Regardless the fact that the disease specific proteins are generally expressed in the whole body, the degeneration of a particular brain region is a common feature of polyQ disorders, as in other neurodegenerative diseases. This occurs along with the presence of insoluble ubiquitinated aggregates, due to increased accumulation of degradation-resistant protein toxic fragments. Protein aggregates often results when misfolded proteins production surpasses the degradative cell's rate, through proteolytic systems and molecular chaperones which are addressed to prevent aggregation (e.g. HSP70/40; Goldberg, 2003, for review). The ubiquitin-proteasome system (UPS) is an adenosine triphosphate (ATP)-dependent *via* for protein degradation. ATP is required for ubiquitin activation trough an ubiquitin-activating enzyme, E1, which is further transported by a specific ubiquitin-carrier protein, E2. An ubiquitin ligase, E3, then catalyzes the assembly of the ubiquitin chain to a specific protein, targeting it towards the 26S proteasome for degradation (Goldberg, 2003, for review).

Another important process involved in the turnover and recycling of proteins, as well as the clearance of damaged organelles (e.g. mitochondria), is macroautophagy, by means of lysosomal digestion. Part of the cytosol and its contents are enclosed by double-membrane structures named autophagosomes/autophagic vacuoles and, in order for degradation to occur through lysosomal acidic hydrolases, autophagosomes have to fuse with lysosomes forming autophagolysosomes (Reggiori and Klionsky, 2005, for review). In neurons, this process is particularly relevant since the reduction of injured cell components by their redistribution through cell division is not possible (Wong and Cuervo, 2010, for review). Komatsu *et al.* (2006) elegantly demonstrated that the absence of autophagy in the central nervous system (CNS) leads to a severe neurological disorder and neurodegeneration in mice deficient for CNS autophagy-related protein 7 (Atg7), an ubiquitin-like activating enzyme essential for autophagy (Komatsu *et al.*, 2006). Interestingly, these authors observed that the lack of autophagy in neurons resulted in

ubiquitin-containing inclusion bodies accumulation although proteasome function was unaffected. Likewise, Hara *et al.* (2006) reported similar results in mice deficient for Atg5. Supporting the benefic role of autophagy in the CNS Sekiguchi and colleagues (2012) proved that rapamycin-induced autophagy (through mammalian target of rapamycin, mTOR, signaling pathway inhibition) reduced neural tissue damage and locomotor impairment in mice after spinal cord injury (Sekiguchi *et al*., 2012).

In polyQ expansion diseases, the UPS and autophagy (e.g. macroautophagy) pathways have been described to be impaired (Bence *et al*., 2001; Wong and Cuervo, 2010, for review). One of the signs of altered autophagy associated to neurodegeneration is the abnormal number of autophagosomes observed in the affected neurons (Wong and Cuervo, 2010, for review). Deregulation of autophagy in HD will be further discussed in *section 1.2.3* of this chapter.

However, the role of protein aggregation is still on debate. It is not completely elucidated whether expanded polyQ proteins toxicity derives from visible aggregates or from smaller intermediate species (e.g. protofibrils and microaggregates) generated during the aggregation process; investigation in this field suggests that smaller aggregates are toxic, whereas large aggregates are cytoprotective (Bauer and Nukina, 2009, for review).

1.2. HUNTINGTON´S DISEASE

HD is the most prevalent neurodegenerative disease among the polyQ-expansion disorders. HD was first accurately described by George Huntington in 1872 on his paper entitled “On Chorea” (see Huntington, 2003)[1]. HD is a fatal hereditary autosomal dominant and progressive neurodegenerative disease characterized by psychiatric disturbances, chorea (the Greek word for dance), dementia and rigidity (in the adult this is particularly observed in late HD stages), affecting both genders with the same frequency. In the juvenile form seizures are also common. The highest prevalence is in Europe and North America, with approximately 1 case per 10,000 (Vonsattel and DiFiglia, 1998 and Zuccato *et al.,* 2010, for review). An extremely high prevalence was found within members of Venezuelan families (Negrette, 1955). This led to the foundation of the Venezuela HD project, which was central for the discovery of the transcript associated

[1] *"On Chorea" by George Huntington, M.D., originally appeared in The Medical and Surgical Reporter: A Weekly Journal (Philadelphia: S.W. Butler), vol. 26, no. 15 (April 13, 1872), pp. 317—332*.

with the disease named *IT15* (Interesting Transcript 15), found to be located on chromosome 4 (Gusella *et al*., 1983). In 1993 the gene was completely identified and named *HD* or *huntingtin* (*htt*) gene (The Huntington's Disease Collaborative Research Group, 1993), which encodes the protein huntingtin (Htt). HD is caused by an expansion of CAG trinucleotide repeats in the coding region of the HD gene. Thus, under pathological conditions Htt presents a polyQ expansion at the N-terminal and is termed mutant Htt (mHtt). This has driven the development of genetic models both *in vitro* and *in vivo,* hence opening new perspectives in HD research. Presently, HD has still no cure or effective neuroprotective treatment.

1.2.1. Disease symptomatology and pathology

The average age of onset of HD is usually between 35 and 45 years of age; 10% of disease cases have a juvenile onset, starting at early 20's (Zuccato *et al.*, 2010, for review). In the majority of the cases (which are middle-age onset), death of the patients occurs 15 to 20 years after disease commencement, whereas in the juvenile cases death may occur after seven to ten years. The expansion of CAG repeats is inversely correlated with the age of disease onset, although other genetic and environmental factors might influence the age of first HD symptoms, particularly for the middle-age onset cases (Rubinsztein *et al*., 1997; Holbert *et al*., 2001; Wexler *et al*., 2004). Unstable CAG repeat length ranges from 6–35 in normal individuals, 35–39 displaying incomplete penetrance (in this case HD carriers may exhibit symptoms later in life) and more than 40 CAGs show full penetrance, establishing the pathology (Wexler *et al.,* 2004). CAG repeats above 60 lead to juvenile-onset cases. Interestingly, homozygous mutations do not imply an earlier age of symptoms, but drastically affects the phenotype and the rate of disease progression (Squitieri *et al*., 2003).

The beginning of the disease is usually recognized for the persistence of motor abnormalities, which can vary from involuntary movements of the face, thorax and body members to abnormal ocular movements. Indeed, the eye saccadic movement is used to evaluate HD occurrence (Berardelli *et al*., 1999). Although chorea is the main hallmark of the disease, dementia and depression are two of the frequently observed clinical features in persons carrying the HD mutation. Typical symptoms involve mood and behavioral disturbance, memory impairment and personality changes, generally occurring before the beginning of motor dysfunctions. Thus, antidepressant and antipsychotic drugs are often

prescribed to HD patients. Nevertheless, according to Shiwach and Norbury (1994), depression or psychiatric symptoms are not substantial signs indicative of later neurological dysfunction. Choreiform movements develop in 90% of patients but in the juvenile forms they can be absent. Instead, juvenile patients may suffer from severe muscle rigidity and bradykinesia (Seneca *et al*., 2004). Weight loss is another typical feature of advanced HD, despite the high nutritional intake (Morales *et al*., 1989), along with a severe cognitive impairment.

Neuropathologically, the degenerative process begins in the striatum. The majority (about 95%) of striatal neurons are medium spiny projecting neurons (MSNs), which synthesize gamma-aminobutyric acid (GABA) as their primary inhibitory neurotransmitter (Chesselet and Delfs, 1996). There are two subpopulations of MSN, according to their involvement in the "indirect" or "direct" pathway, which are discussed in the following paragraphs. Within the striatum, the caudate nucleus degenerates first; later, putamen deterioration is also detected, resulting in global striatal shrinkage and a consequent dilation of the lateral ventricles, commonly observed in postmortem human brains at a late HD state (Fig. 1.1.) (Robitaille *et al*., 1997).

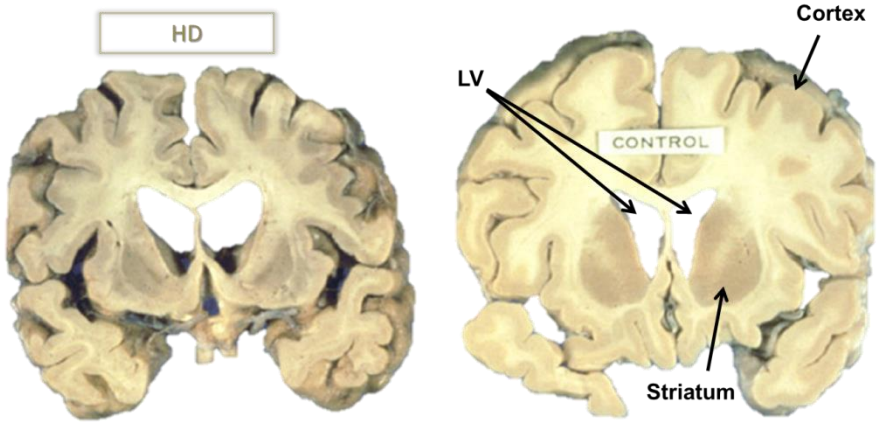

Figure 1.1. – Huntington's disease human brain. Comparison between a normal (control) brain (on the right) with a human brain affected by HD (on the left). **LV** – lateral ventricles (adapted from http://news.softpedia.com/news/Your-Brain-Degenerating-by-Itself-74375.shtml).

The striatum is part of subcortical nuclei called basal ganglia, which are involved in the control of movement. These structures do not directly receive or send sensory information to the spinal cord. Instead, the input of information is mainly received from the cortex into the striatum and the output follows the thalamus back to the cortex route.

The two major neuronal motor pathways were previously described by Albin and colleagues (1989): the "direct pathway", which promotes movement, and the "indirect pathway", responsible for the inhibition of motor activity (Fig. 1.2.). Both may be initiated with an excitatory stimulus (e.g. the release of glutamate from the cortex) into the striatum (putamen and caudate nucleus). Consequently, striatal neurons release GABA, an inhibitory stimulus. If it follows the "direct pathway", GABA is released (from GABAergic MSNs expressing substance P, dynorphin and D1 dopamine receptors) directly into the globus pallidus internal segment (Gpi) and *substantia nigra pars reticulata* (SNpr). In turn, these inhibited nuclei release less GABA into the thalamus, which becomes less inhibited and release more glutamate into the cortex, thus promoting movement. In contrast, if striatum-derived GABA follows the "indirect pathway", this inhibitory neurotransmitter is released (from GABAergic MSNs expressing enkephalin and D2 dopamine receptors) into the globus pallidus external segment (Gpe), inhibiting Gpe GABA-release into the subthalamic nucleus (STN), which in turn, increases the excitatory input of glutamate into the Gpi/SNpr. These structures become more excited and produce more GABA, therefore inhibiting thalamus function and reducing motor activity. Dopaminergic neurons derived from the *substantia nigra pars compacta* (SNpc) are largely known to modulate movement through the release of dopamine into the striatum which enhances the direct pathway and inhibits the indirect pathway. These nigra-striatal pathways are affected in Parkinson's disease.

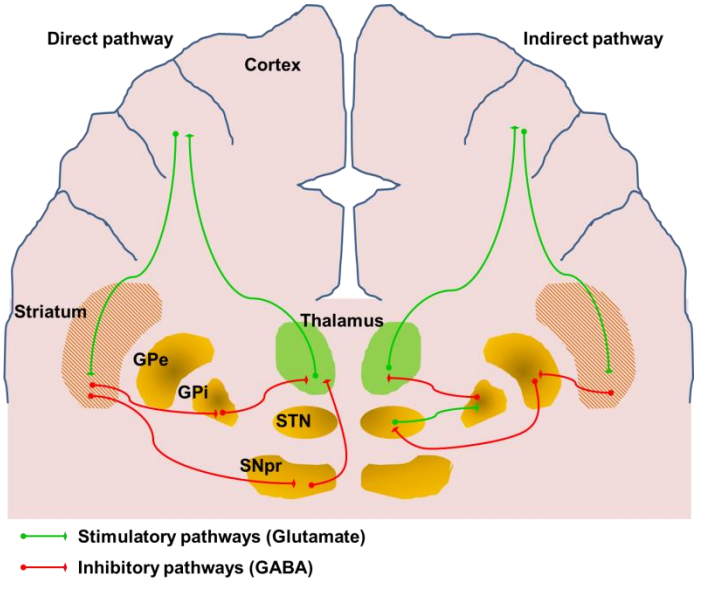

Figure 1.2. – Neuronal motor pathways. Schematic figure representing basal ganglia neuronal "direct" and "indirect" pathways. **GPe** – globus pallidus external segment; **Gpi** – globus pallidus

internal segment; **SNpr** – *substantia nigra pars reticulata*; **STN** – subthalamic nucleus (adapted from Andrews and Brooks, 1998).

Later, it was found that the STN also receives input from the cortex (Mink and Thach, 1993; Nambu *et al*., 2000) and sends outputs to the Gpi/SNpr, inhibiting the thalamus and cortex. This is called the 'hyperdirect pathway' (Nambu *et al.,* 1996) and is not compromised in HD. Instead, striatal GABAergic neurons belonging to the "indirect pathway" (i.e. projecting to the Gpe) are the main neuronal population affected in early and middle HD stages (Reiner *et al.*, 1988), thus impairing the "indirect pathway" (inhibitory) and favoring the "direct pathway" (excitatory). As described previously in this chapter, GABAergic striatal MSNs of the indirect pathway express enkephalin and are enriched in D2 dopamine receptor (Reiner *et al.,* 1988; Albin *et al*., 1991). On the other hand, striatal interneurons, including medium-sized aspiny cholinergic interneurons containing somatostatin, neuropeptide Y or nicotinamide adenine dinucleotide phosphate (NADPH) diaphorase (or nitric oxide synthase) and parvalbumin are relatively spared (Ferrante *et al.,* 1985; Graveland *et al*., 1985; Ferrante *et al.,* 1987a; Ferrante *et al*., 1987b; Sieradzan and Mann, 2001). Ultimately, in the most advanced stages of the disease, the overall of GABAergic neuronal population is lost, even the MSNs involved in the excitatory direct pathway, resulting in a severe motor dysfunction and bradykinesia.

HD severity has been graded based on striatal degeneration in *post mortem* tissues and related to the extent of clinical disability, as determined by the neuropathologist Jean Paul Vonsattel in 1985. The scale goes from grade 0 (30-40% neuronal loss in the head of the caudate nucleus, as revealed after precise histological examination) to grade 4 (the most severe HD cases with atrophy of the striatum and up to 95% neuronal loss) (Vonsattel *et al.,* 1985).

While the striatum is the most affected brain region in HD, the cerebral cortex (particularly layers III, V, and VI), globus pallidus, thalamus, subthalamic nucleus, *substantia nigra*, white matter, hypothalamus and cerebellum (although affected in a less extent) also display signs of significant atrophy in grades 3 and 4 HD subjects (Hedreen *et al.,* 1991; Zuccato *et al*., 2010, for review). Diana Rosas and colleagues confirmed that the volume of almost all brain structures was significantly reduced in HD patients, particularly the cortex, and further revealed that such changes take place before symptoms appear (Rosas *et al,* 2003, 2005 and 2006). Therefore, this is another brain area commonly accepted to be affected in HD.

1.2.2. The protein huntingtin – wild-type *versus* mutant and their roles in HD pathogenesis

1.2.2.1. Possible roles of wild-type huntingtin

The human *HD* gene is located in the beginning of the short arm of chromosome 4 at position 4p16.3 and translates into Htt (of approximately 350 kDa), which is ubiquitously expressed in the body, particularly in brain and testis. In the brain, it is present mainly in the cerebellar cortex, the neocortex, the striatum and the hippocampus (Schmitt *et al*., 1995) and is expressed predominantly in neurons (Sapp *et al*., 1997). Wild-type (WT) Htt is essentially cytosolic (where it can localize with organelles, such as the endoplasmic reticulum and mitochondria), although the protein can also locate in nuclear and perinuclear sites, particularly in its mutant form, when forming aggregates (Hoogeveen *et al*., 1993; Sapp *et al*., 1997; Tao and Tartakoff, 2001; Kegel *et al*., 2002). Htt does not display structural homology with any other known proteins and its function is still not completely understood. However, Htt or its fragments are able to interact with nearly 50 proteins, participating in diverse cellular roles including clathrin-mediated endocytosis, apoptosis, vesicle transport, cell signaling, morphogenesis and transcriptional regulation (as elegantly reviewed in Zuccato *et al.,* 2010). In the nucleus of normal and HD human fibroblasts, and in normal mouse brain and striatal cells, full-length (FL) WT Htt was shown to interact with the transcriptional co-repressor C-terminal binding protein (CtBP; Kegel *et al*., 2002); moreover Boutell *et al.* (1999) have previously demonstrated the interaction of Htt with the C-terminal region of the nuclear receptor co-repressor (N-CoR), in rat and human, using a yeast two-hybrid system. The interaction of Htt with several transcription factors seems to reflect an obvious role of Htt in the control of gene expression. Indeed, WT Htt promotes the expression of brain-derived neurotrophic factor (BDNF), which has been ascribed as an important neurotrophin involved in striatal neuron survival and which is decreased in HD brains (as discussed in *section 1.2.4* of this chapter).

Htt also seems to be required for normal embryogenesis. Nasir and coworkers (1995) reported that Htt knock-out (KO) mice die at embryonic day 7.5; in addition, Dragatsis and co-authors (2000) showed that inactivation of the mouse homologue of the *HD* gene (*Hdh*) at post-natal stages (using Cre/loxP site-specific recombination strategy) in brain and testis led to progressive neurodegeneration and sterility unveiling the role of Htt in

cell survival. Moreover, WT Htt inhibits caspase-9 thus decreasing apoptosis (Rigamonti *et al.,* 2001). Surprisingly, Htt KO neurons differentiate and develop functional synapses *in vitro* (Metzler *et al.,* 1999).

Htt is composed by 36 HEAT-like repeats, which may explain its involvement in cellular trafficking. The HEAT repeat domain is a protein domain found in several cytoplasmic proteins (Fig. 1.3.). The acronym *HEAT* rises from four of those proteins: Htt, elongation factor 3 (EF3), protein phosphatase 2A (PP2A), and the yeast phosphatidylinositol 3-kinase (PI3K) target of rapamycin (TOR)-1 (Andrade and Bork, 1995) and are mostly found in proteins implicated in intracellular trafficking and chromosomal segregation. This suggests that Htt may facilitate the formation of multiple complexes, analogous to other HEAT repeat proteins (Takano and Gusella, 2002), some of which are referred herein. Huntingtin-associated protein (HAP)-1, along with dynactin p150, forms one of these functional complexes and is involved in microtubule-dependent vesicular transport, also interacting with beta-tubulin (Engelender *et al*., 1997; Li *et a*l., 1998; Gauthier *et al.,* 2004). Huntingtin-interacting protein (HIP)-1, actin and clathrin comprise another complex that is required for vesicle endocytosis (Waelter *et al*., 2001). Inositol 1,4,5-trisphosphate (IP_3) receptor type 1 (IP_3R1)-HAP1A-Htt ternary complex was shown to be implicated in intracellular calcium signaling (Tang *et al.,* 2003). Other Htt protein association occurs with the postsynaptic density 95 (PSD-95) protein, which is responsible for clustering and activation of *N*-methyl-D-aspartate (NMDA) receptors in the postsynaptic membrane; indeed, mHtt-induced sensitization of NMDA receptors and neuronal apoptosis was associated to decreased binding of mHtt with PSD-95 (Sun *et al*., 2001).

A functionally active nuclear export signal (NES) sequence and a less active nuclear localization signal (NLS) were found in the C-terminus of Htt (Fig. 1.3.), suggesting that Htt may shuttle between the nucleus and the cytoplasm and may also be involved in nucleus-cytosolic transport of other molecules (Xia *et al.,* 2003).

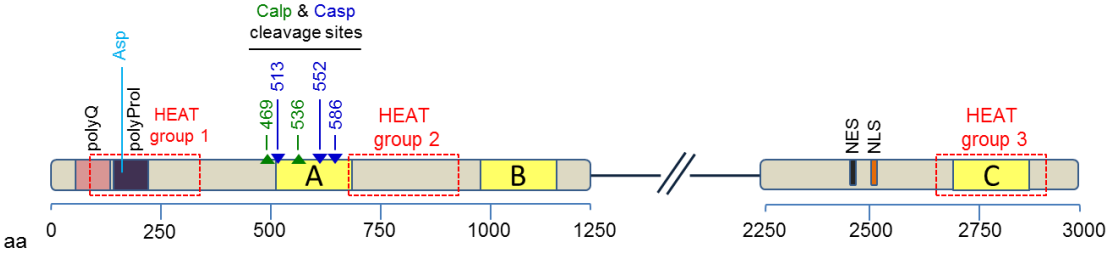

Figure 1.3. – Huntingtin (Htt) amino acid (aa) sequence and cleavage consensus sites. Schematic diagram of Htt protein aa sequence with the main proteases domains. **polyQ** –

polyglutamine tract followed by the **polyProl** – polyproline sequence. **Asp** (light blue), **Calp** (green) and **Casp** (blue) indicates the aspartyl, calpains and caspase cleavage sites, respectively, and their aa position. Boxes in yellow: regions cleaved preferentially in the cerebral cortex, **B**; in the striatum, **C**; or both, **A**. **NES** – Nuclear Export Signal. **NLS** – Nuclear Localization Signal. (based on Zuccato *et al*, 2010).

This hypothesis is further supported by Htt perinuclear and nuclear distribution and by the fact that the first 17 amino acids preceding the polyQ region interact with the translocated promoter region (TPR), a nuclear pore protein which exports proteins from the nucleus. PolyQ expansion impairs Htt nuclear export and depletion of the ten amino acids in the N-terminal Htt, responsible for Htt-TPR interaction, increased Htt nuclear accumulation (Cornett *et al*., 2005).

Htt has different protease domains and it was demonstrated that, besides cysteinyl aspartate-specific proteinases (caspases), both normal and mHtt are cleaved by calpains (cysteine proteinases) and aspartyl proteases (Kim *et al.,* 2001; Lunkes *et al*., 2002), all cleaving the protein within the N-terminal region (Fig. 1.3.), thus supporting the toxic fragment hypothesis of HD pathogenesis (see below *section 1.2.2.2.*).

WT Htt has been assigned with an anti-apoptotic role given that it might block apoptotic pathways by inhibiting the formation of an apoptosome complex, thus preventing caspases-3 and -9 activation (Rigamonti *et al.,* 2000; Rigamonti *et al.,* 2001), or by direct interaction with caspase-3, inhibiting its proteolytic activity (Zhang *et al*., 2006). It has also been shown that Htt inhibits pro-apoptotic HIP-1 protein interactor (HIPPI)-HIP1 complex formation by interacting with HIP1 which, once detached from Htt, associates with HIPPI leading to caspase 8 activation (Gervais *et al*., 2002). Furthermore, Htt is an AKT (or protein kinase B, PKB) substrate, which triggers cell survival pathways (Gervais *et al*., 2002; Rangone *et al*., 2004; Zuccato *et al*., 2010, for review); Htt overexpression rescues mHtt-induced toxicity in cellular models, reinforcing the notion that the pro-survival function of Htt might be affected by the mutation (Cattaneo *et al.,* 2001; Sipione and Cattaneo, 2001; Leavitt *et al.,* 2006).

As mentioned before, WT Htt associates with vesicular transport. Indeed, it was previously shown that neuronal compartments containing vesicle-associated proteins are Htt-enriched. WT Htt associates with clathrin-coated vesicles in normal and HD fibroblasts, thus influencing vesicle transport in the secretory and endocytic pathways (Velier *et al*., 1998). Furthermore, it was demonstrated that WT Htt is necessary for the normal axonal transport in *Drosophila*, and that neuronal depletion of WT Htt, or the

presence of the polyQ protein, disrupts axonal trafficking leading to neuronal degeneration (Gunawardena *et al.,* 2003). In mammals, WT Htt is also involved in fast axonal trafficking of organelles, such as mitochondria. Trushina *et al*. (2004) showed that in embryonic striatal neurons derived from Htt KO mice mitochondria dynamics was altered. Consisting with these results, BDNF vesicular trafficking in neuronal cells (transfected with BDNF and WT FL-Htt) was shown to be enhanced by WT Htt (involving HAP1 and dynactin p150 subunit, two crucial components of molecular motors), and that BDNF transport can be weakened when Htt levels are reduced (Gauthier *et al.,* 2004).

1.2.2.2. Role of mutant huntingtin in HD pathogenesis

Several studies have suggested that Htt mutation results in a gain of function of mHtt that is toxic to the cell (toxic gain of function). Conversely, a loss of protective function of normal Htt has been also reported, due to its decreased expression and/or sequestration into the aggregates by interacting with the mutant protein. Indeed, both may contribute to the disruption of intracellular homeostasis, ultimately leading to neuronal dysfunction and death (Gil and Rego, 2008, for review). Accordingly, different mechanisms have been proposed to explain the pathological role of mHtt (Fig. 1.4.).

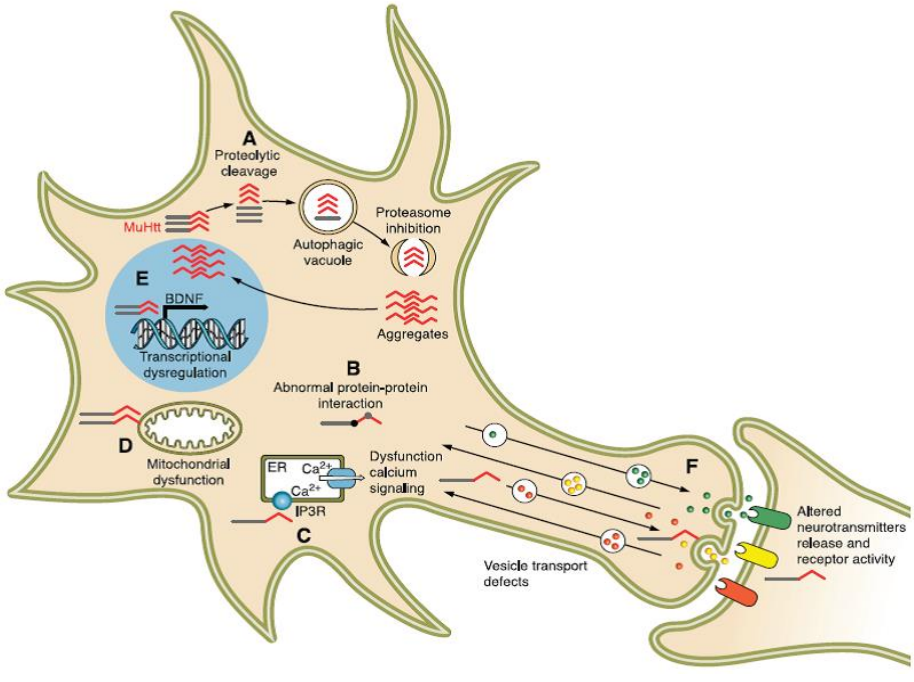

Figure 1.4. – Cellular pathogenic mechanisms in Huntington's disease. Proposed altered mechanisms, which might be inter-dependent rather than exclusive. **A** – mutant Htt (muHtt)

suffers a conformational change leading to partial unfolding or abnormal folding of the protein. FL-muHtt is cleaved by proteases in the cytoplasm and fragments are ubiquitinated to be degraded by the proteasome, which becomes less efficient in HD. Proteasome activity and autophagy are events implicated in cell protection against muHtt toxic insults by enhancing its clearance. **B** – N-terminal fragments (polyQ stretch) accumulate in the cell cytoplasm and interact with several proteins leading to impairment of calcium signaling and homeostasis (**C**) and mitochondrial dysfunction (**D**). **E** – N-terminal muHtt fragments translocate to the nucleus impairing gene transcription and/or forming intranuclear inclusions. **F –** muHtt alters vesicular transport and recycling (image from Zuccato *et al.*, 2010).

Excitotoxicity is the first pathogenic mechanism attributed to neuronal dysfunction in HD. Excitotoxicity broadly refers to the toxic actions of excitatory amino acids, namely glutamate, which results in cell death. Glutamate is the main excitatory neurotransmitter in the mammalian CNS; thereby neuronal excitotoxicity generally means the death of neurons due to abnormal exposure to glutamate and subsequent overactivation of glutamate receptors (reviewed in Fan and Raymond, 2007).

The striatum is innervated by cortical excitatory glutamatergic processes. Thus, overactivation of glutamate receptors might result from increased glutamate release from cortical afferents and/or reduced uptake of glutamate by glial cells, increasing glutamate levels in the synaptic cleft. Among the glutamate receptors the NMDA receptor (NMDAR) is the most relevant in excitotoxic processes. Overactivation of NMDARs is related to intracellular calcium signaling, mitochondrial activity and apoptotic pathways; indeed, increased intracellular calcium concentration has been observed in striatal neurons from symptomatic HD, which correlates with disease progression (Zeron *et al.*, 2002; Tang *et al*., 2003; Fan and Raymond, 2007, for review). Expression of FL mHtt in MSNs was previously shown to facilitate endoplasmic reticulum calcium release in response to enhanced IP_3 formation (Tang *et al.,* 2003). Intracellular calcium is responsible for different events, such as activation of calpains, protein kinase C, endonucleases, phospholipase A2, which may lead to necrotic or apoptotic cell death (Lynch and Guttmann, 2002). Accordingly, increased NMDAR-mediated current density associated with NMDAR overactivation have been closely associated with augmented intracellular free calcium levels and MSN neuronal death in several HD mouse models (Levine *et al*., 1999; Cepeda *et al.,* 2001; Zeron *et al.,* 2002, 2004). As mentioned before, Htt interacts with PSD-95, which is known to associate with and modulate NMDARs function and excitatory signaling (Aarts *et al.,* 2002). In addition, neurons with high calcium buffer capacity (e.g. calbindin positive) in the striatum are not so affected (Ferrer *et al.,* 1994).

NMDAR ligand binding was found to be decreased at pre- and early symptomatic stages in the human HD striatum (Albin *et al*., 1990; DiFiglia, 1990), suggesting that neurons expressing high levels of NMDAR are the most affected and are lost in early HD. At symptomatic stages, nuclear accumulation of mHtt alter transcription and might down-regulate NMDAR expression, as suggested through protein analyses in mouse models and human brain tissue (reviewed in Fan and Raymond, 2007). However, contradictory reports in HD mouse models demonstrated an increased susceptibility to excitotoxic insults (e.g. YAC128 mice) (Zeron *et al*., 2002, 2004), while others showed a complete resistance to excitotoxicity (e.g. R6/2 mice) (Hansson *et al.,* 1999). This might be due to the different characteristics of the transgenic models, given that the YAC128 HD mice model expresses FL human mHtt, opposing to what is observed in R6/2 and N171–82Q transgenic mice models, which only express the N- terminal portion of the protein and display an accelerated HD phenotype.

Striatal neurons excitotoxic sensitivity might also be related to dysfunction of other neurotransmitter receptors, such as A2 adenosine (A2A) receptors, as well as cannabinoid (CB) receptors, which may regulate corticostriatal glutamate release (Tarditi *et al.,* 2006; Maccarrone *et al.,* 2007). In addition, A2A receptor function was found to be altered in cell and animal models of HD (Varani *et al*. 2001; Tarditi *et al.,* 2006). A2A receptors are co-expressed and interact with D2 dopamine receptors on GABAergic enkephalin neurons in the striatum (belonging to the “indirect” pathway, responsible for regulation of motor activity and which are highly affected in HD). Moreover, Varani and co-workers (2001) showed that A2A receptor is particularly altered in cells expressing truncated mHtt, compared to cells expressing the FL protein. In fact, FL mHtt seems to be processed gradually, leading to the accumulation of N-terminal fragments (Li *et al,* 2000), opposing the higher toxicity of truncated mHtt (Wellington *et al.,* 2000). Tarditi *et al*. (2006) demonstrated that R6/2 mice exhibit increased A2A receptor number in the striatum, and a transient insensitivity of the receptor to adenosine antagonists, before the onset of motor symptoms. However, A2A receptors messenger ribonucleic acid (mRNA) levels decrease along with disease progression, not reflecting into a decrease in receptor protein levels, which might be due to a reduction in receptor turnover, as a compensatory mechanism to counteract the decrease in A2A mRNA (Tarditi *et al.,* 2006).

An important finding in HD pathogenesis was the observation of Htt as a substrate for proteolytic cleavage by caspases (Goldberg *et al*., 1996), namely caspase-3. The fact

that cellular toxicity relates to the presence of Htt fragments raised the toxic fragment hypothesis, which postulates that proteolytic cleavage of Htt results in toxic fragments bearing polyQ stretches. These fragments accumulate, further activating other proteolytic caspases and ultimately leading to cell death. Additionally to caspase-3, Htt is cleaved *in vitro* by caspases -2, -6, and -7. Caspase-6-mediated Htt cleavage is particularly toxic. Indeed, inhibition of caspase-6, but not caspase-3, mHtt cleavage site protects against striatal atrophy and neurotoxicity and prevents YAC128 mice motor dysfunction (Graham *et al.*, 2006). Furthermore, calpains, which are a family of calcium-dependent intracellular cysteine proteases, associates to alterations of calcium homeostasis, and its activation was previously demonstrated in human HD tissue (Kim *et al.,* 2001; Gafni and Ellerby, 2002). Cleavage of Htt by calpains is directly proportional to polyQ repeat length. Calpains generate smaller Htt fragments than caspases cleavage and therefore are more toxic to cells (Hackam *et al.,* 1998). Hence, it has been shown that inhibition of calpains and caspases or the modification of their cleavage site in Htt prevent its proteolysis and reduces mHtt toxicity in *in vitro* and *in vivo* HD models (Ona *et al*., 1999; Sanchez *et al.,* 1999; Wellington *et al*., 2000; Gafni and Ellerby, 2002).

The pioneer report of Perutz and coworkers (1994) based on electron microscopy and X-ray diffraction analysis showed that polyQ forms cylindrical β-sheets, which interact via hydrogen bonds, forming “polar zippers” that in turn promote protein aggregation and precipitation (Perutz, 1994; Perutz *et al.,* 1994; Perutz *et al.,* 2002). Interestingly, Htt starts to aggregate *in vitro* after 35-48 glutamine residues, corresponding to the threshold of HD symptomatology (Scherzinger *et al*., 1997).

Insoluble protein aggregates in the form of neuronal intranuclear inclusions (NIIs), formed by mHtt, are found in HD (DiFiglia *et al*., 1997), and are mainly present in the striatum and cortex. The exact role of these aggregates remains unclear, and contradictory protective/toxic roles have been attributed to NIIs (Klement *et al.,* 1998; Saudou *et al*., 1998; Kim *et al*., 1999; Rubinsztein *et al*., 1999; Yang *et al*., 2002). Nevertheless, aggregates are an important HD hallmark. They are present in neurons of all cortical layers and in medium sized striatal neurons of HD carriers, mostly in juvenile than in adult patients (DiFiglia *et al*., 1997). Moreover, protein aggregates have been described in both FL and truncated HD transgenic mice. Nuclear and cytoplasmic inclusions differ in their composition. Nuclear aggregates are mostly composed by the N-terminal mHtt fragments, whereas cytoplasmic inclusions contain both FL and truncated mHtt (Cooper *et al.,* 1998;

Martindale *et al.,* 1998). HD progression in humans and animal models correlates with the accumulation of nuclear aggregates (Boutell *et al*., 1999; Steffan *et al*., 2000; Zoghbi and Orr, 2000; Nucifora *et al*., 2001; Ross, 2002). One mechanism of aggregation recently proposed supports the involvement of the first 17 amino acids in Htt which are rearranged in the form of oligomers with polyQ sequences exposed on their surface (Thakur *et al*., 2009). The process of aggregation might be related to an impairment of UPS and its consequent diminished capacity in degrading mHtt, despite the fact that mHtt is targeted for degradation (reviewed in Gil and Rego, 2008 and Zuccato *et al.,* 2010), since large aggregates were found to colocalize with ubiquitin and chaperones in cell and animal models, as well as in human brains. Concordantly, proteasomal inhibition was observed in the brain and in peripheral tissues (e.g. fibroblasts) derived from HD patients (Seo *et al.,* 2004).

Protein aggregation may not be sufficient to cause neurodegeneration and rather be a cell attempt to sequester toxic soluble fragments (Saudou *et al.*, 1998; Kuemmerle *et al.*, 1999). Indeed, Short-Stop HD mice, which express an *Hdh* mutated gene, truncated after intron II, exhibit aggregates but do not display behavioral dysfunction or neuronal loss (Slow *et al*., 2005). Moreover, aggregate-containing neurons showed increased survival compared to neurons that were aggregate-free (Arrasate *et al*., 2004). Supporting these findings, the expression of a dominant negative ubiquitin-conjugating enzyme in a cellular model of HD, eliminated aggregates but increased mHtt toxicity (Saudou *et al*., 1998). Indeed, Htt oligomers are currently viewed as the most toxic species. Hence, aggregation seems to be an attempt to inactivate toxic species although, later in time, the accumulation of large aggregates may lead to cell dysfunction.
As discussed below, aggregates are able to sequester several proteins, such as transcription factors, resulting in transcriptional abnormalities and can block axonal and dendritic trafficking, causing neuronal damage (Gunawardena *et al*., 2003; Lee *et al.,* 2004). Accordingly, investigators have sought to reduce protein aggregation, using compounds such as sugar trehalose, which demonstrated positive results by diminishing neuronal pathology in the transgenic mouse model R6/2 (Smith *et al*., 2001; Sanchez *et al.*, 2003; Tanaka *et al*., 2004).

Toxicity of Htt aggregates has been attributed to the recruitment of other proteins composed by polyQ tracts, which may lose their function upon aggregation. Some of the

polyQ-containing proteins are transcription factors and transcriptional regulators such as cyclic adenosine monophosphate (cAMP)-response element (CRE)-binding protein (CREB) binding protein (CBP) (Zuccato *et al.,* 2010, for review). Within the nucleus, mHtt has been shown to increase toxicity in cell models and transgenic mice (KIement *et al*., 1998; Saudou *et al*., 1998; Peters *et al.,* 1999) and alter normal Htt activity. Moreover, mHtt interaction with acetyltransferase domains of transcription factors, affects histone acetylation and chromatin structure (Steffan *et al.,* 2001). In a work with purified proteins expressed in *Escherichia coli,* Schaffar and colleagues (2004) showed that soluble/oligomeric mHtt interacts with TBP and CBP prior to aggregation, impairing their normal activity. In fact, the activity of well-known transcriptional systems like the CRE/CREB regulation system was severely reduced in HD (e.g. Cha, 2007).

Deregulation of gene transcription have an important role in HD, mostly through a reduction of gene transcripts (Luthi-Carter *et al.,* 2000; Nucifora *et al.,* 2001; Wyttenbach *et al.,* 2001; Sipione *et al*., 2002), which in turn may downregulate important cell survival factors, but also through the overexpression of pro-apoptotic genes (Garcia *et al.,* 2002). HD transcriptional deregulation was first perceived in *post-mortem* HD human brains, as some signaling neuropeptides and neurotransmitter receptors mRNA were reduced in striatal neurons (Norris *et al*., 1996; Arzberger *et al*., 1997). Importantly, a set of genes associated with transcription, neurotransmission, intracellular signaling, calcium homeostasis and cytoskeletal proteins are altered as disease progresses (Chan *et al.,* 2002, Luthi-Carter *et al.,* 2002; Sipione *et al.,* 2002), as determined by decreased mRNA levels, at early and late HD stages. Interestingly, increased polyQ-induced gene expression was correlated with decreased Htt size, as observed in HD mouse models carrying Htt with different protein length (Chan *et al.,* 2002). Other studies showed that gene deregulation precedes the onset of symptoms, which might indicate an important role for modified transcription regulation in HD (Cha, 2007). Transcription deregulation might result not only from the interaction of soluble mHtt with the activity of transcription factors, but also through the disruption of coactivator complexes on gene promoters (Zuccato *et al*., 2010). Interestingly, gene expression data in the forebrain of the BDNF conditional KO mice correlated with those observed in the human HD caudate, strongly evoking BDNF cortical loss as one of the main causes of striatal damage in HD (Strand *et al.,* 2007).

Gene expression regulation involves the modification of chromatin structure by transcription factors and enzymes, and histones are the main target of these changes, being modified through acetylation, methylation, phosphorylation, ubiquitination, and SUMOylation (Gil and Rego, 2008 and Zuccato *et al*, 2010, for review). Histones acetylation and deacetylation are fundamental processes for gene expression regulation and depend on the interaction between histone acetyl transferases (HATs), that add acetyl groups to chromatin thus opening it and promoting gene transcription, and histone deacetylases (HDACs) that remove acetyl groups, inducing chromatin condensation and, consequently, gene repression (Gil and Rego, 2008 and Zuccato *et al*, 2010, for review). Thus, in an attempt to restore transcriptional activity, some authors overexpressed neuroprotective transcription factors (Steffan *et al.,* 2000; Holbert *et al.,* 2001; Nucifora *et al*., 2001) and inhibited HDACs, which were shown to reduce polyQ toxicity in cell lines, transgenic flies and mouse models of HD (McCampbell *et al*., 2001; Steffan *et al*., 2001; Ferrante *et al*., 2003; Hockly *et al.*, 2003; Oliveira *et al*, 2006).

Mutant Htt cleavage, aggregation and toxicity can also be prevented by Htt phosphorylation (Saudou *et al.,* 1998; Humbert *et al*., 2002; Rangone *et al.,* 2004). Previous reports demonstrated Htt phosphorylation on serine-421 by AKT (Humbert *et al*., 2002; Rangone *et al.,* 2004) and at serine-434, -1181, and -1201 by the cyclin-dependent kinase 5 (Cdk5), which reduced caspase-mediated Htt cleavage and diminished aggregate formation and toxicity (Luo *et al*., 2005). According to these results, inhibition of Htt proteolysis and/or the use of Htt phosphorylation-inducing factors (e.g. insulin-like growth factor 1, IGF-1) could be a good strategy to delay HD progression.

1.2.3. Mitochondrial dysfunction and cell death in HD

A few years ago, the accidental ingestion of 3-nitropropionic acid (3-NP) in humans led to the discovery of striatal susceptibility to mitochondrial impairment (Ludolph *et al.,* 1991). 3-NP inhibits tricarboxylic acid cycle by irreversibly inhibiting mitochondrial succinate dehydrogenase or complex-II (Alston *et al*., 1977; Coles *et al.,* 1979), and its systemic administration in rats was shown to induce selective basal ganglia lesions, and progressive locomotor deterioration (Beal *et al.,* 1993; Borlongan *et al.*, 1995), resembling HD pathology.

Mitochondrial dysfunction is involved in excitotoxicity, oxidative stress and gene deregulation, thus contributing to HD pathogenesis (for review see Gil and Rego, 2008 and Zuccato *et al.,* 2010). mHtt has been shown to associate with mitochondrial outer membrane and its N-terminus direct binds to mitochondria altering their normal function. Moreover, mHtt promotes cytochrome c release, triggering cell apoptosis, by reducing the required calcium levels needed to induce mitochondrial permeability transition (MPT) pore opening (Choo *et al*., 2004).

Energy metabolism impairment is another feature of HD pathology. This is evidenced by decreased production of ATP, increased lactate levels, decreased N-acetylaspartate and creatine, as well as deficits in mitochondrial respiratory chain complexes-I, -II, -III and -IV activities in HD affected brain regions (Zuccato *et al.,* 2010, for review). Moreover, Panov and co-workers showed that mitochondrial membrane potential is decreased in HD patient's lymphoblasts and transgenic mice brain, demonstrating the occurrence of mitochondrial defects in both central and peripheral tissues (Panov *et al*., 2002, 2003).

Deficient mitochondrial calcium handling has been also associated with HD. Mitochondria isolated from the whole brain of YAC72 mice (expressing FL human mHtt) display deficient calcium uptake several months before evidence for behavioral or pathological symptoms (Panov *et al.,* 2002). Similarly, lymphoblast mitochondria derived from HD patients (and particularly those with a juvenile form) were more sensitive to calcium stimuli and displayed decreased mitochondrial membrane potential for lower calcium concentrations, as compared to mitochondria isolated from healthy individuals (Panov *et al.,* 2002). Additionally, incubation of normal mitochondria with mHtt mimics the calcium-handling impairment found in human HD mitochondria (Panov *et al.,* 2002, 2003; Choo *et al*., 2004), suggesting that this dysfunction might result from a direct deleterious effect of mHtt on the outer mitochondrial membrane.

Reduced mitochondrial calcium-handling was also observed in other tissues such as skeletal muscle of late symptomatic R6/2 mice, which is in agreement with muscle cell degeneration (Gizatullina *et al*., 2006). Interestingly, results obtained from different HD mouse models seems to converge to a tissue-specific sensitivity to calcium-handling, particularly striatal mitochondria, which appear to be more sensitive to calcium than cortical mitochondria (Brustovetsky *et al*., 2005). However, calcium loading capacity is apparently increased in isolated mitochondria from transgenic and knock-in (KI) HD mice brain (Brustovetsky *et al*., 2005; Oliveira *et al.,* 2007), and is associated to a severe phenotype (Oliveira *et al.,* 2007). Results obtained using isolated mitochondria posed

pertinent questions concerning the measurement of calcium handling in mitochondria outside their cellular context thus, *in situ* studies performed in primary striatal neurons from YAC128 transgenic mice demonstrated that mitochondria failed to restore calcium homeostasis after NMDAR transient activation, compared with neurons from WT mice littermates (Oliveira *et al*., 2006, 2007).

Mitochondrial function and oxidative stress are indirectly regulated by transcription factors (Cha, 2007). mHtt was shown to interact with p53, increasing its levels and transcriptional activity. Consequently, two pro-apoptotic proteins, B-cell lymphoma-2 (Bcl2)-associated X protein (BAX) and p53-upregulated modulator of apoptosis (PUMA), were upregulated along with mitochondrial membrane depolarization (Bae *et al*., 2005). Additionally, Cui and colleagues (2006) showed that mHtt inhibits peroxisome proliferator-activated receptor gamma co-activator 1-alpha (PGC-1α) co-transcriptional activator, a master regulator of genes involved in mitochondrial function and energy metabolism. Accordingly, the expression of these genes was markedly reduced in the disease. Moreover, PGC-1α KO mice exhibited abnormal mitochondria function along with hyperkinesia and striatal degeneration (Cui *et al*., 2006). Corroborating these results, Weydt and colleagues (2006) observed reduced expression of PGC-1α target genes in HD patient and mouse striatum and demonstrated that HD striatal neurons expressing exogenous PGC-1alpha were resistant to 3-NP treatment (Weydt *et al.*, 2006). These data posed mitochondria as a central target of HD neuron pathogenesis, as both a direct interaction of mHtt and transcription deregulation may contribute for their dysfunction.

Mitochondria have been also implicated in cell death, classically classified as apoptotic or necrotic (Kerr *et al.,* 1972). Apoptosis, or programmed cell death, can occur by two pathways: the extrinsic and intrinsic pathways. The extrinsic pathway involves a death receptor and apoptosis is initiated by an external stimulus which leads to the binding of a ligand (e.g. Fas ligand or tumor necrosis factor, TNF, family proteins) to the death receptor in the plasma membrane; the intrinsic pathway depends on mitochondria. Caspases can be activated by both pathways. In mammals, caspase family can be divided into “initiator” (caspase-1, -2, -4, -5, -8, -9, -10, -11, and -12), and downstream “executioner” (or “effector”) caspases (caspase-3, -6, -7, and -14). Initiator caspases respond to pro-apoptotic stimuli further cleaving executioner procaspases, which in turn cleave target proteins (for a review, see Yi and Yuan, 2009).

During the early phase of apoptosis, upstream caspases might be activated, such as caspase-8 following activation of death receptors in the extrinsic pathway. Effector caspases are subsequently activated, namely caspase-3, either directly (independently of mitochondrial alterations) or indirectly, through the cleavage of BH3 interacting-domain death agonist (Bid), a pro-apoptotic member of Bcl-2 family. Truncated Bid (tBid) can associate with other pro-apoptotic proteins (e.g. Bax), mediating mitochondria outer membrane permeabilization, which further induces the release of apoptogenic factors, such as cytochrome c, and elicits apoptosis (reviewed by Mattson, 2000; Pattison *et al.,* 2006 and Kroemer *et al*., 2007). Mitochondria in apoptotic cells show increased production of reactive oxygen species and calcium levels, which trigger the formation of the permeability transition pore (PTP), with the consequent release of cytochrome c, second mitochondria-derived activator of caspase/direct inhibitor of apoptosis (IAP) binding protein with a low pI (Smac/DIABLO) and Omi stress-regulated endoprotease/high temperature requirement protein A2 (Omi/HtrA2) and subsequent activation of effector caspases (extensively reviewed in Kroemer *et al*., 2007); on the other hand, mitochondrial proteins may release the organelle through pores formed by Bcl-2 pro-apoptotic members, such as Bax, after its translocation to the mitochondrial membrane (Mattson, 2000, for review). Within the cytosol, cytochrome c forms a complex with apoptotic protease-activating factor-1 (Apaf1), procaspase-9 and deoxyATP, the apoptosome, leading to caspase-9 activation (initiator caspase of the intrinsic pathway), which further activates the executioner caspase-3 (Pattison *et al*., 2006, for review). Apoptosis is associated with plasma membrane alterations, such as membrane blebbing and translocation of phosphatidylserine to the outer leaflet of the plasma membrane (which activates cell phagocytosis by macrophages/microglia) and ultimately leads to condensed and fragmented chromatin/desoxyribonucleic acid (DNA) (Mattson, 2000, for review).

Apoptosis may be also mediated by mitochondrial release of apoptosis-inducing factor (AIF), which acts through a caspase-independent pathway. AIF is a mitochondrial intermembrane flavoprotein that is released from the mitochondria and translocated to the nucleus in response to specific death signals, causing initial chromatin condensation and DNA fragmentation (Daugas *et al.,* 2000). AIF appears to function downstream of Bax and is released from mitochondria before cytochrome c (Daugas *et al.,* 2000; Cregan *et al.,* 2002). Corroborating AIF role in apototosis, Cregan and collaborators (2002) showed that blocking AIF function significantly protected against cell death (Cregan *et al.,* 2002).

Despite its downstream role in the apoptotic pathway, caspase-dependent apoptosis (particularly caspase-3) has been described as one of the main events in HD neuronal death, since caspase activation was previously shown to be involved in Htt cleavage (Ona *et al.,* 1999; Sanchez *et al.,* 1999). Furthermore, fragmented chromatin was observed in HD striatal tissues. Accordingly, minocycline, a tetracycline antibiotic, which was shown to inhibit caspase-1 and cytochrome c release, ameliorated HD-related symptoms in HD mice models (Berger, 2000) and in patients (Bonelli *et al*., 2004).

Autophagy, namely macroautophagy, has also been suggested as an alternative form of HD cell death and was previously demonstrated in HD brain, and in animal and cellular models of HD (Kegel *et al*., 2000; Petersén *et al*., 2001a; Larsen and Sulzer, 2002). Indeed, accumulation of Htt aggregates resistant to proteasomal degradation seems to stimulate cell death by autophagy (Ventruti and Cuervo, 2007). On the other hand, autophagy might represent a pathway to increase cell survival given that protein aggregation and cell loss can be reduced following autophagy activation. Previous studies showed that removal of toxic forms of mHtt from the cytosol may occur through autophagy (Sarkar and Rubinsztein, 2008), whereas WT and mHtt present in the nucleus are normally degraded by the proteasome (Iwata *et al*., 2009).

Further evidences supporting the autophagic hypothesis is the fact that an inhibitor of the autophagic pathway, mTOR, is sequestered within polyQ aggregates in HD cell models, transgenic mice, and human patients, inducing autophagy and thus eliminating mHtt fragments (Ravikumar *et al*., 2004). An interesting and more recent work by Martinez-Vicente *et al*. (2010) revealed a miscarried function of the autophagic/lysosomal system, in different cell and mouse HD models and in striatal tissue from HD patients. The authors observed that autophagosomes are formed in HD cells and further fuse with lysosomes, forming the autophagolysosomes, but the autophagosomes in HD cells exhibited diminished efficiency in confiscating cellular components, leading to increased levels of protein aggregates, lipid stores and dysfunctional mitochondria, observed in HD (Martinez-Vicente *et al*., 2010).

Whether striatal neuronal cell death occurs autonomously or involves other brain regions remains to be clarified. It has become evident that deregulation of synaptic glutamate levels leading to enhanced NMDAR activation and BDNF deregulation (see next section) from the cortex might result in excitotoxicity and trophic factor deprivation of striatal neurons, respectively. Furthermore, the high levels of dopamine released into the

striatum can activate oxidative stress and autophagic pathways (Petersén *et al.,* 2001a). In contrast, other events, such as mitochondrial impairment, protein aggregation, gene transcriptional changes and Htt cleavage, may occur independently of changes in intercellular communication.

1.2.4. Brain-derived neurotrophic factor and TrkB receptor in HD

BDNF is a neurotrophic factor that belongs to the family of neurotrophins (NT), along with nerve growth factor (NGF), NT-3 and NT-4/5. Neurotrophins bind to two distinct receptors: one selective member of the tropomyosin-receptor-kinase (Trk) receptor and all four bind to the p75 neurotrophin receptor with low affinity. BDNF preferentially binds to TrkB receptor. TrkB can be alternatively spliced into two variants: a FL and a truncated (T) form, the latter divided into isoforms, T1 and T2. The binding of BDNF to FL-TrkB causes receptor homodimerization, internalization and induces its autophosphorylation at several tyrosine residues. On the other hand, the T-TrkB is thought to inhibit FL-receptor mediated pathways (Haapasalo *et al.,* 2001), thus modulating the trophic effect of BDNF. Moreover, it was previously demonstrated that T-TrkB in astrocytes and Schwann cells stores and controls BDNF release, according to the extracellular concentration of BDNF (Rubio, 1997; Alderson *et al.,* 2000).

FL-TrkB might also be activated in a NT-independent manner, by transactivation, the process by which TrkB phosphorylation is induced following other receptor activation (Lee and Chao, 2001), such as A2A receptor. A2A receptor activation induces translocation of TrkB receptors to lipid rafts and amplifies the biological effects of TrkB-mediated BDNF function in the nervous system (Assaife-Lopes *et al*., 2010; Sebastião *et al.*, 2011, for review). BDNF binding to FL-TrkB receptor activates different signaling pathways, namely the PI3K/AKT pathway, the mitogen-activated protein kinase (MAPK)/extracellular-signal-regulated kinase (ERK) pathway and the phospholipase C-gamma1 (PLC-γ1) pathway (Barbacid, 1994).

BDNF is mainly produced in the cortex by neurons in layers V and VI and further transported anterogradely to the striatum where it is released and interacts with TrkB receptors located on GABAergic striatal neurons (Marty *et al.,* 1997). Low levels of BDNF protein were also demonstrated in the striatum of HD patients and mice (Ferrer *et al*., 2000; Zuccato *et al.*, 2001; Ginés *et al*, 2003a). Striatal neurons express both forms of T- and FL-TrkB variants and adenosine A2A receptor. In the R6/2 HD mice model it was

demonstrated that administration of an A2A receptor agonist delays motor dysfunction and mHtt aggregation (Chou *et al*., 2005) and alters NMDAR subunit composition, indicating decreased susceptibility to excitotoxicity, which was observed specifically in the striatum, strongly suggesting A2A receptor-mediated neuroprotection selective for BDNF-deficient HD pathology (Ferrante *et al*., 2010).

It is well documented the importance of BDNF for MSNs, the most affected neuronal population in HD. This neutrophin is a potent survival factor for striatal neurons (Ventimiglia *et al.,* 1995) and induces the differentiation of striatal GABA-, calbindin- and dopamine and cAMP regulated phosphoprotein (DARPP-32)-neurons (Nakao *et al*., 1995). Indeed, BDNF KO mice die prematurely (Jones *et al.*, 1994; Ivkovic *et al.*, 1997). Homozygote mutants die within 2 days after birth, although some animals survive up to 2-4 weeks (Jones *et al.*, 1994). Furthermore, postnatal forebrain ablation of BDNF induces striatal dendrite dysfunction in conditional KO mice (Baquet *et al.*, 2004). These animals developed similar symptoms as HD transgenic mice, namely a reduction of striatum volume, neuronal loss and a clasping behavior (Baquet *et al*., 2004). Altogether, these data strongly confirmed the importance of the neurotrophin in MSNs survival and integrity of dendrite morphology.

Interestingly, in excitotoxic HD animal models, BDNF and TrkB receptor are upregulated after exposure to quinolinic acid (QA, an endogenous agonist of NMDARs), 3-NP or colchicine lesions in the striatum, suggesting an endogenous neuroprotective role (Alberch *et al.,* 2004). In addition, intrastriatal administration of BDNF protected striatal neurons from excitotoxicity *in vivo* (Martinez-Serrano and Bjorklund, 1996; Bemelmans *et al*., 1999; Perez-Navarro *et al.,* 2000; Gratacos *et al.,* 2001). Recently, Gomes *et al.* (2012) was able to show the differential expression levels of T- and FL-TrkB receptors after an excitotoxic stimulus. Accordingly, FL-TrkB receptors are degraded *in vitro* (in cultured hippocampal and striatal rat neurons exposed to glutamate) and *in vivo* (after kainate hippocampal injection) while T-TrkB is upregulated (Gomes *et al*., 2012). The authors suggested that the change observed in TrkB isoforms expression may partially be responsible for a change in BDNF function, from a neurotrophic to a neuroprotective function. Furthemore, BDNF neuroprotection during hippocampal neuronal excitotoxic stimulation was mediated by T-TrkB (Gomes *et al*., 2012), thus attributing a new role to the truncated receptor other than being a dominant negative TrkB receptor form (Haapasalo *et al*., 2001).

Besides neuroprotection, BDNF was also demonstrated to promote neurogenesis in the adult brain (Zigova *et al*., 1998; Pencea *et al*., 2001).

As described above, MSNs largely depend on cortex-derived BDNF. Therefore, several studies proposed that BDNF might have an important role in HD, since striatal BDNF levels were decreased in HD patients, transgenic mice models and cell cultures (Zuccato *et al.*, 2001). However, no changes were detected in the cerebral cortex and in the hippocampus (Zuccato *et al*., 2010, for review). YAC72 transgenic mouse model of HD overexpressing FL human mHtt displayed a marked reduction in BDNF mRNA and protein levels in the cerebral cortex and striatum, similar to the reduced production of the neurotrophin observed in HD human brain (Zuccato *et al.,* 2001; Zuccato *et al.,* 2010, for review).

HD is characterized by reduced BDNF gene transcription. Htt interacts with repressor element-1 (RE1)-silencing transcription factor (REST), which controls cortical BDNF expression, and is decreased by polyQ expansion. WT Htt associates with REST and neuron restrictive silencer factor (NRSF), among other proteins, in the cytoplasm. Conversely, mHtt induces REST/NRSF release from the complex, promotes its accumulation in the nucleus and binding to RE1/neuron restrictive silencer element (NRSE) within the BDNF promoter II, which is subsequently activated leading to decreased BDNF transcription (Zuccato *et al.,* 2003). mHtt may also affect BDNF transcription by altering the transcriptional activity of other transcription factors important for the regulation of BDNF promoters (Zuccato *et al.,* 2010, for review). Another proposed cause for BDNF decreased levels in the HD striatum (Ferrer *et al.,* 2000; Zuccato *et al*., 2001; Zuccato *et al.,* 2003) is the reduced transport of BDNF vesicles along the cortico-striatal afferents, observed in homozygous mHtt KI cells (Gauthier *et al.,* 2004). Meanwhile, other studies demonstrated that mitochondrial transport was also affected in endogenous Htt depleted systems or in cells carrying mHtt (Orr *et al.,* 2008; Zuccato *et al.,* 2010, for review). BDNF vesicle transport also appears to depend on Htt phosphorylation at serine-421 by AKT. Upon phosphorylation, Htt promotes anterograde transport, but if not phosphorylated BDNF vesicles are more likely to undergo retrograde transport (Colin *et al,* 2008). In HD, reduced phosphorylation of Htt at serine-421 was demonstrated in cellular and animal models and in postmortem human tissues, which might impair BDNF transport (Warby et *al*., 2005; Colin *et al*, 2008).

1.3. HD MODELS

HD research largely depends on animal and cellular models, since limited information is given by *post-mortem* human brain or even peripheral human cells. Since HD is caused by a single mutation, the introduction of the mutant gene into non-human primate, mouse, fly, fish, and worm has generated disease models. Interestingly, the first "polyQ model" was developed almost 50 years ago, when the aggregation properties of polyQ stretches were discovered in a test tube (Krull *et al*., 1965). These simple cell-free systems are appropriate models to investigate the biochemical parameters involved in protein conformational change, sequestration and aggregation, as well as to screen chemical compounds which may interfere with these processes (Perutz, 1994; Perutz *et al*., 1994; Scherzinger *et al.,* 1997; Perutz *et al.,* 2002; Schaffar *et al.,* 2004).

1.3.1. HD Animal models

Before the emergence of genetic models, different toxins were delivered to rodents and primates to reproduce a HD-like phenotype (Brouillet *et al*., 1999; Zuccato *et al.,* 2010, for review). The over-stimulation of glutamate receptors with excitatory amino acids directly injected in the rodent striatum, such as ibotenic acid, kainic acid (KA) (a non-NMDAR agonist), NMDA or QA induced neuronal death by excitotoxicity (McGeer and McGeer, 1976; Bruyn and Stoof, 1990; Zuccato *et al.,* 2010, for review). KA and QA are the two most common neurotoxins used to produce rodent and non-human primate HD models. The activation of these excitotoxic pathways suggests that excitotoxicity might be a relevant event in HD pathology. Another strategy to induce striatal degeneration consists in the systemic administration of mitochondrial toxins like 3-NP and malonate (irreversible and reversible inhibitors of complex-II, respectively), implicating mitochondrial dysfunction in disease pathogenesis (as described before). 3-NP leads to ATP depletion and reproduces a specific striatal degeneration of GABAergic neurons and thus its use is based on the hypothesis that chronic impairment of mitochondrial metabolism may induce neuronal death. These chemically induced models are able to reproduce the regional selectivity of HD neuropathology, but do not mimic the progressive pathophysiological mechanisms induced by the mutated HD gene. Therefore, their interest has decreased in favor of the mHtt-based models; nevertheless, they are still useful tools to test HD

therapeutic strategies, such as neuronal protection and restoration, as these models are normally associated with neuronal death.

The development of transgenic models led to a significant advance in HD research, allowing determining the first molecular changes associated with the disease, find some of the activated toxic pathways and test effective therapies. The simplest genetic animal model of HD is the invertebrate nematode *Caenorhabditis elegans* with only 302 neurons (Faber *et al*., 1999; Holbert *et al*., 2001; Parker *et al*., 2001; Faber *et al*., 2002), which allows performing biochemical and morphological studies, and even behavioral tests. Because it is transparent, *C. elegans* models permit longitudinal live imaging studies *in vivo* with standard microscopy equipment.

Another invertebrate model for HD is the fruit fly *Drosophila melanogaster*, which displays progressive neurodegeneration of photoreceptors, disruption of axonal transport and nuclear inclusions, leading to early cell death (Jackson *et al.*, 1998; Steffan *et al.*, 2001; Gunawardena *et al.*, 2003).

Transgenic HD flies or worms are easy to produce and are suitable models to screen for genetic or chemical modifiers, which would interfere with the polyQ-induced pathology *in vivo*.

Mammals, particularly the mouse (*Mus musculus*), are the most commonly used animals to model HD. Three types of mouse models have been developed: KO, KI and transgenic models.

Htt KO models were the first to be generated but, as mentioned before, the animals did not overcome the embryonic stage. Nevertheless, KO models revealed the crucial role of Htt during embryogenesis. To date, several rodent models have been developed to study the effects of mutated HD gene and each model exhibits unique phenotypes (for review see Zuccato *et al*., 2010 and Gil-Mohapel *et al.*, 2011). Thus, some discrepancies observed between studies may result from the use of different genetic HD models, since these models differ in the size of the expressed Htt fragment, the number of CAG repeats, the promoter driving the transgene and consequently the expression of the mutant protein, as well as the background strain (Table 1.2.).

Table 1.2. – Common rodent genetic HD models.

Model	1) Construct 2) Promoter	CAG repeats	Expression level	Background strain	1) Life Span 2) Symptoms onset	1) Neuropathology 2) Behavior 3) Other
Knock-in						
HdhQ92-111 mice (Wheeler *et al.* 1999, 2000)	1) mouse *htt* exon 1 replaced with human m*htt* exon 1 2) mouse *htt*	92-111	100%	129Sv x C57BL/6J	1) normal 2) 96 wk	1) NIIs, striatal neuropil aggregates, no brain atrophy or cell loss, neuronal cells w/degenerative morphology, gliosis 2) No symptoms 3) N.O.
Hdh(CAG)140 -150 mice (Lin *et al.* 2001; Menalled *et al.* 2003)	1) polyQ (CAG repeats) inserted in mouse *htt* gene 2) mouse *htt*	140-150	N.D.	129/Ola × C57BL/6J	1) normal 2)2-4 mo	1) NIIs, cell dysfunction, gliosis, axonal degeneration 2) Clasping, motor deficits 3) Reduced size
Transgenic (FL)						
YAC72 mice (Hodgson *et al.* 1999)	1) YAC FL-h*htt* 2) h*htt*	72	30-50%	FVB/N	1) normal 2) 6 wk	1) Selective striatal cell death 2) Hyperkinesia followed by hipokinesia 3) Body weight loss
YAC128 mice (Slow *et al*. 2003)	1) YAC FL-h*htt* 2) h*htt*	128	75%	FVB/N	1) normal 2) 8-12 wk	1) Striatal inclusions, selective striatal and cortical cell death and atrophy 2) Hyperkinesia followed by hipokinesia, cognitive deficits, depressive-like behavior 3) Body weight increase
BACHD mice (Gray *et al*. 2008)	1) BAC FL-h*htt* 2) h*htt*	97	N.D.	FVB/NJ	1) normal 2) 12 wk	1) Neuropil mHtt inclusions (few in cortex and striatum), brain atrophy, reduced cortical and striatal volume 2) Motor deficits 3) Body weight increase
Transgenic (truncated)						
R6/1 mice (Mangiarini *et al.* 1996)	1) Exon1 of h*htt* 2) h*htt*	113	31%	CBA x C57BL/6J	1) 32-40 wk 2) 15-21 wk	1) NIIs and neuropil aggregates, limited cell loss, brain atrophy, cell dysfunction 2) Behavior and motor deficits 3) Body weight loss

R6/2 mice (Mangiarini *et al.* 1996)	1) Exon1 of h*htt* 2) h*htt*	144	75%	CBA x C57BL/6J	1) 12-15 wk 2) 5-6 wk	1) NIIs and neuropil aggregates, limited cell loss, brain atrophy, cell dysfunction 2) rapid deterioration of cognitive and motor functions 3) weight loss, diabetes, cardiac dysfunction
N171-82Q mice (Schilling *et al.* 1999)	1) first 171 aa of h*htt* 2) mouse prion protein	82	10-20%	C3H/HEJ x C57BL/6J	1) 24-30 wk 2) 10wk	1) NIIs, striatal neurodegeneration 2) motor deficits 3) NO
HD rat (von Hörsten *et al.* 2003)	1) Exon1 of h*htt* 2) rat *htt*	51	N.D.	Sprague Dawley	1) 24 mo 2) 40-50 wk	1) NIIs, specific striatal cell loss and atrophy, cell dysfunction 2) Cognitive deficits and progressive motor dysfunction 3) Body weight loss

aa – amino acids; **BAC** – Bacterial Artificial Chromosome; **FL –** full-length; ***htt*** – *huntingtin* gene; **h*htt*** – human *htt*; **m*htt*** – mutant *htt;* **mo** – month; **N.D**. – not determined; **NIIs** – Neuronal Intranuclear Inclusions; **N.O**. – not observed; **YAC** – Yeast Artificial Chromosome; **wk** – week (adapted from Zuccato *et al.,* 2010, and Gil-Mohapel *et al*., 2011).

KI mice derived from the insertion of a polyQ stretch into the mouse *HD* gene homologue and the offsprings include both heterozygous and homozygous animals (for review see Gil-Mohapel *et al.*, 2011). The mutated gene is then expressed under its natural promoter and in its appropriate genomic context. KI mice develop behavioral abnormalities at a very early stage, before any neuropathological changes are observed. They are characterized by hyperactivity followed by hypoactivity and gait abnormalities, which resembles the progression of motor symptoms in HD patients (Lin *et al.,* 2001; Menalled and Chesselet, 2002; Wheeler *et al.,* 2002). mHtt microaggregates can be observed at an early disease stage (2–6 months of age) but NIIs are detected only at later stages (10–18 months of age) (Wheeler *et al.,* 2000; Lin *et al.,* 2001; Menalled and Chesselet, 2002). The degree of neuropathology is positively correlated with polyQ expansion. Mice carrying less CAG repeats (e.g. Hdh94) show aggregates and NIIs exclusively in the striatum, whereas mice with longer stretches (e.g. Hdh150 mice, with 150 CAGs) show a more widespread brain distribution of aggregates (Lin *et al.,* 2001; Menalled and Chesselet, 2002). Importantly, cell loss and gliosis are usually absent (for review see Gil-Mohapel *et al.*, 2011).

Transgenic HD models can derive from either truncated- or FL-Htt expressing rodents. Since their generation in 1996, the R6 lines (R6/1 and R6/2) are the most common transgenic HD mice models. These mice express exon 1 of the human *HD* gene (corresponding to ~ 3% of the entire gene) with 115 and 150 CAG repeats, respectively (Mangiarini *et al.,* 1996). The phenotype and neuropathology developed in R6 mice reproduce several features of HD in humans, including progressive motor deterioration characterized by an initial hyperactive phase, followed by a hypoactive phase, and cognitive impairment (reviewed in Gil-Mohapel *et al.*, 2011). Neuropathologically, these mice display significant brain atrophy along with striatal volume reduction (Mangiarini *et al.,* 1996). Indeed, MSN exihibit reduced soma area by about 20%, as well as reduced dendritic arborizations and spine density (Gil-Mohapel *et al.*, 2011, for review). Accumulation of ubiquitinated nuclear and cytoplasmic inclusions of mHtt altered levels of neurotransmitters and their receptors and compromised gene expression can be also observed in the R6 mice (Gil and Rego, 2008 and Gil-Mohapel *et al.*, 2011, for review). Some peripheral features have been also described, such as decreased body weight (also seen in HD patients), diabetes and neuroendocrine abnormalities (Mangiarini *et al.,* 1996; Gil and Rego, 2008 and Gil-Mohapel *et al.*, 2011, for review). These animlas die prematurely (Mangiarini *et al.,* 1996). A loss of hypothalamic neurons was also reported in end-stage R6/2 mice, which is also observed in human HD patients (Petersén *et al.,* 2005; van der Burg *et al.,* 2008) and might explain alterations in the circadian rhythm (including sleep disturbances), metabolic changes and weight loss.

Other truncated transgenic animals are produced through the expression of an N-terminal fragment of Htt with 171 amino acids carrying 18 (N171-18Q), 44 (N171-44Q), or 82 (N171-82Q) glutamine residues (Schilling *et al.,* 1999). Animals with 82Q express relatively low levels of the transgene. Similarly to the R6 lines, these mice die prematurely, display loss of body weight and behavioral abnormalities. NIIs and neuritic aggregates of mHtt have been also detected in N171-82Q mice (Schilling *et al.,* 1999).

In 2003, von Hörsten and colleagues developed the first transgenic rat model for a neurodegenerative disease. In this model, a fragment of the HD gene with 51 CAG repeats was expressed under the control of the endogenous rat Htt promoter (von Hörsten *et al.,* 2003). These animals showed an adult and progressive onset of symptoms, including reduced anxiety, cognitive impairment and motor dysfunction with the appearance of chorea-like movements (von Hörsten *et al.,* 2003; Gil-Mohapel *et al.*, 2011, for review). The HD transgenic rat brain exhibited NIIs as well as striatal volume

reduction and neuronal loss and die around 24 months of age, with marked decrease in body weight associated with a severe muscular atrophy (von Hörsten *et al.,* 2003).

Another strategy for generating transgenic mouse models is the use of a transgene bearing FL human *HD* gene with different CAG lengths. Human *HD* gene is then expressed under the control of different promoters, including cytomegalovirus (CMV) or endogenous Htt promoter (Gil-Mohapel *et al.*, 2011, for review).

Among the various FL transgenic models, bacterial artificial chromosome (BAC) mice is a recent HD model generated by introduction of BAC enclosing complete human Htt locus of 170 kb with an expansion of 97 CAG into FvB fertilized eggs (Gray *et al*. 2008). BAC transgenic mouse model of HD (BACHD) express FL-mHtt, display progressive motor deficits and recapitulate the adult-onset pattern of mHtt aggregation observed in HD. BACHD show selective neuropathology in the cortex and striatum independently of early nuclear accumulation of aggregated Htt; indeed, these animals have stable levels of FL-mHtt and fewer amounts of mHtt N-terminal fragments, present in both the nucleus and cytoplasm (Gray *et al*. 2008).

The most common FL transgenic model is the yeast artificial chromosome (YAC) mice, which express the FL human *HD* gene with 18, 46, 72 (Hodgson *et al.,* 1999) or 128 (Slow *et al.,* 2003) CAG repeats. YAC128 mice have been the most extensively characterized. First symptoms include hyperkinesia in an early stage (around 3 months of age) followed by the onset of motor deficits and ultimately hypokinesia (Graham *et al.,* 2006; van Raamsdonk *et al.,* 2005, 2007). YAC128 transgenic HD mice also develop mild cognitive deficits, as well as a depressive-like phenotype at 3 months of age and neuropathologically exhibit marked atrophy of striatum, globus pallidus and cortex (at ~9 months of age) (Slow *et al*., 2003; van Raamsdonk *et al.,* 2005). Interestingly, 12 month-old YAC128 mice display selective degeneration of striatal MSNs (van Raamsdonk *et al.,* 2005) and Htt inclusions in striatal cells can be detected in older end-stage animals (i.e., at 18 months of age) (Slow *et al*., 2003). Neuronal dysfunction and loss before mHtt intranuclear inclusions sustain the hypothesis that inclusions may result from cellular dysfunction and/or have a protective role in the beginning of the disease (Saudou *et al*., 1998; for review see Gil and Rego, 2008). At the peripheral level, YAC128 mice display increased body weight and testicular atrophy and degeneration (van Raamsdonk *et al.,* 2005, 2006 and 2007).

1.3.2. HD Non-animal models

Other HD models are obtained by the expression of mHtt, an Htt fragment or a polyQ expansion in different cell types, including yeast, cell lines, or primary neuronal cultures. Yeast (*Saccharomyces cerevisiae*) provides a useful tool for the screening of genes involved in aggregate formation, to study potential polyQ-induced toxicity and for the rapid screening of chemical compounds (Lindquist *et al.,* 2001; Muchowski *et al.,* 2002). HD cell lines allow the stable or inducible expression of WT Htt or mHtt, and thus are also useful models to study disease mechanisms and for screening potential therapies (for review see Zuccato *et al.*, 2010).

Neuronal cell lines or primary neuronal cultures may be obtained from HD KI and transgenic mice striatum and cultured *in vitro*. These cells express mHtt in a physiological manner, although the absence of a severe phenotype, nuclear inclusions or no apparent cell death likely restrains the study of HD pathology (Trettel *et al.*, 2000; Petersén *et al*., 2001b; Zeron *et al*., 2004; Bauer and Nukina, 2009, for review). Primary striatal neurons transfected with mHtt have shown typical HD features, such as protein aggregation and neuronal death (Saudou *et al*., 1998). Unfortunately, the low transfection rate significantly constrains their use.

Recently, differentiated human neurons derived from HD patients induced pluripotent stem cells (iPSCs) appear to be useful tools in the research of neurodegenerative diseases, particularly in their underlying causes as well as the possibility of addressing new drug targets (Peng and Zeng, 2011, for review). The pivotal report of Takahashi and Yamanaka (2006) about mouse fibroblast reprograming back to a pluripotent state using four transcription factors (Oct4, Sox2, Klf4, and c-Myc) has been successfully followed by others using different somatic lineages and other species including human (Peng and Zeng, 2011, for review). In HD field, Park and colleagues (2008) obtained fibroblasts from a young HD patient which were transduced with retroviruses that expressed the four key transcription factors (Oct4, Sox2, Klf4, and c-Myc), thus successfully producing iPSCs. These cells display human ESC characteristics when grown in co-culture with mouse embryonic feeder fibroblasts (Park *et al.,* 2008). Later, another group managed to differentiate the HD-specific iPSC originally obtained by Park *et al*. (2008) into neurons

with striatal characteristics (Zhang *et al.*, 2010). These cells contained the same expanded CAG tract like the HD patient fibroblasts and HD fibroblast-derived iPSC.
This approach might be useful in the analysis of neurodegenerative diseases. Furthermore, the use of patient specific iPSCs might help to understand how mutant genes, such as *HD*, influence cellular homeostasis, which is crucial especially when investigating disease mechanisms and potential therapeutics.

1.4. ADULT NEUROGENESIS

In the mammalian brain, adult neurogenesis was first demonstrated in 1962 by Altman and co-workers. Although neurogenesis is almost complete at birth, it is widely accepted that neural stem cells (NSC) are present in the adult brain mainly in two neurogenic regions, the subventricular zone (SVZ) in the lateral ventricles and the subgranular zone (SGZ) in the hippocampus dentate gyrus (DG) (Gage, 2000; Doetsch, 2003). Stem cells are characterized by their capacity for self-renewal through cell division and for generating specialized cell type(s).
In the adult SVZ, glial fibrillary acidic protein (GFAP)-expressing cells (type B cells or radial glia-like cells) are considered the stem cells of the brain. These cells self-renew and give rise to rapidly dividing progenitor cells (transit-amplifying type C cells) which originate migrating neuroblasts (type A cells) (Fig. 1.5). The neuroblasts migrate through the rostral migratory stream (RMS) and reach the olfactory bulb where they differentiate into interneurons and are thought to play a role in olfactory discrimination. In SGZ, radial glia-like type B cells give rise to immature cells (D cells) which divides and differentiate locally into granular neurons (type G cells) (Fig. 1.5) (Alvarez-Buylla and Verdugo, 2002; Alvarez-Buylla *et al*., 2002; Doetsch, 2003), which may play a role in learning and memory formation.

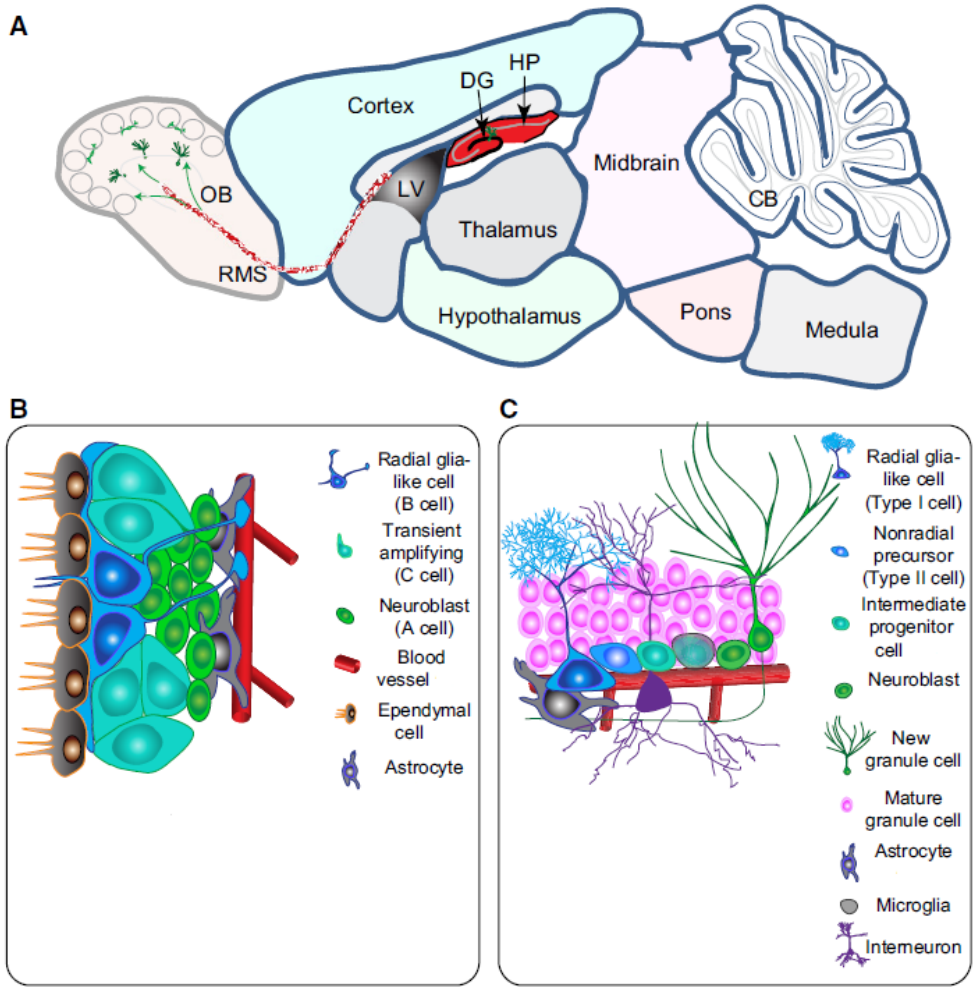

Figure 1.5. – Neurogenic regions of adult brain. A: sagittal section diagram of an adult rodent brain with the two neurogenic regions in the adult brain: dentate gyrus (**DG**) in the hippocampus (**HP**), and the lateral ventricle (**LV**) with the rostral migratory stream (**RMS**) to the olfactory bulb (**OB**). **B**: Schematic illustration of the neural stem cell niche in the subventricular zone (**SVZ**). **C**: Schematic illustration of the neural stem cell niche in the subgranular zone (**SGZ**) in the DG (adapted from Ming and Song, 2011).

Both intrinsic and extrinsic mechanisms regulate different aspects of adult neurogenesis. Among others, neurotrophins, growth factors, cytokines, and hormones are major regulators of neurogenesis in the adult brain (reviewed in Hagg, 2009). BDNF is one of the neurotrophins involved in neuroblast survival, through TrkB receptor activation (Bath *et al*., 2008). BDNF and NGF can also activate the p75 neurotrophin receptor in a sub-population of highly proliferative precursor cells, within the stem cell niche of the rat SVZ, which are responsible for neuron production in both newborn and adult animals (Young *et*

al., 2007). NGF and NT-3 were shown to enhance survival of new hippocampal neurons and to promote hippocampal neurogenesis. Glial cell-derived neurotrophic factor (GDNF) infusion into the post-ischemic rat striatum induced SVZ proliferation, recruitment of neuroblasts into the striatum and promoted new neurons survival (Kobayashi *et al.,* 2006). Similarly, basic fibroblast growth factor (FGF-2) also stimulates neurogenesis in the hippocampus, as reviewed by Hagg (2009). Moreover, de Chevigny showed that simultaneous infusion of the endogenous epidermal growth factor (EGF) receptor ligand, transforming growth factor (TGF)-alfa, with nanogg, in rat dopamine-depleted striatum originate a large number of migrating multipotent neural progenitors (de Chevigny *et al.*, 2008). One important neural cytokine (a family of neurotrophic factors) is ciliary neurotrophic factor (CNTF), which was demonstrated to play an important role in adult CNS neurogenesis, since CNTF KO mice displayed reduced neurogenesis (Yang *et al*., 2008).

Neurogenesis can also be promoted by therapeutic agents like neurotrophic factors (described in the last paragraph) and medications affecting neurotransmitters, such as antidepressants (e.g. serotonin re-uptake inhibitors), which increase neural progenitor proliferation and dendritic development and enhance the survival of newborn neurons in the adult hippocampus (reviewed in Hagg *et al.,* 2009 and Ming and Song, 2011). The neurotransmitters dopamine and glutamate play known roles in neurogenesis (Hagg, 2009, for review). Interestingly, SVZ neuroblast populations are differentially affected by ionotropic (e.g. GLU_{K5}-containing kainate receptor, by limiting neuroblast migration) and metabotropic (e.g. mGluR5 receptor, by activating SVZ proliferating cells) glutamate receptors-induced calcium levels (Platel *et al.*, 2008), supporting the notion that there are different populations of NSC and neuroblasts in the CNS (Merkle *et al*., 2007).
However, it is not always clear whether pharmacological manipulations act directly on neural precursors and newborn neurons or indirectly, through modulation of their niche.

Surprisingly, the involvement of specific apoptosis-associated molecules in mouse NSC differentiation (e.g. p53, caspases and Bcl-2 proteins) was also shown, as reviewed by Solá *et al*. (2013). Another family of proteins associated with apoptosis, calpains, is also involved in the regulation of several cellular processes, such as cell cycle, migration, autophagy and synaptic plasticity and, recently, calpains -1 and -2 were shown to participate in NSC self-renewal (e.g. calpain-1 represses glial and neural differentiation)

and NSC differentiation (e.g. calpain-2 is a potential modulator of gliogenesis) (Santos *et al*., 2012).

Caspase signaling, in particular, cause the activation of the specific nuclease caspase-activated DNase (CAD), and the caspase-3/CAD regulate cell differentiation by increasing the expression of critical regulatory genes (reviewed in Solá *et al*., 2013). Caspase determine cell fate in an apoptotic and nonapoptotic controlled manner to regulate proper cell differentiation and maturation in the developing nervous system. Some processes where caspases are involved are the innate immune response, neural regeneration, NSC fate and differentiation, and neural activation. Corroborating the role of caspases in cell differentiation, it was shown that caspase-3-deficient hematopoietic stem cells proliferate more and differentiate later (Solá *et al*., 2013, for review).

Interestingly, caspase-3 and -8 were also shown to be involved in the induction of nuclear reprogramming of iPSCs; for instance inhibition of caspase 8 completely blocked iPSC induction, while inhibition of caspase 3 only partially blocked the same process, supporting a relevant role of caspases in stem cell biology apart from cell death (Li *et al*., 2010).

1.4.1. Neurogenesis in HD

Neurogenesis in HD is a controversial subject from which opposing data has emerged. Initial studies using the transgenic R6/1 and R6/2 mice revealed a dramatic reduction in adult hippocampal neurogenesis (Lazic *et al.,* 2004; Gil *et al.,* 2004). In pre-symptomatic R6/1 mice no changes in hippocampal cell proliferation were observed, but at 20 weeks of age a significant reduction of new DG cells was detected. The number of HD mature neurons was also decreased at later stages due to reduced cell survival and differentiation (Lazic *et al*., 2004 and 2006). Interestingly, in R6/2 animals, hippocampal cell proliferation was negatively affected shortly after 2 weeks of age (before the onset of behavioral symptoms), which is in accordance with the faster disease progression observed in R6/2 line (for review see Gil-Mohapel *et al.,* 2011). A progressive decrease in cell proliferation parallels the disease course, and end-stage R6/2 mice exhibit reduced DG cell number (by about 70%), associated to a reduction in neuronal maturation and differentiation, like in R6/1 animals, along with decreased expression of polysialylated neural cell adhesion molecule (PSA-NCAM). However, other authors did not observe differences in DG cell proliferation in both R6/1 (Grote *et al.*, 2005) and R6/2 (Jin *et al.,*

2005; Phillips *et al.,* 2005) mice, which might be related to the use of different mouse colonies or proliferation assays (reviewed in Gil-Mohapel *et al.,* 2011). Similar results to those obtained in R6 lines were recently obtained with the FL HD transgenic YAC128 mouse, since it was demonstrated that adult hippocampal neurogenesis was selectively affected in young and particularly in old mice, along with reduced number of mature new neurons (Simpson *et al.,* 2011). In the transgenic HD rat model a significant and progressive decrease in adult hippocampal cell proliferation was also observed (Kandasamy *et al.,* 2010). Thus, data collected from different HD animal models seem to converge into evidences for a progressive decline in hippocampal neurogenesis, constituting a novel neuropathological feature observed in early HD stages.

In contrast to the neurogenic deficits observed in the SGZ, SVZ proliferation and differentiation was relatively unchanged in these mice models (for review, see Gil-Mohapel *et al.*, 2011). Neurospheres derived from the SVZ of adult R6/2 and WT showed the same proliferative capacity (Phillips *et al.,* 2005). Nevertheless, migration of SVZ-derived neuroblasts through RMS was diminished in R6/2 mice (Gil *et al.*, 2005; Moraes *et al*., 2009). Interestingly, increased SVZ proliferating progenitor cells was described in HD *post-mortem* human brain, which might occur in response to the greater number of degenerating neurons that is present in the adjacent striatum (Curtis *et al*., 2003, 2005). Moreover, *in vitro* studies showed that neural stem precursor cells isolated from the SVZ of HD KI mice showed increased neural progenitors and neurogenesis (Lorincz and Zawistowski, 2009). Conversely, transgenic R6/2 SVZ-derived neural stem cells have increased self-renewal capacity when compared to WT cells, but no increase in the formation of new neurons (Batista *et al.,* 2006). Indeed, these data are contradictory to Phillips *et al.* (2005) probably due to differences in technical procedures, given that, at the age of 8 weeks, both authors obtained similar results. Interestingly, Batista and colleagues (2006) studied neurosphere proliferative capacity at 4.5, 8 and 12 weeks of age (the study conducted by Philipps *et al*. (2005) only evaluated adult neurosphere proliferation at 8 weeks of age), and reported that the increase in the number of R6/2 neurospheres observed at 8 weeks (when R6/2 mice display behavioral deficits) progresses with age (at 12 weeks), whereas at 4.5 weeks the number of WT and R6/2 neurospheres was unchanged.

Nevertheless, the differences observed between KI and transgenic mice-derived SVZ neurospheres might be related to differences inherent to these genetic models. In addition, excitotoxic-induced SVZ neurogenesis was observed after QA lesion in a rat

model of HD (Tattersfield *et al.,* 2004). Together, these results suggest that the increase in SVZ neurogenesis might depend on the extent of neuronal loss. In fact, the absence of cell death in the R6 striatum may account for by the absence of increased SVZ proliferation in these mice (Gil-Mohapel *et al.*, 2011, for review). Because HD striatal cell loss is reproduced in late-stage YAC128 mice (Slow *et al*., 2003), one would expect to observe an increase in SVZ proliferation; however, no significant differences were detected (Simpson *et al.,* 2011).

1.5. OBJECTIVES

HD is a complex neurodegenerative disorder involving several pathological pathways reflecting multiple symptoms and several mechanisms underlying the more selective striatal degeneration. In this study we focused in two of these pathological mechanisms, the deficits in BDNF and mitochondrial dysfunction, which have been previously documented to occur in several HD models and HD-affected human cells (e.g. Zuccato *et al*, 2001; Oliveira *et al.*, 2006; Ferreira *et al.*, 2010). Therefore, the main objective of this work was to investigate the role of BDNF and BDNF-mediated TrkB receptor activation and the involvement of modified mitochondrial function in HD mice and human peripheral samples, by determining their role in neuronal differentiation and HD pathogenesis.

Specifically, we investigated:

- Whether BDNF and TrkB receptor-overexpression could mediate the activation of survival pathways and ameliorate striatal cell death. For that purpose, we used a retroviral-based strategy to induce BDNF and TrkB overexpression in a striatal cell line, expressing endogenous wild-type and full-length mutant huntingtin, with 7 and 111 glutamines, respectively (*Chapter 2*);

- The role of BDNF and the involvement of mitochondrial function in neuronal differentiation of SVZ-derived cells isolated from YAC128 transgenic mice, expressing full-length human mutant huntingtin, at 6 and 10 months of age (*Chapter 3*);

- Differential deregulation of mitochondrial respiratory chain complexes I-IV in human peripheral blood platelets mitochondria obtained from pre-symptomatic and symptomatic HD carriers *versus* age-matched control individuals (*Chapter 4*).

CHAPTER 2

BDNF AND TRKB RECEPTOR OVEREXPRESSION RESCUE CELL DEATH IN HUNTINGTON'S DISEASE MOUSE STRIATAL CELLS

Chapter based on the following manuscript:

Ana Silva, Luana Naia, Alejandro Dominguez, Márcio Ribeiro, Joana Rodrigues, Otília V. Vieira, Volkmar Lessmann and A. Cristina Rego (2013). BDNF and TrkB receptor overexpression rescue cell death in Huntington's disease mouse striatal cells (*Manuscript submitted to* Journal of Neurochemistry)

2.1 Abstract

Several cellular mechanisms have been proposed to explain Huntington's disease (HD) pathogenesis, largely affecting GABAergic striatal neurons. Brain-derived neurotrophic factor (BDNF) is one important neurotrophin implicated in the survival of striatal neurons. In this work we analysed how transduced preproBDNF and/or full-length (FL)-TrkB receptors mediate the activation of AKT and ERK pathways and rescue cell death in HD mice striatal cells. We found that mutant cells express higher levels of BDNF than wild-type (WT) cells, although both BDNF-overexpressing cells release similar amounts of pro- and mature BDNF. Decreased AKT activation in HD cells was rescued following BDNF or TrkB overexpression, in co-cultures of BDNF/TrkB- or in TrkB-overexpressing cells exposed to recombinant BDNF. Activated ERK was also enhanced in HD BDNF/TrkB co-cultures and in both TrkB overexpressing-cells and in control/untransduced cells stimulated with BDNF. Under basal conditions, caspase-3 activation in HD cells was significantly decreased in both BDNF and TrkB overexpressing cells and in TrkB overexpressed cells exposed to recombinant BDNF. Protection against staurosporine-induced cell death in HD cells, evaluated by caspase-3-like activation and DNA condensation/fragmentation, was observed in TrkB overexpressing cells exposed to BDNF. These results highlight the importance of BDNF-induced activation of AKT mediated by FL-TrkB receptor in heightening the survival of HD striatal cells.

2.2 Introduction

HD is an autosomal, progressive and fatal neurodegenerative disorder caused by an unstable expansion of CAG repeats in the *HD* gene, coding for mutant huntingtin (mHtt), with an abnormal polyglutamine (polyQ) tract at its N-terminus (Huntington's Disease Collaborative Research Group, 1993). Symptoms usually occur in mid-life and include involuntary movements and psychiatric disturbances; neuropathogically, the main HD hallmark is the selective loss of GABAergic medium spiny neurons (MSNs) in the striatum. Death of the patients occurs 15-20 years after the disease onset (Gil and Rego, 2008, for review). WT Htt is ubiquitously expressed and seems to play an important role in cell survival (Zuccato *et al*., 2003, Gil and Rego, 2008, for review). The mutation has been suggested to alter WT Htt function and to promote a gain of function of FL-mHtt and/or of its short N-terminal fragments (Wellington *et al*., 2002; Li and Li, 2004). Nevertheless, the mechanisms underlying neuronal dysfunction induced by polyQ expansion are still not entirely understood.

Under normal conditions, MSNs receive input of BDNF from the cortex (Canals *et al*., 2001) and thus BDNF mRNA and protein levels were found in HD human cortex (Zuccato *et al.*, 2001). On the other hand, low levels of BDNF protein were demonstrated in the striatum (caudate and putamen) of HD patients (Ferrer *et al*., 2000), as well as in the striatum and cortex of HD mice (Zuccato *et al.*, 2001; Ginés *et al*, 2003a). Interestingly, cultured rat cortical and striatal neurons demonstrated comparable levels of BDNF/TrkB protein and BDNF mRNA (Ma *et al*., 2012). Importantly, Zuccato and collaborators previously demonstrated that mHtt impairs transcription of BDNF in cultured central nervous system cells overexpressing FL-mHtt, in the cerebral cortex of HD transgenic mice and in cortical tissue from HD patients (e.g. Zuccato *et al.*, 2001, 2003). Moreover, BDNF axonal transport was further shown to be reduced in HD neuronal cells derived from knock-in (KI) mice (Gauthier *et al*., 2004). Decreased TrkB mRNA and protein levels were also reported in HD striatal cells and human patients (Ginés *et al*., 2006; Zuccato *et al*., 2008; Ginés *et al*., 2010), largely suggesting that mHtt interferes with BDNF-TrkB-mediated signaling pathways.

BDNF-induced signaling is mediated primarily by its binding to the high affinity receptor TrkB. Activation of TrkB initiates three major intracellular signaling

cascades: i) the well-characterized mitogen activated protein kinase (MAPK)/extracellular signal-regulated kinases (ERK) cascade; ii) activation of a phosphatidylinositol-3-kinase pathway involving AKT1, and iii) TrkB mediated activation of phospholipase C-gamma (PLCγ) which produces inositol triphosphate (IP_3) and diacylglycerol (DAG) and increases intracellular free calcium (e.g. Chao *et al.,* 2006*;* Reichardt, 2006; Murray and Holmes, 2011, for review). MAPK/ERK is essential for neurogenesis, neurite outgrowth and promotes cell survival by inducing prosurvival genes and also by inhibiting proapoptotic proteins. On the other hand, apoptosis is also suppressed via phosphatidylinositol 3-kinase (PI3K). PI3K activates AKT which sequesters pro-apoptotic proteins in the cytoplasm, thus impairing their binding to transcriptional targets in the nucleus (Murray and Holmes, 2011, for review). AKT is a serine-threonine pro-survival kinase in neurons, acting through the phosphorylation of several substrates (Franke *et al.,* 2003), including elements of cell death machinery and transcription factors of the forkhead family. The forkhead box transcription factors classe O (FoxO) family is negatively regulated by the PI3K–AKT signaling pathway in response to growth factors and neurotrophic factors (Calnan and Brunet, 2008), thus suppressing apoptosis, while mammalian target of rapamycin (mTOR) activation inhibits autophagy (Laplante and Sabatini, 2009). BDNF-induced TrkB activation ultimately leads to neuronal differentiation, survival, migration and maturation of striatal neurons (Perez-Navarro *et al*., 2000; Petridis and El Maarouf, 2011). BDNF-mediated signaling is also involved in neuronal synaptic transmission and in preventing MSNs apoptosis, protecting GABAergic neurons against several insults (Petersén *et al*., 2001; Bath and Lee, 2010; Murray and Holmes, 2011, for review). Our lab previously showed the protective role of BDNF against apoptosis and in regulating transcription in cortical neurons exposed to 3-nitropropionic acid, a complex II irreversible inhibitor (Almeida *et al*., 2009, 2010).

Taking into account the evidence of altered neurotrophic support involved in HD pathogenesis (Zuccato *et al.*, 2010, for review) and the importance of testing novel tools that could rescue the HD phenotype in striatal cells, in the present study we studied the influence of BDNF and TrkB receptor overexpression on the activation of AKT and ERK signaling pathways and on cell death parameters in striatal cells derived from KI HD mice transduced with retroviral vectors encoding for

preproBDNF and FL-TrkB receptors. Data highlight the importance of heightening the levels of BDNF and TrkB receptors in striatal cell survival.

2.3 Material and Methods

2.3.1. Reagents

Penicillin-streptomycin, Geneticin, trypsin 5% EDTA and Hoechst 33342 were purchased from GIBCO (Invitrogen Life Technologies, Paisley, UK). Foetal calf serum (FCS) was obtained from BioWhittaker Molecular Applications (Rockland, MD, USA). Efficiency DH5α Competent Cells and propidium iodide were from Invitrogen (Invitrogen Life Technologies, Paisley, UK). Pfu DNA polymerase enzyme, dNTPs and LigaFast Rapid DNA Ligation System were purchased from Promega (Madison, WI, USA). QIAquick PCR purification Kit, QIAquick Gel extraction Kit and Qiagen Plasmid Maxi Kit were obtained from Qiagen (Hilden, Germany). Fugene 6 Transfection Reagent was from Roche (Roche Diagnostics, Mannheim, Germany). Hexadimethrine bromide (polybrene), puromycin, staurosporin, bromophenol blue, phenylmethylsufonyl fluoride (PMSF), dithiothreitol (DTT), protease cocktail inhibitor (chymostatin, leupeptin, antipain, pepstatin A), mouse anti-α-tubulin were purchased from Sigma Chemical Co. (St. Louis, MO, USA). BIORAD Protein Reagent was from Biorad (BioRad, Hercules, CA, USA). N-acetyl-Asp-Glu-Val-Asp-AFC (Ac-DEVD-AFC) was obtained from Calbiochem (Darmstadt, Germany). Recombinant human brain-derived neurotrophic factor (rhBDNF) was purchased from Peprotech (Rocky Hill, NJ, USA). Mouse anti-huntingtin (Htt, MAB2166) and mouse anti-polyglutamine (1C2) were obtained from Millipore (EMD Millipore Corporation, Billerica, MA, USA). Rabbit anti-BDNF and rabbit anti-TrkB were from Santa Cruz Biotechnology Inc. (Santa Cruz, CA, EUA). Rabbit anti-AKT, mouse anti-phospho (-P)-AKT, rabbit anti-p44/42 MAPK and anti-P-p44/42 MAPK (ERK 1/2 and P-ERK 1/2, respectively), were from Cell Signaling (Beverly, MA, USA). Polyvinylidene difluoride (PVDF) membrane, enhanced chemifluorescence reagent (ECF) and alkaline phosphatase-linked anti-rabbit and anti-mouse secondary antibodies were purchased from Amersham Biosciences (Buckinghamshire, UK).

2.3.2. Striatal neuronal cell lines

Immortalized wild-type ST*Hdh*Q7 (clone 2aA5) and homozygous mutant ST*Hdh*Q111 (clone 109-1A) striatal neural progenitor cells, expressing endogenous WT and FL-mHtt, with 7 and 111 glutamines, respectively, were generated from WT *Hdh*Q7 and homozygous *Hdh*Q111 KI littermate embryos (Trettel *et al*., 2000) and kindly donated by Dr. Marcy E. MacDonald (Department of Neurology, Massachusetts General Hospital, Boston, USA). Cells were grown at 33ºC in Dulbecco's modified Eagle's medium (DMEM) supplemented with 10% FCS, 10 mM HEPES, 12 mM $NaHCO_3$, 1% penicillin/streptomycin and 400 mg/ml G418. Whenever necessary (~70% confluence) cells were harvested by trypsinization and subcultured.

2.3.3. Plasmids and virus production

Plasmids. Original preproBDNF tagged to enhanced Green fluorescent protein (eGFP) inserted in the Clontech pEGFP-N1 vector has been described previously (by Haubensak *et al.*, 1998) and was used to generate BDNF-mCherry viral vectors. TrkB-eGFP, also inserted in pEGFP-NI vector (Clontech), was previously described (Watson *et al*., 1999), and kindly provided by Dr. Rosalind Segal (DANA-FARBER Cancer Institute, Boston, MA, USA). The plasmid with the red fluorophore mCherry coding sequence was kindly provided by Dr. Roger Y. Tsien (Howard Hughes Medical Institute Laboratoires, Univ. California, San Diego, USA). The retroviral (RV) backbone pBABE-PURO and pVSV-G were kindly made available by Dr. Otília V. Vieira (CNC, University of Coimbra).

To subclone the genes of interest into pBABE-puro RV vector (under the SV40 promoter with a resistant gene to puromycin), restriction sites for EcoRI and SalI were inserted in preproBDNF-eGFP (EcoRI: 5'-TTTGAATTCGAGTGATGACCATC-3'; SalI: 5'-TTTGTCGACTTACTTGTACAGCTCGTCC-3') and TrkB-eGFP (EcoRI: 5'-TTTGAATTCATGTCGCCCTGGCCGAG-3'; SalI described primer) with Pfu DNA polymerase, through the PCR technique. PCR product was purified using QIAquick PCR purification Kit and digested with EcoRI and SalI enzymes. preproBDNF-eGFP and TrkB-eGFP purified genes were thus subcloned into the RV vector pBABE-PURO previously digested with EcoRI and SalI and purified with QIAquick Gel extraction kit. Subcloning was performed using LigaFast Rapid DNA Ligation System and the product was transformed with Efficiency DH5α Competent bacteria

cells. DNA from positive colonies was amplified by Qiagen Plasmid Maxi Kit. All experimental procedures based-kits were done according to manufacturer's instructions.

To make pBABE-preproBDNF-mCherry, eGFP was excised from pBABE-preproBDNF-eGFP vector with AgeI and SalI enzymes and the AgeI and SalI restriction sites were inserted in mCherry plasmid (AgeI: 5'-TTTACCGGTAATGGTGAGCAAGGGCG-3'; SalI: 5'-TTTGTCGACCTACTTGTACAGCTCGTCC-3').

To make pBABE-eGFP, BamHI (5'-TTTggatccatggtgagcaagggcgag-3') and SalI (previously described primer) restriction sites were inserted in the original preproBDNF-eGFP vector to cut eGFP and further subcloned it into pBABE-PURO RV vector.

Retroviruses production. Retroviruses were produced using Phoenix-gp packaging cells. Phoenix cells are based on Moloney Murine Leukemia Virus and allow gene delivery to almost all dividing mammalian cell types. This system contains the *gag* (group-specific antigen, which encodes for core and structural proteins of the virus) and the *pol* (polymerase, which encodes for reverse transcriptase, protease and integrase) genes and allows for pseudotyping with alternative envelope proteins. We used as an envelope protein VSV-G (Vesicular Stomatitis Virus, glycoprotein G) which helps viruses enter host cells (http://www.stanford.edu/group/nolan/retroviral_systems/retsys.html).

Human Phoenix gag-pol packaging cell line (www.stanford.edu/group/nolan/retroviral_systems/phx.html; obtained from the American Type Culture Collection with authorization by Garry Nolan, School of Medicine, Stanford University, Stanford, CA) was kept in high-glucose DMEM (supplemented with 10% FBS, 44 mM $NaHCO_3$, 1 mM sodium pyruvate and 1% penicillin/streptomycin). Nearly confluent cells (~80%) in 10-cm dishes were transfected in Optimem serum and antibiotic-free medium with 2.5 µg DNA (ratio 6:1) and pVSV-G (0.25 µg), using Fugene as the transfection reagent, in accordance to manufacturer's protocol. Twenty-four hours post-transfection, the medium was changed to low-glucose DMEM (DMEM-LG without glucose, supplemented with 5.5 mM glucose, 4 mM L-glutamine, 10% FBS, 44 mM $NaHCO_3$, and 1% penicillin/streptomycin) and placed at 32 °C. Supernatant were collected every 24 h for up to five days and filtered through a 0.45-µm syringe filter. The

same batches of viruses were then concentrated by ultracentrifugation (50000 xg for 2 h), resuspended in DMEM-LG plus 10 mM HEPES, frozen in liquid nitrogen and kept at -80 ºC until use.

2.3.4. Cell transduction

ST*Hdh*Q7 and ST*Hdh*Q111 striatal cells were plated in twelve-well plates (40000 per well) and transduced with retrovirus (50 µL) encoded for preproBDNF-mCherry, TrkB-eGFP and eGFP (infection control). Ultraconcentrated viruses were delivered to cells simultaneously with polybrene (hexadimethrine bromide), a cationic polymer which neutralizes charge repulsion between virions and sialic acid on cell surface, thus increasing the efficiency of cell infection with the retrovirus (Davis *et al*., 2004). Polybrene (4 µg/mL) was added and cells were allowed to grow and passed to six-well plates. Cells were selected with puromycin (10 µg/mL) until nearly 100% of cells were positive for eGFP or mCherry and then experiments were performed. Some data was also compared to untransduced/control (CTR) cells.

2.3.5. Incubation with staurosporine and recombinant BDNF

Puromycin-selected cells were plated in 10 cm petri dishes, in uncoated glass coverslips in a twelve-well plate, or in 96-well plate, for western blotting, cell death or caspase-3-like activity analysis, respectively. Nearly confluent cells (~80%) were then incubated with staurosporine (STS, 10 nM), an apoptotic inducer. Control and TrkB-eGFP-expressing cells were also treated with rhBDNF (20 ng/mL) 15 min before and during STS insult and experiments were performed 24 h later. For co-cultures, preproBDNF-mCherry and TrkB-eGFP-expressing cells (1:1) were plated simultaneously, maintained for up to 24 h in culture and treated as described above.

2.3.6. Cell extracts and Western blotting analysis

Cells were washed in PBS (Phosphate Buffered Saline, pH 7.4) and lysed in iced-cold RIPA buffer (150 mM NaCl, 50 mM Tris-HCl, 5 mM EGTA, 1% Triton X-100; 0.5% deoxycholate (DOC) and 0.1% sodium dodecyl sulfate (SDS), pH 7.5) supplemented with 1 mM PMSF, 1 mM DTT, phosphatase inhibitors (1 mM sodium orthovanadate, 25 mM NaF) and 1:1000 protease cocktail inhibitor (1 µg/ml chymostatin, 1 µg/ml leupeptin, 1 µg/ml antipain, 5 µg/ml pepstatin A). After 30 min in RIPA buffer, cells were scraped, collected and centrifuged (1000 *xg*) for 10 min,

at 4ºC, and the pellet was discarded. Protein concentration was determined by Biorad Protein Assay. Equivalent amounts of protein were denaturated with 6x concentrated sample buffer (0.35 M Tris, 36% glycerol, 10.28% SDS, 0.6 M DTT, 0.012% bromophenol blue), at 95ºC for 5 min, separated on a 10% SDS-polyacrylamide gel (SDS-PAGE) and electroblotted onto PVDF membrane. Membranes were further blocked in 5% skim milk in Tris buffer saline (25 mM Tris-HCl, pH 7.6, 150 mM NaCl) plus 0.1% Tween (TBS-T), for 1 h at room temperature (RT). Incubations with primary antibodies (in TBS-T/5% milk) were performed overnight, at 4ºC: mouse anti-huntingtin (MAB2166) 1:250, rabbit anti-BDNF 1:500, mouse anti-polyglutamine (1C2), rabbit anti-TrkB, rabbit anti-AKT, mouse anti-P-AKT (ser473), rabbit anti-ERK1/2 and anti-P-ERK1/2 (Thr202/Tyr204 of ERK1), all at 1:1000, and mouse anti-tubulin 1:10000, used as a loading control. Membranes were washed with TBS-T and incubated for 1 h at RT with alkaline phosphatase-linked secondary antibodies (anti-rabbit or anti-mouse IgG, 1:20,000, in TBS-T/5% milk). After washing in TBS-T, proteins in the membranes were incubated with ECF (5 min, RT). Immunoreactive bands were visualized by alkaline phosphatase activity that catalyses the conversion of ECF substrate to a highly fluorescent product reagent. This product strongly fluoresces at 540–560 nm when the blots are illuminated with UV light (maximum excitation at 430 nm), by using a BioRad Versa Doc 3000 Imaging System (BioRad, Hercules, CA, USA).

For determining BDNF release, 24 h after plating cell culture medium (1 mL) was collected from nearly confluent cells and centrifuged at 1000 x*g* for 10 min, at 4ºC. After denaturation with sample buffer (6x concentrated), at 95ºC for 5 min, equivalent amounts (v) were applied in the gel and Western blotting was performed as previously described.

2.3.7. Caspase protease activity assay

For measurement of caspase 3-like activity, the culture media was removed and cells were washed two times in PBS. Lysis buffer (25 mM HEPES, 2 mM $MgCl_2.6H_2O$, 1 mM EDTA, 1 mM EGTA, pH 7.5) supplemented with 2 mM DTT, 100 µM PMSF, 1:1000 protease inhibitor cocktail (chymostatin, pepstatin A, leupeptin, and antipain, 1 mg/ml) and 0.04% Triton X-100 was added to cells, for 30 min, at 4ºC. Cells were then scraped and part of the cellular lysate was used to determine protein content (BIORAD Protein Assay). CHAPS buffer, containing 25 mM HEPES,

10% (m/v) sucrose and 0.1% (m/v) 3-((3-cholamidopropyl) dimethylammonio)-1-propane- sulfonate) (CHAPS), at pH 7.5, supplemented with 2 mM DTT and 15 µM of fluorimetric substrate Ac-DEVD-AFC, were further added to wells. Immediately after, fluorescence was read for 1 h at 37ºC (excitation: 400 nm; emission: 505 nm) in a fluorometer microplate reader (Spectramax Gemini, Molecular Devices, Sunnyvale, CA, USA). Upon reading, the amount of protein of each sample was determined. The values obtained are expressed as relative fluorescence units (RFU) per minute per milligram protein for each condition.

2.3.8. Cell death

Cells were washed with microscopy buffer (120 mM NaCl, 3.5 mM KCl, 0.4 mM KH_2PO_4, 20 mM HEPES, 5 mM $NaHCO_3$, 1.2 mM Na_2SO_4 and 15 mM glucose) supplemented with 1.2 mM $MgCl_2$ and 1.3 mM $CaCl_2$, pH 7.4. Cells were further incubated with Hoechst 33342 (2 µg/mL, a blue permeable fluorescent dye, which binds to DNA, to determine fragmented/condensed nucleus) and propidium iodide (PI) (4 µg/mL, a non-membrane permeable red fluorescent dye that binds to DNA, for necrotic cell evaluation), during 8 and 3 min, respectively, in the dark. Live cells were analyzed by fluorescence microscopy. Images from five different fields in each coverslip were acquired in a fluorescence microscope Axioskop 2 Plus (Zeiss, Jena, Germany) and cells were counted using ImageJ Launcher (version 1.44p, NIH). Fragmented/condensed nucleus labeled with Hoechst 33342 (apoptotic-like cells) and cell nucleus labeled with PI (necrotic cells) were determined as a percentage of total cells (stained with Hoechst).

2.3.9. Statistical analysis

Results are presented as the mean ± SEM of the indicated number of experiments. Data were analyzed with two-way ANOVA with Bonferroni post-test using GraphPad Prism version 5.0 for Windows, GraphPad Software, San Diego California USA (www.graphpad.com). $P < 0.05$ was considered significant.

2.4. Results

The expression of Htt in control WT and mutant striatal cell lines was first analysed. As observed in Fig. 2.1A, a band corresponding to mHtt (polyQ detection using the 1C2 antibody) was evident in mutant homozygous cells only (upper panel), which matched the higher molecular weight band detected with the antibody against Htt (MAB2166), observed in the middle panel.

BDNF and TrkB receptor-mediated signaling were previously demonstrated to be reduced in HD (e.g. Zuccato *et al.,* 2001; Ginés *et al.,* 2006, 2010). In the present study, we genetically transformed WT and mutant mice striatal cell lines in which BDNF or TrkB receptor expression levels is not significantly affected (as described below), to overexpress preproBDNF-mCherry and TrkB-eGFP. These cells were transduced with RV vectors (Fig. 2.1B), in order to examine the role of BDNF or TrkB overexpression in rescuing HD striatal cell death. Although striatal cells do not synthetize high amounts of BDNF, cortical BDNF production seems to depend on striatal target integrity (Zuccato and Cattaneo, 2007, for review). Thus, a mutant striatal cell model overexpressing BDNF may help to understand how the effects of the mutation can be alleviated by released BDNF in an autocrine and paracrine manner. After transduction, the cells were selected with puromycin, allowing the establishment of preproBDNF-mCherry, TrkB-eGFP and eGFP (used as infection control) overexpressing cell lines. Stable infection was tightly checked through the analysis of mCherry and eGFP fluorescence in both WT and mutant striatal cells (Fig. 2.1C).

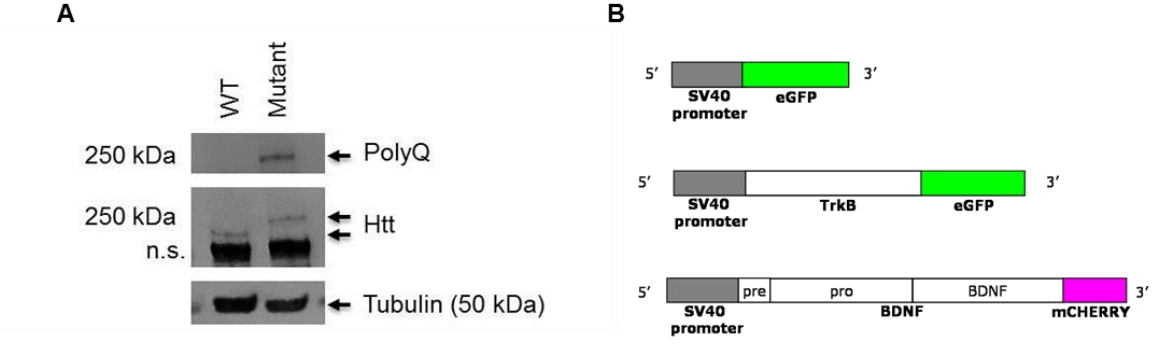

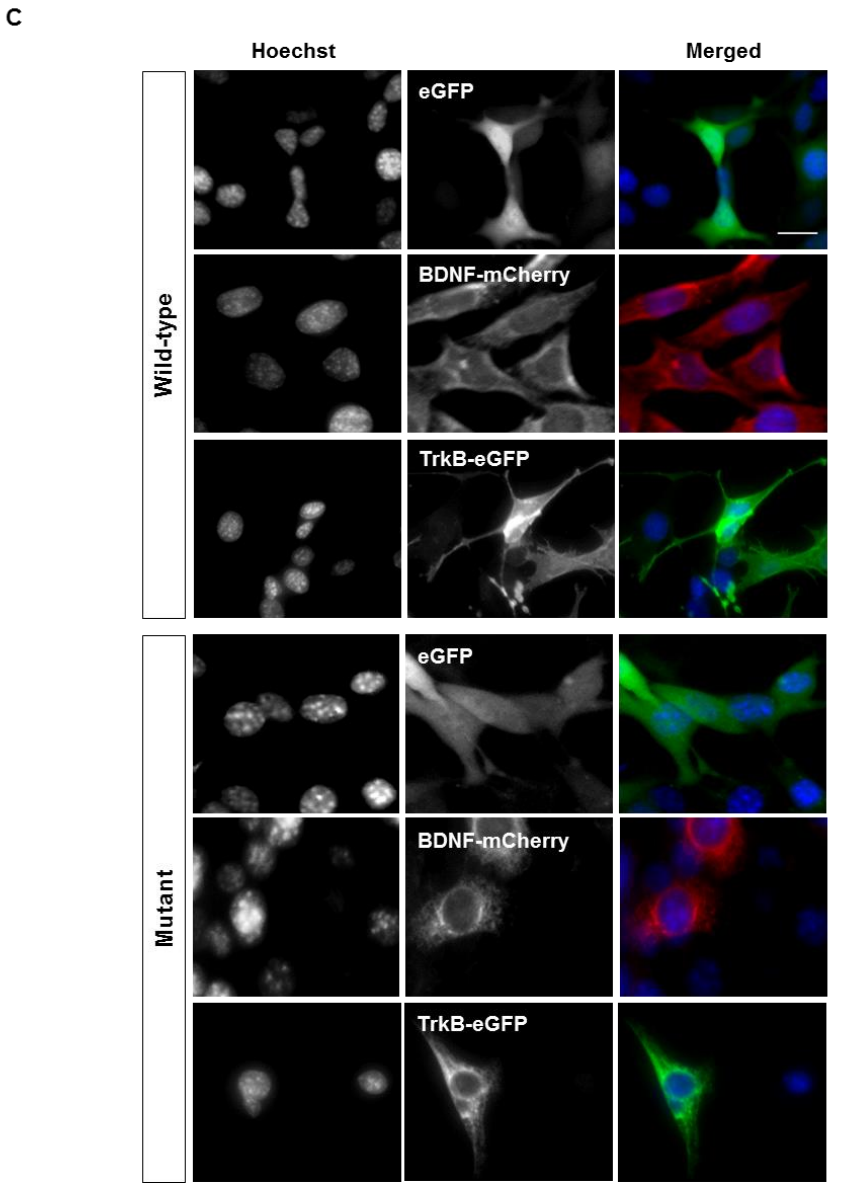

Figure 2.1 – Establishment of transduced wild-type and mutant striatal cell lines with BDNF or TrkB retrovirus. (**A**) Western blotting analysis of wild-type (WT) and mutant huntingtin (Htt), the latter retaining polyglutamine (polyQ) expansion. (**B**) Representation of the structure of the retroviral vectors (RV): eGFP (control of infection), TrkB-eGFP and preproBDNF-mCherry, which were subcloned in the RV backbone pBABE-PURO, under the SV40 promoter. (**C**) Representative fluorescence images of WT and mutant striatal cells transduced with eGFP, TrkB-eGFP and preproBDNF-mCherry. The cells were selected with puromycin (10 µg/mL) after infection. Scale bar = 20 µm. n.s. – non specific.

We next examined BDNF and TrkB receptor protein levels by Western blotting in WT and mutant control and transduced cell lines (Fig. 2.2). BDNF is synthesized as

a 32 kDa precursor and this proneurotrophin is then processed in the *trans*-Golgi or in secretory vesicles into mature BDNF with 14 kDa (Mowla *et al*., 2001; Lessmann and Brigadski, 2009, for review). The unprocessed protein can also be released to the extracellular medium and further activate TrkB receptors (Mowla *et al*., 2001) or other intracellular pathways, including apoptotic cell death cascades through activation of p75 receptors (e.g. Teng *et al*., 2005). BDNF intermediate form of 28 kDa is also a product of proBDNF cleavage, but it seems to be generated through a distinct processing pathway; indeed, its role has not been defined yet (Mowla *et al*., 2001). In the present study, both 28 kDa and pro- (32 kDa) BDNF were considered as proBDNF. According to Fig. 2.2C, CTR (untransduced) mutant cells express slightly higher levels of proBDNF than WT cells although, both WT and mutant cells exhibited similar but very low levels of mature BDNF. Importantly, BDNF-mCherry transduced cells produced higher levels of BDNF species (pro- and mature BDNF), compared to CTR cells, particularly the mature form (Fig. 2.2A and B). Taking into account the increase in mature protein in mutant cell extracts, we further verified the BDNF accumulated in the extracellular medium (24 h culture medium from nearly confluent cell culture) in mutant *versus* WT cells. Interestingly, both BDNF-overexpressing WT and mutant cells released similar amounts of BDNF and pro-BDNF to the medium (Fig. 2.2D, E).

Ginés and co-workers (2006, 2010) previously observed a marked reduction in FL-TrkB receptor mRNA and protein (total and cell surface) levels in HD striatal cell lines. In our study, we also detected slight differences in the levels of endogenous FL-TrkB receptors between CTR WT and mutant cells (Fig. 2.2G). We then evaluated TrkB receptor expression levels in TrkB-eGFP overexpressing cells. Both WT and mutant infected cells similarly produced more FL-TrkB receptor, compared to endogenous levels observed in CTR cells (Fig. 2.2F). In contrast, the levels of truncated (T)- receptor were barely unaffected in TrkB-eGFP overexpressing cells transduced with a RV vector encoding the FL-TrkB receptor.

Notably, the infection procedure did not affect the endogenous expression levels of either BDNF or TrkB, since no differences were observed between CTR and eGFP-expressing cells (Fig. 2.2A, D, F).

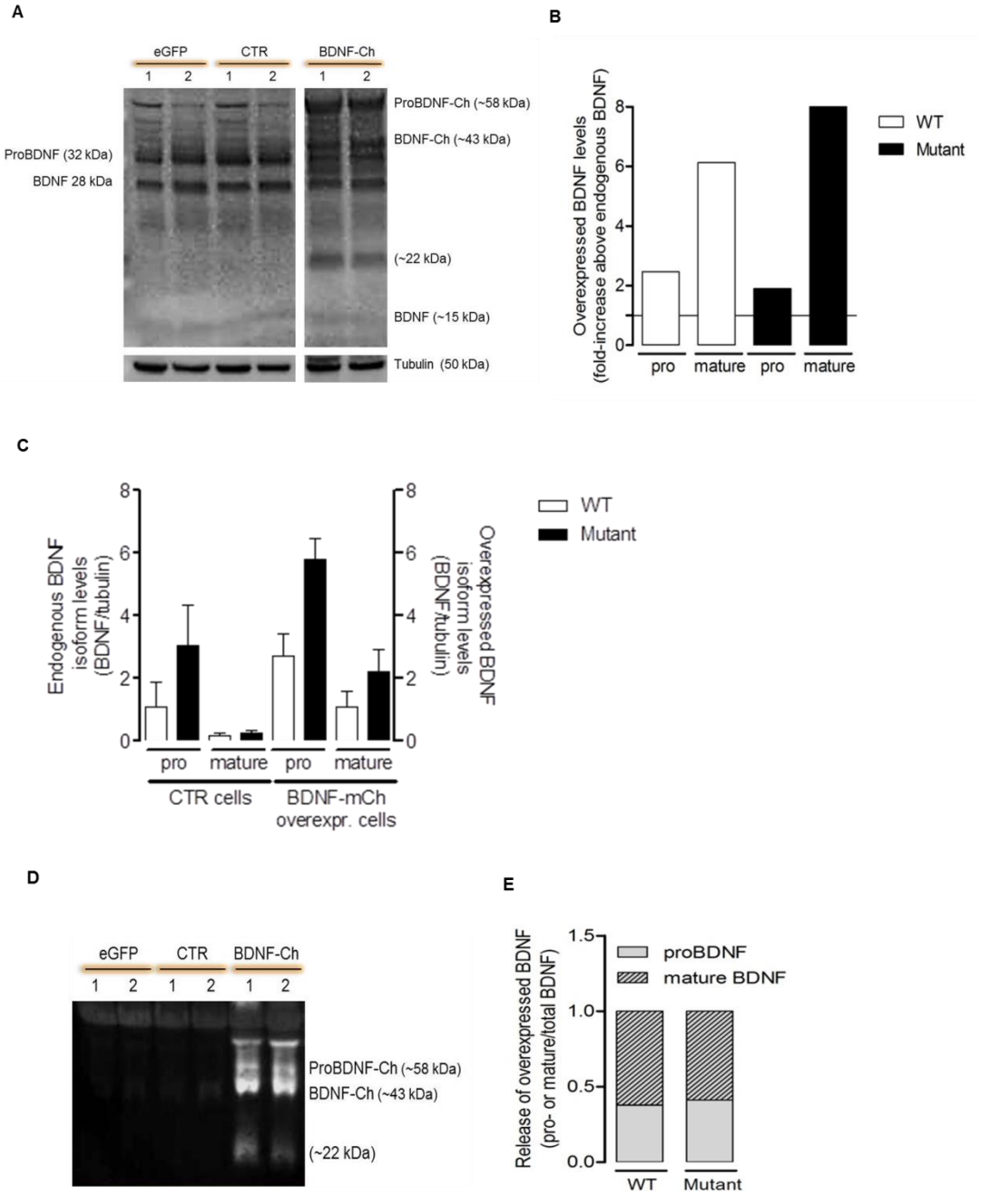
A
eGFP
CTR
BDNF-Ch
1 2 1 2 1 2
ProBDNF (32 kDa)
BDNF 28 kDa
ProBDNF-Ch (~58 kDa)
BDNF-Ch (~43 kDa)
(~22 kDa)
BDNF (~15 kDa)
Tubulin (50 kDa)
B
Overexpressed BDNF levels
(fold-increase above endogenous BDNF)
WT
Mutant
pro
mature
pro
mature
C
Endogenous BDNF
isoform levels
(BDNF/tubulin)
Overexpressed BDNF
isoform levels
(BDNF/tubulin)
WT
Mutant
pro
mature
pro
mature
CTR cells
BDNF-mCh
overexpr. cells
D
eGFP
CTR
BDNF-Ch
1 2 1 2 1 2
ProBDNF-Ch (~58 kDa)
BDNF-Ch (~43 kDa)
(~22 kDa)
E
Release of overexpressed BDNF
(pro- or mature/total BDNF)
proBDNF
mature BDNF
WT
Mutant

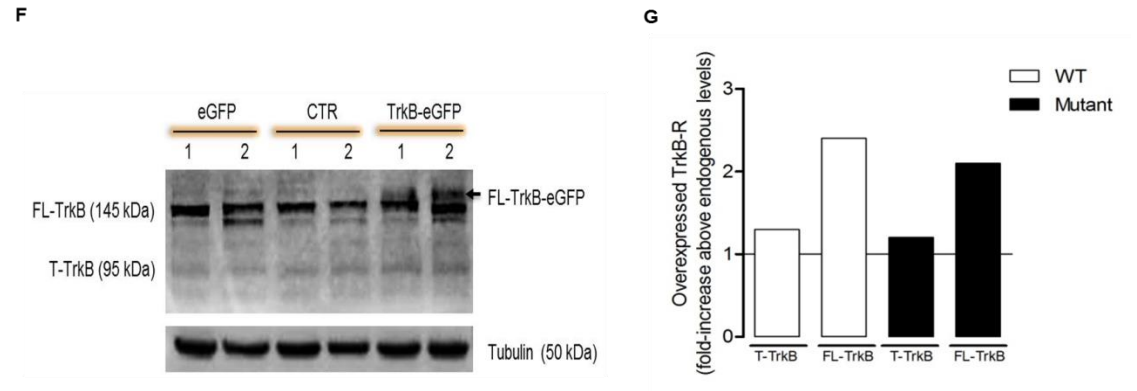

Figure 2.2 – BDNF and TrkB receptor protein levels in transduced wild-type and mutant striatal cell lines. (**A**-**E**) Protein levels of intracellular and extracellular levels of pro- and mature BDNF forms. (**A, D**) Representative Western blots showing pro- (double band of 58 kDa, corresponding to unprocessed BDNF-mCh) and mature BDNF-mCh (corresponding to 43 kDa band) were detected in transduced wild-type and mutant cell extracts (**A**) and in extracellular media (**D**). Pro- and mature BDNF protein levels expressed by wild-type (WT) and HD mutant BDNF-overexpressing cells were calculated as fold-increase above endogenous protein levels, detected in CTR cells (**B**). In **C**, endogenous levels of pro- and mature BDNF were evaluated by Western blotting in control/untransduced (CTR)- and preproBDNF-mCherry (mCh)-overexpressing cells. In **E**, extracellular levels of pro- and mature BDNF were determined and calculated relatively to total BDNF. (**F**-**G**) TrkB receptor protein levels. In **F**, representative Western blot of data depicted in **G**. Full length (FL-) and truncated (T-) TrkB receptor protein levels produced by WT and mutant TrkB-eGFP overexpressing cells were calculated as fold-increase relatively to CTR-untransduced cells (**G**). Data in graphs are the mean ± S.E.M. of 3-5 independent experiments. 1 – WT cells; 2 – HD mutant cells.

Next, we evaluated the activation of AKT (Ser473) and ERK (Thr202/Tyr204 of ERK1) signaling pathways in CTR and transduced striatal cell lines (Fig. 2.3A, B), and after exposure of CTR and TrkB cells to rhBDNF, for 24 h. We found no significant differences in the activation of AKT or ERK signaling pathways in CTR *versus* eGFP expressing cells (not shown); therefore in these experiments we used non-infected cells as controls to facilitate the comparison between transduced cells and CTR cells exposed to exogenous rhBDNF (+B). Mutant CTR cells showed lower levels of phosphorylated AKT protein, but only a slight decrease in ERK activation, compared to WT cells (Fig 2.3A, B). Nevertheless, overexpression of BDNF and TrkB, respectively, *per se* induced a significant activation of AKT in mutant cells (Fig. 2.3A). Moreover, overexpressed FL-TrkB in mutant cells stimulated with BDNF, either derived from BDNF-overexpressing cells (BDNF/TrkB co-culture) or exogenously added (+B), lead to AKT-pathway activation (Fig. 2.3A),

suggesting that the receptor is still functional in mutant cells and can mediate AKT signaling cascade after 24 h of BDNF stimulus. Enhanced ERK phosphorylation levels were detected in TrkB overexpressing cells after co-cultured with BDNF-transduced cells (Fig 2.3B, BDNF/TrkB); a slight increase in ERK activation was also observed in TrkB overexpressing cells after BDNF incubation (Fig 2.3B, TrkB +B). Interestingly, upregulation of ERK was also observed in mutant CTR cells following BDNF exposure (Fig. 2.3B; CTR +B).

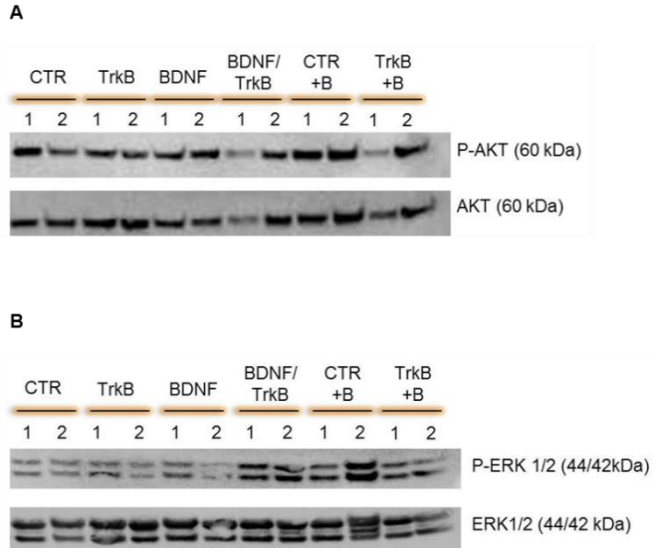

Figure 2.3 – Influence of BDNF and TrkB overexpression on AKT and ERK activation in transduced *versus* untransduced wild-type and mutant striatal cells. Levels of phosphorylated AKT (**A**) and ERK1/2 (**B**) were evaluated by Western blotting in total lysates of WT and mutant control/untransduced (CTR) cells and cells overexpressing TrkB-eGFP (TrkB) or BDNF-mCherry (BDNF). BDNF/TrkB stands for co-cultures of BDNF and TrkB transduced cells. Control and TrkB-overexpressing cells were also exposed to 20 ng/mL BDNF (+B) for 24 h. The images show representative blots of 3-12 independent experiments. 1 – WT cells; 2 – HD mutant cells.

Finally, we determined whether overexpression of BDNF or TrKB receptor rescued features of cell death in HD mutant cells. Caspase-3 is an effector caspase, which once triggered, leads to DNA fragmentation and apoptosis. Thus, we determined caspase-3 activation, the number of fragmented/condensed nucleus and evaluated necrotic cell death by PI staining in TrkB and BDNF overexpressing cells, after BDNF/TrkB co-culture, and following exposure to exogenous rhBDNF (20 ng/mL, 15 min before STS insult, when applied) in CTR and TrkB-expressing cells. Under

basal conditions, CTR HD mutant striatal cells exhibited significant increased caspase-3-like activity and enhanced the number of fragmented/condensed chromatin, compared to WT cells (Fig. 2.4A, C), whereas no changes were observed in necrotic cell death (Fig. 2.4E). To gain additional insights on the efficiency of striatal cell protection evoked by BDNF and TrkB overexpression, we also determined whether cell death parameters were altered after a mild apoptotic insult with STS (10 nM), for 24 h, which was shown to slightly increase caspase-3 activation and fragmented/condensed nuclei, without causing necrotic cell death (Fig. 2.4B, D, F). Overexpression of TrkB receptor or BDNF significantly diminished caspase-3 activity in mutant cells (Fig. 2.4A). Moreover, exposure of TrkB-expressing cells to BDNF (TrkB+B) also decreased caspase-3-like activity in mutant cells. However, no significant changes were observed when considering the number of apoptotic or necrotic cells in cells non-exposed to STS (Fig. 2.4C and E). STS-evoked caspase-3-like activity was prevented in TrkB-overexpressing cells subjected to BDNF exposure only (Fig. 2.4B). In contrast, DNA fragmentation was prevented in STS-treated mutant TrkB-expressing cells and in both CTR and TrkB-expressing cells following exogenous exposure to BDNF (Fig. 2.4D).

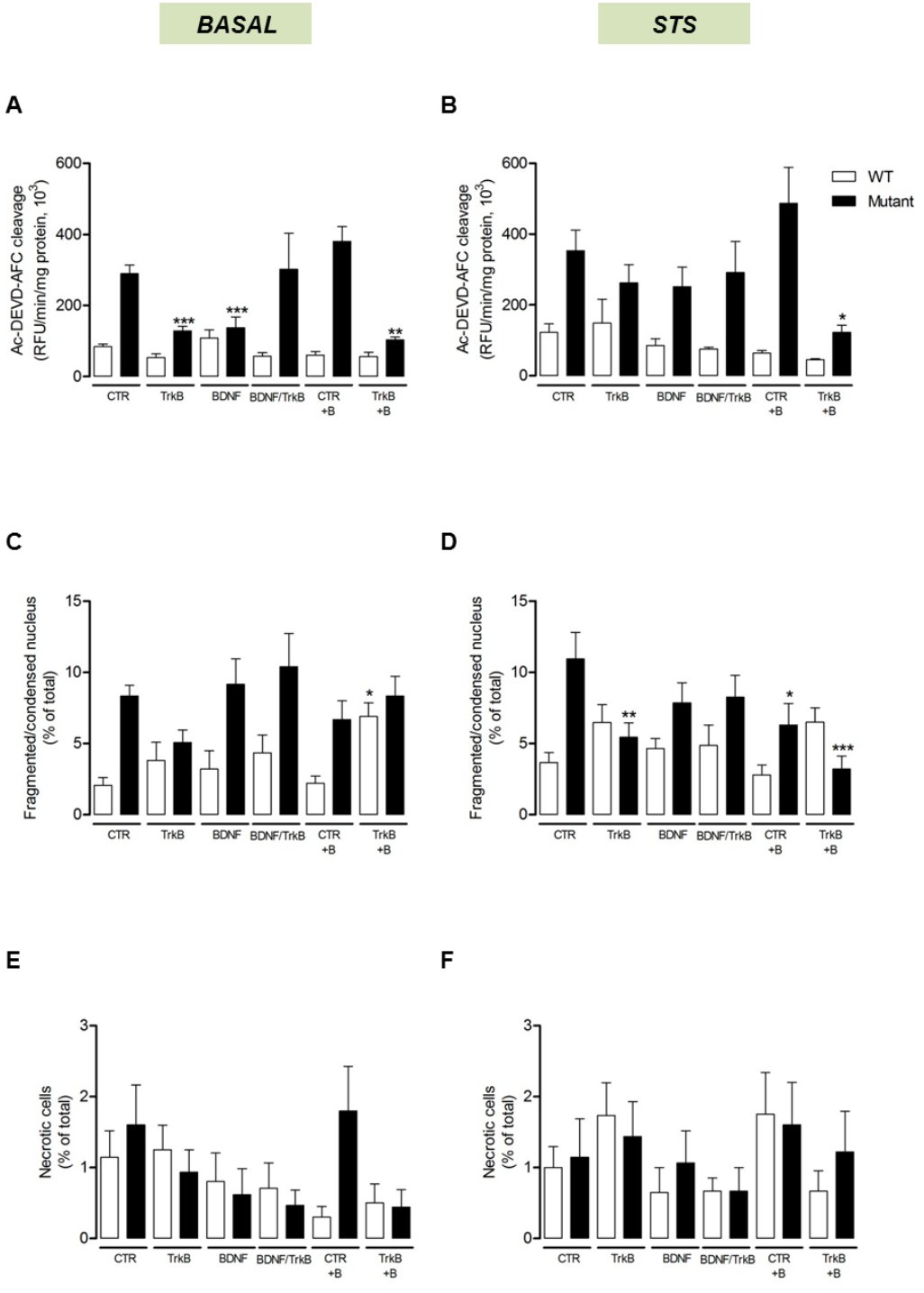

Figure 2.4 – Effect of BDNF and TrkB RV infection on cell death in wild-type and mutant striatal cells. Striatal wild-type (WT) and mutant control-untransduced (CTR) and transduced cells were incubated with staurosporine (STS, 10 nM), an apoptotic inducer, for 24 h (**B, D** and **F**). Control and TrkB-eGFP cells were also pre-treated with 20 ng/mL BDNF (+B) 15 min before and during STS exposure. (**A**-**B**) Caspase-3 activity was measured in basal conditions (**A**) and after STS insult (**B**) by following the cleavage of Ac-DEVD-AFC

fluorimetric substrate. The activity was expressed as relative fluorescence units (RFU) per minute per milligram protein for each condition. Results are depicted as the mean ± S.E.M. of 2-5 independent experiments, in triplicates. (**C**-**F**) Plated cells were stained with Hoechst 33342 (2 µg/mL) plus propidium iodide (4 µg/mL) to determine apoptotic (fragmented/condensed chromatin, **C** and **D**) and necrotic cell death (**E** and **F**). Live cell nucleus were counted in five different fields per coverslip. Images were acquired by fluorescence microscopy. Average of cells counted per field in 5 different fields (WT/mutant): *Basal* – CTR (103/113), TrkB (98/96), BDNF (103/92), BDNF/TrkB (104/152), CTR +B (148/88), TrkB +B (158/85); *STS* – CTR (118/75), TrkB (102/144), BDNF (105/109), BDNF/TrkB (97/141), CTR +B (113/88), TrkB +B (152/47). Data is depicted as the mean ± S.E.M. of 3 independent experiments. Statistical analysis: two-way ANOVA with Bonferroni post-test, *P<0.05, **P<0.01 and ***P<0.001, compared to CTR cells.

Discussion

Transduction of striatal cell lines with RV vectors encoding for preproBDNF and FL-TrkB was shown to enhance endogenous BDNF levels and its release as well as to increase the levels of FL-TrkB receptors, respectively, in both WT and mutant cells. BDNF or TrkB overexpression induced AKT activation in mutant cells, which was also detected after the co-culture of BDNF and TrkB transduced mutant cells, and following exposure of mutant TrkB-overexpressing cells to rhBDNF. Likewise, mutant co-cultures and both mutant TrkB-overexpressing and CTR cells stimulated with rhBDNF displayed increased phosphorylation of ERK. Of interest, TrkB and BDNF overexpression significantly reduced caspase-3 activity in mutant cells; moreover, STS-induced apoptotic cell death was largely rescued in FL-TrkB overexpressing mutant cells exposed to BDNF, correlating with AKT activation. Overall, our data strongly suggest the importance of BDNF-mediated TrkB activation in preventing striatal cell death and bring new perspectives regarding the targeting of FL-TrkB receptor for the treatment of HD.

BDNF is synthesized as a precursor protein (preproBDNF) in endoplasmic reticulum which, following cleavage of the signal peptide, is transported to the Golgi and allocated into either constitutive or regulated secretory vesicles (Mowla *et al*., 1999; Lessmann and Brigadski, 2009). Therefore, BDNF can be secreted by both constitutive and regulated pathways, the latter in response to neuronal activity. proBDNF can be converted into mature BDNF intracellularly, in the trans-Golgi by endoproteases such as furin, or in immature secretory granules by proprotein convertases (Mowla *et al*., 1999; Lessmann and Brigadski, 2009). BDNF was also described to be processed extracellularly by tissue plasminogen activator/plasmin

(Pang *et al.,* 2004). More recently, Matsumoto and colleagues (2008) reported that proBDNF is processed intracellularly and is secreted only in its mature form in cultured hippocampal neurons (Matsumoto *et al.,* 2008). proBDNF binds to sortilin and has been classically described to preferentially interact with p75 pan neurotrophin receptor, triggering different signaling cascades, namely cell survival (*via* activation of nuclear factor kappa-light-chain-enhancer of activated B cells, NF-kB) or cell death (involving c-Jun N-terminal kinase, JNK) (Teng *et al.,* 2005; Cunha *et al*., 2010, for review). In our study we observed higher levels of proBDNF in mutant cells, compared to WT cells, which could contribute to mHtt-linked striatal cell death. We also show that striatal mutant cells express higher levels of mature BDNF, when compared to WT cells, after infection with BDNF encoding retrovirus, which could anticipate deficient release of BDNF caused by mHtt. Nevertheless, data obtained in transduced cells show similar extracellular accumulation of pro- and mature BDNF in WT and mutant cells. Indeed, mature BDNF activates specifically the tyrosine receptor TrkB. Different TrkB isoforms are generated by alternative splicing resulting in a functional FL-TrkB, containing a long cytoplasmic region with a catalytic tyrosine protein kinase domain, and three truncated splice variants: T1, T2, and T-Shc that have the complete extracellular region and transmembrane domain, but differ in their short cytoplasmic tails and lack the kinase domain (Klein *et al*., 1990; Middlemas *et al.,* 1991; Stoilov *et al*., 2002). Truncated forms inhibit FL receptor signaling by sequestering BDNF or functioning as dominant negative receptors by heterodimerization with FL-TrkB (Haapasalo *et al.,* 2001).

PI3K-mediated AKT activation (at Ser473) was previously shown to prevent mHtt-induced cell death and intranuclear inclusion formation by directly acting on Htt protein through Ser421 phosphorylation (Humbert *et al.*, 2002). Ginés and colleagues (2003) previously hypothesized that compensatory pro-survival pathways might be activated in mutant cells to counteract metabolic dysfunction due to mHtt expression. The authors showed increased AKT activation in mutant cells, which was not observed in our study. However, in Ginés work (2003) cells were serum-deprived for 3 h before cell extracts, which might account for the inconsistent results. Corroborating our data, Colin and co-authors (2005) reported a downregulation of AKT in the brain of a HD rat model, even before neuronal degeneration, and in post-mortem samples of human brain, at a final stage of the

disease. In the latter case, AKT was down-regulated by caspase-3 cleavage, as previously suggested by Humbert *et al*. (2002), who observed the accumulation of a shorter fragment (49 kDa) of AKT in the striatum of HD patients. Caspase-3 mediated cleavage of AKT generating an inactive AKT fragment was also reported by other investigators (Bachelder *et al*., 1999; François and Grimes, 1999; Rokudai *et al.* 2000). Interestingly, Colin et al. (2005) observed increased levels of AKT in peripheral cells (e.g. lymphoblasts and lymphocytes) from HD patients, although AKT specific activity (defined by phosphorylation at Ser473) was reduced in these human cells. In our experiments, AKT activation was positively influenced by BDNF and TrkB overexpression in the striatal mutant cells, which further promoted cell survival pathways; indeed, caspase-3 mediated apoptotic cell death was significantly reduced in cells expressing increased levels of BDNF or TrkB alone. Correlation between AKT activation and decreased cell death parameters (caspase-3 activation and fragmented/condensed nuclei) was also observed following BDNF exposure in cells overexpressing TrkB, revealing that both proteins are required for complete rescue of apoptotic-like cell death.

In the present study both CTR WT and mutant cells displayed increased ERK1/2 activation upon rhBDNF exposure, which is also contradictory to previous published data by Ginés *et al.* (2010), who reported a reduction in mutant ERK1/2 activation mediated by BDNF. Again, differences between these studies may be accounted for by the methodology used, since these authors used 100 ng/mL BDNF, and AKT or ERK activation were analyzed up to 30 min later, while in the present work the cells were exposed to 20 ng/mL BDNF, for 24 h. In our study, BDNF-mediated ERK1/2 phosphorylation was also observed in TrkB-overexpressing WT and mutant cells, which might be also related to decreased activity of caspase-3 and DNA condensation/fragmentation. Moreover, co-cultures of transduced cells (BDNF/TrkB) favored both AKT and ERK1/2 signaling pathways, although it was not reflected into inhibition of apoptotic cell death. When considering apoptosis, not all stimuli affecting caspase-3 activity effectively altered chromatin fragmentation, which may be accounted for by the difficulty to examine fragmented chromatin in proliferating striatal cell line. Nevertheless, STS-induced apoptosis involving caspase-3 activation and DNA fragmentation/condensation, as previously observed by us in HD mutant striatal cell line (Rosenstock *et al*., 2011), was completely

rescued in TrkB-overexpressing HD mutant cells exposed to BDNF, underlying an important role of TrkB receptors in HD striatal cells.

Our data further suggest that different sources of BDNF (through BDNF overexpression or exogenous transient administration), which reflect different exogenous levels of BDNF, as well as TrkB receptor accessibility, evoke distinct pathways activation. In a context other than HD, it has been shown that transient or sustained activation of TrkB receptors depends on BDNF concentration and administration (acute or gradual), leading to different kinetics of ERK activation/phosphorylation (Ji *et al*., 2005, 2010). Previously published data (e.g. Haapasalo *et al*., 2002) strongly indicated that BDNF activation of TrkB receptors on cell surface, signals the recruitment of more TrkB receptors from the cytoplasm to the plasma membrane, thus implicating the existence of an intracellular pool of TrKB receptors located in vesicles, which can be promptly recruited to the cell surface upon an activation signal. Then, Trk receptors can follow two alternate endocytic pathways: 1) recycling to the plasma membrane, or 2) trafficking to lysosomes, which constitutes the degradative pathway characterized by down-regulation of cell surface receptors and decreased responsiveness to ligand (Chen *et al*., 2005). Thus, prolonged BDNF exposure can decrease responsiveness of TrkB receptors, which are downregulated by internalization from the plasma membrane (Haapasalo *et al*., 2002), and may then be sorted to the degradative pathway upon activation (Chen *et al.,* 2005). This could help to explain the decrease in BDNF-mediated ERK phosphorylation in HD cells transduced with BDNF, similarly to what was observed in mutant striatal cells after exposure to 100 ng/mL BDNF (Ginés *et al*., 2010). Conversely, lower BDNF concentrations (20 ng/mL) or higher expression of FL-TrkB receptors plus BDNF (as in the BDNF/TrkB system) increased ERK activation. Indeed, BDNF-induced TrkB phosphorylation was not largely altered in mutant compared to WT cells (Ginés *et al.,* 2010). According to these authors, mHtt selectively impaired TrkB receptor-mediated ERK1/2 activation through a reduction in p52/p46Shc adapter protein expression, increasing mutant cells vulnerability to oxidative stress; therefore, deficient ERK1/2 activation was proposed to contribute for HD neurodegeneration (Ginés *et al*., 2010), since ERK1/2 activation was described to play an important neuroprotective role in promoting cell survival in response to oxidative stress (Han and Holtzman,

2000) and in preventing caspase-3 mediated cell death in cells expressing FL-mHtt (Wu *et al.*, 2002).

By thoroughly examining the effects of enhanced endogenous BDNF release (in cells overexpressing BDNF), its exogenous application, and the expression of FL-TrkB receptors, the present data reinforce the positive role of BDNF and functional TrkB receptors in HD striatal cells survival through a pathway mainly involving AKT, given that sustained AKT activation was observed after 24 h only in mutant cells, particularly in BDNF and TrkB overexpressing cells (exposed or not to rhBDNF), which probably reflects into a reduction in caspase-3 activity. On the other hand, ERK phosphorylation levels were highly enhanced when BDNF and FL-TrkB were overexpressed (e.g. BDNF/TrkB) or BDNF was exogenously added (e.g. in CTR or TrkB transduced cells), both in mutant and WT cells, suggesting that ERK activation may stimulate signaling events other than cell survival, as corroborated by modified activity of caspase-3. Moreover, data herein suggest that BDNF and TrkB bear complementary roles against dysfunctional mechanisms underlying HD pathology, reinforcing their potential benefit as HD therapies.

CHAPTER 3

CHARACTERIZATION OF SUBVENTRICULAR ZONE-DERIVED PROGENITOR CELLS FROM MILD AND LATE SYMPTOMATIC YAC128 MOUSE MODEL OF HUNTINGTON'S DISEASE

Chapter based on the following manuscript:

Ana Silva, Elisabete Ferreiro, Ildete L Ferreira, João MR Cardoso, Joana Rodrigues, Michael R Hayden and A. Cristina Rego (2013). Characterization of subventricular zone-derived progenitor cells from mild and late symptomatic YAC128 mouse model of Huntington's disease (*Manuscript submitted to* Human Molecular Genetics)

3.1. Abstract

Huntington's disease (HD) is caused by the expansion of CAG repeats at the *HD* gene, leading to the expression of mutant huntingtin (mHtt) and to selective striatal neuronal loss, frequently associated with mitochondrial dysfunction and decreased support by brain-derived neurotrophic factor (BDNF). New neurons derived from the subventricular zone (SVZ) are apparently not able to rescue HD pathological features. Therefore, in this study we analyzed the proliferation, migration and differentiation potential of adult SVZ-derived cells from mild (6 month-old, mo) and late (10-mo) symptomatic HD YAC128 mice expressing full-length (FL)-mHtt, *versus* age-matched wild-type (WT) mice. YAC128 and WT cells showed similar profile in proliferation and cell cycle phases. However 6 mo YAC128 SVZ-derived cells exhibited higher migratory capacity, and higher number of MAP2+ and synaptophysin+ cells, compared to WT cells, which was promoted following exposure to BDNF. BDNF-evoked neuronal differentiation was diminished in 10 mo cells, correlating with decreased levels of TrkB receptors at this age. Interestingly, 6 mo YAC128 SVZ-derived cells also showed increased intracellular Ca^{2+} levels in response to KCl, which was promoted by BDNF, evidencing the presence of differentiated neurons. In contrast, KCl and BDNF induced-Ca^{2+} responses were diminished in 10 mo YAC128 cells, suggestive of decreased differentiation capacity of these cells along with lower mitochondrial membrane potential and increased mitochondrial Ca^{2+} accumulation, compared to 6 mo YAC128 cells. Data evidence age-dependent reduced migration and decreased acquisition of a neuronal phenotype, accompanied by decreased mitochondrial function in SVZ-derived cells from YAC128 mice through HD symptomatic phases.

3.2. Introduction

HD is the most prevalent polyglutamine disorder, caused by an expansion of CAG repeats in the *HD* gene, encoding for mHtt. Neuropathologically, HD is characterized by a selective degeneration of striatal (γ-aminobutyric acid (GABA)ergic and cortical neurons (e.g. Davies and Ramsden, 2001; Gil and Rego, 2008, for review). Under normal conditions, GABAergic medium spiny neurons (MSN) receive BDNF input from the cortex (Canals *et al*., 2001). BDNF binding to TrkB receptors activates intracellular pathways leading to neuronal differentiation, survival, migration and maturation of striatal neurons (Perez-Navarro *et al*., 2000; Petridis and El Maarouf, 2011). BDNF also mediates the modulation of synaptic transmission between neurons and the inhibition of apoptotic pathways in MSN, thus protecting GABAergic neurons against several insults (Petersén *et al*., 2001; Bath and Lee, 2010, for review).

Concordantly, in a previous study, we showed that BDNF efficiently promotes the differentiation of neural progenitor cells into a GABAergic neuronal phenotype (Silva *et al*., 2009); moreover, we showed that BDNF has a protective role against apoptosis and regulates transcription in cortical neurons treated with 3-nitropropionic acid (Almeida *et al.,* 2009, 2010). Importantly, mHtt was previously shown to repress the transcription of BDNF (Zuccato *et al*., 2001, 2003) and to reduce the axonal transport of this neurotrophin (Gauthier *et al*., 2004). Supporting these results, Xie *et al.* (2010) demonstrated that overexpression of BDNF in the forebrain rescues many disease phenotypes in YAC128 mice expressing human FL-mHtt, including prevention of loss and atrophy of striatal neurons. Additionally, decreased TrkB mRNA and protein levels were reported in HD striatal cells and human patients (Ginés *et al.,* 2006, Zuccato *et al*., 2008). Other HD pathological mechanisms include modified intracellular calcium homeostasis and mitochondrial dysfunction, which are believed to contribute to neuronal dysfunction and death of striatal MSNs (for review see Gil and Rego, 2008; Rosenstock *et al*., 2010).

Neural stem cells (NSC) are present in the adult in two main neurogenic regions, the subventricular zone (SVZ), near the striatum, the most affected area in HD, and the subgranular zone (SGZ) of the hippocampus (Gage, 2000; Doetsch, 2003). In adult SVZ, glial fibrillary acidic protein (GFAP)-expressing cells self-renew and give rise to progenitor cells that originate migrating neuroblasts (Alvarez-Buylla *et al*., 2002; Doetsch, 2003). NSC can be grown *in vitro* as neurospheres (NS), composed by restricted progenitors and a small number of multipotent stem cells (Reynolds and Weiss, 1996), which

proliferate in response to mitogens (*e.g.* epidermal growth factor, EGF) (Reynolds *et al*., 1992; Vescovi *et al.*, 1993; Gage, 2000). The differentiation of NSC is thought to be determined by factors present in the NSC niche, namely growth factors (Ahmed *et al*., 1995; Takahashi *et al.*, 1999; Benoit *et al.*, 2001; Bosch *et al*., 2004), such as BDNF, and extracellular matrix (ECM) proteins (Jacques *et al*., 1998; Danen and Sonnenberg, 2003, for review; Flanagan *et al*., 2006). Among these, fibronectin (FN) is one of the important ECM proteins secreted by cells in the niche (Alvarez-Buylla and Lim, 2004), as well as by neurospheres (Campos *et al*., 2004). Importantly, FN has been implicated in NSC proliferation, migration and GABAergic neuronal differentiation (Jacques *et al*., 1998; Silva *et al*., 2009).

In HD *post-mortem* human brain, increased SVZ proliferating progenitor cells was previously observed (Curtis *et al*., 2003, 2005). In HD mice models (e.g YAC128 and R6/1; see Simpson *et al*., 2011), SVZ neurogenesis and neuronal differentiation was unchanged, however SVZ neuroblast migration through the rostral migratory stream (RMS) was diminished in R6/2 mice, expressing human mHtt exon 1 (Gil *et al.*, 2005; Moraes *et al*., 2009). In contrast, neural stem precursor cells isolated from the SVZ of HD KI mice showed increased number of neural progenitors and neurogenesis (Lorincz and Zawistowski, 2009), rising opposing data that may be accounted by the different characteristics of these HD mice models. However, multipotent NSC are apparently not able to rescue the pathological features of neurodegenerative disorders, including HD (for review Winner *et al.,* 2011 and Curtis *et al*. 2012,) and the causes are not yet fully clarified.

Taking this into account, in this work we aimed to characterize proliferation and differentiation potential of HD *versus* (*vs*) WT SVZ-derived cells, using the YAC128 HD mice model at mild (6 months of age) and late (10 months of age) symptomatic stages of HD-related phenotypes. Indeed, YAC128 mice expressing human FL-mHtt were previously demonstrated to exhibit HD symptoms beginning around 3 months of age. The symptoms are essentially behavioral until in 9 mo animals, with hyperkinesis first manifested in 3 mo mice, followed by a progressive motor deficit at 6 months and advancing to hypokinesis by 12 months of age. Degeneration begins around 9 mo, and striatal neuronal loss is seen at 12 mo (Slow *et al*, 2003; van Raamsdonk, *et al*., 2005). In the present study we used SVZ cells cultured as NS derived from 6 and 10 mo YAC128 animals to mimic mild symptomatic HD, at a stage the symptoms are mainly behavioral, and late symptomatic HD, when brain degeneration may be evident. We studied the

proliferation, cell cycle and migration with a focus on neuronal differentiation of SVZ cells isolated from adult YAC128 HD mice *vs* WT littermates. Our data reveal changes in SVZ-derived cells through the HD symptomatic-like phase of disease progression in YAC128 mice, which should be taken into account when investigating new approaches to promote SVZ-derived neuronal differentiation and delay HD neuropathology.

3.3. Materials and Methods

3.3.1. Reagents

Proteinase K was purchased from ROCHE (Roche Diagnostics, Mannheim, Germany). DMEM:F-12 (1:1) + GlutaMAX medium, B27 supplement, penicillin-streptomycin, Hoechst 33342 were purchased from GIBCO (Invitrogen Life Technologies, Paisley, UK). Alexa Fluor-594 anti-mouse IgG, Alexa Fluor-488 anti-rabbit IgG, rhodamine-123 (Rh123) and Fura-2-acetoxymethyl ester (Fura-2/AM) were obtained from Molecular Probes (Invitrogen Life Technologies, Paisley, UK). Foetal calf serum (FCS) was obtained from BioWhittaker Molecular Applications (Rockland, MD, USA). EGF and BDNF were purchased from Peprotech (Rocky Hill, NJ, USA). Ethidium bromide, DNAse I type IV, papain, accutase, poly-L-lysine (PLL), FN, glycine, saponin, phenylmethylsufonyl fluoride (PMSF), dithiothreitol (DTT), protease cocktail inhibitor (chymostatin, leupeptin, antipain, pepstatin A), carbonylcyanide-p-trifluoromethoxyphenylhydrazone (FCCP), oligomycin, histamine, mouse monoclonal anti-microtubule associated protein (MAP)-2, mouse anti-α-tubulin and mouse anti-actin were obtained from Sigma Chemical Co. (St. Louis, MO, USA). Rabbit anti-synaptophysin, mouse anti-huntingtin (Htt, MAB2166) and mouse anti-polyglutamine (1C2) were purchased from Millipore (EMD Millipore Corporation, Billerica, MA, USA). Rabbit anti-BDNF and rabbit anti-TrkB were from Santa Cruz Biotechnology Inc. (Santa Cruz, CA, EUA). Biorad Protein Reagent was from BIORAD (BioRad, Hercules, CA, USA). Polyvinylidene difluoride (PVDF) membrane, enhanced chemifluorescence reagent (ECF) and alkaline phosphatase-linked anti-rabbit and anti-mouse secondary antibodies were purchased from Amersham Biosciences (Buckinghamshire, UK). DAKO fluorescence mounting medium was from DakoCytomation (Glostrup, Denmark).

3.3.2. Animals

Hemizygous YAC128 transgenic mice (HD53 line) expressing human mHtt with 128 glutamines and non-transgenic (WT) littermates (kindly provided by Prof. Michael Hayden, University of British Columbia, Vancouver, Canada) were housed in animal facilities with controlled-temperature room and maintained on 12 h light/dark cycle. Food and water were available *ad libitum*. The mice offsprings resulting from WTxYAC128 (FVB/N background) crosses were genotyped and adult females and males with three (*Supplementary data*), six and ten months of age were used. All animals and experiments were performed in accordance to the Helsinki Declaration, EU guidelines (86/609/EEC).

3.3.3. Genotyping

DNA was extracted from mouse tails for PCR analysis, using primers for detection of left and right YAC arm (LYA and RYA, respectively), in a previously described procedure (Hodgson *et al*., 1996; Slow *et al*., 2003). Briefly, a piece of tail from each animal was collected and the DNA extracted., The tissue was incubated with 300 µL of Lysis Buffer (50 mM Tris, 100 mM NaCl, 5 mM EDTA, 0.5% SDS, pH 8.2) and 30 µL of Proteinase K (10 mg/mL, in mili-Q sterile water) overnight at 56 ºC, at 500 r.p.m.. The digested tissue was then carefully mixed and centrifuged (20800 x*g* for 3 min at 4 ºC). Supernatant was transferred to a new eppendorf and 200 µL of concentrated NaCl solution was added in order to precipitate proteins. After 20 min in ice, supernatant was centrifuged (208001 x*g* for 15 min at 4 ºC). The second supernatant was collected and 500 µL iced ethanol (100%) was added. The mixture was placed in a tube rotator, at 40 r.p.m. for 15 min at room temperature (RT) and further centrifuged (20800 x*g*, for 5 min at 4 ºC) to precipitate DNA content. Supernatant was carefully discarded and 700 µL iced-cold ethanol (70%) was added. After centrifugation (6800 x*g* for 8 min at 4 ºC), DNA pellet was left at RT to dry out. DNA was further dissolved in 200 µL T.E. (10 mM Tris, 1 mM EDTA, pH 8) and quantified using a micro-volume spectrophotometer. Genotype was determined through a triplex PCR (according to Dr. Michael Hayden's Laboratory protocol). A 25 µL PCR reaction was prepared as follows: 10 ng/µL of sample DNA, 2X PCR Reaction Buffer, 2 mM $MgCl_2$, 200 µM dNTP, 0.4 µM of each upstream and downstream primers, 0.08 U of TAQ DNA polymerase and sterile mili-Q water up to a final volume of 25 µL (94 °C for 3 min; 35 cycles at 94 °C for 30 sec, at 63 °C for 30 sec, at 72 °C for 30 sec; 72 °C for 10 min). The primers used are described. For the Right YAC Arm (RYA1): 5'- CTT GAG ATC GGG CGT TCG ACT CGC -3' and (RYA2) 5'- CCG CAC CTG TGG CGC CGG TGA

TGC -3'; Left YAC Arm (LYA1): 5'- CCT GCT CGC TTC GCT ACT TGG AGC -3' and (LYA2) 5'- GTC TTG CGC CTT AAA CCA ACT TGG -3'; Actin (forward): 5'- GGA GAC GGG GTC ACC CAC AC -3'; Actin (reverse): 5'- AGC CTC AGG GCA TCG GAA CC -3'. PCR products were loaded in a 1.7% agarose gel and stained with ethidium bromide. Photographs were taken in Gel-Doc XR Imaging System (BioRad, Hercules, CA, USA). A sample was considered as positive (transgenic) when all the RYA (170 bp), LYA (230 bp) and actin (450 bp) bands were amplified.

3.3.4. Isolation of Neural Stem/Precursor Cells

Neural stem/precursor cells were isolated from the SVZ of adult YAC128 and WT mice littermates. Followed decapitation, brains were immediately dissected. Cerebellum and olfactory bulbs were removed and the brain was placed in an acryl brain matrix (Stoelting, Illinois, USA). A single coronal cut (~2 mm) from frontal brain, anterior to the optic chiasm was done, exposing the lateral ventricles and SVZ, as described previously (Lorincz and Zawistowsk, 2009). The walls of the ventricles, corresponding to the SVZ, were bilaterally dissected with a forceps and incubated in an enzymatic solution (40 µg/mL DNAase I Type IV and 30 U/mL papain in DMEM:F-12 (1:1) + GlutaMAX), for 30 min at 37ºC. Following the incubation time, 10% FCS was added to the enzymatic solution to stop tissue digestion, and the cellular suspension was centrifuged at 200 x*g,* for 5 min. The pellet was resuspended in culture medium (DMEM:F-12 (1:1) + GlutaMAX, plus 10,000 units/mL of penicillin, 10 mg/mL streptomycin), 2% B-27 supplement, and 20 ng/mL EGF) and cells were cultured into T25 uncoated flasks. After four days in culture, fresh culture medium with EGF was added to culture flasks. The cells were grown as NS (floating aggregates) in a 95% air/5% CO_2 humidified atmosphere, at 37°C. After five days, the spheres were mechanically dissociated into a single cell suspension (*passaging*) with a Gilson pipette (200 µL) and re-cultured with fresh proliferation medium. Experiments were done in NS with two to a maximum of five cell passages.

3.3.5. Cell extracts and Western blotting analysis

NS were centrifuged (150 x*g*, 5 min) to remove culture medium and washed in PBS (Phosphate Buffered Saline, pH 7.4) before cellular extracts procedure. Cells were lysed in ice-cold RIPA buffer (150 mM NaCl, 50 mM Tris-HCl, 5 mM EGTA, 1% Triton X-100; 0.5% deoxycholate (DOC) and 0.1% sodium dodecyl sulfate (SDS), at pH 7.5) supplemented with 1 mM PMSF, 1 mM DTT, phosphatase inhibitors (1 mM sodium

orthovanadate, 25 mM NaF) and 1:1000 protease cocktail inhibitor (1 µg/mL chymostatin, 1 µg/mL leupeptin, 1 µg/mL antipain, 5 µg/mL pepstatin A). After 15 min in RIPA, samples were resuspended, centrifuged at 1000 x*g* for 10 min, at 4ºC, and the supernatant used for protein quantification by Biorad Protein Assay (BioRad, Hercules, CA, USA). Equivalent amounts of protein were denaturated with 6x concentrated sample buffer (0.35 M Tris, 36% glycerol, 10.28% SDS, 0.6 M DTT, 0.012% bromophenol blue), at 95ºC, for 5 min, separated on a 10% SDS-polyacrylamide gel (SDS-PAGE) and electroblotted onto PVDF membrane. Membranes were further blocked in 5% skim milk in Tris buffer saline (25 mM Tris-HCl, pH 7.6, 150 mM NaCl) plus 0.1% Tween-20 (TBS-T), for 1 h (RT). Incubations with primary antibodies (in TBS-T/5% milk) were performed overnight, at 4ºC: mouse anti-huntingtin 1:250, mouse anti-polyglutamine 1:1000, rabbit anti-BDNF 1:500, rabbit anti-TrkB 1:1000 and mouse anti-actin or α-tubulin 1:10,000, as loading control. Membranes were washed with TBS-T and incubated for 1 h at RT with alkaline phosphatase-linked secondary antibodies (anti-rabbit or anti-mouse IgG, 1:20,000, in TBS-T/5% milk). After washing in TBS-T, proteins in the membranes were incubated with ECF (5 min, RT). Immunoreactive bands were visualized by alkaline phosphatase activity that catalyses the conversion of ECF substrate to a highly fluorescent product reagent. This product strongly fluoresces at 540–560 nm when the blots are illuminated with UV light (maximum excitation at 430 nm), by using a BioRad Versa Doc 3000 Imaging System (BioRad, Hercules, CA, USA).

3.3.6. Proliferation and Cell Cycle

Dissociated NS were cultured on 100 µg/mL PLL (prepared in borate buffer solution) coated wells. After three days, cells were incubated with 5-ethynyl-2'-deoxyuridine (EdU, 10 µM), which incorporates into DNA during active DNA synthesis. Cells were fixed in 70% ethanol overnight (experimental protocol modified by Carreira *et al.*, 2010) 4 h after EdU incubation. Cells were detached with accutase (15 min, 37ºC) and proliferation was assessed using Click-iT® EdU Alexa Fluor® 488 Flow Cytometry Assay Kit (Invitrogen, Paisley, UK), according to manufacturer's instructions. Briefly, detection of EdU incorporation was based on a copper-catalyzed reaction between an azide (conjugated to Alexa Fluor 488 dye) and an alkyne (EdU). The advantage of this method is that the fluorescent azide, because of its small size, can penetrate the chromatin and access the EdU, thus denaturation of DNA is not required. Fixed cells were then incubated with

Alexa Fluo 488 azide and copper sulfate, for 30 min, and then incubated with RNAse plus the nuclear dye 7-aminoactinomycin D (7-AAD) for 30 min.

Cells were analyzed by FACS on a standard BD FACSCalibur flow cytometer (BD Biosciences, San Jose, CA) equipped with a 15 mW, air-cooled, 488 nm argon-ion laser for excitation of Alexa Fluor 488 and 7-AAD. EdU/Alexa Fluor 488 fluorescence was collected through a 530/30 nm bandpass filter and displayed on four-decade log scales. Fluorescence emission from 7-AAD was collected through a 670 nm longpass filter using linear amplification. The flow cytometer was calibrated with fluorescent standard microbeads (CaliBRITE Beads; BD Biosciences, San Jose, CA, USA) for accurate instrument setting. Photomultiplier tube voltage and spectral compensation were established using cells single-stained with EdU, Alexa Fluor 488, EdU/Alexa Fluor 488 or 7-AAD. For doublet discrimination, in addition to FL3 heights (7-AAD fluorescence), FL3 area and width were measured. At least ten thousand events were collected per sample. Analysis of the multivariate data was performed with BD CellQuestTM Pro software. Cell cycle analysis of DNA histograms was performed with ModFit LT 3.0.

3.3.7. Migration Assay

Single NS were plated on µ-slides (8 wells, IBIDI, Martinsried, Germany) coated with 100 µg/mL PLL or 10 µg/mL FN (prepared in PBS), in cell culture medium. In order to follow cells migrating out of each NS, transmission images were acquired every 30 min from time 0 (0 min) until 3 h after plating, in a laser scanning microscope LSM 510 META (Zeiss, Jena, Germany). Cell migration were analyzed using ImageJ Launcher (version 1.44p, NIH), to assess cellular mean velocity and maximum length achieved, taking the soma as a reference point.

3.3.8. Differentiation Assay and Immunocytochemistry

Single NS were seeded on PLL (100 µg/mL) or FN (10 µg/mL, pre-treated with PLL) coated coverslips, without the mitogen EGF, for seven days. To induce neuronal differentiation, cells were exposed to 5 ng/mL BDNF in duplicate wells and BDNF renewed every 48 h. Neuronal differentiation was further assessed by immunocytochemistry. For this purpose, cells were fixed in methanol-acetone (1:1) for 10 min, at 4ºC, washed and further incubated with 20 mM glycine, for 10 min. Cells were then permeabilized with 0.1% saponin for 30 min. Incubation with the primary antibodies against MAP2 and rabbit synaptophysin (1:200, diluted in saponin solution), was

performed for 1 h, at RT. Following this time, the cells were washed in saponin solution and incubated with the secondary antibodies mouse Alexa Fluor 594 and rabbit Alexa Fluor 488 (1:200, in saponin solution), for 1 h at RT. Nuclei were stained with 2 µg/mL Hoechst 33342, for 8 min and then washed with PBS. The coverslips were mounted on DAKO mounting medium. Images from five different fields of each coverslip were acquired in a fluorescence microscope Axioskop 2 Plus (Zeiss, Jena, Germany) and cells were counted using ImageJ Launcher (version 1.44p, NIH). Representative images were acquired in a fluorescence microscope Axioskop 2 Plus (Zeiss, Jena, Germany).

3.3.9. Single cell simultaneous analysis of cytoplasmic free calcium and mitochondrial membrane potential

Single cell and simultaneous analysis of cytoplasmic free calcium and mitochondrial membrane potential ($\Delta\Psi m$) were based on Ward *et al.* (2000) and Rego *et al*. (2001). Briefly, 7-day BDNF-treated cells were washed in Krebs medium (132 mM NaCl, 1 mM KCl, 2.5 mM $CaCl_2$, 1 mM $MgCl_2$, 10 mM glucose, 10 mM Hepes, pH 7.4) and further incubated in loading medium (Krebs medium plus 0.1% fatty acid free BSA) plus 1.3 µM Rh123, in quench-mode, for 5 min at RT. Then, glass coverslips were transferred to loading medium plus 0.02% pluronic acid and 5 µM Fura-2/AM, for 40 min at 37ºC. After a washing step, simultaneous intracellular calcium levels and Rh123 fluorescence were recorded for 25 minutes by exciting cells at 340 and 380 nm for Fura-2 and 548 nm for Rh123. From the fifth to the seventh minute, cells were stimulated with 50 mM KCl (isosmotic substitution of NaCl for KCl), washed three times and from ten to twelve minute, cells were incubated with 100 µM histamine (Agasse, *et al*., 2008 based protocol, with some modifications). Complete mitochondrial depolarization was achieved at 15 min by simultaneously adding 2 µM FCCP, a protonophore that collapses $\Delta\Psi m$, and 2 µg/ml oligomycin, which prevents H^+ flux through ATP synthase and thus ATP hydrolysis. At the end of each experiment 2 µM ionomycin was added in order to obtain maximum Fura-2 fluorescence. Data were recorded by using an inverted fluorescence microscope Axiovert 200 (Carl Zeiss, Jena, Germany) equipped with a dual band pass emission filter (510/40 and 600/60 nm) and with a Lambda DG4 apparatus (Sutter Instruments company, Novato, CA, USA). Emitted fluorescence was collected with the objective PlanNeofluar 40x/0,75 (Carl Zeiss, Jena, Germany) and driven to a CoolSNAP HQ digital camera (Roper Scientific, Trenton, NJ, USA). The system was controlled by MetaFluor software (Molecular Devices, Sunnyvale, USA). Data analysis was performed with systematic

custom scripts of Mathworks Matlab 2009a (32 bits) for fluorescence time course parameterization. For each coverslip, cell responses were normalized to the basal levels of the time-course. Values of peak amplitude were calculated at each stimulus instant, for Fura-2 and Rh123 fluorescence time-course. Each experiment condition was assayed at least in three different coverslips from three independent culture preparations.

3.3.10. Statistical analysis

Data were the mean ± S.E.M of the experiments defined in figure legends. Statistical analysis was performed by two-way Analysis of Variance (ANOVA) with Bonferroni post-hoc test, using SPSS V.19. software. P value <0.05 was considered significant.

3.4. Results

3.4.1. SVZ-derived neurospheres display age-dependent cell cycle changes, but no differences in proliferation or early apoptotic events

SVZ-derived neurospheres from YAC128 *vs* WT mice with 6 and 10 months of age were initially assessed for analysis of protein expression levels of endogenous Htt and FL-mHtt by Western blotting. According to Fig. 3.1A (middle panel), two bands can be observed in YAC128-derived cells, corresponding to WT and mHtt, as evaluated by using the MAB2166 antibody. The presence of mHtt in YAC128-derived neurospheres was confirmed with the 1C2 antibody, which binds to polyglutamine (polyQ) tract (Fig. 3.1A, upper panel) and matches the higher molecular weight band visualized with MAB2166.

We further determined if proliferation and cell cycle status were altered in YAC128 NS. In these experiments, dissociated cells were plated on PLL-coated wells. In order to evaluate cell proliferation, EdU was added to cells 4 h before fixation. Cell cycle (Fig. 3.1 B-D), EdU incorporation (Fig. 3.1E) and early apoptosis (Fig. 3.1F) profile were analyzed in SVZ NS from YAC128 and WT mice. Because cell cycle events are inherently dynamic, we could not determine how many cells were in G0, G1 or in G2 and M, or either between phases. Thus, we assumed the nomenclature of cell cycle phases as G0/G1, G2/M and Sub G0/apoptotic (Fig. 3.1B, D and F). According to Fig. 3.1, differences are age-related since no significant differences in cell cycle phases, proliferation status or apoptosis were detected between YAC128 and WT SVZ-derived

NS. We did not observe significant genotype-related differences in the phases of the cell cycle in cells from early-symptomatic 3 mo mice either (*Supplementary data*, Fig. S3.1). Both WT and YAC128 cells were arrested in G0/G1 stage at 6 mo (Fig. 3.1B, S3.1A), while at 10 mo a higher number of cells were at S phase (Fig. 3.1C) and G2/M phases (Fig. 3.1D). Nevertheless, no significant age or genotype differences were observed in proliferation (Fig. 3.1E, S3.1D) or early apoptotic events (Fig. 3.1F, S3.1E).

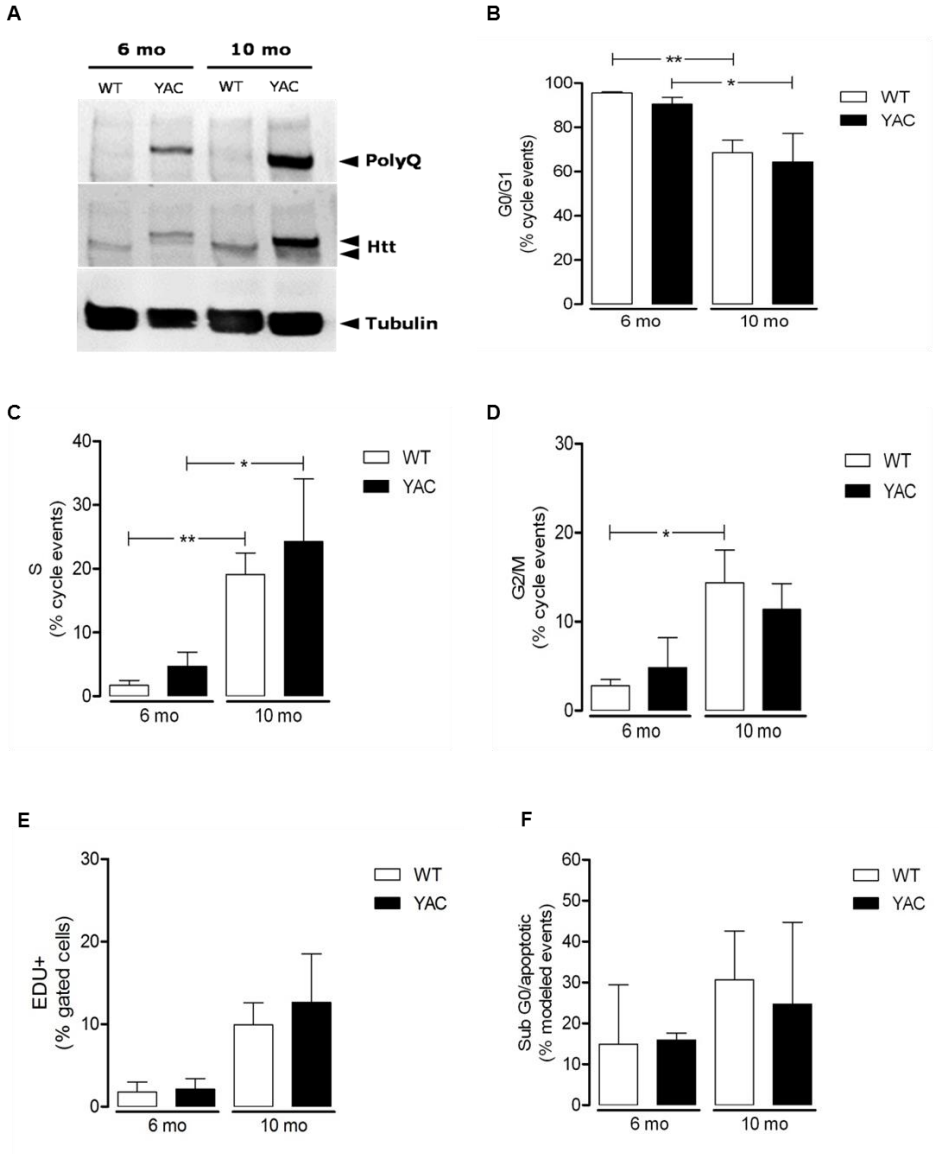

Figure 3.1 – Huntingtin protein levels, cell cycle, proliferation and early apoptotic events in WT and YAC128 SVZ-derived neurospheres. Cells were isolated from 6 and 10 mo WT and YAC128 mice SVZ and kept in culture as NS in the presence of EGF (20 ng/mL). (**A**) Cell extracts were performed after 5 passages; expression of wild-type Htt and FL human mHtt were confirmed by Western blotting, using tubulin as control (**A**, lower panel). Htt protein was present both in WT

and YAC128 cells (**A**, middle panel). A high molecular weight band corresponding to mHtt can be detected in YAC128-derived cells only, as confirmed using the 1C2 antibody against the polyglutamine (PolyQ) tract (**A**, upper panel). Decreased intensity of PolyQ band in 6 mo NS from YAC128 appears to be accounted for by decreased protein loading, as observed by tubulin labeling. Cell cycle (**B**-**D**), proliferation (**E**) and early apoptosis (**F**) profile were analyzed by Flow Cytometry, as described in Methods section. After 2-4 passages, NS were plated on PLL wells for 3 days. EdU was added to the cells 4 h before fixation (70% ethanol, overnight). Data are the mean ± S.E.M. of two to four independent analysis from 6 mice (3 WT and 3 YAC128) with 6 months of age, and 5 mice (3 WT and 2 YAC128) with 10 months of age. Statistics (two-way ANOVA with Bonferroni post-hoc test): *P<0.05, ** P<0.01.

3.4.2. SVZ-derived cells from mild symptomatic HD mice exhibit increased migration – role of extracellular matrix

Cell migration towards a target region is involved in the replacement of injured cells and the components of ECM are extremely important in this process. FN is one of the ECM proteins known to promote cell migration and differentiation (Tate *et al*., 2002; Flanagan *et al*., 2006; Silva *et al*., 2009). In this context, we analyzed if cell migration (determined by mean velocity and maximal length attained) of YAC128 SVZ-derived cells was compromised when compared to WT cells. For this purpose, WT and YAC128 NS from 6 and 10 mo mice were plated on PLL or FN for 3 h. Interestingly, YAC128 NS-derived cells from mild symptomatic (6 mo), but not 10 mo, mice showed higher migratory capacity than WT cells when plated on both PLL (Fig. 3.2A-D) and FN (Fig. 3.2E-H). YAC128 cells derived from 6 mo mice displayed higher mean velocity than WT cells plated in PLL (Fig. 3.2A), although the maximum distance achieved was similar (Fig. 3.2B). However, in FN coated dishes, both parameters were increased in YAC128 NS derived from youngest mice (Fig. 3.2E, F); Moreover, FN promoted migration of both WT and YAC128 cells, compared to PLL, at both ages. WT and YAC128 cell populations plated on FN showed increased velocity values (Fig 3.2E) at 6 mo (P<0.05, WT; P<0.01, YAC128) and at 10 mo (P<0.01, for WT and YAC128 cells), compared to PLL (Fig. 3.2A). WT cells attained greater distance in FN (Fig. 3.2F) at 10 mo (P<0.01) and YAC128 cells at both ages (P<0.001 for 6 mo; P<0.01 for 10 mo), compared to PLL (Fig. 3.2B). Interestingly, migration process appeared to begin sooner in cells plated on FN than on PLL (Fig. 3.2, image *arrows* indicate some migratory cells).

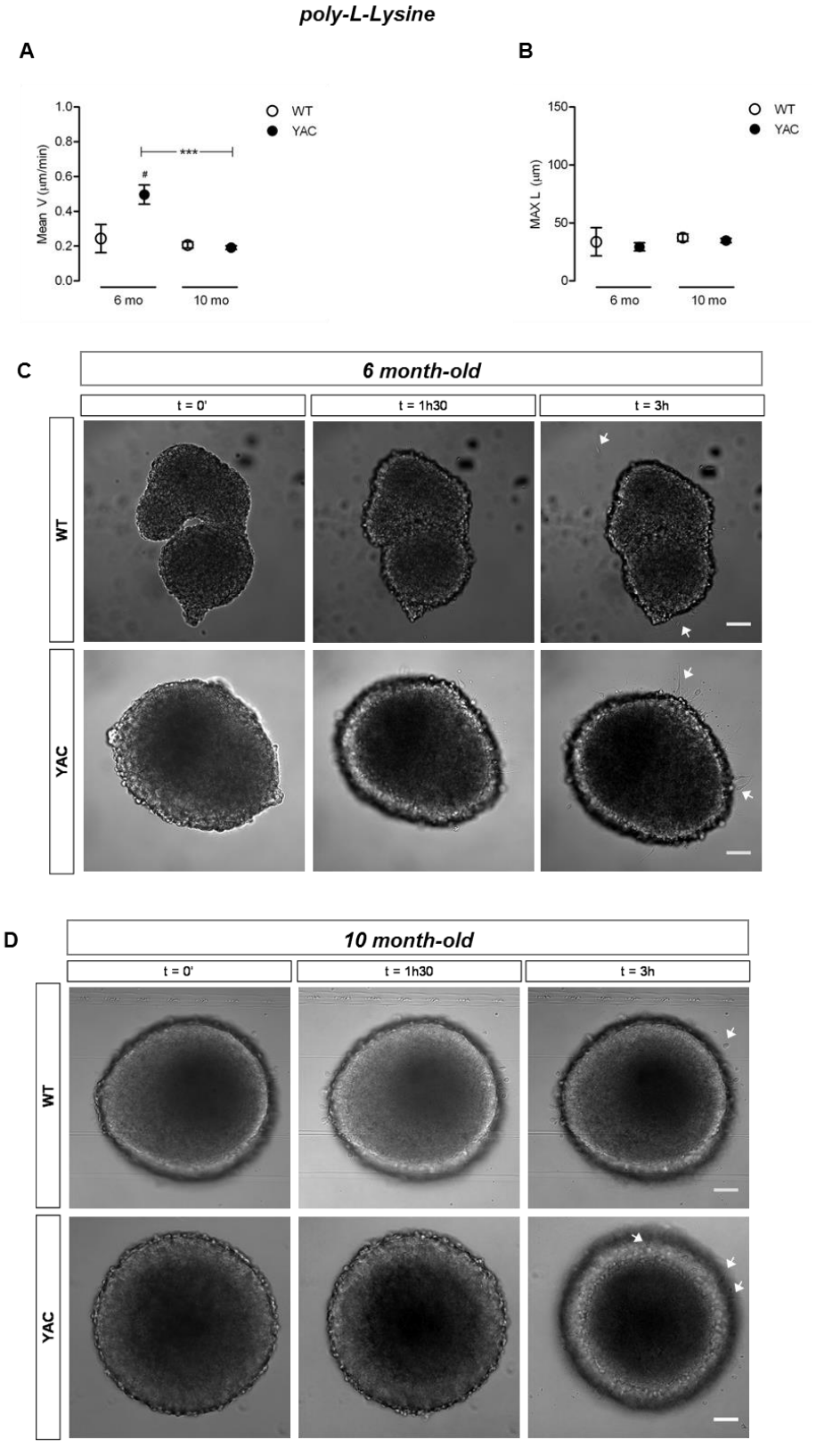
poly-L-Lysine
A
B
Mean V (µm/min)
1.0
0.8
0.6
0.4
0.2
0.0
WT
YAC
***
#
6 mo
10 mo
MAX L (µm)
150
100
50
0
C
6 month-old
t = 0'
t = 1h30
t = 3h
WT
YAC
D
10 month-old

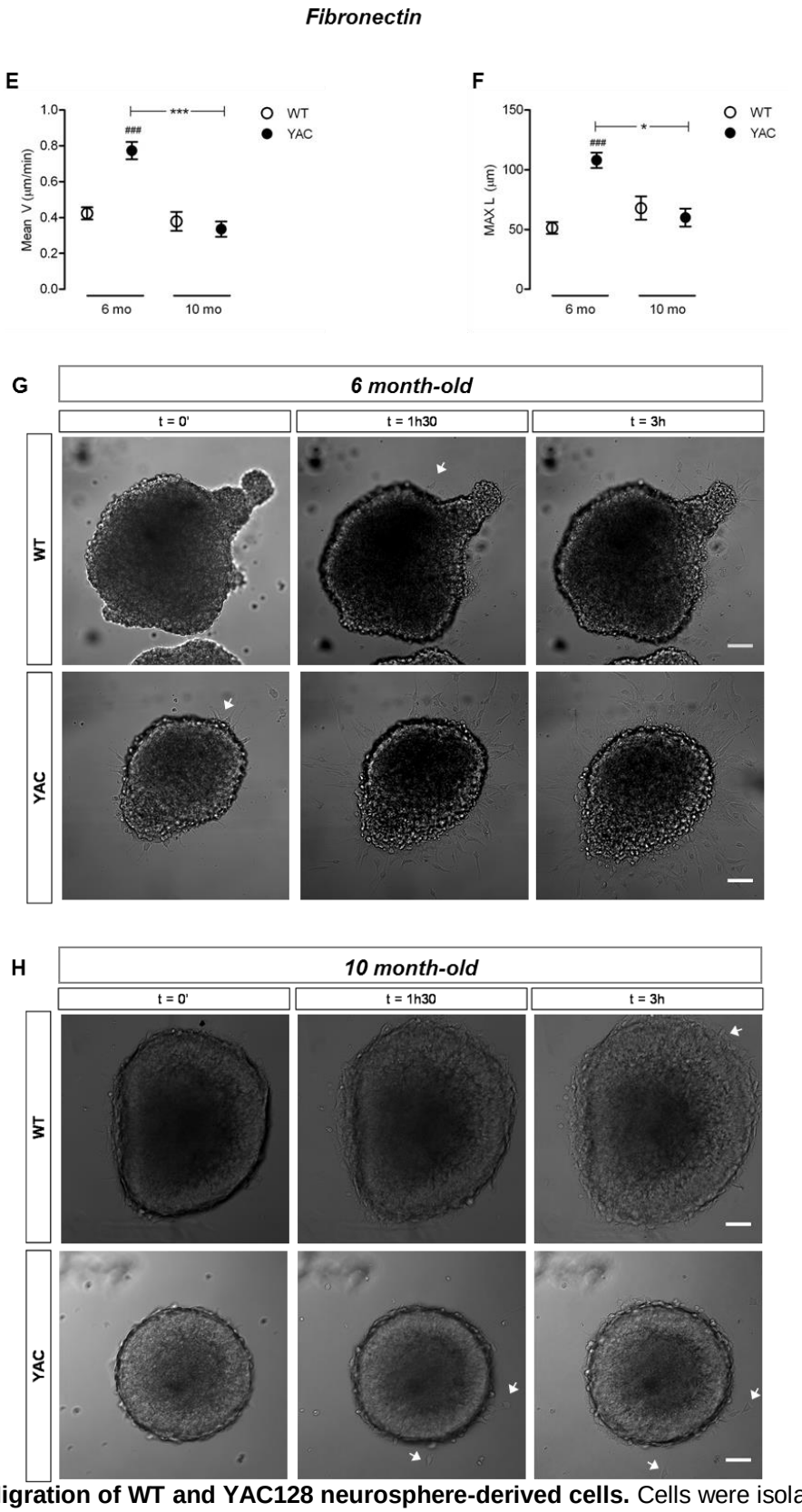

Figure 3.2 – Migration of WT and YAC128 neurosphere-derived cells. Cells were isolated from WT and YAC128 mice SVZ, at 6 and 10 mo and kept in culture as NS in the presence of EGF (20

ng/mL). After 2-4 passages, cells were plated on PLL or FN-covered wells, in cell culture medium, for 3 h. Confocal transmission images were acquired every 30 min up to 3 h (See *Supplementary Data* for representative cell migration movies). Cell mean velocity (Mean V) and maximum distance (MAX L) achieved in PLL (**A** and **B**) and FN (**E** and **F**) was determined using ImageJ software. The cell soma was used as reference point. Representative images of NS obtained from WT and YAC128 at 6 (**C** and **G**) and 10 mo (**D** and **H**), at time zero (left panels), and after 1 h 30 min (middle panels) and 3 h (right panels) after platting (*arrows* indicate some migratory cells; scale bar = 50 µm). Data are the mean ± S.E.M. of three independent experiments in NS derived from 6 mice (3 WT and 3 YAC128) with 6 months of age and 6 mice (3 WT and 3 YAC128) with 10 months of age. Average number of migratory cells analysed out of the NS (*per* experiment): *PLL*: 6 mo n = 9/13 (WT/YAC128), 10 mo n= 12/10 (WT/YAC128); *FN*: 6 mo n=17/23 (WT/YAC128), 10 mo n = 12 (WT and YAC128). Statistical analysis (two-way ANOVA with Bonferroni post-hoc test): $^{\#}$ P<0.05 and $^{\#\#\#}$ P<0.001, compared to WT; * P<0.05 and *** P<0.001, compared to 6 mo mice.

3.4.3. SVZ-derived cells from mild symptomatic HD mice show increased differentiation into neuron-like cells – effect of BDNF and extracellular matrix

We further examined the neuronal differentiation potential of WT and YAC128 cells. The neurotrophin BDNF was previously shown to stimulate both migration and differentiation in the adult rat brain (Benraiss *et al*., 2001; Zigova *et al*., 1998). Thus, to determine possible differences in neuronal differentiation potential of SVZ-derived cells from YAC128 and WT animals, NS were cultured on PLL or FN-coated coverslips for 7 days, in the absence (-) or presence (+) of a physiological concentration of BDNF (5 ng/mL) (e.g. Petridis and El Maarouf, 2011).

Genotype-related differences regarding neuronal differentiation (considering the number of MAP2+ cells) were observed in 6 mo cells plated on PLL, but not in 10 mo cells (Fig. 3.3A, C and 3.3D, F). At early stage of HD YAC128 mice, at 3 months of age, no differences in neuronal differentiation were detected between YAC128 and WT cells either (data not shown). At 6 mo, YAC128 cells not only were more prone to differentiate into neuronal-like cells (MAP2+ cells; Fig. 3.3A), but also showed increased synapse labeling (synaptophysin positive cells, Synapt+; Fig. 3.3B), when compared to WT cells. Moreover, differentiation into MAP2+ and Synapt+ cells was enhanced by BDNF (5 ng/mL) in NS derived from YAC128 mice at 6 months of age; nevertheless, no changes in Synapt+ were observed in WT cells subjected to BDNF stimulus. Older WT cells, but not YAC128 cells, responded to BDNF stimulus, resulting in more MAP2+ cells (Fig. 3.3D, F). Conversely, Synapt+ labeling of both WT and YAC128 10 mo cells was positively influenced by the neurotrophin (+BDNF, Fig. 3.3E, F).

Despite the increased migration promoted by plating the NS on FN, and in contrast with the differences in neuronal differentiation observed in NS plated on PLL, no major genotype-related differences were observed regarding MAP2 or synaptophysin labeling in cells plated on FN, either at 6 or 10 mo, before and after exposure to BDNF (Fig. 3.3G-I and 3.3J-L). The non-responsiveness of FN-plated cells to BDNF may be accounted for by enhanced differentiation under basal conditions. Indeed, both 6 mo and 10 mo WT population showed a higher number of MAP2+ cells when plated on FN, compared to PLL, in the absence of BDNF ($P<0.001$; Fig. 3.3G, J *vs* 3.3A, D, respectively). On the other hand, under basal conditions, 10 mo WT and YAC128 cells plated on FN showed increased Synapt+ labeling, compared to PLL ($P<0.05$, Fig. 3.3K *vs* 3.3E), suggesting that FN may promote synapse formation.

In the present work, we observed that age is an important factor affecting neuronal differentiation. Accordingly, older cells retained a lower capacity to differentiate into neurons, as evaluated by a decreased number of MAP2+ ($P<0.001$) and Synapt+ ($P<0.01$, WT; $P<0.001$, YAC128) cells obtained from 10 (Fig. 3.3D-F) *vs* 6 (Fig. 3.3A-C) mo mice-derived cells plated on PLL. Moreover, 10 mo NS plated on FN showed a decrease in MAP2+ cells ($P<0.001$, WT; $P<0.01$, YAC128), compared to 6 mo NS (Fig. 3.3J, L and 3.3G, I). Despite this, the number of Synapt+ cells plated on FN was not affected by aging (Fig. 3.3H and 3.3K).

Poly-L-Lysine

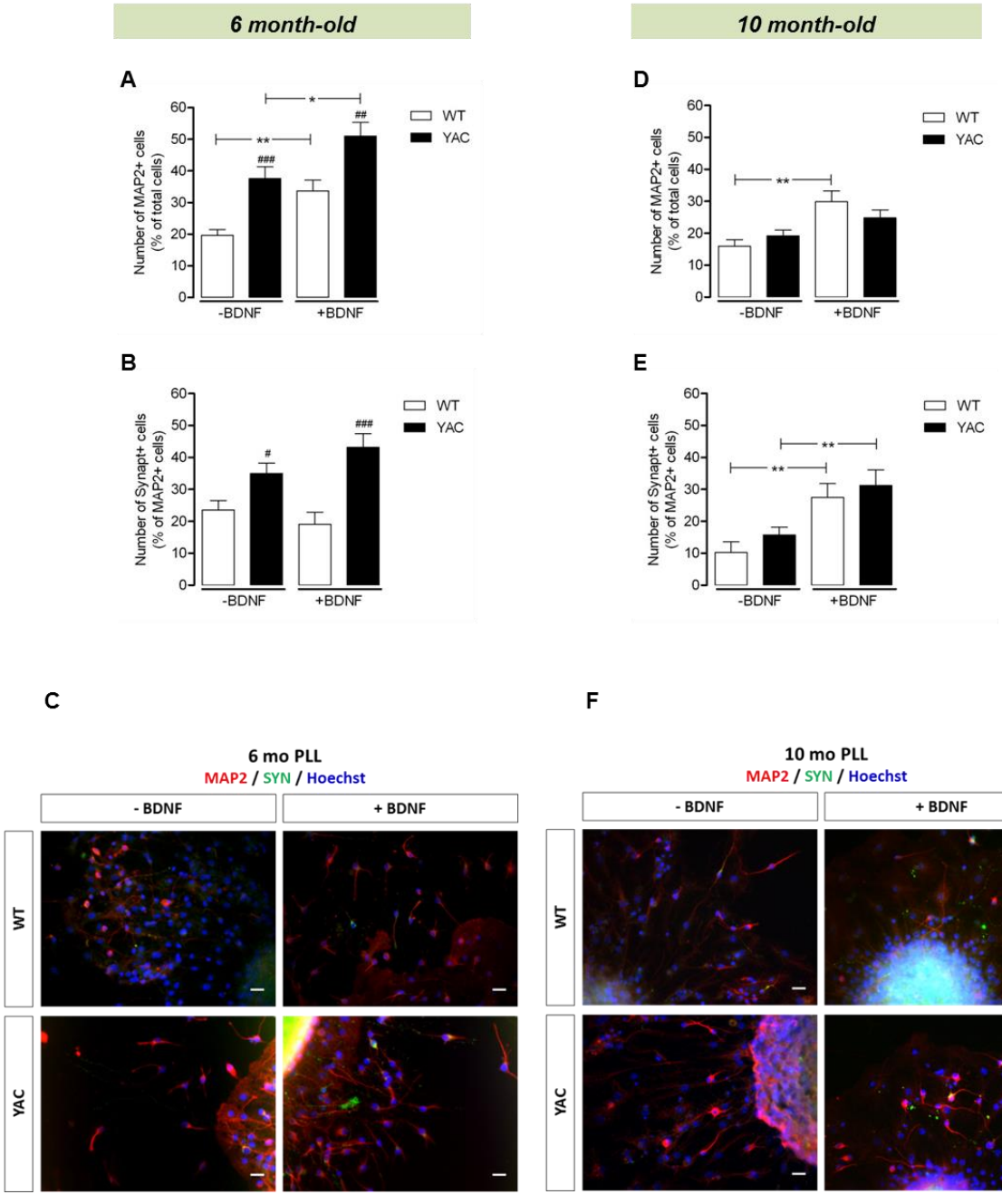

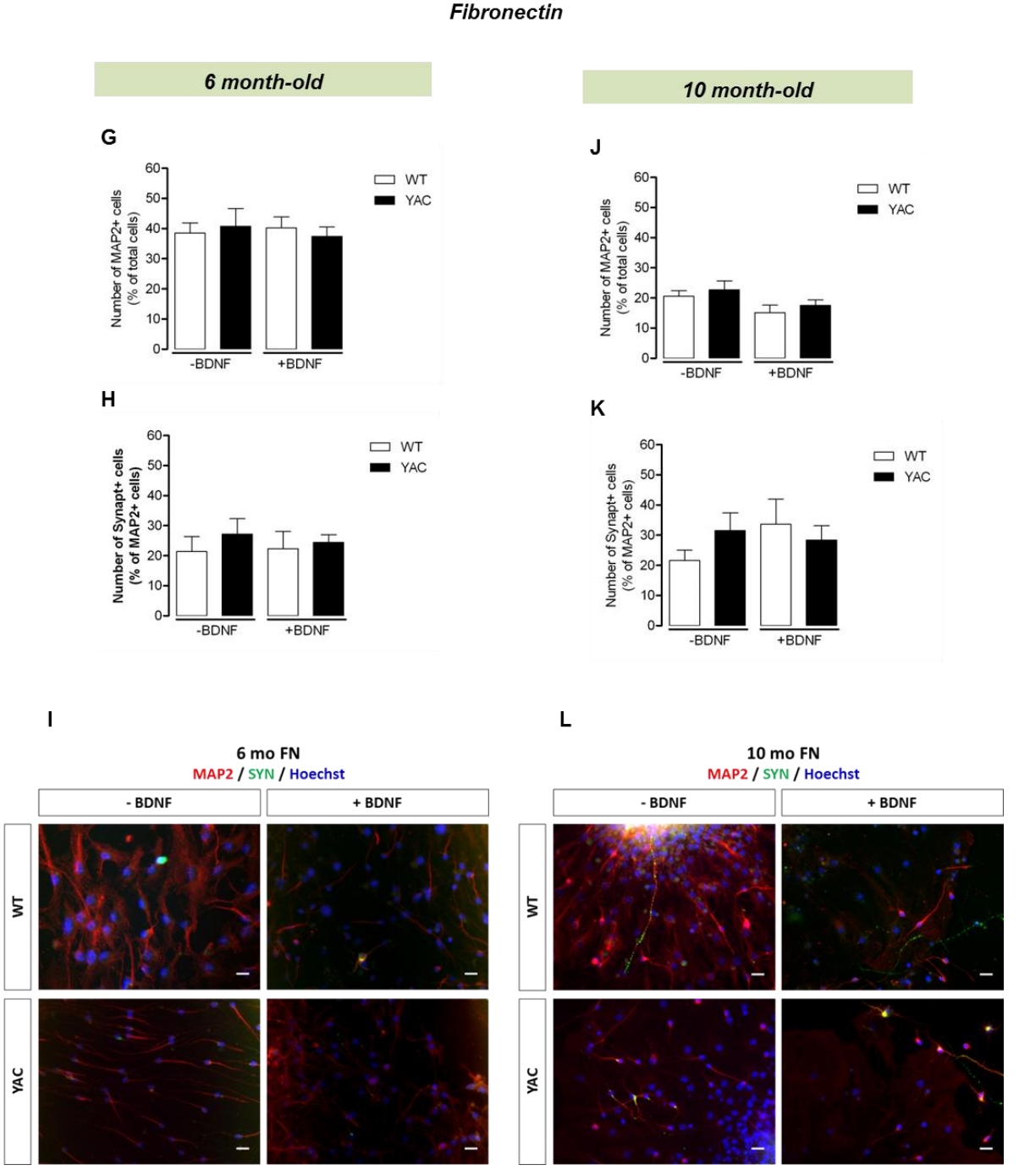

Figure 3.3 – Neuronal differentiation of WT and YAC128 neurosphere-derived cells. Cells were isolated from WT and YAC128 mice SVZ, at 6 and 10 mo and maintained in culture as NS in the presence of EGF (20 ng/mL). After 2-4 passages, cells were plated on PLL or FN covered coverslips, without EGF and let to differentiate for 7 days, in the absence (-) or presence (+) of BDNF (5 ng/mL). Cells were stained with anti-microtubule-associated protein (MAP)-2 (a neuronal marker) or with anti-synaptophysin (Synapt+; SYN, in images) (marker for synaptic vesicles) and exposed to Hoechst (2 µg/mL), which binds to DNA (nuclear marker). Data depicted in graphs correspond to the percentage of MAP2+ and Synapt+ cells plated on PLL at 6 (**A** and **B**) and 10

months of age (**D** and **E**), and on FN at 6 (**G** and **H**) and 10 months of age (**J** and **K**). **C** and **F** (PLL, 6 and 10 mo) and **I** and **L** (FN, 6 and 10 mo) show fluorescence representative images of cells undergoing differentiation (scale bar = 20 μm). Data are the mean ± S.E.M. of three independent experiments per condition, using 6 mice (3 WT and 3 YAC128) with 6 or 10 months of age. Average of cells counted, *per* field, in 5 different fields (-BDNF/+BDNF), in: i) *PLL*, at 6 mo WT= 142/89 or YAC128= 83/61; ii) *PLL* at 10 mo WT= 75/55 or YAC128= 84/53; iii) *FN* at 6 mo WT= 72/113 or YAC128= 70/86; and iv) *FN* at 10 mo WT= 77/70 or YAC128= 78/79. Statistics (two-way ANOVA with Bonferroni post-hoc test): $^{\#}$ P<0.05, $^{\#\#}$ P<0.01 and $^{\#\#\#}$ P<0.001, compared to WT; *P<0.05 and ** P<0.01, compared to BDNF.

3.4.4. Age-dependent reduced levels of BDNF forms and TrkB receptors in SVZ-derived neurospheres

In order to explain genotype and age-dependent differences in response to BDNF, we further determined the levels of BDNF and its receptor, TrkB, in 6 and 10 mo NS obtained from WT and YAC128 mice (Fig. 3.4). BDNF is synthesized as a 32 kDa precursor that is processed in the *trans*-Golgi or in secretory vesicles into mature BDNF (14 kDa) (e.g. Mowla *et al*., 2001). The 28 kDa form is also a product of proBDNF cleavage, but it seems to be generated through a distinct process (Mowla *et al*., 2001). Western blotting analysis of pro-, mature and the intermediate form of 28 kDa of BDNF revealed that all forms of BDNF tend to decrease with age, both in WT and YAC128 NS (Fig. 3.4A-C and 3.4F; see also *Supplementary data*, Fig. S3.2A-C). Data were significantly different in WT cells for proBDNF (Fig. 3.4A) and BDNF 28 kDa (Fig. 3.4C) forms. In 10 mo YAC128 NS the reduction in proBDNF was also significantly different when compared to pre-symptomatic 3 mo mice (P<0.05; *Supplementary data*, Fig. S3.2). A correspondent, although non-significant, age-dependent decrease in 28 kDa form and mature BDNF (15 kDa) were also observed (Fig. S3.2B, C).

Likewise, we observed a significant decrease in FL- and truncated (T-) TrkB receptor protein levels due to aging, but not to genotype (Fig. 3.4D, E and F). Indeed, WT NS showed a reduction in FL-TrkB (Fig. 3.4D) and both WT and YAC128 NS showed decreased T-TrkB receptor levels (Fig. 3.4E) at 10 months of age. Although statistically not significant NS derived from mild symptomatic YAC128 mice have slightly lower TrkB expression levels than WT mice (Fig. 3.4D, E). T-TrkB protein levels were significantly increased in WT (P<0.001) and YAC128 cells (P<0.05) at 6, compared to 3 mo (*Supplementary data*, Fig. S3.2); nevertheless, levels of FL-TrkB receptors displayed a trend for an age-dependent decrease in NS from YAC128 mice, from 3 to 10 mo

(*Supplementary data*, Fig. S3.2). Indeed, decreased response to BDNF-induced differentiation in aged NS (Fig. 3.3) may be in agreement with decreased levels of FL-TrkB receptors.

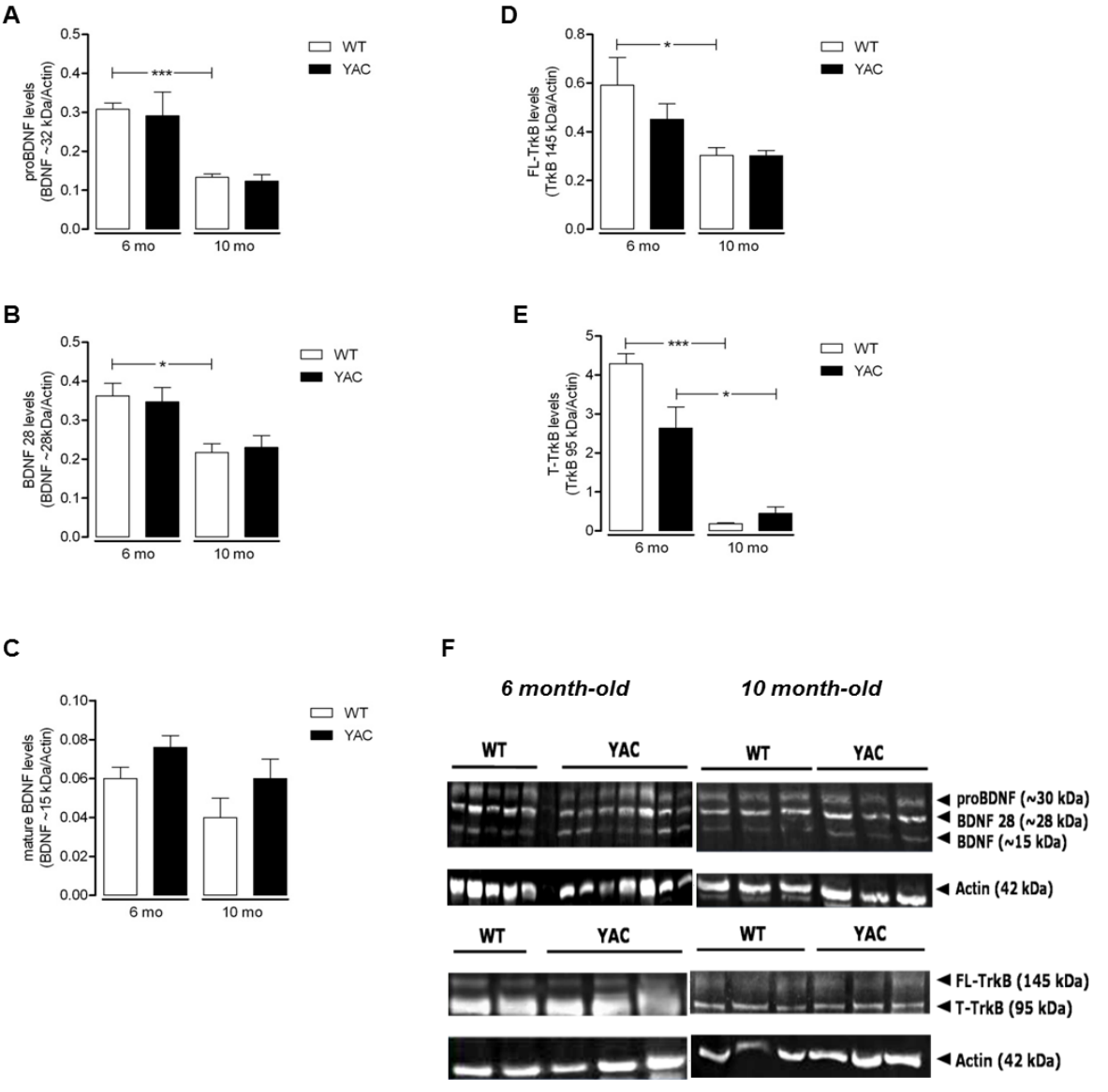

Figure 3.4 – Protein levels of BDNF forms and TrkB receptors in WT and YAC128 SVZ-derived neurospheres. Cells were isolated from 6 and 10 mo WT and YAC128 mice SVZ and kept in culture as NS in the presence of EGF (20 ng/mL). Cell extracts were performed after 5 passages and analyzed by Western blotting. (**A**-**C**) Protein levels of pro, intermediate form of 28 kDa and mature BDNF. (**D**-**E**) Protein levels of full length (FL)- and truncated (T-) TrkB receptor. Protein expression levels were normalized for actin. (**F**) Representative Western blots. Data are the mean ± S.E.M. of three to ten independent analysis from 13 (5 WT and 8 YAC128) 6 mo mice

and 6 (3 WT and 3 YAC128) 10 mo mice. Statistics (two-way ANOVA with Bonferroni post-hoc test): * P<0.05, *** P<0.001.

3.4.5. SVZ-derived cells from mild symptomatic HD mice exhibited increased KCl-mediated Ca^{2+} response and higher mitochondrial membrane potential

Taking into account that measurement of intracellular free Ca^{2+} (Ca^{2+}_i) oscillation is a practical way to characterize functional undifferentiated *vs* differentiated cells (Agasse *et al*., 2008), we further characterized *in situ* Ca^{2+}_i and $\Delta\Psi m$ changes by single cell simultaneous analysis of Fura-2 and Rh123 fluorescence, respectively, in response to potassium chloride (KCl) followed by histamine (His) stimulation, based on previously described protocols (Agasse *et al*., 2008; Ward *et al*. 2000; Rego *et al.,* 2001). Agasse and co-authors (2008) showed that mature SVZ-derived neurons were mostly KCl responsive, whereas immature cells responded more to His. In initial experiments we applied the protocol based on KCl and His stimulation to embryonic (E17) rat cortical neurons after eight days in culture; in these cells about 94% of cells responded to KCl, against 6% His-responsive cells (supplementary Fig. S3.3A). Cells were also exposed simultaneously to FCCP (protonophore that collapses $\Delta\Psi m$) and oligomycin (ATP synthase inhibitor that prevents H^+ flux through ATP synthase and thus ATP hydrolysis under conditions affecting mitochondrial respiratory chain function) to induce complete mitochondrial depolarization (e.g. Ward *et al*., 2000; as depicted in supplementary Fig. S3.3B).

YAC128 cells plated on PLL obtained from 6 mo mice showed an increase in Ca^{2+}_i levels in response to KCl, when compared to WT cells, which was enhanced in the presence of BDNF (Fig. 3.5A), suggesting the presence of more committed neuronal cells in YAC128 cells at this age. Cells from 6 mo YAC128 mice also exhibited a large rise in Ca^{2+}_i in response to His, further evidencing the presence of undifferentiated cells. Interestingly, the response evoked by His was significantly decreased in BDNF-treated YAC128 cells, which might reflect maturation of neuronal progenitors promoted by BDNF treatment. Notably, Ca^{2+}_i changes were mostly accompanied by slight alterations in Rh123 fluorescence; fluorescence increase results from the release of probe from mitochondria and thus slight mitochondrial depolarization, whereas a decrease in fluorescence reflects increased mitochondrial uptake due to probe quenching within the organelle and thus slight increased mitochondrial membrane potential (Fig. 3.5B, F and J). Interestingly,

while BDNF treatment caused a slight depolarization in KCl-responsive YAC128 cells, the neurotrophin slightly increased mitochondrial potential in YAC128 cells responding to His. After these stimuli, 6 mo-YAC128 cells displayed high mitochondrial Rh123 release induced by FCCP plus oligomycin (to completely depolarize mitochondria and thus release the total accumulated probe), compared to WT cells (Fig. 3.5D), reflecting increased $\Delta\Psi m$, which was associated with slight increased mitochondrial Ca^{2+} retention (Fig. 3.5C).

In older cells plated on PLL, slight differences in Ca^{2+}_i levels were mainly due to BDNF exposure. BDNF improved the Ca^{2+}_i response of 10 mo YAC128 cells to KCl, and the Ca^{2+}_i response of both WT and YAC128 cells to His (Fig. 3.5E). Along with the increase in Ca^{2+}_i, BDNF exposure also slightly depolarized mitochondria following KCl or His stimuli (Fig. 3.5F). Interestingly, 10 mo YAC128 cells were less responsive to KCl or His stimuli, when compared to 6 mo cells in terms of Ca^{2+}_i ($P<0.001$) (Fig. 3.5E *vs.* 3.5A). Notably, in contrast to 6 mo cells, 10 mo YAC128 KCl-responsive cells exhibited slight mitochondrial depolarization (Fig. 3.5F). Nevertheless, complete mitochondrial depolarization with FCCP plus oligomycin did not evoke a differential release of Rh123 from the organelle in untreated 10 mo YAC128 cells, in contrast to 6 mo cells, suggesting the presence of less polarized mitochondria in late, compared to mild, symptomatic YAC128 cells (Fig. 3.5H *vs.* 3.5D). Interestingly, YAC128 mitochondria at 10 months of age retained larger amounts of Ca^{2+} (Fig. 3.5G), compared to WT cells and to 6 mo YAC128 cells. Conversely, treatment with BDNF significantly improved mitochondrial membrane potential in 10 mo cells plated on PLL (Fig. 3.5H). Interestingly, the number of fragmented/condensed nuclei (determined by Hoechst staining) was positively influenced by aging. WT and YAC128 cells plated on PLL showed higher number of apoptotic-like cells at 10 mo than at 6 mo, independently of BDNF stimuli (data not shown).

Because 10 mo SVZ NS plated on FN showed a decrease in neuronal differentiation compared to 6 mo NS, we further determined the effects of KCl and His in Ca^{2+}_i and $\Delta\Psi m$ changes in SVZ NS derived from mice at the older age (Fig. 3.5I-L). Remarkably, the effects seen at 10 months of age in YAC128 cells (when compared to WT cells) plated on PLL were exacerbated in cells plated on FN, namely decreased Ca^{2+}_i levels following KCl and His stimuli and enhanced KCl-induced mitochondrial depolarization (Fig. 3.5I, J); moreover, the latter was almost completely ameliorated by BDNF. Although no genotype-related changes were observed in total mitochondrial accumulation of Rh123 or Ca^{2+}, exposure to BDNF significantly decreased mitochondrial Ca^{2+} accumulation and

increased mitochondrial membrane potential (evidenced through increased Rh123 accumulation), as observed after complete mitochondrial depolarization with FCCP plus oligomycin (Fig. 3.5K, L).

6 month-old

Poly-L-Lysine

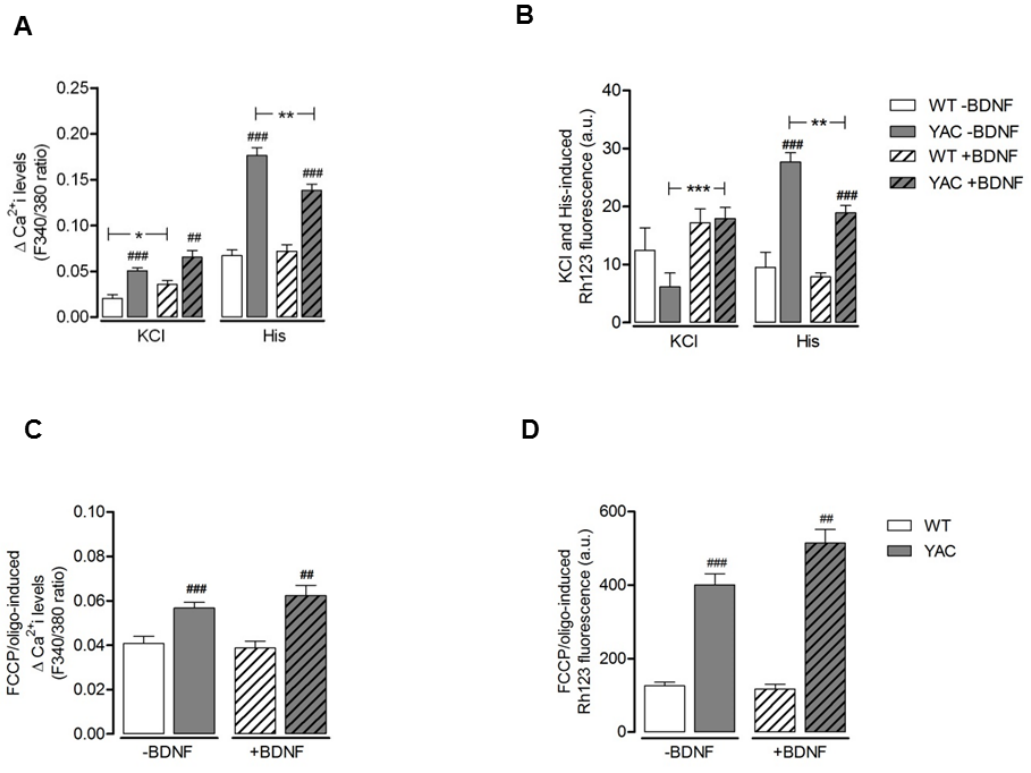

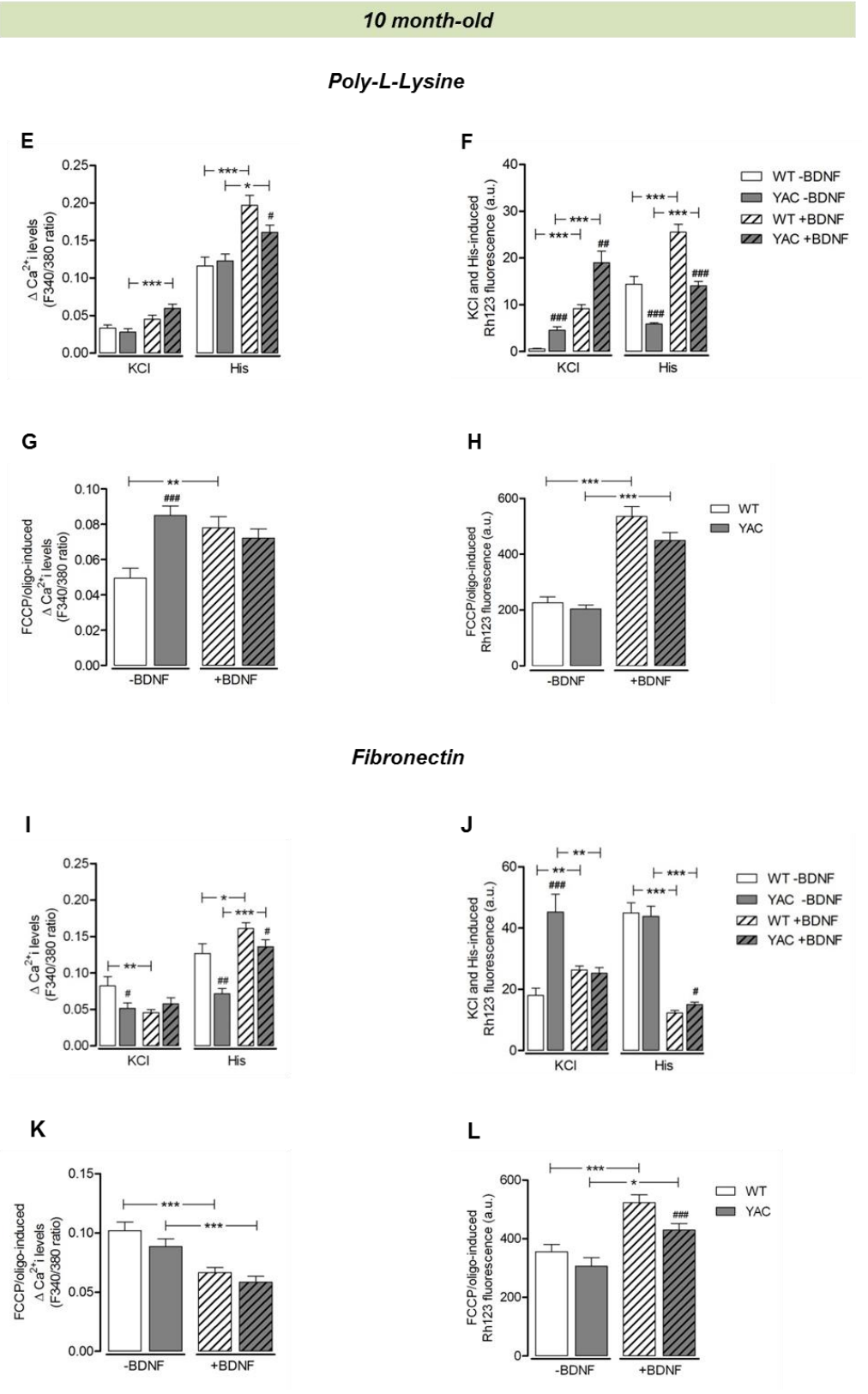

Figure 3.5 – Single cell analysis of intracellular Ca^{2+} levels and mitochondrial membrane potential of WT and YAC128 neurosphere-derived cells. Cells were isolated from WT and

YAC128 mice SVZ, at 6 (**A-D**) and 10 (**E-L**) mo and kept in culture as NS in the presence of EGF (20 ng/mL). After 2-4 passages, cells were plated on PLL (**A-H**) or FN (**I-L**) covered coverslips, without EGF, and let to differentiate for 7 days, in the absence or presence of BDNF (5 ng/mL). Cells were washed in Krebs medium and incubated with rhodamine 123 (Rh123, 1.3 µM), in quench-mode for 5 min and further loaded with Fura-2/AM (5 µM) for 45 min before stimulation with KCl (50 mM) for 2 min, followed by histamine (His, 100 µM), for another 2 min. Cells were then exposed to oligomycin (oligo, 2 µg/mL) plus FCCP (2 µM). *In situ* single cell analysis of intracellular Ca^{2+} levels (**A, E** and **I**) and transient alterations in mitochondrial membrane potential ($\Delta\Psi_m$) (**B**, **F** and **J**) were determined by following the changes, respectively, in 340/380 nm ratio of Fura-2 and Rh123 fluorescence in the cell body. Mitochondrial Ca^{2+} accumulation (**C, G** and **K**) and Rh123 accumulation, defining overall mitochondrial $\Delta\Psi_m$ (**D, H** and **L**), were evaluated after exposure to FCCP/oligo. At the end of the experiment, ionomycin (2 µM) was added to the culture in order to obtain maximum Fura-2 fluorescence (not shown). Data are the mean ± S.E.M. of three independent experiments per condition, using 6 mice (3 WT and 3 YAC128) with 6 or 10 months of age. Average number of analyzed cells (-BDNF/+BDNF) obtained from young and aged mice: i) **PLL**, *6 mo*: WT n= 69/70, YAC128 n= 158/160; ii) **PLL**, *10 mo*: WT n= 55/96, YAC128 n= 162/115; iii) **FN**, *10 mo*: WT n= 101/124, YAC128 n= 82/84. Statistical analysis (two-way ANOVA with Bonferroni post-hoc test): $^{\#}$ P<0.05, $^{\#\#}$ P<0.01 and $^{\#\#\#}$ P<0.001, compared to WT; * P<0.05, ** P<0.01 and *** P<0.001, compared to BDNF.

3.5. Discussion

This work demonstrates that expression of human FL-mHtt does not impair cell cycle and proliferation or induce early apoptosis in YAC128 mice SVZ-derived NS. Interestingly, mild symptomatic YAC128 NS cells showed increase migration and neuronal differentiation, along with higher KCl-responsiveness to Ca^{2+}_i rise and higher mitochondrial potential, compared to WT cells. Notably, these changes were lost in late (10 mo) symptomatic YAC128 SVZ-derived cells, and further exacerbated after plating the NS on FN. This work reveals significant age-dependent differences concerning the involvement of calcium handling, mitochondrial function and BDNF effect in SVZ-derived cells from transgenic HD mice along the symptomatic-like stages of the disease.

The cell cycle profile of SVZ NS-derived cells showed significant differences related to aging rather than to genotype, which appears to be in agreement with Lorincz and Zawistowsk (2009). These authors reported similar results with embryonic stem cells (ESC) lines derived from HD KI mice. The authors showed that the proportion of undifferentiated ESC in the cell cycle phase G1, or S and G2/M was not significantly different between *Hdh*CAG7 and *Hdh*CAG150 ESC cell lines. In our study, G0/G1 arrest of 6 mo cells might be in part due to a cell cycle exit in order to undergo differentiation.

Nevertheless, proliferation and early apoptosis were similar in WT and YAC128 SVZ-derived cells.

An important cell event that is implicated in the replacement of injured cells is migration. Cells need to migrate from their origin site towards their target region via a substrate or other cells (e.g. Jacques *et al.,* 1998); therefore, ECM proteins play a crucial role is this process. ECM can be secreted by cells in the stem cell niche (Alvarez-Buylla and Lim, 2004) as well as in the neurosphere system (Campos *et al*., 2004). Interestingly, YAC128 NS-derived cells plated on PLL showed improved migration in comparison with WT cells at mild symptomatic mice. This could be due to the presence of more committed cells (i.e. progenitor cells) in YAC128 NS than in the WT NS at this age. Concordantly, in YAC128 cells at 6 months of age we observed a rise in intracellular Ca^{2+} following histamine stimulus. Soares and Sotelo (2004) previously demonstrated that adult SVZ progenitors migrate further than neural stem cells. Nevertheless, such difference was no longer observed in cells derived from late (10 mo) symptomatic animals. The different profile response to histamine of 6 and 10 mo cells might indicate the presence of different types of cells, under different degrees of differentiation. The fact that YAC128 SVZ-derived cells showed enhanced migration, increased immature His-responsive cells and increased neuronal differentiation (as discussed next) may reflect the maintenance of an equilibrium between immature cells and neuronal progenitors and/or neurons. Interestingly, aging *per se* apparently leads to more histamine-responsive WT cells, suggestive of less neuronal committed progenitor cells; concordantly, older NS exhibit increased number of EdU+ cells.

FN is one of the ECM proteins known to promote cell migration and differentiation (Tate *et al*., 2002; Flanagan *et al*., 2006; Silva *et al*., 2009). Interestingly, in our study, FN promoted both cell velocity and migratory distance of WT and YAC128 cells, at 6 and 10 mo. These results are in agreement with Kearns and co-workers (2003) who registered higher velocity of cerebellar neurospheres derived from post-natal mice in FN, compared to laminin, another ECM protein. Moreover, cells plated on laminin showed lower velocity and took longer time to reach maximal velocity than cells plated on FN (Kearns *et al.,* 2003).

Along with increased migratory capacity, 6 mo YAC128 SVZ-derived cells plated on PLL exhibited increased neuronal differentiation (MAP2+ and Synapt+ cells), which was promoted by BDNF. These data revealed a YAC128 cell population committed to neuron phenotype, in agreement with data shown by Lorincz and Zawistowsk (2009); previously,

these authors demonstrated that HD SVZ-derived stem cells (from KI mice) had increased neural progenitors and neurogenesis compared to WT cells, which was related to elevated expression of transcripts involved in neuronal differentiation. Gene ontology analysis identified migration, transcriptional regulation, morphogenesis and receptor binding as processes mediating increased neuronal differentiation of *Hdh*CAG150 ESCs (Lorincz and Zawistowsk, 2009). These authors also observed that synaptophysin, a protein important in synaptic transmission, appeared earlier and was more reactive in *Hdh*CAG150 compared to *Hdh*CAG7. It is worth noticing that, in general, our data observed at mild symptomatic stages (6 mo) are in agreement with Lorincz and Zawistowsk (2009); however, the authors only used P20 animals in their experiments and thus did not evaluate differences in aged animals.

Indeed, in our study, we further evaluate the effect of aging. We demonstrate decreased neuronal differentiation evoked by BDNF in 10 mo YAC128 cells plated on PLL (compared to 6 mo cells) that can be related with an age-dependent decrease in FL-TrkB receptors. Despite this, at this late stage, WT cells responded significantly to exogenous BDNF when considering MAP2+ labeling, suggesting that formation of new neurons may be dependent on BDNF-evoked activation of relevant intracellular signaling pathways. Notwithstanding, BDNF exposure also favored 10 mo WT and YAC128 synapse formation, which might reflect increased neuron maturation. BDNF binds preferentially to TrkB receptor, and is widely described as an important neurotrophin in neuronal differentiation, mainly regulating neuron maturation and viability (Perez-Navarro *et al*., 2000; Canals *et al.*, 2001; Petersén *et al*., 2001; Bath and Lee, 2010, for review). Interestingly, different concentrations of BDNF have different biological effects on SVZ-cells, as recently described by Petridis and colleagues (2011). Concentrations of BDNF in the physiological range (e.g. 1 ng/mL) stimulated migration, whereas doses of 10 ng/mL or higher induced SVZ cell differentiation and reduced migration (Petridis and El Maarouf, 2011). The low concentration of BDNF used in the present study (5 ng/mL) was able to evoke SVZ cell differentiation.

Furthermore, we show an age-, but not genotype-, dependent decrease in BDNF levels in the SVZ NS cells. In contrast, BDNF levels were previously demonstrated to be reduced in the cortex and striatum of HD patients as well as in mouse and cell models of the disease (Zuccato and Cattaneo, 2007, for review) and recently TrkB receptors were also reported to be decreased (Zuccato *et al*., 2008; Ginés *et al*., 2006). In prior studies, BDNF and TrkB mRNA were also evaluated in hippocampal neural progenitor cells (NPC)

derived from adult mice (Li *et al*., 2008). These cells expressed TrkB receptors and responded to BDNF. The authors also showed that ablation of TrkB in NPC, but not in differentiated neurons, impaired hippocampal proliferation and neurogenesis *in vivo* and that the dividing cells were more prone to prematurely exit the cell cycle (Li *et al*., 2008). Even though 10 mo WT cells showed a significant reduction in pro- and 28 kDa-BDNF levels, no changes were observed in mature BDNF. The maintenance of relatively similar levels of intracellular mature BDNF might reflect deficient release of the neurotrophin in aged cells. YAC128 NS also appeared to have slightly more mature BDNF protein, at both ages. Because proBDNF levels were not different between WT and YAC128 cells, its processing into the mature form does not seem to be affected, again raising the question of whether the observed results may be due to a deficient release of BDNF in HD cells, as a consequence of altered transport of BDNF-containing vesicles as observed previously in neuronal cells derived from KI mice (Gauthier *et al*., 2004).

Mature neurons are excitable cells and thus membrane depolarization occurs in response to KCl, which is paralleled with an increase in intracellular Ca^{2+} levels via voltage sensitive calcium channels (VSCC). KCl depolarization is attributable to neuronal differentiation, since VSCC are absent or expressed at very low levels in neural precursor cells (Sah *et al*., 1997; Maric *et al*., 2000). Furthermore, less differentiated cells stimulated with histamine also display increased Ca^{2+} levels due to the activation of histamine receptor 1 (H1R), expressed in immature SVZ cells, and leading to the mobilization of Ca^{2+} from intracellular stores, as demonstrated in prior studies (Tran *et al*., 2004, Agasse *et al*., 2008; Molina-Hernández and Velasco, 2008). Therefore, evidence for increased neuronal differentiation potential of YAC128 cells from mild symptomatic animals was corroborated by an increased response to KCl, when compared to WT cells. Importantly, KCl-evoked increased intracellular Ca^{2+} levels were not observed in older cells, largely supporting the results from MAP2+ labeling. Older YAC128 SVZ-derived cells displayed more depolarized mitochondria following the KCl stimulus, implicating mitochondrial depolarization without significant neuronal differentiation. Neuronal differentiation evoked by BDNF was further supported by the rise in Ca^{2+} in KCl-responsive SVZ-derived cells; interestingly, BDNF counteracted the changes in $\Delta\Psi_m$ following the KCl and His stimuli. Importantly, YAC128 mice mitochondria retained more Ca^{2+} than WT SVZ-derived cells, at 6 and particularly at 10 mo, concordantly with mitochondrial depolarization at later stages of the disease. Improved mitochondrial Ca^{2+} loading capacity was previously shown by us in mitochondria isolated from old YAC mice brain (Oliveira *et al*., 2007),

supporting a possible compensatory mechanism in the HD mice model. Importantly, plating the SVZ NS cells on FN largely promoted cell migration and neuronal differentiation (in the absence of BDNF) at 6 mo, which is in accordance with the effect of FN in promoting cell migration and differentiation (Tate *et al*., 2002; Flanagan *et al*., 2006; Silva *et al*., 2009). Moreover we have previously demonstrated that FN *per se* significantly induced a specific neuronal phenotype (i.e. GABAergic) of neurosphere-derived cells from post-natal mice brain (Silva *et al.*, 2009). Furthermore, the ECM FN exacerbated the effects observed in older (10 mo) YAC128 SVZ NS cells plated on PLL, namely by evidencing decreased neuronal differentiation and increased mitochondrial depolarization in KCl-responsive cells, which were ameliorated by BDNF, further supporting the protective effects of this neurotrophin.

Adult SVZ has been described to drive new neurons. However, these cells are not able to successfully replace the dying cells in several neurodegenerative disorders, such as HD, in a way that could circumvent major disabilities caused by neurodegeneration, an issue that still remains to be clarified. In this context, in the present work we verified important differences between HD and WT cells related to cell differentiation along disease progression, which are accompanied by altered mitochondrial function. While in an undifferentiated state (e.g. NS), no genotype-related differences were observed; following differentiation in mild symptomatic conditions, YAC128-derived SVZ cells exhibited apparently compensatory mechanisms by promoting neurogenesis and increasing cell function, as revealed through the analysis of mitochondrial function. In contrast, aged YAC128 SVZ cells showed evidences of decreased neurogenic potential and mitochondrial dysfunction. Thus, our work brings new insights related with changes calcium handling, mitochondrial function and BDNF effects and their impact on neuronal differentiation in YAC128 SVZ-derived cells along disease progression, pointing out that strategies aimed to impact on SVZ-directed neurogenesis in HD might be more efficacious in early stages of symptomatology.

CHAPTER 3 SUPPLEMENTARY FIGURES

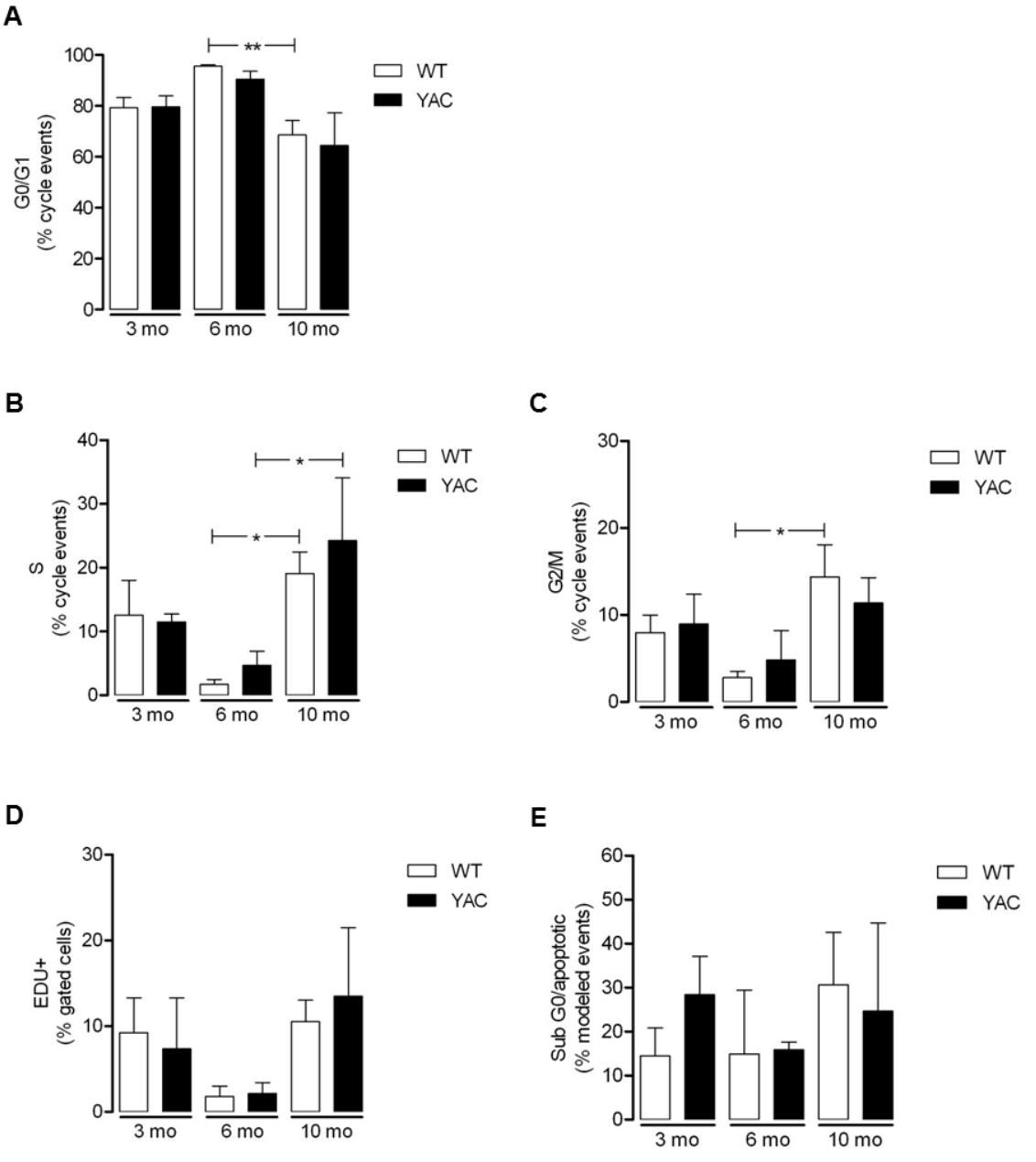

Fig. S3.1 – Cell cycle, proliferation and early apoptotic events of WT and YAC128 neurosphere-derived cells. Cells were isolated from WT and YAC128 mice SVZ at 3, 6 and 10 month-old (mo) and kept in culture as neurospheres in the presence of EGF (20 ng/mL). After 2-4 passages, cells were plated in poly-L-lysine wells for 3 days. EdU was added to the cells 4 h before fixation (70% ethanol overnight). Cell cycle (**A**-**C**), proliferation (**D**) and early apoptosis (**E**) profile were analyzed by Flow Cytometry, as described in Methods section. Data are the mean ± S.E.M. of two to four independent analysis from 6-7 (3 WT and 3-4 YAC128) mice for each age, at 3, 6 or 10 months of age. Statistics: two-way ANOVA and Bonferroni post-hoc test - * $P<0.05$, ** $P<0.01$.

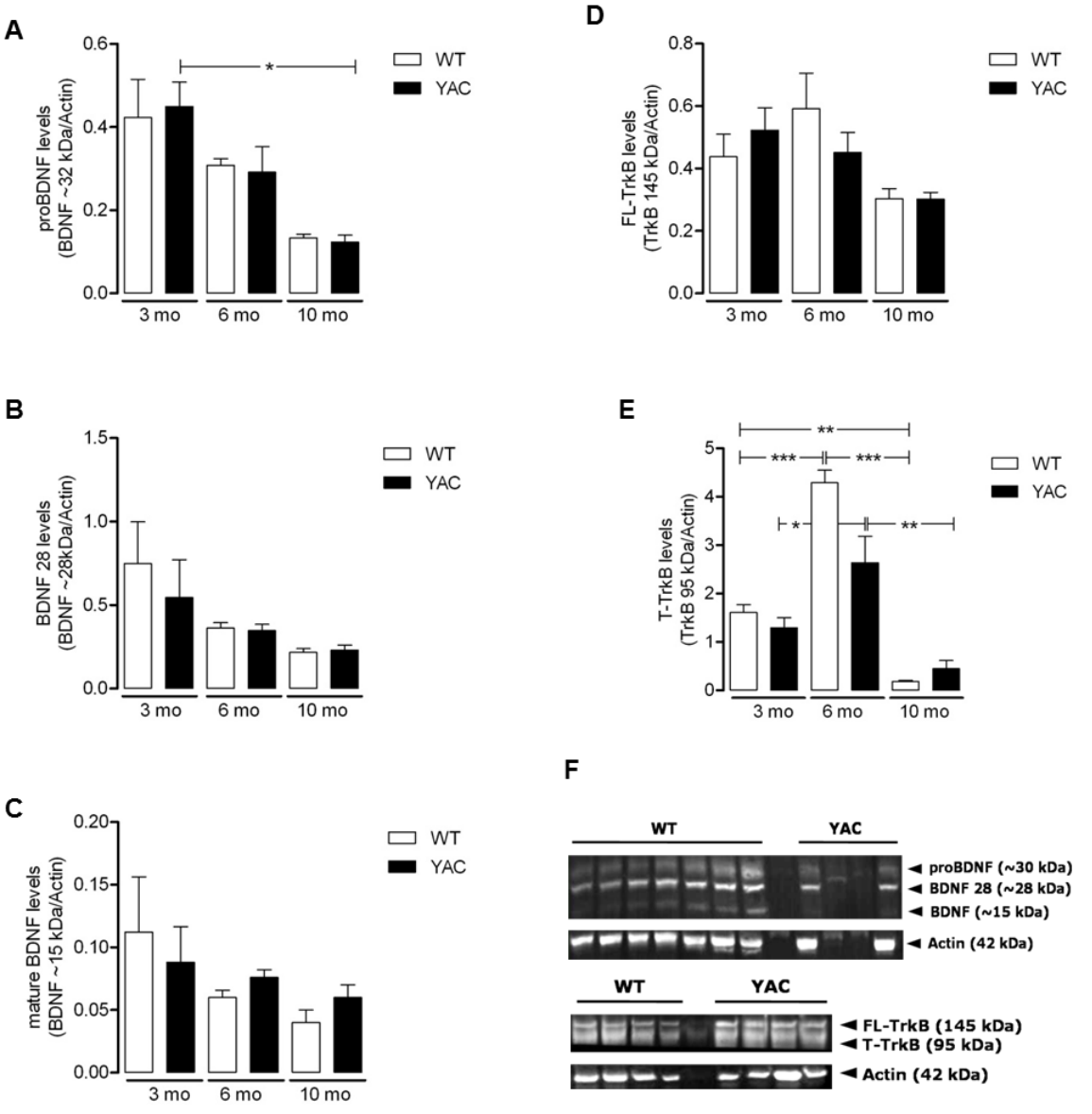

Fig. S3.2 – Protein levels of BDNF forms and TrkB receptors in WT and YAC128 SVZ-derived neurospheres. Cells were isolated from 3, 6 and 10 mo WT and YAC128 mice SVZ and kept in culture as NS in the presence of EGF (20 ng/mL). Cell extracts were performed after 5 passages and analyzed by Western blotting. (**A**-**C**) Protein levels of pro, intermediate form of 28 kDa and mature BDNF. (**D**-**E**) Protein levels of full length (FL)- and truncated (T-) TrkB receptor. Protein levels were normalized for actin. (**F**) Representative Western blot images of the experiments with neurospheres derived from 3 mo mice. Data are the mean ± S.E.M. of three to ten independent analysis from 12 (7 WT and 5 YAC) 3 mo mice, 13 (5 WT and 8 YAC128) 6 mo mice and 6 (3 WT and 3 YAC128) 10 mo mice. Statistical analysis (two-way ANOVA and Bonferroni post-hoc test): * $P<0.05$, ** $P<0.01$ and *** $P<0.001$.

A

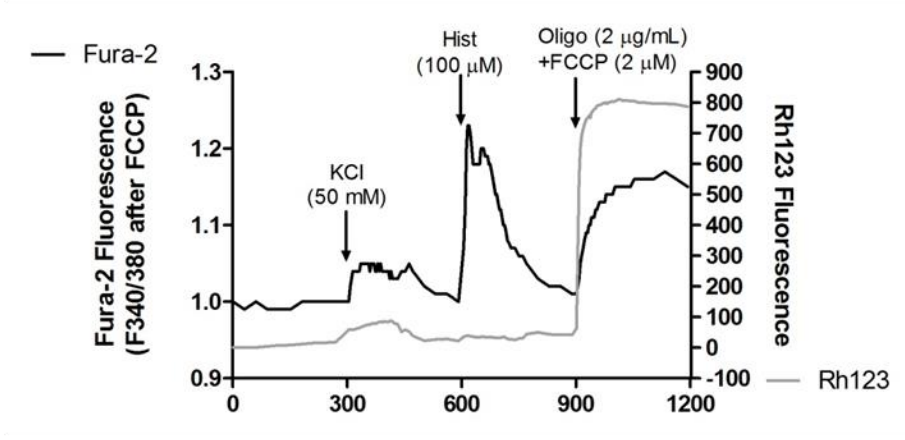

B

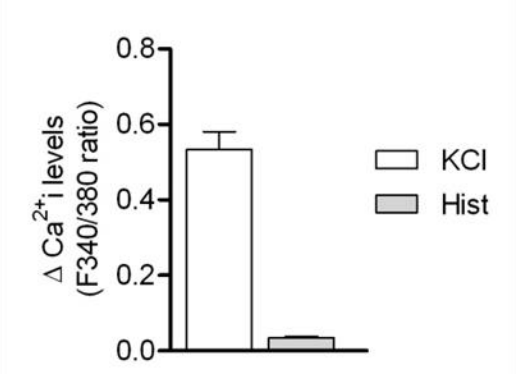

Fig. S3.3 – Single cell analysis of intracellular Ca^{2+} levels and mitochondrial membrane potential procedure. (A) Intracellular Ca^{2+} levels and mitochondrial membrane potential analysis in neurosphere-derived cells (data depicted in Fig. 5). Cells were washed in Krebs medium and incubated with rhodamine 123 (Rh123, 1.3 μM), in quench-mode, for 5 min and further loaded with both Rh123 and Fura-2/AM (5 μM) for 45 min, before stimulation with KCl (50 mM) for 2 min, followed by histamine (His, 100 μM), for another 2 min. Cells were then exposed to oligomycin (oligo, 2 μg/mL) plus FCCP (2 μM). *In situ* single cell analysis of intracellular Ca^{2+} levels and transient alterations in mitochondrial membrane potential ($\Delta\Psi_m$) were determined by following the changes, respectively, in 340/380 nm ratio of Fura-2 and Rh123 fluorescence in the cell body. Mitochondrial Ca^{2+} accumulation and Rh123 accumulation, defining overall mitochondrial $\Delta\Psi_m$, were evaluated after exposure to FCCP/oligo. At the end of the experiment, ionomycin (2 μM) was added to the culture in order to obtain maximum Fura-2 fluorescence (not shown). (**B**) As a control, E17 rat cortical neurons were differentiated for 8 days *in vitro* (DIV) using the same protocol of differentiation; as expected, neuron-like cells showed higher response to KCl compared to His.

CHAPTER 4

MITOCHONDRIAL RESPIRATORY CHAIN COMPLEX ACTIVITY AND BIOENERGETIC ALTERATIONS IN HUMAN PLATELETS DERIVED FROM PRE-SYMPTOMATIC AND SYMPTOMATIC HUNTINGTON'S DISEASE CARRIERS

Chapter based on the following manuscript:

Ana Silva, Sandra Almeida, Mário Laço, Ana Duarte, Joana Domingues, Catarina R Oliveira, Cristina Januário and A. Cristina Rego (2012). Mitochondrial respiratory chain complex activity and bioenergetic alterations in human platelets derived from pre-symptomatic and symptomatic Huntington's disease carriers (*Manuscript submitted to* Mitochondrion)

4.1. Abstract

Mitochondrial dysfunction has been implicated in Huntington's disease (HD) pathogenesis. We analysed the activity of mitochondrial complexes (Cx) I-IV, protein levels of selected Cx subunits and adenine nucleotides in platelet mitochondria from pre-symptomatic *versus* symptomatic HD human carriers and age-matched control individuals. Mitochondrial platelets exhibited reduced activity of citrate synthase in pre-symptomatic and Cx-I in pre-symptomatic and symptomatic HD carriers. Positive correlation between Cx activity and protein subunits was observed for Cx-I and Cx-II in symptomatic HD patient's mitochondria. Moreover, AMP increased in mitochondria from pre-symptomatic HD carriers. Results highlight mitochondrial changes occurring before the onset of HD clinical symptoms.

4.2. Introduction

HD is an autosomal, progressive and fatal neurodegenerative disorder caused by an expansion of CAG repeat in the exon 1 of HD gene, leading to an abnormal polyglutamine (polyQ) tract at the N-terminus of the huntingtin (Htt) protein (Huntington's Disease Collaborative Research Group, 1993). Clinically, HD is characterized by involuntary movements, behavioral disturbances and progressive dementia; neuropathologically, the main HD hallmark is the selective death of striatal medium spiny neurons and mutant Htt (mHtt) aggregates forming nuclear inclusions. Death of the patients occurs 15-20 years after the disease onset (for review, Gil and Rego, 2008). The mutation has been described to induce a loss of function of wild-type (WT) Htt and a gain of function of full-length (FL)-mHtt and/or of its short N-terminal fragments (Wellington et al., 2002; Li and Li, 2004). The mechanisms underlying neuronal death following polyQ expansion still remain inconclusive, but mitochondrial dysfunction has been reported as a relevant pathway in cell degeneration in HD (for review Gil and Rego, 2008; Rosenstock et al, 2010). Indeed, previous studies demonstrated that mHtt localizes to mitochondria in brain tissue (e.g. Panov *et al.,* 2002; Yu *et al*., 2003) and mitochondrial dysfunction was evident in human and mice models of HD (e.g. Oliveira *et al.,* 2006; Ferreira *et al.,* 2010). Mitochondrial enzyme complexes (Cx) are formed by the assembly of both nuclear- (n-) and mitochondrial- (mt-) encoded protein subunits, with the exception of Cx-II. In humans, nicotinamide adenine dinucleotide (NADH)–ubiquinone oxidoreductase or NADH dehydrogenase (Cx-I) comprises at least 45 subunits (38 n-encoded and 7 mt-encoded) (Pagniez-Mammeri *et al*., 2012), succinate–ubiquinone oxidoreductase or succinate dehydrogenase (Cx-II) is formed by 4 n-encoded subunits, ubiquinol-cytochrome c reductase (Cx-III) comprises 11 subunits (10 n-encoded and 3 mt-encoded), cytochrome c oxidase (COX or Cx-IV) has 13 subunits (10 n-encoded and 3 mt-encoded), and ATP synthase (Cx-V) is composed by 14 subunits (12 n-encoded and 2 mt-encoded) (Sue and Schon, 2000, for review).

Mitochondrial Cx activities have been shown to be compromised in HD. Reduced activity of Cx-II, -III and -IV was previously reported in HD human basal ganglia (Gu *et al.,* 1996; Browne *et al.,* 1997). Mitochondrial Cx-I, -II and -III activities were also found to be decreased in peripheral cells/tissues, namely Cx-I in platelets (Parker *et al*., 1990) and muscle (Arenas *et al*., 1998) and Cxs-II/III in skeletal muscle (Turner *et al.,* 2007), which could be accounted for by the presence of mHtt in these tissues. Mitochondrial

abnormalities in Cx-I and particularly Cx-IV were also described in lymphoblasts from HD patients (Sawa *et al*., 1999). However, no alterations in mitochondrial Cx activities were observed in other studies performed in HD human platelets (Powers *et al*., 2007) or in HD cybrid (cytoplasmic hybrid cells) lines, an ex-vivo human peripheral cell model based on the fusion of teratocarcinoma NT2 mitochondrial DNA-depleted cells with platelets derived from symptomatic HD patients (Swerdlow *et al.,* 1999; Ferreira *et al*., 2010). Taking into account contradictory results obtained in human platelets, the aim of this work was to evaluate changes in components of mitochondrial respiratory chain in human peripheral platelets derived from pre-symptomatic HD carriers (pre-HD) versus symptomatic HD patients and age-matched control individuals. Thus, we determined mitochondrial Cx activities, selected n- and mt-encoded subunit protein levels, and mitochondrial energy levels in platelet mitochondrial fractions. Our data show significant changes in mitochondrial complexes activities in pre-HD carriers and positive correlation with subunit protein levels in symptomatic HD patient's platelet mitochondria containing Htt fragments. Data reinforce the occurrence of mHtt-associated mitochondrial modifications before the onset of clinical symptoms.

4.3. Material and Methods

4.3.1. Reagents

Biorad Protein Reagent was from Biorad (BioRad, Hercules, CA, USA). Prostaglandin I2, decyl-Ubiquinone, acetyl-CoA, cytochrome c, NADH and anti-alpha (α)-tubulin were purchased from Sigma Chemical Co. (St. Louis, MO, USA). Antibodies against mitochondrial Cx-I NADH dehydrogenase (mitochondrial-encoded ND6 subunit (20 kDa) and nuclear-encoded ion-sulfur protein, 3 subunit (30 kDa)); Cx-II succinate dehydrogenase (nuclear-encoded ion-sulfur protein subunit (30 kDa) and flavoprotein subunit (70 kDa)) and Cx-IV cytochrome c oxidase, COX (mitochondrial-encoded subunit I (COX I, 57 kDa) and nuclear-encoded subunit Vb (COX Vb, 13 kDa)) were purchased from Molecular Probes (Invitrogen, Eugene, OR, USA). Anti-HSP60 and anti-Htt (MAB2166) were obtained from Millipore (EMD Millipore Corporation, Billerica, MA, USA). Polyvinylidene difluoride (PVDF) membrane, enhanced chemifluorescence reagent (ECF) and alkaline phosphatase-linked anti-mouse secondary antibody were purchased from Amersham Biosciences (Buckinghamshire, UK).

4.3.2. Participants

Patients were characterized according to the Unified Huntington's Disease Rating Scale (UHDRS) (Huntington Study Group, 1996). Seven genetically and clinically confirmed HD symptomatic patients, motor score from UHDRS greater than 4 points, eight pre-HD carriers and eight healthy controls (CTR) without any neurological disease were included in this study. The CAG repeats were between 43 ± 1.1 (36 to 45 CAG repeats) in pre-HD, and 44 ± 0.8 (41 to 48 CAG repeats) in symptomatic HD carriers (Table 4.1). All subjects gave informed consent for this study. Prescribed medication and the number of individuals medicated are also described in Table 4.1.

4.3.3. Platelet isolation

Human blood was drawn and collected in proper collecting tubes with anticoagulant, under direct supervision of a neurologist at Coimbra University Hospital Centre. Platelet isolation was performed according to the method described by Krige *et al.* (1992) with modifications. The blood was centrifuged at 200 x g for 10 min, at room temperature (RT). The supernatant – PRP (platelet-rich plasm) was collected and prostaglandin I2 was added at a final concentration of 0.07 nM. The PRP was centrifuged at 1000 x g for 20 min (RT) and resultant pellet resuspended in Tyrodes buffer (150 mM NaCl, 5 mM HEPES, 0.55 mM NaH2PO4, 7 mM NaHCO3, 2.7 mM KCl, 5.6 mM glucose, 1 mM EDTA-K2, pH 7.4), in an equal volume of PRP. The suspension was centrifuged at 1000 x g for 10 min (RT). The pellet was resuspended in Tyrodes buffer and centrifugations were repeated twice (in a total of three). At the end of the final centrifugation, the pellet was resuspended in 5 mL of homogenization buffer (0.25 mM sacarose, 10 mM TRIS-HCl, 1 mM EDTA-K2, at pH 7.4).

4.3.4. Isolation of mitochondrial fraction

Isolation of mitochondrial fractions from human platelets was performed according to the method described by Krige *et al* (1992) with some modifications. In brief, the cell suspension was transferred into a Parr bomb and subjected to pressurization with nitrogen at 1200 psi for 20 min, on ice. After release of N2 the homogenate was collected and further centrifuged at 1000 x g, for 15 min (4ºC). The supernatant was collected and kept at 4ºC. The pellet was further resuspended in cold homogenization buffer (6 mL) to lyse remaining cells and the procedure was repeated. The second supernatant was added to the first and further centrifuged at 8500 x g for 10 min (4ºC). The supernatant

was removed and the mitochondria-enriched pellet was resuspended in cold homogenization buffer (~150 mL), frozen in liquid N2 and kept at -80ºC. Mitochondrial-enriched fractions showed strong staining for heat shock protein (HSP)-60, a mitochondrial chaperone, and weak labeling for α-tubulin, a cytoskeletal protein (Fig. 4.1).

4.3.5. Measurement of mitochondrial respiratory chain complexes activities

Isolated platelet mitochondria were assayed for the activity of Cx I-V by spectrophotometry.

NADH–ubiquinone oxidoreductase assay – Cx-I activity was determined at 340 nm by following the decrease in NADH absorbance due to ubiquinone (50 µM) reduction to ubiquinol (Ragan *et al*., 1987). Cx-I activity was expressed in nanomoles per minute per milligram of protein and correspond to the rotenone (10 µM) sensitive rate.

Succinate–ubiquinone oxidoreductase assay – Cx-II activity was monitored at 600 nm by following the reduction of 6,6-dichlorophenolindophenol (DCPIP) (74 µM) by ubiquinol resulting from this reaction (Hatefi *et al*., 1978). Cx-II activity was expressed in nanomoles per minute per milligram of protein and corresponds to Cx-II inhibitor, thenoyltrifluoroacetone (TTFA), sensitive rate.

Ubiquinol–cytochrome c reductase assay – Cx-III activity was monitored at 550 nm by following the ubiquinol reduction of cytochrome c. The assay was started by adding the sample to the reaction mixture (35 mM K_2HPO_4, pH 7.2, 1 mM EDTA, 5 mM $MgCl_2$, 1 mM KCN, 5 µM rotenone) containing 15 µM cytochrome c and 15 µM ubiquinol, at 30ºC. Cx-III activity was expressed in rate constant (k) per minute per milligram of protein.

Cytochrome c oxidase assay – Cx-IV activity was determined at 550 nm by measuring the oxidation of reduced cytochrome c (15 µM) by cytochrome c oxidase (Wharton *et al*., 1967). Cx-IV activity was expressed in rate constant (k) per minute per milligram of protein.

Citrate synthase (CS) assay - CS activity was performed at 412 nm following the reduction of 5,5'-dithio-bis(2-nitrobenzoic acid) (200 µM) in the presence of acetyl-CoA (200 µM) and oxaloacetate (100 µM) (Coore *et al*., 1971). CS activity was expressed in nanomoles per minute per milligram of protein.

4.3.6. Cell extracts and Western blotting analysis

Equivalent amounts of protein, determined by the Biorad Protein Assay, were denaturated with sample buffer (0.06 M Tris, 6% glycerol, 1.7% SDS, 0.1 M DTT, 0.002%

bromophenol blue), at 95ºC for 5 min, separated on a 10% SDS-polyacrylamide gel (SDS-PAGE) and electroblotted onto PVDF membrane. Membranes were blocked in 5% skim milk in Tris buffer saline (25 mM Tris-HCl, pH 7.6, 150 mM NaCl) plus 0.1% Tween (TBS-T), for 1 h (RT). Incubations with primary antibodies (in TBS-T/5% milk) were performed overnight, at 4ºC: anti-Cx-I (20 kDa) 1:500, anti-Cx-I (30 kDa) 1:1000, anti-Cx-II (30 kDa) 1:80, anti-Cx-II (70 kDa) 1:1000, anti-COX Vb 1:250, anti-COX I 1:1000, anti-Htt 1:250, anti-HSP60 1:1000 and anti-α-tubulin 1:10,000. Membranes were washed with TBS-T and incubated for 1 h at RT with alkaline phosphatase-linked secondary antibody anti-mouse IgG (1:20,000), in TBS-T plus 5% milk. After extensively washed in TBS-T membranes were incubated with ECF (5 min, RT). Immunoreactive bands were visualized by alkaline phosphatase activity that catalyses the conversion of ECF substrate to a highly fluorescent product reagent. This product strongly fluoresces at 540–560 nm when the blots are illuminated with UV light (maximum excitation at 430 nm), by using a BioRad Versa Doc 3000 Imaging System (BioRad, Hercules, CA, USA).

4.3.7. Measurement of adenine nucleotides

Isolated platelet mitochondria were assayed for adenosine triphosphate (ATP), adenosine diphosphate (ADP), and adenosine monophosphate (AMP) by separation in a reverse-phase high-performance liquid chromatograph, with detection at 254 nm, as described by Stocchi *et al*. (1985). The chromatographic apparatus used was a Beckman-System Gold, consisting of a 126 Binary Pump Model and 166 Variable UV detector, controlled by a computer. Detection wavelength was 254 nm, and the column used was a Lichrospher 100 RP-18 (5 μm) from Merck (Darmstadt, Germany). An isocratic elution with 100 mM phosphate buffer (KH_2PO_4, pH 6.5) and 1.0% methanol was performed with a flow rate of 1 ml/min. The required time for each analysis was 6 min. Peak identity was determined by the retention time compared with standards. The amounts of ATP, ADP and AMP were determined by a concentration standard curve, and the results were presented as nmol/mg protein. Energy charges were calculated using the formula: ½ [(ATP + 2 ADP)/(ATP + ADP + AMP)].

4.3.8. Statistical analysis

Results are presented as the mean ± SEM of the indicated number of samples. Data were analyzed with one-way ANOVA with Bonferroni post-test using GraphPad Prism

version 5.0 for Windows, GraphPad Software, San Diego California USA, www.graphpad.com. P<0.05 was considered significant.

4.4. Results

Mitochondrial-enriched fractions isolated from platelets of healthy individuals (CTR), pre-HD and symptomatic HD carriers with similar mean CAG repeat length (Table 4.1) showed strong staining for HSP60, a mitochondrial protein, and a weak tubulin labelling, indicative of successful enrichment of the faction (Fig. 4.1A).

Table 4.1 – Characterization of control and HD carrier participants.

	CTR n=8	**Pre-symptomatic (pre-HD) n=8**	**Symptomatic (HD) n=7**
Gender	2 M; 6 F	3 M; 5 F	2 M; 5 F
Age (years)	37 ± 5.8 (23-75)	41 ± 4.2 (21-64)	54 ± 3.7 (43-66)
CAG repeats	n.d.	43 ± 1.1 (36-45)	44 ± 0.8 (41-48)
Medication (**Active compound**) [nº individuals]	Anxiolytic benzodiazepine derivative (**Ethyl loflazepate**) [1 in 8]	Antagonist of the NMDA receptors (**Amantadine hydrochloride)** Anxiolytic, benzodiazepines (**Alprazolam**) [1 in 8]	Anxiolytic, benzodiazepines (**Alprazolam, Diazepam**) [3 in 7] Anti-psychotic (**Haloperidol, Risperidone**) [3 in 7] Anti-epileptic (**Topiramate**) [1 in 7] Anti-depressant (**Mirtazapine**) [1 in 7]

CTR – Control, healthy individuals; pre-symptomatic (pre-HD) HD carriers, not subjected to neuroleptic therapeutics; HD – symptomatic Huntington's disease patients under therapy. M- male; F- female. Data are the mean±S.E.M. Minimum and maximum values for each parameter are depicted in brackets. Square brackets indicate the number of individuals under medication. n.d.- not determined.

Although we could not detect a band of ~350 kDa corresponding to FL-Htt in any of the samples analyzed, two juxtaposed bands corresponding to a molecular weight of ~250

kDa appeared in the HD symptomatic samples only (Fig. 4.1B), probably resulting from Htt cleavage, similarly as described by Orr and colleagues (2008).

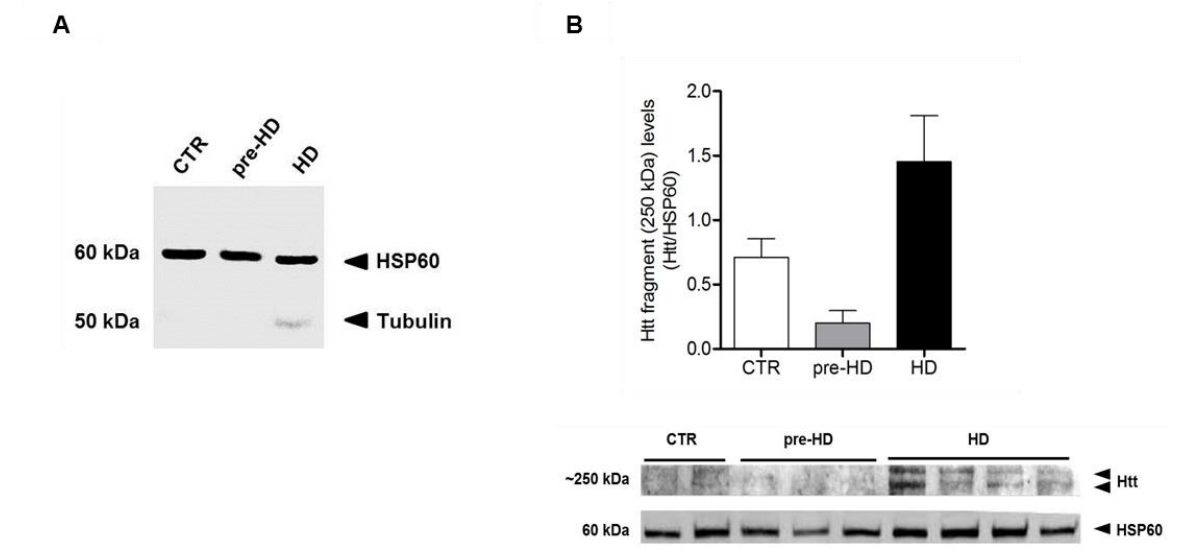

Figure 4.1 – Characterization of mitochondrial fractions isolated from human platelets. (**A**) Representative Western blot for mitochondrial-enriched fractions obtained from platelets of control (CTR), pre symptomatic (pre-HD) and HD symptomatic (HD) individuals showing a strong staining for HSP60, a mitochondrial protein, and weak tubulin labeling, a cytoskeletal cytosolic protein. (**B**) Human platelet-derived mitochondrial fractions were analyzed by Western blotting for the presence of Htt using the MAB2166 antibody. Two bands were observed in mitochondrial samples isolated from HD symptomatic patients, corresponding to high MW Htt fragments (~250 kDa). The image shows a representative blot of the data depicted in the graph. The results are the mean ± S.E.M. of 2-4 experiments. CTR – Control; pre-HD – pre-symptomatic HD carriers; HD – symptomatic Huntington's disease patients.

Next, we determined the activity of CS and mitochondrial respiratory chain Cx I-IV in the same mitochondrial-enriched fractions. Importantly, the activity of CS (a mitochondrial marker enzyme localized in the matrix) decreased significantly in mitochondrial samples from pre-HD individuals (Fig. 4.2A). This it is not likely due to incorrect procedure regarding mitochondrial isolation, since no differences were observed in the levels of the mitochondrial protein HSP60 (Fig. 4.1A), suggesting that CTR, pre-HD and HD have similar amount of intact mitochondria. Taking into account that the decrease in CS activity may reflect inherent mitochondrial dysfunction, the activities of mitochondrial respiratory chain complexes were not normalized to CS. According to our data, Cx-I activity was significantly reduced in both pre-HD and symptomatic HD carriers (Fig. 4.2B), whereas a significant increase in the activity of Cx-IV was detected in platelet mitochondrial fractions

derived from HD patients only (Fig. 4.2E). Conversely, no significant differences in Cx-II or Cx-III were observed in pre-HD or symptomatic HD carriers (Fig. 4.2C, D).

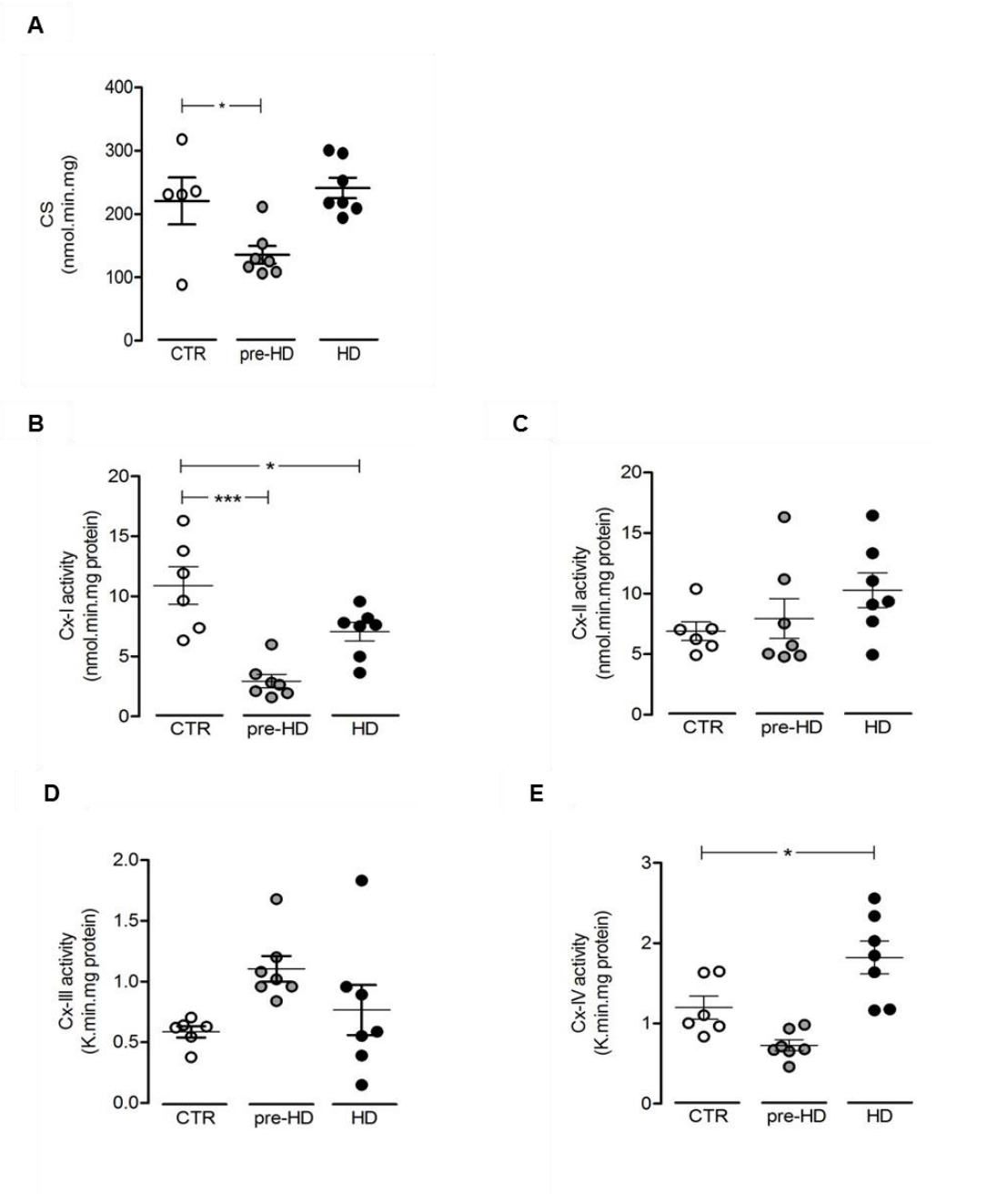

Figure 4.2 – Activity of mitochondrial respiratory chain complexes I-IV and citrate synthase. Mitochondrial respiratory chain complexes (Cxs) and citrate synthase (CS) activities were determined in mitochondrial fractions isolated from human platelets. Data are the mean ± S.E.M. of 6-7 independent samples, expressed as nmol/min/mg of protein (CS), Cxs I and II, in **A-C**) or k/min/mg of protein (Cxs III and IV, in **D**-**E**). Statistical analysis: One-way ANOVA with Bonferroni post-test. *P<0.05 and ***P<0.001. CTR – Control; pre-HD – pre-symptomatic HD carriers; HD – symptomatic Huntington's disease patients.

Taking into account the alterations detected in mitochondrial Cx activities, we further determined whether these were related to modifications in the levels of mitochondrial complex subunits. Because not all protein subunits could be examined (considering the high number of protein subunits of mitochondrial respiratory Cxs), we analyzed nuclear (n)- and mitochondrial (mt)-encoded subunits of Cxs I and IV and n-encoded subunits of Cxs II, for which there are commercially available antibodies. In particular, we determined the protein levels of: i) Cx-I mt-encoded ND6 (20 kDa) and n-encoded ion-sulfur protein 3 (30 kDa) subunits (Fig. 4.3A, B); ii) Cx-II n-encoded ion-sulfur (30 kDa) and flavoprotein (70 kDa) subunits (Fig. 4.3C, D); and iii) Cx-IV mt-encoded subunit I (COX I, 57 kDa) and n-encoded subunit Vb (COX Vb, 13 kDa) (Fig. 4.3E, F). The mt-encoded COX I subunit (Cx-IV) was decreased in both pre-HD and symptomatic HD carriers, compared to CTR individuals (Fig. 4.3E). No significant differences were observed in other protein subunits of Cx-I (mt- 20 kDa and n-encoded 30 kDa subunits, Fig. 4.3A, B), Cx-II (30 kDa, Fig. 4.3C) or the n-encoded COX Vb subunit of Cx-IV (Fig. 4.3F) between HD carriers and control individuals. Unchanged levels of ATP synthase subunit d were also observed (supplementary Fig. S4.1).

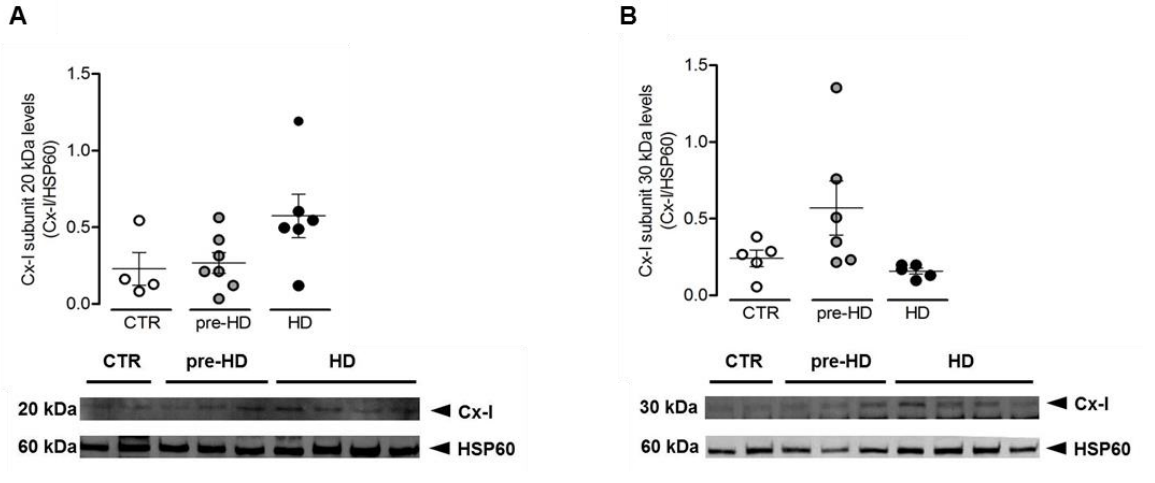

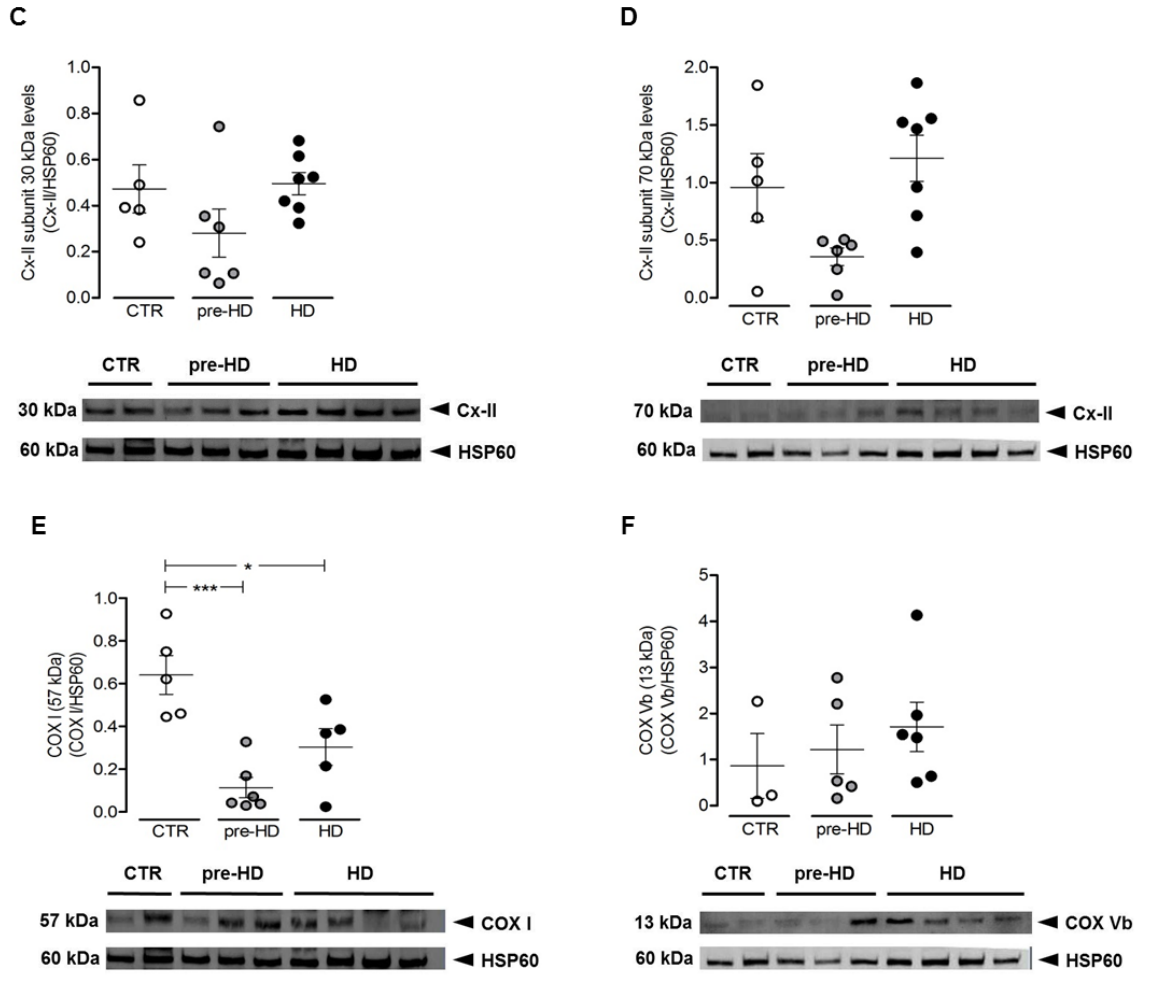

Figure 4.3 – Protein levels of selected mitochondrial complex subunits encoded by mitochondrial or nuclear DNA. Protein expression levels of mitochondrial complex (Cx) subunits in platelet mitochondria isolated from healthy control (CTR), pre-HD individuals and symptomatic HD patients (HD), were analysed by Western blotting. The graphs and representative blots show the protein levels of: (**A**) mt-encoded (20 kDa) and (**B**) n-encoded (30 kDa) Cx-I subunits; (**C**) n-encoded 30 kDa and (**D**) 70 kDa Cx-II subunits; (**E**) mt-encoded subunit I (COX I) and (**F**) n-encoded subunit COX Vb Cx-IV subunits. Data are the mean ± S.E.M. of 3-5 (CTR), 5-6 (pre-HD) and 4-7 (HD) independent samples. Levels of each complex were normalized for HSP60, a mitochondrial marker. Statistical analysis: One-Way ANOVA with Bonferroni post-test. *P<0.05 and ***P<0.001.

Because individual differences could be accounted for by a close correlation between the Cx activities and the protein levels of single Cx subunits, we further determined the correlation coefficients and related statistical parameters between the activity and protein levels of individual subunits of mitochondrial Cxs I, II and IV for each sample derived from control, pre-HD or symptomatic HD individuals. Data depicted in Table 4.2 shows

significant positive correlations in the case of Cx-I 20 kDa (mt-encoded) or Cx-II 30 kDa (n-encoded) subunits and the respective Cx activities in symptomatic HD samples only. These positive correlations indicate the importance of these Cx subunits in defining the activity of the respective subunits, which is particularly relevant in the case of Cx-I exhibiting significant decreased activity in HD patients under conditions that did not affect mitochondrial integrity/mass, as examined by the maintenance in CS activity. None of the others Cx subunits analyzed in this work seem to have largely contributed for modified mitochondrial Cx activities (Table 4.2).

Table 4.2 – Statistic values of correlation between mitochondrial complexes (Cx) activity and complex subunits expression levels.

	CTR						pre-HD						HD					
Complexes	Cx-I		Cx-II		Cx-IV		Cx-I		Cx-II		Cx-IV		Cx-I		Cx-II		Cx-IV	
Subunits	20 kDa	30 kDa	30 kDa	70 kDa	COX I	COX Vb	20 kDa	30 kDa	30 kDa	70 kDa	COX I	COX Vb	20 kDa	30 kDa	30 kDa	70 kDa	COX I	COX Vb
Pearson's r *Spearman's r	-0.5*	0.8*	0.8*	-0.4*	NA	0.4*	-0.55	-0.21	-0.29	0.33	0.09	0.51	0.84	-0.51	0.82	-0.49	0.35	0.55
P value (2-tailed)	1	0.33	0.33	0.75	NA	0.75	0.33	0.73	0.63	0.57	0.9	0.37	0.03	0.37	0.02	0.26	0.49	0.34
Correlation significance (α=0.05)	ns	ns	ns	ns	NA	ns	ns	ns	ns	ns	ns	ns	#	ns	#	ns	ns	ns
R^2	-	-	-	-	NA	-	0.3	0.04	0.08	0.11	0.01	0.26	0.7	0.26	0.68	0.24	0.12	0.3

Correlation was analysed between the activity (data depicted in Fig. 4.2) and the expression levels (data depicted in Fig. 4.3) of mitochondrial complex (Cx-)-I Cx-II and Cx-IV in control (CTR), pre-symptomatic (pre-HD) and Huntington's disease (HD)/symptomatic mitochondrial platelets. Data correspond to matched results (complex activity as in Fig. 4.2 and protein expression levels as in Fig. 4.3, obtained from the same individual samples).

*nonparametric Spearman correlation coefficient (data did not pass Kolmogrov-Smirnov normality test). In this case, R^2 was not calculated. NA – not applied (due to small data); ns – not significant; # $P<0.05$

We further determined possible differences in adenine nucleotide levels in control and HD mitochondrial platelets. Although no significant differences were observed in mitochondrial ATP and ADP levels, or ATP/ADP and AMP/ATP ratio (Fig. 4.4A, B, D, E), between control and pre-HD individuals or HD patient platelets, a ~3-fold increase in AMP levels occurred in platelet mitochondria from pre-HD individuals, when compared to the controls or HD/symptomatic mitochondria (Fig. 4.4C).

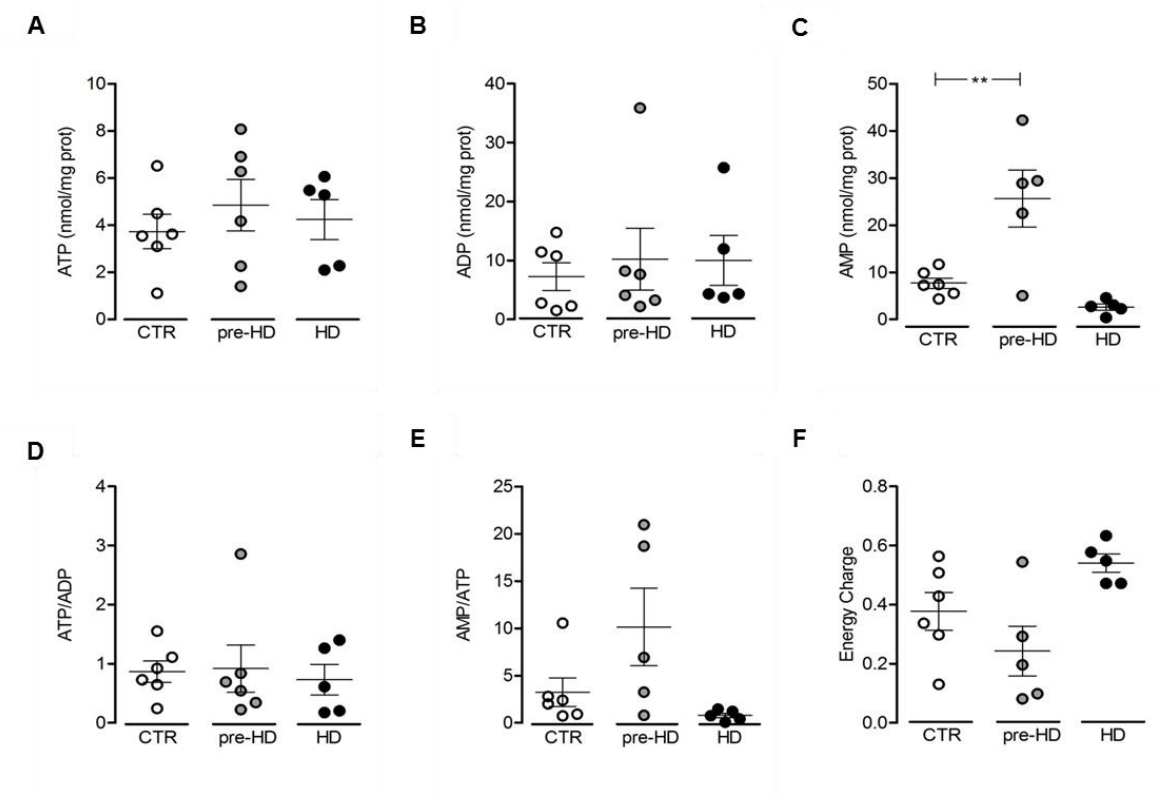

Figure 4.4 – Analysis of adenine nucleotides in human mitochondrial platelets. Adenine nucleotides were measured in mitochondrial fractions isolated from platelet of healthy controls (CTR), pre-HD and Huntington's disease/symptomatic patients (HD). Levels of ATP (**A**), ADP (**B**) and AMP (**C**) were determined by reverse-phase high-performance liquid chromatography. In (**D**) is depicted the ratio between ATP and ADP levels and in (**E**) the ratio between AMP and ATP levels. The energy charge (determined based on the formula EC= ½ [(ATP + 2 ADP)/(ATP + ADP + AMP)]) is represented in (**F**). Data are the mean ± S.E.M. of 5-6 independent samples. Statistical analysis: One-Way ANOVA with Bonferroni post-test. **P< 0.01.

4.5. Discussion

In the present work we observed decreased mitochondrial Cx-I and CS activities and increased AMP levels in platelets from pre-HD (and without medical treatment) human HD carriers. Platelet mitochondria isolated from symptomatic HD patients exhibited increased Cx-IV activity, despite decreased levels of mt-encoded COX I subunit, and decreased activity of Cx-I. Moreover, Cx-I mt-encoded ND6 (20 kDa) and ion-sulfur Cx-II (30 kDa) subunits showed positive correlations with the respective Cx activities in platelet mitochondria from HD patients only, revealing an important role of these subunits in defining the changes in Cx activities in platelet mitochondria. Interestingly, although pre-HD and symptomatic HD individuals carried similar mean CAG repeat lengths, only mitochondria isolated from HD symptomatic patients exhibited Htt high MW fragments.

Conflicting evidence for the role played by impaired mitochondrial complex activity in HD arise from the fact that different studies examine different type of cells at different disease stages. Our data seems to be in agreement with a prior study by Parker and colleagues (1990), who showed that mitochondrial Cx-I activity was reduced in HD platelets. Moreover, reduced Cx-I was found in muscle of HD patients and in R6/2 mice (Arenas *et al.*, 1998; Gizatullina *et al*., 2006). However, in the latter study, the authors also reported a decrease in Cx-IV activity. Impairments in Cxs-II, -III, and -IV were also detected in post-mortem HD human brain (Brennan *et al*., 1985; Gu *et al*., 1996; Tabrizi *et al*., 1999), at the final stage of the disease. Interestingly, Seo and co-workers (2008) did not find noticeable modifications in Cx-II activity in R6/2 mice striatal cells at 13 weeks of age (end-stage), but in YAC72 mice at 16 months of age (chronic stage) Cx-II was drastically increased. In this study the authors suggested a compensatory increase in Cx II/IIII activity in striatal cells to counterbalance mHtt toxicity (Seo *et al*., 2008). Nonetheless, another study using a higher number of early HD patient carriers, compared to our study, showed no significant differences in the activity of CS or Cx-I in platelet mitochondria (Powers *et al*., 2007). However, these authors did not discriminate between pre-HD and symptomatic HD carriers. Based on *in vivo* positron emission tomography (PET) measurements of cerebral mitochondrial oxidative metabolism (in Parkinson's disease and HD patients, *versus* normal controls), and *ex vivo* determinations of platelet Cx-I and Cxs I+III activities, performed on blood collected immediately before PET studies, Powers and colleagues (2011) further reported that platelet electron transport system (ETS) activity is not a good measure of brain ETS activity. Cxs I-IV activities were not altered in

pre-symptomatic or grade I HD brains (Guidetti *et al.*, 2001), or in a striatal cell line derived from KI mice (Milakovic and Johnson, 2005) either. Similarly, we did not find significant changes in the activities of mitochondrial respiratory chain Cxs I–IV in HD cybrids, generated by fusing platelets of symptomatic HD patients with mitochondria-depleted cells, compared to control cybrids (Ferreira *et al.*, 2010). Nevertheless, the HD cells were more prone to mitochondrial-dependent apoptosis, particularly after exposure to toxic stimuli such as 3-nitropropionic acid or staurosporine (Ferreira *et al.*, 2010) and showed modified cellular bioenergetics due to inherent dysfunction of mitochondrial pyruvate dehydrogenase activity (Ferreira *et al*., 2011). Unchanged Cxs activities in HD cybrids could be accounted for some repopulation of NT2 mitochondria in cybrid lines, variability in Cxs activities for each experimental group, and/or the fact that reduction of Cx-I is more evident in mitochondria from pre-HD than symptomatic HD carriers, suggesting that the disease stage at which platelet cells are isolated may impact on mitochondrial activity. Considering other peripheral cell types, we have previously reported a reduction in mitochondrial membrane potential and increased apoptotic markers in mononuclear blood cells from HD patients, particularly in B lymphocytes (Almeida *et al.*, 2008), which could resemble some changes verified in HD brain. Therefore, although we cannot extrapolate the data obtained in peripheral cells to particular mitochondrial changes occurring in the brain, the analysis of defined biochemical parameters in these cells may be used in the future to discriminate different disease stages.

Data generated in the present study also showed significant positive correlations between the activity of Cxs I or II, respectively, with Cx-I mt-encoded ND6 subunit (20 kDa) or the ion-sulfur Cx-II subunit (30 kDa) subunits, revealing an important role of these subunits in defining the changes in Cx activities in platelet mitochondria from symptomatic HD carriers. These data may be relevant when considering that mitochondria from HD carriers had significant reduced Cx-I activity compared to platelet mitochondria isolated from control individuals. In this regard, changes in mt-encoded subunit expression as a result of mtDNA lesions (mtDNA deletions, variations and/or oxidation) have been described to contribute to HD pathogenesis (e.g. Banoei *et al*., 2007; Acevedo-Torres *et al*., 2009).

Importantly, we found Htt fragments with high molecular weight in mitochondria from symptomatic, but not in pre-HD, HD carriers. These data appear to be in agreement with the previous observation that high MW N-terminal specific mHtt fragments associate with

mitochondria in an age-dependent manner in Hdh(CAG)150 KI mouse brain (Orr *et al*., 2008). Mutant Htt interaction with the mitochondrial membrane has also been shown in YAC72 transgenic mice neuronal mitochondria (Panov *et al.,* 2002) and in HD striatal cells (Choo *et al*., 2004). Interestingly, these fragments can induce the opening of the mitochondrial permeability transition pore as demonstrated by Choo and colleges in mitochondria from mouse liver (Choo *et al*., 2004). It has been shown that WT and mHtt fragments are originated when the FL protein is proteolytically cleaved by caspases, calpain and/or aspartic endopeptidases (e.g. Lunkes *et al*., 2002; Wellington *et al*., 2002; Gafni *et al.,* 2004).

In addition to decreased Cx-I activity and reduced CS activity, mitochondria from pre-HD platelets showed increased AMP levels and a trend for increased AMP/ATP ratio. This observation might be relevant considering the role of AMP in regulating key metabolic enzymes, such as the AMP-activated protein kinase (AMPK) (Suter *et al*, 2006), an important enzyme responsible for regulating the cellular uptake of glucose, β-oxidation of fatty acids and mitochondrial biogenesis, or phosphofructokinase-1, the most important control site in the mammalian glycolytic pathway. In accordance with altered AMP levels, we observed a slight (non-statistically significant) alteration in energy charge. Indeed, cell energy charge is a sensitive indicator of cell energy status (Atkinson, 1968) and AMP may function as a mediator of energy metabolism (Ramaiah *et al*., 1964), since cellular concentrations of AMP change more drastically than ATP or ADP levels. The ATP levels or ATP/ADP ratio were unchanged in HD carriers, which may be due to apparent compensatory activities of mitochondrial Cxs (e.g. decreased Cx-I activity accompanied by increased Cx-IV activity in HD patient's platelets). In contrast with our data, mitochondrial ATP was impaired in HD striatal cell lines (Milakovic and Johnson, 2005). The translation of ATP and ADP small changes into relatively large changes in AMP concentration is accomplished by adenylate kinase, a sensitive indicator of the cellular energy state. Thus, any system that supervise cellular energy status respond to AMP (or the AMP/ATP ratio) rather than ADP (or the ADP/ATP ratio) with higher sensitivity and fidelity to stress signals (for review, Hardie and Hawley, 2001 and Dzeja and Terzic, 2009). Furthermore, adenylate kinase functions to conserve cellular nucleotide pool through AMP re-phosphorylation back to ADP and ATP (Dzeja and Terzic, 2009).

In the present work, platelet mitochondrial fractions were isolated from medicated and non-medicated individuals, as depicted in Table 4.1. Although HD symptomatic carriers were highly medicated, we did not find significant differences between medicated and

non-medicated individuals within the same HD carrier group. Previous studies showed that many psychotropic medications (including antidepressants, antipsychotics and benzodiazepines) may induce mitochondrial damage (Neustadt and Pieczenik, 2008, for review; Hroudova and Fisar, 2010). In this regard, the intrinsic mitochondrial alterations closely associated to the disease should be taken into account when prescribing therapeutics and developing new drugs. Given that some of the symptomatic HD patients were medicated and that some mitochondrial changes were evident in platelets derived from pre-HD carriers, but not seen in HD symptomatic patients (such as altered CS activity or increased AMP levels), we hypothesize that the therapies used may have protected the platelets against disease-related mitochondrial changes.

In summary, mitochondrial Cxs activities and their correlation with defined subunit expression warrants further investigation, by taking into account the type of tissue and disease progression, which may help to reveal selective targets for future HD therapeutic research. Moreover, by using human peripheral blood cells, this work reinforces the idea that dysfunction of mitochondrial Cxs may occur very early during HD progression and that cytoprotective agents may be beneficial if used at early/pre manifest phases of the disease.

CHAPTER 4 SUPPLEMENTARY FIGURE

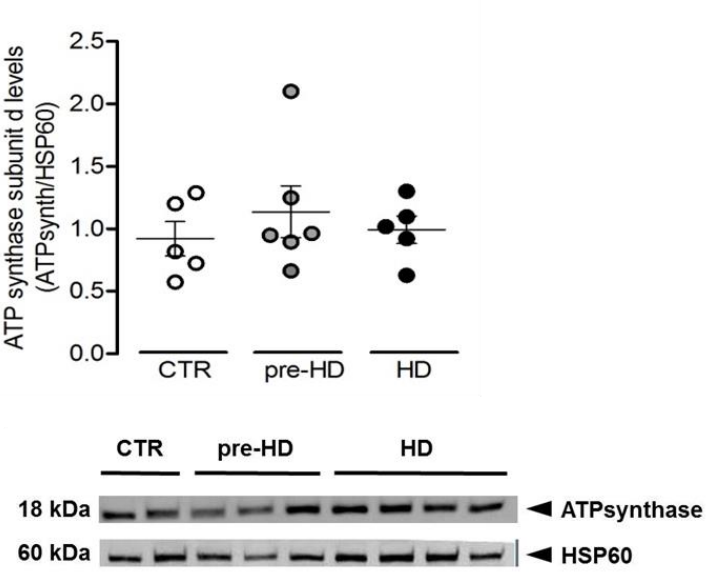

Fig. S4.1 – **Protein levels of ATPsynthase subunit d.** Protein levels of ATPsynthase subunit d were analysed by Western blotting (anti Cx-V (ATPsynthase), subunit d: Molecular Probes, Invitrogen, Eugene, OR, USA; 1:100) in platelet mitochondria isolated from healthy controls (CTR), pre-HD individuals and symptomatic HD patients (HD). Data are the mean ± S.E.M. of 5-6 independent samples. Levels of ATPsynthase subunit d were normalized for HSP60, a mitochondrial marker.

CHAPTER 5

FINAL CONCLUSIONS

Final Conclusions

Globally, data herein obtained from different HD paradigms brought new insights about the underling pathological mechanisms occurring in HD. In particular, the significant roles of functional mitochondria and the neurotrophic support promoted by BDNF in HD pathology are greatly reinforced.

Functional BDNF-mediated signalling through FL-TrkB receptors plays an essential role in rescuing HD striatal cells from apoptosis. BDNF synthesis is not generally associated with striatal cells. Nevertheless, the model in which HD striatal cells were transduced with preproBDNF contributed with relevant information regarding BDNF/TrkB protection and BDNF processing in HD. Apart from a defect in BDNF transcription (e.g. Zuccato *et al*., 2001, 2003), data presented in *Chapter 2* of this thesis suggests that BDNF release might be affected, since HD cells exhibiting higher intracellular levels of pro- and mature BDNF released similar amounts of these forms of the protein, when compared to WT cells; in addition, BDNF was preferentially located in vesicles retaining a perinuclear localization in HD cells, suggesting that it might be trapped in the Golgi apparatus. Surprisingly, HD cells tend to produce and only slightly release more pro-BDNF than WT cells, which might account for by striatal cell death associated with the disease; therefore, it would be interesting to evaluate proBDNF-mediated stimulation of p75 receptors, classically associated with cell death (Teng *et al*., 2005; Cunha *et al*., 2010, for review). Furthermore, the activity of endoproteases (e.g. furin), which process pro- into mature BDNF in the trans-Golgi (Lessmann and Brigadski, 2009, for review) should be also investigated. Yet, overexpression of BDNF and TrkB (either stimulated or not (±) with exogenous rhBDNF) in HD cells diminished caspase-3 activation, which seems to be related with increased activation of AKT and/or ERK pathways. These results are in accordance with previous studies, demonstrating that functional activity of FL-TrkB are essential for neuronal survival in HD (reviewed in Zuccato and Cattaneo, 2007). Moreover, data herein presented strongly support TrkB receptors as potential therapeutic candidates to be explored in the context of HD. However, sustained ERK activation observed in WT (TrkB, TrkB +rhBDNF and BDNF/TrkB co-cultures) and HD (CTR + rhBDNF and BDNF/TrkB co-cultures) transduced-cells could not always be related to a decrease in apoptotic features, suggesting that different cell mechanisms might be

triggered (e.g. cell growth, differentiation, maturation). Considering that caspase-3 is involved in cell differentiation (reviewed in Solá *et al*., 2013) and that prolonged ERK activation can be associated with neuronal apoptosis (Cagnol *et al*., 2006), other cell processes such as cell cycle and differentiation, activation of death receptors (e.g. p75) and mitochondrial release of apoptogenic factors (e.g. cytochrome c; caspase-independent AIF release) should be considered. Moreover, BDNF concentration and administration need to be accurately evaluated concerning HD therapeutic approaches. It became clear that acute, exogenous addition of low BDNF concentrations (e.g. 20 ng/mL; 5 ng/mL were also tested without significant results - data not shown) displayed different cell responses compared to endogenously produced BDNF (from transduced cells); this is particularly relevant in HD TrkB-overexpressing cells, probably due to receptor overstimulation or desensitization (Haapasalo *et al*., 2002), an effect that HD cells were unable to counteract. Nevertheless, the transduced HD cell model was shown to suitably unveil the role of the neurotrophin and its selective receptor in mediating neuroprotection in HD striatal cells.

Interestingly, 5 ng/mL of BDNF were able to promote *in vitro* neuronal differentiation of WT and YAC128 SVZ-derived cells, with no effect on cell survival or migration (not shown). While no genotype related differences were detected in proliferation and cell cycle phases of undifferentiated cells, improved migratory ability and neuronal differentiation/maturation (determined by MAP-2+/synaptophysin+ staining and Ca^{2+}_i raise upon KCl stimulus), were observed in YAC128 cells, compared to WT, at a mild HD stage. The same proliferative capacity of WT and HD NSC/progenitor cells, and enhanced neuron differentiation were also confirmed by others (Lorincz and Zawistowsk, 2009; Phillips *et al.,* 2005); therefore mHtt does not seem to interfere with NSC self-renewal, but it may influence neural stem/progenitors differentiation into neurons. Affected cells might compensate HD-induced neuronal dysfunction by exacerbating intrinsic cellular mechanisms to repair and/or substitute damaged cells, which is ultimately lost along the progression of the disease. In fact, SVZ-derived cells, from mild symptomatic YAC128 mice, exhibited characteristics of more committed population, than the WT counterpart, as observed by increased migration (as in Soares and Sotelo, 2004) and Ca^{2+}_i following histamine stimulus. HD cells at mild disease stage also exhibited improved mitochondrial function than WT cells, corroborating a hypothetic cell compensatory mechanism. This seems to be an inherent feature of HD cells, probably due to the presence of mHtt rather than cell adjustment to counteract a toxic milieu.

These cells respond promptly to differentiation stimuli, such as BDNF or fibronectin; however, the specific neuronal phenotype acquired in this process should be further examined. Although increased neurogenesis has been related in stressed or injured brain, the replacement of dead neurons in severe conditions, such as neurodegenerative diseases, occurs without success, which has been attributed to hostile surroundings. Fibronectin was previously shown to induce a GABAergic phenotype in neurosphere-derived neuronal cells (Silva *et al*., 2009); thus, if functional GABAergic neurons were obtained from HD SVZ cells, one should carefully consider ameliorate cell environment by promoting the natural ECM fibronectin in early diseased brain. *Chapter 3* focused mainly in neuronal differentiation, as neurons are the most affected cell population in HD. However, it would be interesting to future evaluate the differentiation potential, and possible interplay with mitochondrial function, of HD neuronal supporting cells (e.g. oligodendrocytes and astrocytes) at different stages of the disease.

In this work it is proposed that mitochondrial alterations are an early event in disease progression. This extends beyond brain context, given that peripheral HD cells (e.g. platelets) derived from pre-symptomatic HD carriers showed increased AMP levels (denoting altered cellular energy status) and decreased activities of citrate synthase and mitochondrial Cx-I, compared to age-matched controls. Though one should be careful about extrapolating data obtained in peripheral cells to brain changes (Powers *et al.,* 2011), biochemical analysis in these cells may be useful to discriminate different disease stages. With the advance course of the disease, mitochondrial platelets from symptomatic HD patients showed increased Cx-IV activity (probably to oppose reduced Cx-I activity) and interesting significant and positive correlation was observed between Cx-I activity and 20 kDa mitochondrial-encoded subunit. Modifications in mitochondrial-encoded subunit expression due to mtDNA lesions was previously reported to contribute to HD pathogenesis (Banoei et al., 2007; Acevedo-Torres *et al*., 2009); accordingly, it would be important to deeply investigate potential correlations of other mitochondrial- and nuclear-encoded subunits and their respective complexes activities. This could bring new insights about the role of individual complex subunit expression levels in response to altered activity, which could lead to the discovery of new HD therapeutical targets.

Considering the study of selective targets and therapeutic approaches for HD, our results strengthen the importance of the neurotrophin BDNF, and the need of attention when choosing the concentrations and the delivery methods, based on tissue context and best

timing for therapeutic intervention. Furthermore, TrkB receptor showed successful outcomes concerning HD cell survival, therefore opening new perspectives about its use as a potential therapeutic candidate. Thus, improving supportive cell milieu and targeting mitochondria in the early course of the disease are apparently good neuroprotective strategies that may help ameliorate and/or counteract disease progression.

REFERENCES

REFERENCES

Aarts M, Liu Y, Liu L, Besshoh S, Arundine M, Gurd JW, Wang YT, Salter MW and Tymianski M (2002). Treatment of ischemic brain damage by perturbing NMDA receptor- PSD-95 protein interactions. Science 298:846-850.

Acevedo-Torres K, Berríos L, Rosario N, Dufault V, Skatchkov S, Eaton MJ, Torres-Ramos CA and Ayala-Torres S (2009). Mitochondrial DNA damage is a hallmark of chemically induced and the R6/2 transgenic model of Huntington's disease. DNA Repair (Amst). 8:126-36.

Agasse F, Bernardino L, Silva B, Raquel R, Grade S and Malva JO (2008). Response to Histamine Allows the Functional Identification of Neuronal Progenitors, Neurons, Astrocytes, and Immature Cells in Subventricular Zone Cell Cultures. Rejuvenation Research 11(1):187-200.

Ahmed S, Reynolds BA and Weiss S. (1995). BDNF enhances the differentiation but not the survival of CNS stem cell-derived neuronal precursors. J. Neurosci. 15:5765-5778.

Alberch J, Perez-Navarro E and Canals JM (2004). Neurotrophic factors in Huntington's disease. Prog Brain Res 146:195-229.

Albin RL, Young AB and Penney JB (1989). The functional anatomy of basal ganglia disorders. Trends Neurosci 12:366-375.

Albin RL, Young AB, Penney JB, Handelin B, Balfour R, Anderson KD, Markel DS, Tourtellotte WW and Reiner A (1990). Abnormalities of striatal projection neurons and N-methyl-D-aspartate receptors in presymptomatic Huntington’s disease. N Engl J Med 322:1293–1298.

Albin RL, Qin Y, Young AB, Penney JB and Chesselet MF (1991). Preproenkephalin messenger RNA-containing neurons in striatum of patients with symptomatic and presymptomatic Huntington's disease: an in situ hybridization study. Ann Neurol 30:542-549.

Alderson RF, Curtis R, Alterman AL, Lindsay RM and DiStefano PS (2000). Truncated trkB mediates the endocytosis and release of BDNF and neurotrophin-4/5 by rat astrocytes and Schwann cells in vitro. Brain Res. 871:210–222.

Almeida S, Sarmento-Ribeiro AB, Januário C, Rego AC and Oliveira CR (2008). Evidence of apoptosis and mitochondrial abnormalities in peripheral blood cells of Huntington's disease patients. Biochem Biophys Res Commun. 374(4):599-603.

Almeida S, Laço M, Cunha-Oliveira T, Oliveira CR and Rego AC (2009). BDNF regulates BIM expression levels in 3-nitropropionic acid-treated cortical neurons. Neurobiol. Dis. 35(3):448-56.

Almeida S, Cunha-Oliveira T, Laço M, Oliveira CR and Rego AC (2010). Dysregulation of CREB activation and histone acetylation in 3-nitropropionic acid-treated cortical neurons: prevention by BDNF and NGF. Neurotox. Res. 17(4):399-405.

Alston TA, Mela L and Bright HF (1977). 3-Nitropropionate, the toxic substance of Indigofera, is a suicide inactivator of succinate dehvdrogenase. Proc Natl Acad Sci USA 74(9):3767-3771.

Altman J (1962). Are New Neurons Formed in the Brains of Adult Mammals? Science 135(3509):1127-1128.

Alvarez-Buylla A and Garcia-Verdugo JM. (2002). Neurogenesis in adult subventricular zone. J. Neurosci. 22:629-634.

Alvarez-Buylla A, Seri B, Doetsch F (2002). Identification of neural stem cells in the adult vertebrate brain. Brain Res Bull. 57(6):751-8.

Alvarez-Buylla A and Lim DA. (2004). For the long run: maintaining germinal niches in the adult brain. Neuron 41:683-686.

Andrade MA and Bork P (1995). HEAT repeats in the Huntington's disease protein. Nat Genet 11:115-116.

Andrews TC and Brooks DJ (1998). Advances in the understanding of early Huntington's disease using the functional imaging techniques of PET and SPET. Molecular Medicine Today 4(12):532–539

Arenas J, Campos Y, Ribacoba R, Martin M.A, Rubio JC, Ablanedo P and Cabello A (1998). Complex I defect in muscle from patients with Huntington's disease. Ann. Neurol. 43:397-400.

Arrasate M, Mitra S, Schweitzer ES, Segal MR and Finkbeiner S (2004). Inclusion body formation reduces levels of mutant huntingtin and the risk of neuronal death. Nature 431:805–810.

Arzberger T, Krampfl K, Leimgruber S and Weindl A (1997). Changes of NMDA receptor subunit (NR1, NR2B) and glutamate transporter (GLT1) mRNA expression in Huntington's disease–an in situ hybridization study. J Neuropathol Exp Neurol 56:440–454.

Assaife-Lopes N, Sousa VC, Pereira DB, Ribeiro JA, Chao MV and Sebastião AM (2010). Activation of Adenosine A2A Receptors Induces TrkB Translocation and Increases BDNF-Mediated Phospho-TrkB Localization in Lipid Rafts: Implications for Neuromodulation J Neurosci. Jun 30(25):8468-8480.

Atkinson DE (1968). The energy charge of the adenylate pool as a regulatory parameter. Interaction with feedback modifiers. Biochemistry 7:4030-4034.

Bachelder R.E., Ribick M.J., Marchetti A., Falcioni R., Soddu S., Davis K.R. and Mercurio A.M. (1999). p53 inhibits alpha 6 beta 4 integrin survival signaling by promoting the caspase 3-dependent cleavage of AKT/PKB. J. Cell Biol. 147(5):1063-1072.

Bae BI, Xu H, Igarashi S, Fujimuro M, Agrawal N, Taya Y, Hayward SD, Moran TH, Montell C, Ross CA, Snyder SH and Sawa A (2005). p53 mediates cellular dysfunction and behavioral abnormalities in Huntington's disease. Neuron 47: 29–41.

Banoei MM, Houshmand M, Panahi MS, Shariati P, Rostami M, Manshadi MD and Majidizadeh T (2007). Huntington's disease and mitochondrial DNA deletions: event or regular mechanism for mutant huntingtin protein and CAG repeats expansion?! Cell Mol Neurobiol 27:867-75.

Baquet ZC, Gorski JA and Jones KR (2004). Early striatal dendrite deficits followed by neuron loss with advanced age in the absence of anterograde cortical brain-derived neurotrophic factor. J Neurosci 24:4250-4258.

Barbacid M (1994). The Trk family of neurotrophin receptors. J Neurobiol. 25(11):1386-403.

Bath KG, Mandairon N, Jing D, Rajagopal R, Kapoor R, Chen ZY, Khan T, Proenca CC, Kraemer R, Cleland TA, Hempstead BL, Chao MV and Lee FS (2008). Variant brain-derived neurotrophic factor (Val66Met) alters adult olfactory bulb neurogenesis and spontaneous olfactory discrimination. J Neurosci 28:2383–2393.

Bath KG and Lee FS (2010). Neurotrophic factor control of adult SVZ neurogenesis. Dev. Neurobiol. 70(5):339-349.

Batista CM, KippinTE, Willaime-Morawek S, Shimabukuro MK, Akamatsu W and van der Kooy D (2006). A progressive and cell non-autonomous increase in striatal neural stem cells in the Huntington's disease R6/2 mouse. J. Neurosci. 26:10452–10460.

Bauer PO and Nukina N (2009). The pathogenic mechanisms of polyglutamine diseases and current therapeutic strategies. J Neurochem 110(6):1737-65.

Beal MF, Brouillet E, Jenkins BG, Ferrante RJ, Kowall NW, Miller JM, Storey E, Srivastava R, Rosen BR and Hyman BT (1993). Neurochemical and histologic characterization of striatal excitotoxic lesions produced by the mitochondrial toxin 3-nitropropionic acid. J Neurosci. 13(10):4181-4192.

Bemelmans AP, Horellou P, Pradier L, Brunet I, Colin P and Mallet J (1999). Brain-derived neurotrophic factor-mediated protection of striatal neurons in an excitotoxic rat model of Huntington's disease, as demonstrated by adenoviral gene transfer. Hum Gene Ther 10:2987-2997.

Bence NF, Sampat RM and Kopito RR (2001). Impairment of the ubiquitin-proteasome system by protein aggregation. Science 292:1552-1555.

Benoit BO, Savarese T, Joly M, Engstrom CM, Pang L, Reilly J, Recht LD, Ross AH and Quesenberry PJ. (2001). Neurotrophin channeling of neural progenitor cell differentiation. J. Neurobiol. 46:265-280.

Benraiss A, Chmielnicki E, Lerner K, Roh D and Goldman SA (2001). Adenoviral brain-derived neurotrophic factor induces both neostriatal and olfactory neuronal recruitment from endogenous progenitor cells in the adult forebrain. J. Neurosci. 21:6718-31.

Berardelli A, Noth J, Thompson PD, Bollen EL, Curra A, Deuschl G, van Dijk JG, Topper R, Schwarz M and Roos RA (1999). Pathophysiology of chorea and bradykinesia in Huntington's disease. Mov Disord 14:398-403.

Berger A (2000). Minocycline slows progress of Huntington’s disease in mice. BMJ 321:370.

Bonelli RM, Hödl AK, Hofmann P and Kapfhammer HP (2004). Neuroprotection in Huntington's disease: a 2-year study on minocycline. Intl Clin Psychopharmacol 19:337–342.

Borlongan CV, Koutouzis TK, Freeman TB, Cahill DW and Sanberg PR (1995). Behavioral pathology induced by repeated systemic injections of 3-nitropropionic acid mimics the motoric symptoms of Huntington's disease. Brain Res. 697(1-2):254-257.

Bosch M, Pineda J R, Sunol C, Petriz J, CattaneoE, Alberch J and Canals JM. (2004). Induction of GABAergic phenotype in a neural stem cell line for transplantation in an excitotoxic model of Huntington's disease. Exp. Neurol. 190:42-58.

Boutell JM, Thomas P, Neal JW, Weston VJ, Duce J, Harper PS and Jones AL (1999). Aberrant interactions of transcriptional repressor proteins with the Huntington's disease gene product, huntingtin. Hum Mol Genet 8:1647-1655.

Brennan WA Jr, Bird ED and Aprille JR (1985). Regional mitochondrial respiratory activity in Huntington's disease brain. J Neurochem 44:1948-1950.

Brouillet E, Conde F, Beal MF and Hantraye P (1999). Replicating Huntington's disease phenotype in experimental animals. Prog Neurobiol 59:427-468.

Browne SE, Bowling AC, MacGarvey U, Baik MJ, Berger SC, Muqit MM, Bird ED and Beal MF (1997). Oxidative damage and metabolic dysfunction in Huntington's disease: selective vulnerability of the basal ganglia. Ann. Neurol. 41:646-653.

Brustovetsky N, LaFrance R, Purl KJ, Brustovetsky T, Keene CD, Low WC and Dubinsky JM (2005). Age-dependent changes in the calcium sensitivity of striatal mitochondria in mouse models of Huntington's Disease. J Neurochem 93: 1361–1370.

Bruyn RP and Stoof JC (1990). The quinolinic acid hypothesis in Huntington's chorea. J Neurol Sci 95:29-38.

Cagnol S, Van Obberghen-Schilling E and Chambard JC. Prolonged activation of ERK1,2 induces FADD-independent caspase 8 activation and cell death (2006). Apoptosis 11(3):337-346.

Calnan DR and Brunet A (2008). The FoxO code. Oncogene 27(16):2276-88.

Campos LS, Leone DP, Relvas JB, Brakebusch C, Fassler R, Suter U and Ffrench-Constant C. (2004). Beta1 integrins activate a MAPK signalling pathway in neural stem cells that contributes to their maintenance. Development 131:3433-3444.

Canals JM, Checa N, Marco S, Akerud P, Michels A, Perez-Navarro E, Tolosa E, Arenas E and Alberch J. (2001). Expression of brain-derived neurotrophic factor in cortical neurons is regulated by striatal target area. J. Neurosci. 21:117-124.

Carreira BP, Morte I, Inácio A, Costa G, Rosmaninho-Salgado J, Agasse F, Carmo A, Couceiro P, Brundin P, Ambrósio AF, Carvalho CM and Araújo IM (2010). Nitric Oxide Stimulates the

Proliferation of Neural Stem Cells Bypassing the Epidermal Growth Factor Receptor. Stem Cells 28:1219-1230.

Cattaneo E, Rigamonti D, Goffredo D, Zuccato C, Squitieri F and Sipione S (2001). Loss of normal huntingtin function: new developments in Huntington's disease research. Trends Neurosci 24:182-188.

Cepeda C, Ariano MA, Calvert CR, Flores-Hernandez J, Chandler SH, Leavitt BR, Hayden MR and Levine MS (2001). NMDA receptor function in mouse models of Huntington disease. J Neurosci Res 66:525-539.

Cha JH. Transcriptional signatures in Huntington's disease (2007). Pro Neurobiol 83: 228–248.

Chan EY, Luthi-Carter R, Strand A, Solano SM, Hanson SA, DeJohn MM, Kooperberg C, Chase KO, DiFiglia M, Young AB, Leavitt BR, Cha JH, Aronin N, Hayden MR and Olson JM (2002). Increased huntingtin protein length reduces the number of polyglutamine-induced gene expression changes in mouse models of Huntington's disease. Hum Mol Genet 11:1939–1951.

Chao MV, Rajagopal R and Lee FS (2006). Neurotrophin signalling in health and disease. Clin Sci (Lond) 110:167–173.

Chen ZY, Ieraci A, Tanowitz M and Lee FS (2005). A Novel Endocytic Recycling Signal Distinguishes Biological Responses of Trk Neurotrophin Receptors. Mol Biol Cell 16(12):5761–5772.

Chesselet MF and Delfs JM (1996). Basal ganglia and movement disorders: an update. Trends Neurosci 19:417-422.

Choo YS, Johnson GV, MacDonald M, Detloff PJ and Lesort M (2004). Mutant huntingtin directly increases susceptibility of mitochondria to the calcium-induced permeability transition and cytochrome c release. Hum Mol Genet 13:1407-1420.

Chou SY, Lee YC, Chen HM, Chiang MC, Lai HL, Chang HH, Wu YC, Sun CN, Chien CL, Lin YS, Wang SC, Tung YY, Chang C and Chern Y (2005). CGS21680 attenuates symptoms of Huntington's disease in a transgenic mouse model. J Neurochem. 93(2):310-20.

Coles CJ, Edmondson DE and Singer TP (1979). Inactivation of succinate dehydrogenase by 3-Nitropropionate. J Biol Chem 254:516l-5167.

Colin E, Régulier E, Perrin V, Dürr A, Brice A, Aebischer P, Déglon N, Humbert S and Saudou F (2005). AKT is altered in an animal model of Huntington's disease and in patients. Eur J Neurosci (6):1478-88.

Colin E, Zala D, Liot G, Rangone H, Borrell-Pages M, Li XJ, Saudou F and Humbert S. (2008). Huntingtin phosphorylation acts as a molecular switch for anterograde/retrograde transport in neurons. EMBO J 27:2124–2134.

Cooper JK, Schilling G, Peters MF, Herring WJ, Sharp AH, Kaminsky Z, Masone J, Khan FA, Delanoy M, Borchelt DR, Dawson VL, Dawson TM and Ross CA (1998). Truncated NH2-terminal fragments of huntingtin with expanded glutamine repeats form nuclear and cytoplasmic aggregates in cell culture. Hum Mol Genet 7:783–790.

Coore HG, Denton RM, Martin BR and Randle PJ (1971). Regulation of adipose tissue pyruvate dehydrogenase by insulin and others hormones. Biochem. J. 125:115–127.

Cornett J, Cao F, Wang CE, Ross CA, Bates GP, Li SH and Li XJ (2005). Polyglutamine expansion of huntingtin impairs its nuclear export. Nat Genet. 37(2):198-204.

Cregan SP, Fortin A, MacLaurin JG, Callaghan SM, Cecconi F, Yu SW, Dawson TM, Dawson VL, Park DS, Kroemer G and Slack RS (2002). Apoptosis-inducing factor is involved in the regulation of caspase-independent neuronal cell death. J Cell Biol 158(3):507-517.

Cui L, Jeong H, Borovecki F, Parkhurst CN, Tanese N and Krainc D (2006). Transcriptional repression of PGC-1alpha by mutant huntingtin leads to mitochondrial dysfunction and neurodegeneration. Cell 127: 59–69.

Cunha C., Brambilla R. and Thomas K.L. (2010) A simple role for BDNF in learning and memory? Front. Mol. Neurosci. 3(1):1-14.

Curtis MA, Penney EB, Pearson AG, van Roon-Mom WM, Butterworth NJ, Dragunow M, Connor B and Faull RL (2003). Increased cell proliferation and neurogenesis in the adult human Huntington's disease brain. Proc. Natl. Acad. Sci. USA 100(15):9023-7.

Curtis MA, Penney EB, Pearson J, Dragunow M, Connor B and Faull RL (2005). The distribution of progenitor cells in the subependymal layer of the lateral ventricle in the normal and Huntington's disease human brain. Neuroscience 132(3):777-88.

Curtis MA, Low VF and Faull RL (2012). Neurogenesis and progenitor cells in the adult human brain: a comparison between hippocampal and subventricular progenitor proliferation. Dev Neurobiol. 72(7):990-1005.

Danen EH and Sonnenberg A (2003). Integrins in regulation of tissue development and function. J. Pathol. 201:632-641.

Daugas E, Susin SA, Zamzami N, Ferri KF, Irinopoulou T, Larochette N, Prévost MC, Leber B, Andrews D, Penninger J and Kroemer G (2000). Mitochondrio-nuclear translocation of AIF in apoptosis and necrosis. FASEB J. 14(5):729-739.

Davies S and Ramsden DB (2001). Huntington's disease. Mol. Pathol. 54:409-413.

Davis HE, Rosinski M, Morgan JR and Yarmush ML (2004). Charged Polymers Modulate Retrovirus Transduction via Membrane Charge Neutralization and Virus Aggregation. Biophys J 86(2):1234-42.

de Chevigny A, Cooper O, Vinuela A, Reske-Nielsen C, Lagace DC, Eisch AJ and Isacson O (2008). Fate mapping and lineage analyses demonstrate the production of a large number of striatal neuroblasts after transforming growth factor alpha and noggin striatal infusions into the dopamine-depleted striatum. Stem Cells 26(9):2349-2360.

DiFiglia M (1990). Excitotoxic injury of the neostriatum: a model for Huntington's disease. Trends Neurosci 13:286–289.

DiFiglia M, Sapp E, Chase KO, Davies SW, Bates GP, Vonsattel JP and Aronin N (1997). Aggregation of huntingtin in neuronal intranuclear inclusions and dystrophic neuritis in brain. Science 277:1990-1993.

Doetsch F (2003). A niche for adult neural stem cells. Curr. Opin. Genet. Dev. 13(5):543-550.

Dragatsis I, Levine MS and Zeitlin S (2000). Inactivation of Hdh in the brain and testis results in progressive neurodegeneration and sterility in mice. Nat Genet 26:300-306.

Dzeja P and Terzic A (2009). Adenylate Kinase and AMP Signaling Networks: Metabolic Monitoring, Signal Communication and Body Energy Sensing. Int. J. Mol. Sci. 10:1729-1772.

Engelender S, Sharp AH, Colomer V, Tokito MK, Lanahan A, Worley P, Holzbaur EL and Ross CA (1997). Huntingtin-associated protein 1 (HAP1) interacts with the p150Glued subunit of dynactin. Hum Mol Genet 6:2205-2212.

Faber PW, Alter JR, MacDonald ME and Hart AC (1999). Polyglutamine-mediated dysfunction and apoptotic death of a Caenorhabditis elegans sensory neuron. Proc Natl Acad Sci U S A 96:179-184.

Faber PW, Voisine C, King DC, Bates EA and Hart AC (2002). Glutamine/proline-rich PQE-1 proteins protect Caenorhabditis elegans neurons from huntingtin polyglutamine neurotoxicity. Proc Natl Acad Sci U S A 99:17131-17136.

Fan MM and Raymond LA (2007). N-methyl-D-aspartate (NMDA) receptor function and excitotoxicity in Huntington's disease. Prog Neurobiol. 81(5-6):272-293.

Ferrante RJ, Kowall NW, Beal MF, Richardson EP, Jr., Bird ED and Martin JB (1985). Selective sparing of a class of striatal neurons in Huntington's disease. Science 230:561-563.

Ferrante RJ, Beal MF, Kowall NW, Richardson EP, Jr. and Martin JB (1987a). Sparing of acetylcholinesterase-containing striatal neurons in Huntington's disease. Brain Res 411:162-166.

Ferrante RJ, Kowall NW, Beal MF, Martin JB, Bird ED and Richardson EP, Jr. (1987b). Morphologic and histochemical characteristics of a spared subset of striatal neurons in Huntington's disease. J Neuropathol Exp Neurol 46:12-27.

Ferrante RJ, Kubilus JK, Lee J, Ryu H, Beesen A, Zucker B, Smith K, Kowall NW, Ratan RR, Luthi-Carter R and Hersch SM (2003). Histone deacetylase inhibition by sodium butyrate

chemotherapy ameliorates the neurodegenerative phenotype in Huntington's disease mice. J Neurosci 23:9418-9427.

Ferrante A, Martire A, Armida M, Chiodi V, Pézzola A, Potenza RL, Domenici MR and Popoli P (2010). Influence of CGS 21680, a selective adenosine A(2A) receptor agonist, on NMDA receptor function and expression in the brain of Huntington's disease mice. Brain Res. 1323:184-191.

Ferrè S, O'Connor W, Fuxe K and Ungerstedt U (1993). The striatopallidal neuron a main locus for adenosine-dopamine interaction in the brain. Neurosci. 13:5402–5406.

Ferreira IL, Nascimento MV, Ribeiro M, Almeida S, Cardoso SM, Grazina M, Pratas J, Santos MJ, Januario C, Oliveira CR and Rego AC (2010). Mitochondrial-dependent apoptosis in Huntington's disease human cybrids. Exp. Neurol. 222:243-255.

Ferreira IL, Cunha-Oliveira T, Nascimento MV, Ribeiro M, Proença MT, Januário C, Oliveira CR and Rego AC (2011). Bioenergetic dysfunction in Huntington's disease human cybrids. Exp. Neurol. 231:127– 134.

Ferrer I, Oliver B, Russi A, Casas R and Rivera R (1994). Parvalbumin and calbindin-D28k immunocytochemistry in human neocortical epileptic foci. J Neurol Sci 123:18-25.

Ferrer I, Goutan E, Marin C, Rey MJ and Ribalta T (2000). Brain-derived neurotrophic factor in Huntington disease. Brain Res 866:257-261.

Flanagan LA, Rebaza LM, Derzic S, Schwartz PH and Monuki ES (2006). Regulation of human neural precursor cells by laminin and integrins. J. Neurosci. Res. 83:845-856.

Franke TF, Hornik CP, Segev L, Shostak GA and Sugimoto C (2003).PI3K／AKT and apoptosis: size matters. Oncogene 22:8983–8998.

François F. and Grimes M.L. (1999) Phosphorylation-dependent Akt cleavage in neural cell in vitro reconstitution of apoptosis. J. Neurochem. 73(4):1773-1776.

Franke T.F., Hornik C.P., Segev L., Shostak G.A. and Sugimoto C. (2003) PI3K／Akt and apoptosis: size matters. Oncogene 22:8983–8998.

Gafni J and Ellerby LM (2002). Calpain activation in Huntington's disease. J Neurosci 22:4842-4849.

Gafni J, Hermel E, Young JE, Wellington CL, Hayden MR, and Ellerby LM (2004). Inhibition of calpain cleavage of huntingtin reduces toxicity: accumulation of calpain/caspase fragments in the nucleus. J Biol Chem. 279(19):20211-20.

Gage FH (2000). Mammalian neural stem cells. Science 287:1433-1438.

Garcia M, Vanhoutte P, Pages C, Besson MJ, Brouillet E and Caboche J (2002). The mitochondrial toxin 3-nitropropionic acid induces striatal neurodegeneration via a c-Jun N-terminal kinase/c-Jun module. J Neurosci 22:2174-2184.

Gauthier LR, Charrin BC, Borrell-Pagès M, Dompierre JP, Rangone H, Cordelières FP, De Mey J, MacDonald ME, Leßmann V, Humbert S and Saudou F (2004). Huntingtin Controls Neurotrophic Support and Survival of Neurons by Enhancing BDNF Vesicular Transport along Microtubules. Cell 118(1):127-138.

Gervais FG, Singaraja R, Xanthoudakis S, Gutekunst CA, Leavitt BR, Metzler M, Hackam AS, Tam J, Vaillancourt JP, Houtzager V, Rasper DM, Roy S, Hayden MR and Nicholson DW (2002). Recruitment and activation of caspase-8 by the Huntingtin-interacting protein Hip-1 and a novel partner Hippi. Nat Cell Biol 4:95-105.

Gil JM, Leist M, Popovic N, Brundin P and Petersén A (2004). Asialoerythropoietin is not effective in the R6/2 line of Huntington's disease mice. BMC Neurosci. 5:17.

Gil JM, Mohapel P, Araújo IM, Popovic N, Li JY, Brundin P and Petersén A (2005). Reduced hippocampal neurogenesis in R6/2 transgenic Huntington's disease mice. Neurobiol. Dis. 20(3):744-51.

Gil JM and Rego AC (2008). Mechanisms of neurodegeneration in Huntington's disease. European Journal of Neuroscience 27:2803-2820.

Gil-Mohapel J, Simpson JM, Ghilan M and Christie BR (2011). Neurogenesis in Huntington's disease: can studying adult neurogenesis lead to the development of new therapeutic strategies? Brain Res. 1406:84-105.

Ginés S., Ivanova E., Seong I.S., Saura C.A. and MacDonald M.E. (2003) Enhanced Akt signaling is an early pro-survival response that reflects N-methyl-D-aspartate receptor activation in Huntington's disease knock-in striatal cells. J. Biol. Chem. 278(50):50514-50522.

Ginés S., Seong I.S., Fossale E., Ivanova E., Trettel F., Gusella J.F., Wheeler V.C., Persichetti F. and MacDonald M.E. (2003a) Specific progressive cAMP reduction implicates energy deficit in presymptomatic Huntington's disease knock-in mice. Hum. Mol. Genet. 12:497–508.

Ginés S, Bosch M, Marco S, Gavaldà N, Díaz-Hernández M, Lucas JJ, Canals JM and Alberch J. (2006). Reduced expression of the TrkB receptor in Huntington's disease mouse models and in human brain. Eur J Neurosci. 23(3):649-58.

Ginés S, Paoletti P and Alberch J (2010). Impaired TrkB-mediated ERK1/2 activation in Huntington's disease knock-in striatal cells involves reduced P52/p46 SHC expression. J. Biol Chem. 285(28):21537-48.

Gizatullina ZZ, Lindenberg KS, Harjes P, Chen Y, Kosinski CM, Landwehrmeyer BG, Ludolph AC, Striggow F, Zierz S, Gellerich FN (2006). Low stability of Huntington muscle mitochondria against Ca2+ in R6/2 mice. Ann Neurol 59:407-11.

Goldberg YP, Nicholson DW, Rasper DM, Kalchman MA, Koide HB, Graham RK, Bromm M, Kazemi-Esfarjani P, Thornberry NA, Vaillancourt JP and Hayden MR (1996). Cleavage of huntingtin by apopain, a proapoptotic cysteine protease, is modulated by the polyglutamine tract. Nat Genet 13:442–449.

Goldberg AL (2003). Protein degradation and protection against misfolded or damaged proteins. Nature 426(6968):895-899.

Gomes JR, Costa JT, Melo CV, Felizzi F, Monteiro P, Pinto MJ, Inácio AR, Wieloch T, Almeida RD, Grãos M and Duarte CB (2012). Excitotoxicity downregulates TrkB.FL signaling and upregulates the neuroprotective truncated TrkB receptors in cultured hippocampal and striatal neurons. J Neurosci. 32(13):4610-22.

Graham RK, Deng Y, Slow EJ, Haigh B, Bissada N, Lu G, Pearson J, Shehadeh J, Bertram L, Murphy Z, Warby SC, Doty CN, Roy S, Wellington CL, Leavitt BR, Raymond LA, Nicholson DW and Hayden MR (2006). Cleavage at the caspase-6 site is required for neuronal dysfunction and degeneration due to mutant huntingtin. Cell 125:1179–1191.

Gratacos E, Perez-Navarro E, Tolosa E, Arenas E and Alberch J (2001). Neuroprotection of striatal neurons against kainate excitotoxicity by neurotrophins and GDNF family members. J Neurochem 78:1287-1296.

Graveland GA, Williams RS and DiFiglia M (1985). Evidence for degenerative and regenerative changes in neostriatal spiny neurons in Huntington's disease. Science 227:770-773.

Gray M, Shirasaki DI, Cepeda C, Andre VM, Wilburn B, Lu XH, Tao J, Yamazaki I, Li SH, Sun YE, Li XJ, Levine MS and Yang XW (2008). Full-length human mutant huntingtin with a stable polyglutamine repeat can elicit progressive and selective neuropathogenesis in BACHD mice. J Neurosci 28:6182–6195.

Grote HE, Bull ND, Howard ML, van Dellen A, Blakemore C, Bartlett PF and Hannan AJ (2005). Cognitive disorders and neurogenesis deficits in Huntington's disease mice are rescued by fluoxetine. Eur J Neurosci 22:2081–2088.

Gu M, Gash MT, Mann VM, Javoy-Agid F, Cooper JM, Schapira AH (1996). Mitochondrial defect in Huntington's disease caudate nucleus. Ann Neurol 39:385-9.

Guidetti P, Charles V, Chen EY, Reddy PH, Kordower JH, Whetsell WO Jr, Schwarcz R and Tagle DA (2001). Early degenerative changes in transgenic mice expressing mutant huntingtin involve dendritic abnormalities but no impairment of mitochondrial energy production. Exp Neurol 169:340-50.

Gunawardena S, Her LS, Brusch RG, Laymon RA, Niesman IR, Gordesky-Gold B, Sintasath L, Bonini NM and Goldstein LS (2003). Disruption of axonal transport by loss of huntingtin or expression of pathogenic polyQ proteins in Drosophila. Neuron 40:25-40.

Gusella JF, Wexler NS, Conneally PM, Naylor SL, Anderson MA, Tanzi RE, Watkins PC,Ottina K, Wallace MR, Sakaguchi AY, et al. (1983). A polymorphic DNA marker genetically linked to Huntington's disease. Nature 306:234-238.

Haapasalo A., Koponen E., Hoppe E., Wong G. and Castrén E. (2001) Truncated trkB.T1 Is Dominant Negative Inhibitor of trkB.TK1-Mediated Cell Survival. Biochem. Biophys. Res. Commun. 280:1352–1358.

Haapasalo A, Sipola I, Larsson K, Akerman KE, Stoilov P, Stamm S, Wong G and Castren E (2002). Regulation of TRKB surface expression by brain-derived neurotrophic factor and truncated TRKB isoforms. J Biol Chem 277(45):43160-7.

Hackam AS, Singaraja R, Wellington CL, Metzler M, McCutcheon K, Zhang T, Kalchman M and Hayden MR (1998). The influence of huntingtin protein size on nuclear localization and cellular toxicity. J Cell Biol 141:1097–1105.

Hagg T (2009). From neurotransmitters to neurotrophic factors to neurogenesis. Neuroscientist. 15(1):20-7.Han BH and Holtzman DM (2000). BDNF protects the neonatal brain from hypoxic-ischemic injury in vivo via the ERK pathway. J Neurosci. 20(15):5775-81.

Han B.H. and Holtzman D.M. (2000) BDNF protects the neonatal brain from hypoxic-ischemic injury in vivo via the ERK pathway. J. Neurosci. 20(15):5775-5781.

Hansson O, Petersen A, Leist M, Nicotera P, Castilho RF and Brundin P (1999). Transgenic mice expressing a Huntington's disease mutation are resistant to quinolinic acid-induced striatal excitotoxicity. Proc Natl Acad Sci U S A 96:8727–8732.

Hara T, Nakamura K, Matsui M, Yamamoto A, Nakahara Y, Suzuki-Migishima R, Yokoyama M, Mishima K, Saito I, Okano H and Mizushima N (2006). Suppression of basal autophagy in neural cells causes neurodegenerative disease in mice. Nature 441(7095):885-889.

Hardie DG and Hawley SA (2001). AMP-activated protein kinase: the energy charge hypothesis revisited. BioEssays 23:1112-1119.

Hatefi Y and Stiggall DL (1978). Preparation and properties of succinate: ubiquinone oxidoreductase (complex II). Methods Enzymol. 53:21–27.

Haubensak W, Narz F, Heumann R and Leßmann V (1998). BDNF-GFP containing secretory granules are localized in the vicinity of synaptic junctions of cultured cortical neurons. J Cell Sci 111:1483-1493.

Hedreen JC, Peyser CE, Folstein SE and Ross CA (1991). Neuronal loss in layers V and VI of cerebral cortex in Huntington's disease. Neurosci Lett 133:257-261.

Hockly E, Richon VM, Woodman B, Smith DL, Zhou X, Rosa E, Sathasivam K, Ghazi-Noori S, Mahal A, Lowden PA, Steffan JS, Marsh JL, Thompson LM, Lewis CM, Marks PA and Bates GP (2003). Suberoylanilide hydroxamic acid, a histone deacetylase inhibitor, ameliorates motor deficits in a mouse model of Huntington's disease. Proc Natl Acad Sci U S A 100:2041-2046.

Hodgson JG, Smith DJ, McCutcheon K, Koide HB, Nishiyama K, Dinulos MB, Stevens ME, Bissada N, Nasir J, Kanazawa I, Disteche CM, Rubin EM and Hayden MR (1996). Human huntingtin derived from YAC transgenes compensates for loss of murine huntingtin by rescue of the embryonic lethal phenotype. Hum. Mol. Genet. 5(12):1875-1885.

Hodgson JG, Agopyan N, Gutekunst CA, Leavitt BR, LePiane F, Singaraja R, Smith DJ, Bissada N, McCutcheon K, Nasir J, Jamot L, Li XJ, Stevens ME, Rosemond E, Roder JC, Phillips AG,

Rubin EM, Hersch SM and Hayden MR (1999). A YAC mouse model for Huntington's disease with full-length mutant huntingtin, cytoplasmic toxicity, and selective striatal neurodegeneration. Neuron 23:181–192.

Holbert S, Denghien I, Kiechle T, Rosenblatt A, Wellington C, Hayden MR, Margolis RL, Ross CA, Dausset J, Ferrante RJ and Neri C (2001). The Gln-Ala repeat transcriptional activator CA150 interacts with huntingtin: neuropathologic and genetic evidence for a role in Huntington's disease pathogenesis. Proc Natl Acad Sci U S A 98:1811-1816.

Hoogeveen, AT, Willemsen R, Meyer N, de Rooij E, Roos RAC, van Ommen GB and Galjaard H (1993). Characterization and localization of the Huntington disease gene product. Hum. Mol. Gen. 2:2069-2073.

Hroudova J and Fisar Z (2010). Activities of respiratory chain complexes and citrate synthase influenced by pharmacologically different antidepressants and mood stabilizers. Neuro. Endocrinol. Lett. 31(3):336-42.

Humbert S, Bryson EA, Cordelieres FP, Connors NC, Datta SR, Finkbeiner S, Greenberg ME and Saudou F (2002). The IGF-1/AKT pathway is neuroprotective in Huntington's disease and involves Huntingtin phosphorylation by AKT. Dev Cell 2:831-837.

Huntington G (2003). On chorea. George Huntington, M.D. J Neuropsychiatry Clin Neurosci 15:109-112.

Ivkovic S, Polonskaia O, Farinas I and Ehrlich ME (1997). Brain-derived neurotrophic factor regulates maturation of the DARPP-32 phenotype in striatal medium spiny neurons: studies in vivo and in vitro. Neuroscience 79:509-516.

Iwata A, Nagashima Y, Matsumoto L, Suzuki T, Yamanaka T, Date H, Deoka K, Nukina N and Tsuji S. (2009). Intra-nuclear degradation of polyglutamine aggregates by the ubiquitin proteasome system. J Biol Chem. 280:40282–40292.

Jackson GR, Salecker I, Dong X, Yao X, Arnheim N, Faber PW, MacDonald ME and Zipursky SL (1998). Polyglutamine-expanded human huntingtin transgenes induce degeneration of Drosophila photoreceptor neurons. Neuron 21:633-642.

Jacques TS, Relvas JB, Nishimura S, Pytela R, Edwards GM, Streuli CH and Ffrench-Constant C. (1998). Neural precursor cell chain migration and division are regulated through different beta1 integrins. Development 125:3167-3177.

Ji Y, Pang PT, Feng L and Lu B (2005). Cyclic AMP controls BDNF-induced TrkB phosphorylation and dendritic spine formation in mature hippocampal neurons. Nat. Neurosci. 8:164–172.

Ji Y, Lu Y, Yang F, Shen W, Tang TT, Feng L, Duan S and Lu B (2010). Acute and gradual increases in BDNF concentration elicit distinct signaling and functions in neurons. Nat Neurosci. 13(3):302-9.

Jin K, LaFevre-Bernt M, Sun Y, Chen S, Gafni J, Crippen D, Logvinova A, Ross CA, Greenberg DA and Ellerby LM (2005). FGF-2 promotes neurogenesis and neuroprotection and prolongs survival in a transgenic mouse model of Huntington's disease. Proc. Natl. Acad. Sci. U. S. A. 102:18189–18194.

Jones KR, Farinas I, Backus C and Reichardt LF (1994). Targeted disruption of the BDNF gene perturbs brain and sensory neuron development but not motor neuron development. Cell 76:989-999.

Kandasamy M, Couillard-Despres S, Raber KA, Stephan M, Lehner B, Winner B, Kohl Z, Rivera FJ, Nguyen HP, Riess O, Bogdahn U, Winkler J, von Hörsten S and Aigner L (2010). Stem cell quiescence in the hippocampal neurogenic niche is associated with elevated transforming growth factor-beta signaling in an animal model of Huntington disease. J. Neuropathol. Exp. Neurol. 69:717–728.

Kearns SM, Laywell ED, Kukekov VK and Steindler DA (2003). Extracellular matrix effects on neurosphere cell motility. Exp. Neurol. 182:240-244

Kegel KB, Kim M, Sapp E, McIntyre C, Castano JG, Aronin N and DiFiglia M (2000). Huntingtin expression stimulates endosomal-lysosomal activity, endosome tubulation, and autophagy. J Neurosci 20:7268-7278.

Kegel KB, Meloni AR, Yi Y, Kim YJ, Doyle E, Cuiffo BG, Sapp E, Wang Y, Qin ZH, Chen JD, Nevins JR, Aronin N and DiFiglia M (2002). Huntingtin is present in the nucleus, interacts with the transcriptional corepressor C-terminal binding protein, and represses transcription. J Biol Chem 277:7466-7476.

Kerr JF, Wyllie AH and Currie AR (1972). Apoptosis: a basic biological phenomenon with wide ranging implications in tissue kinetics. Br J Cancer 26:239-257.

Kim M, Lee HS, LaForet G, McIntyre C, Martin EJ, Chang P, Kim TW, Williams M, Reddy PH, Tagle D, Boyce FM, Won L, Heller A, Aronin N and DiFiglia M (1999). Mutant huntingtin expression in clonal striatal cells: dissociation of inclusion formation and neuronal survival by caspase inhibition. J Neurosci 19:964-973.

Kim YJ, Yi Y, Sapp E, Wang Y, Cuiffo B, Kegel KB, Qin ZH, Aronin N and DiFiglia M (2001). Caspase 3-cleaved NH2-terminal fragments of wild-type and mutant huntingtin are present in normal and Huntington's disease brains, associate with membranes, undergo calpain-dependent proteolysis. Proc Natl Acad Sci USA 98:12784–12789.

Klein R., Conway D., Parada L.F. and Barbacid M. (1990) The trkB tyrosine protein kinase gene codes for a second neurogenic receptor that lacks the catalytic kinase domain. Cell 61(4), 647-656.

Klement IA, Skinner PJ, Kaytor MD, Yi H, Hersch SM, Clark HB, Zoghbi HY and Orr HT (1998). Ataxin-1 nuclear localization and aggregation: role in polyglutamine-induced disease in SCA1 transgenic mice. Cell 95:41-53.

Kobayashi T, Ahlenius H, Thored P, Kobayashi R, Kokaia Z and Lindvall O (2006). Intracerebral infusion of glial cell line-derived neurotrophic factor promotes striatal neurogenesis after stroke in adult rats. Stroke 37:2361–2367.

Komatsu M, Waguri S, Chiba T, Murata S, Iwata J, Tanida I, Ueno T, Koike M, Uchiyama Y, Kominami E and Tanaka K (2006). Loss of autophagy in the central nervous system causes neurodegeneration in mice. Nature. 2006 441(7095):880-884

Krige D, Carroll MT, Cooper JM, Marsden CD and Schapira AH. Platelet mitochondria function in Parkinson's disease (1992). The Royal Kings and Queens Parkinson Disease Research Group. Ann Neurol 32:782–8.

Kroemer G, Galluzzi L and Brenner C (2007). Mitochondrial membrane permeabilization in cell death. Physiol Rev. 87(1):99-163.

Krull LH, Wall JS, Zobel H and Dimler RJ (1965). Synthetic Polypeptides Containing Side-chain Amide Groups: Water-Insoluble Polymers. Biochemistry 43:626-633.

Kuemmerle S, Gutekunst CA, Klein AM, Li XJ, Li SH, Beal MF, Hersch SM and Ferrante RJ (1999). Huntington aggregates may not predict neuronal death in Huntington's disease. Ann Neurol 46:842–849.

La Spada AR, Wilson EM, Lubahn DB, Harding AE and Fischbeck KH (1991). Androgen receptor gene mutations in X-linked spinal and bulbar muscular atrophy. Nature 352, 77–79.

La Spada AR and Weydt P (2005). Targeting toxic proteins for turnover. Nat Med. 11(10):1052-3.

Laplante M and Sabatini DM (2009). mTOR signaling at a glance. J Cell Sci 122(Pt 20):3589-94.

Larsen KE and Sulzer D (2002). Autophagy in neurons: a review. Histol Histopathol 17:897-908.
Lazic SE, Grote H, Armstrong RJ, Blakemore C, Hannan AJ, van Dellen A and Barker RA (2004). Decreased hippocampal cell proliferation in R6/1 Huntington's mice. Neuroreport 15: 811–813.

Lazic SE, Grote HE, Blakemore C, Hannan AJ, van Dellen A, Phillips W, Barker RA and (2006). Neurogenesis in the R6/1 transgenic mouse model of Huntington's disease: effects of environmental enrichment. Eur. J. Neurosci. 23:1829–1838.

Leavitt BR, van Raamsdonk JM, Shehadeh J, Fernandes H, Murphy Z, Graham RK, Wellington CL, Raymond LA and Hayden MR (2006). Wild-type huntingtin protects neurons from excitotoxicity. J Neurochem 96:1121–1129.

Lee FS and Chao MV. (2001). Activation of Trk neurotrophin receptors in the absence of neurotrophins. Proc. Nat. Acad. Sci. U.S.A. 98(6):3555-3560.

Lee WC, Yoshihara M and Littleton JT (2004). Cytoplasmic aggregates trap polyglutamine containing proteins and block axonal transport in a Drosophila model of Huntington's disease. Proc Natl Acad Sci U S A 101:3224-3229.

Lessmann V. and Brigadski T. (2009) Mechanisms, locations, and kinetics of synaptic BDNF secretion: an update. Neurosci. Res. 65(1):11-22.

Levine MS, Klapstein GJ, Koppel A, Gruen E, Cepeda C, Vargas ME, Jokel ES, Carpenter EM, Zanjani H, Hurst RS, Efstratiadis A, Zeitlin S and Chesselet MF (1999). Enhanced sensitivity to N-methyl-D-aspartate receptor activation in transgenic and knockin mouse models of Huntington's disease. J Neurosci Res 58:515-532.

Li SH and Li XJ (1998). Aggregation of N-terminal huntingtin is dependent on the length of its glutamine repeats. Hum Mol Genet 7:777-782.

Li H, Li SH, Johnston H, Shelbourne PF and Li XJ (2000). Amino-terminal fragments of mutant huntingtin show selective accumulation in striatal neurons and synaptic toxicity. Nat Genet. 25:385–389

Li SH and Li XJ (2004). Huntingtin and its role in neuronal degeneration. Neuroscientist 10:467-475.

Li Y, Luikart BW, Birnbaum S, Chen J, Kwon CH, Kernie SG, Bassel-Duby R and Parada LF (2008). TrkB regulates hippocampal neurogenesis and governs sensitivity to antidepressive treatment. Neuron 59(3):399-412.

Li F, He Z, Shen J, Huang Q, Li W, Liu X, He Y, Wolf F and Li CY (2010). Apoptotic caspases regulate induction of iPSCs from human fibroblasts. Cell Stem Cell 7(4):508-20.

Lin CH, Tallaksen-Greene S, Chien WM, Cearley JA, Jackson WS, Crouse AB, Ren S, Li XJ, Albin R and Detloff PJ (2001). Neurological abnormalities in a knock-in mouse model of Huntington's disease. Hum. Mol. Genet. 10:37–144.

Lindquist S, Krobitsch S, Li L and Sondheimer N (2001). Investigating protein conformationbased inheritance and disease in yeast. Philos Trans R Soc Lond B Biol Sci 356:169- 176.

Lorincz MT and Zawistowski VA (2009). Expanded CAG repeats in the murine Huntington's disease gene increases neuronal differentiation of embryonic and neural stem cells. Mol. Cell. Neurosci. 40(1):1-13.

Ludolph AC, He F, Spencer PS, Hammerstad J and Sabri M (1991). 3-Nitropropionic acidexogenous animal neurotoxin and possible human striatal toxin. Can J Neurol Sci 18:492-498.

Lunkes A, Lindenberg KS, Ben-Haiem L, Weber C, Devys D, Landwehrmeyer GB, Mandel JL and Trottier Y (2002). Proteases acting on mutant huntingtin generate cleaved products that differentially build up cytoplasmic and nuclear inclusions. Mol Cell 10: 259–269.

Luo S, Vacher C, Davies JE and Rubinsztein DC (2005). Cdk5 phosphorylation of huntingtin reduces its cleavage by caspases: implications for mutant huntingtin toxicity. J Cell Biol 169: 647–656.

Luthi-Carter R, Strand A, Peters NL, Solano SM, Hollingsworth ZR, Menon AS, Frey AS, Spektor BS, Penney EB, Schilling G, Ross CA, Borchelt DR, Tapscott SJ, Young AB, Cha JH and Olson JM (2000). Decreased expression of striatal signaling genes in a mouse model of Huntington's disease. Hum Mol Genet 9:1259-1271.

Luthi-Carter R, Hanson SA, Strand AD, Bergstrom DA, Chun W, Peters NL, Woods AM, Chan EY, Kooperberg C, Krainc D, Young AB, Tapscott SJ and Olson JM (2002). Dysregulation of gene expression in the R6/2 model of polyglutamine disease: parallel changes in muscle and brain. Hum Mol Genet 11:1911–1926.

Lynch DR and Guttmann RP (2002). Excitotoxicity: perspectives based on N-methyl-D-aspartate receptor subtypes. J Pharmacol Exp Ther 300:717-723.

Ma B., Savas J.N., Chao M.V. and Tanese N. (2012) Quantitative analysis of BDNF/TrkB protein and mRNA in cortical and striatal neurons using α-tubulin as a normalization factor. Cytometry A. 81(8):704-717.

Maccarrone M, Battista N and Centonze D (2007). The endocannabinoid pathway in Huntington's disease: a comparison with other neurodegenerative diseases. Prog Neurobiol 81:349–379.

Mangiarini L, Sathasivam K, Seller M, Cozens B, Harper A, Hetherington C, Lawton M, Trottier Y, Lehrach H, Davies SW and Bates GP (1996). Exon 1 of the HD gene with an expanded CAG repeat is sufficient to cause a progressive neurological phenotype in transgenic mice. Cell 87:493-506.

Maric D, Maric I and Barker JL (2000). Developmental changes in cell calcium homeostasis during neurogenesis of the embryonic rat cerebral cortex. Cereb. Cortex 10:561-573.

Martindale D, Hackam A, Wieczorek A, Ellerby L, Wellington C, McCutcheon K, Singaraja R, Kazemi-Esfarjani P, Devon R, Kim SU, Bredesen DE, Tufaro F and Hayden MR (1998). Length of huntingtin and its polyglutamine tract influences localization and frequency of intracellular aggregates. Nat Genet 18:150–154.

Martinez-Serrano A and Bjorklund A (1996). Protection of the neostriatum against excitotoxic damage by neurotrophin-producing genetically modified neural stem cells. J Neurosci 16:4604-4616.

Martinez-Vicente M, Talloczy Z, Wong E, Tang G, Koga H, Kaushik S, de Vries R, Arias E, Harris S, Sulzer D and Cuervo AM. Cargo recognition failure is responsible for inefficient autophagy in Huntington's disease (2010). Nat Neurosci. 13(5):567-76.

Marty S, Berzaghi Mda P and Berninger B (1997). Neurotrophins and activity-dependent plasticity of cortical interneurons. Trends Neurosci 20:198-202.

Matsumoto T, Rauskolb S, Polack M, Klose J, Kolbeck R, Korte M and Barde YA (2008). Biosynthesis and processing of endogenous BDNF: CNS neurons store and secrete BDNF, not pro-BDNF. Nat Neurosci. 11(2):131-133.

Mattson MP (2000). Apoptosis in neurodegenerative disorders. Nat Rev Mol Cell Biol. 1(2):120-129.

McCampbell A, Taye AA, Whitty L, Penney E, Steffan JS and Fischbeck KH (2001). Histone deacetylase inhibitors reduce polyglutamine toxicity. Proc Natl Acad Sci U S A 98:15179-15184.

McGeer EG and McGeer PL (1976). Duplication of biochemical changes of Huntington's chorea by intrastriatal injections of glutamic and kainic acids. Nature 263:517–519.

Menalled LB and Chesselet MF (2002). Mouse models of Huntington's disease. Trends Pharmacol. Sci. 23:32–39.

Menalled LB, Sison JD, Dragatsis I, Zeitlin S and Chesselet MF (2003). Time course of early motor and neuropathological anomalies in a knock-in mouse model of Huntington's disease with 140 CAG repeats. J Comp Neurol 465:11-26.

Merkle FT, Mirzadeh Z and Alvarez-Buylla A (2007). Mosaic organization of neural stem cells in the adult brain. Science 317(5836):381–384.

Metzler M, Chen N, Helgason CD, Graham RK, Nichol K, McCutcheon K, Nasir J, Humphries RK, Raymond LA and Hayden MR (1999). Life without huntingtin: normal differentiation into functional neurons. J Neurochem 72:1009-1018.

Michalik A and Van Broeckhoven C (2003). Pathogenesis of polyglutamine disorders: aggregation revisited. Hum Mol Genet 12 Spec No 2:R173-186.

Milakovic T and Johnson GVW (2005). Mitochondrial Respiration and ATP Production Are Significantly Impaired in Striatal Cells Expressing Mutant Huntingtin. The Journal of Biological Chemistry 280(35):30773-30782.

Middlemas D.S., Lindberg R.A. and Hunter T. (1991). trkB, a neural receptor protein-tyrosine kinase: evidence for a full-length and two truncated receptors. Mol. Cell Biol. 11(1):143-153.

Ming GL and Song H (2011). Adult Neurogenesis in the Mammalian Brain: Significant Answers and Significant Questions. Neuron 70(4):687-702

Mink JW and Thach WT (1993). Basal ganglia intrinsic circuits and their role in behavior. Curr Opin Neurobiol 3:950-957.

Molina-Hernández A and Velasco I (2008). Histamine induces neural stem cell proliferation and neuronal differentiation by activation of distinct histamine receptors. J. Neurochem. 106:706-717.

Moraes L, de Moraes Mello LE, Shimabukuro MK, de Castro Batista CM and Mendez-Otero R (2009). Lack of association between PSA-NCAM expression and migration in the rostral migratory stream of a Huntington's disease transgenic mouse model. Neuropathology 29(2):140-7.

Morales LM, Estevez J, Suarez H, Villalobos R, Chacin de Bonilla L and Bonilla E (1989). Nutritional evaluation of Huntington disease patients. Am J Clin Nutr 50:145-150.

Mowla SJ, Pareek S, Farhadi HF, Petrecca K, Fawcett JP, Seidah NG, Morris SJ, Sossin WS and Murphy RA (1999). Differential sorting of nerve growth factor and brain-derived neurotrophic factor in hippocampal neurons. J Neurosci 19:2069 –2080.

Mowla SJ, Farhadi HF, Pareek S, Atwal JK, Morris SJ, Seidah NG and Murphy RA (2001). Biosynthesis and Post-translational Processing of the Precursor to Brain-derived Neurotrophic Factor. The Journal of Biological Chemistry 276(16):12660-12666.

Muchowski PJ, Ning K, D'Souza-Schorey C and Fields S (2002). Requirement of an intact microtubule cytoskeleton for aggregation and inclusion body formation by a mutant huntingtin fragment. Proc Natl Acad Sci U S A 99:727-732.

Murray P.S. and Holmes P.V. (2011). An overview of brain-derived neurotrophic factor and implications for excitotoxic vulnerability in the hippocampus. Int. J. Pept. 2011:654085.

Nakao N, Brundin P, Funa K, Lindvall O and Odin P (1995). Trophic and protective actions of brain-derived neurotrophic factor on striatal DARPP-32-containing neurons in vitro. Brain Res Dev Brain Res 90:92-101.

Nambu A, Takada M, Inase M and Tokuno H (1996). Dual somatotopical representations in the primate subthalamic nucleus: evidence for ordered but reversed body-map transformations from the primary motor cortex and the supplementary motor area. J Neurosci 16:2671-2683.

Nambu A, Tokuno H, Hamada I, Kita H, Imanishi M, Akazawa T, Ikeuchi Y and Hasegawa N (2000). Excitatory cortical inputs to pallidal neurons via the subthalamic nucleus in the monkey. J Neurophysiol 84:289-300.

Nasir J, Floresco SB, O'Kusky JR, Diewert VM, Richman JM, Zeisler J, Borowski A, Marth JD, Phillips AG and Hayden MR (1995). Targeted disruption of the Huntington's disease gene results in embryonic lethality and behavioral and morphological changes in heterozygotes. Cell 81:811-823.

Negrette A (1955). Corea de Huntington: estudio de una sola familia a traves de varias generaciones. (Universidad de Zulia, Maracaibo, Venezuela).

Neustadt J and Pieczenik SR (2008). Medication-induce d mitochondri al damage and disease. Mol. Nutr. Food Res. 52:780-788.

Norris PJ, Waldvogel HJ, Faull RL, Love DR and Emson PC (1996). Decreased neuronal nitric oxide synthase messenger RNA and somatostatin messenger RNA in the striatum of Huntington’s disease. Neuroscience 72: 1037–1047.

Nucifora FC, Jr., Sasaki M, Peters MF, Huang H, Cooper JK, Yamada M, Takahashi H, Tsuji S, Troncoso J, Dawson VL, Dawson TM and Ross CA (2001). Interference by huntingtin and atrophin-1 with cbp-mediated transcription leading to cellular toxicity Science 291:2423-2428.

Oliveira JM, Chen S, Almeida S, Riley R, Goncalves J, Oliveira CR, Hayden MR, Nicholls DG, Ellerby LM and Rego AC (2006). Mitochondrial-dependent $Ca2^{+}$ handling in Huntington's disease striatal cells: effect of histone deacetylase inhibitors. J Neurosci 26: 11174–11186.

Oliveira JM, Jekabsons MB, Chen S, Lin A, Rego AC, Gonçalves J, Ellerby LM and Nicholls DG (2007). Mitochondrial dysfunction in Huntington's disease: the bioenergetics of isolated and in situ mitochondria from transgenic mice. J. Neurochem. 101:241-9.

Ona VO, Li M, Vonsattel JP, Andrews LJ, Khan SQ, Chung WM, Frey AS, Menon AS, Li XJ, Stieg PE, Yuan J, Penney JB, Young AB, Cha JH and Friedlander RM (1999). Inhibition of caspase-1 slows disease progression in a mouse model of Huntington's disease. Nature 399:263-267.

Orr AL, Li S, Wang CE, Li H, Wang J, Rong J, Xu X, Mastroberardino PG, Greenamyre JT and Li XJ (2008). NH_2-terminal mutant huntingtin associates with mitochondria and impairs mitochondrial trafficking. J Neurosci 28:2783–2792.

Pang PT, Teng HK, Zaitsev E, Woo NT, Sakata K, Zhen S, Teng KK, Yung WH, Hempstead BL and Lu B (2004). Cleavage of proBDNF by tPA/plasmin is essential for long-term hippocampal plasticity. Science 306(5695):487-91.

Pagniez-Mammeri H, Rak M, Legrand A, Bénit P, Rustin P and Slama A (2012). Mitochondrial complex I deficiency of nuclear origin II. Non-structural genes. Mol Genet Metab. 105(2):173-9.

Panov AV, Gutekunst CA, Leavitt BR, Hayden MR, Burke JR, Strittmatter WJ and Greenamyre JT (2002). Early mitochondrial calcium defects in Huntington's disease are a direct effect of polyglutamines. Nat. Neurosci. 5:731-736.

Panov AV, Burke JR, Strittmatter WJ and Greenamyre JT (2003). In vitro effects of polyglutamine tracts on Ca2+-dependent depolarization of rat and human mitochondria: relevance to Huntington's disease. Arch Biochem Biophys 410:1-6.

Park IH, Arora N, Huo H, Maherali N, Ahfeldt T, Shimamura A, Lensch MW, Cowan C, Hochedlinger K and Daley GQ (2008). Disease-specific induced pluripotent stem cells. Cell 134:877-886.

Parker WD Jr, Boyson SJ, Luder AS and Parks JK (1990). Evidence for a defect in NADH: ubiquinone oxidoreductase (complex I) in Huntington's disease. Neurology 40:1231-1234.

Parker JA, Connolly JB, Wellington C, Hayden M, Dausset J and Neri C (2001). Expanded polyglutamines in Caenorhabditis elegans cause axonal abnormalities and severe dysfunction of PLM mechanosensory neurons without cell death. Proc Natl Acad Sci U S A 98:13318-13323.

Pattison LR, Kotter MR, Fraga D and Bonelli RM (2006). Apoptotic cascades as possible targets for inhibiting cell death in Huntington's disease. J Neurol. 253(9):1137-42.

Pencea V, Bingaman KD, Wiegand SJ and Luskin MB (2001). Infusion of brain-derived neurotrophic factor into the lateral ventricle of the adult rat leads to new neurons in the parenchyma of the striatum, septum, thalamus, and hypothalamus. J Neurosci 21:6706-6717.

Peng J and Zeng X (2011). The role of induced pluripotent stem cells in regenerative medicine: neurodegenerative diseases. Stem Cell Res Ther 2(4):32.

Perez-Navarro E, Canudas AM, Akerund P, Alberch J and Arenas, E. (2000). Brain-derived neurotrophic factor, neurotrophin-3, and neurotrophin-4/5 prevent the death of striatal projection neurons in a rodent model of Huntington's disease. J. Neurochem. 75:2190-2199.

Perutz M (1994). Polar zippers: their role in human disease. Protein Sci 3:1629-1637.

Perutz MF, Johnson T, Suzuki M and Finch JT (1994). Glutamine repeats as polar zippers: their possible role in inherited neurodegenerative diseases. Proc Natl Acad Sci U S A 91:5355-5358.

Perutz MF, Finch JT, Berriman J and Lesk A (2002). Amyloid fibers are water-filled nanotubes. Proc Natl Acad Sci U S A 99:5591-5595.

Peters MF, Nucifora FC, Jr., Kushi J, Seaman HC, Cooper JK, Herring WJ, Dawson VL, Dawson TM and Ross CA (1999). Nuclear targeting of mutant Huntingtin increases toxicity. Mol Cell Neurosci 14:121-128.

Petersén A., Larsen K.E., Behr G.G., Romero N., Przedborski S., Brundin P. and Sulzer D. (2001). Brain-derived neurotrophic factor inhibits apoptosis and dopamine-induced free radical production in striatal neurons but does not prevent cell death. Brain. Res. Bull. 56:331-335.

Petersén A, Larsen KE, Behr GG, Romero N, Przedborski S, Brundin P and Sulzer D (2001a). Expanded CAG repeats in exon 1 of the Huntington's disease gene stimulate dopamine-mediated striatal neuron autophagy and degeneration. Hum Mol Genet 10:1243-1254.

Petersén A, Hansson O, Puschban Z, Sapp E, Romero N, Castilho RF, Sulzer D, Rice M, DiFiglia M, Przedborski S and Brundin P (2001b). Mice transgenic for exon 1 of the Huntington's disease gene display reduced striatal sensitivity to neurotoxicity induced by dopamine and 6-hydroxydopamine. Eur J Neurosci 14:1425-1435.

Petersén A, Gil J, Maat-Schieman ML, Björkqvist M, Tanila H, Araújo IM, Smith R, Popovic N, Wierup N, Norlén P, Li JY, Roos RA, Sundler F, Mulder H and Brundin P (2005). Orexin loss in Huntington's disease. Hum. Mol. Genet. 14:39–47.

Petridis AK and El Maarouf A (2011). Brain-derived neurotrophic factor levels influence the balance of migration and differentiation of subventricular zone cells, but not guidance to the olfactory bulb. J. Clinical Neurosci. 18:265-270

Phillips W, Morton AJ and Barker RA (2005). Abnormalities of neurogenesis in the R6/2 mouse model of Huntington's disease are attributable to the in vivo microenvironment. J. Neurosci. 25: 11564–11576.

Platel JC, Dave KA and Bordey A (2008). Control of neuroblast production and migration by converging GABA and glutamate signals in the postnatal forebrain. J Physiol. 586(16):3739-3743.

Powers WJ, Haas RH, Le T, Videen TO, Hershey T, McGee-Minnich L, Perlmutter JS (2007). Normal platelet mitochondrial complex I activity in Huntington's disease. Neurobiol. Dis. 27:99-101.

Powers WJ, Haas RH, Le T, Videen TO, Markham J and Perlmutter JS (2011). Platelet mitochondrial complex I and I + III activities do not correlate with cerebral mitochondrial oxidative metabolism. Journal of Cerebral Blood Flow & Metabolism e1-e5.

Qin ZH, Wang Y, Kegel KB, Kazantsev A, Apostol BL, Thompson LM, Yoder J, Aronin N and DiFiglia M (2003). Autophagy regulates the processing of amino terminal huntingtin fragments. Hum Mol Genet 12:3231-3244.

Ragan CI, Wilson MT, Darley-Usmar VM and Lowe PN (1987). Subfractionation of mitochondria, and isolation of the proteins of oxidative phosphorylation, in Mitochondria, a practical approach. (Darley-Usmar V.M., Rickwood D., Wilson M.T., eds), IRL Press., London, 79–112.

Ramaiah A, Hathaway JA, Atkinson DE. (1964). Adenylate as a metabolic regulator. Effect on yeast phosphofructokinase kinetics. J. Biol. Chem. 239:3619-3622.

Rangone H, Poizat G, Troncoso J, Ross CA, MacDonald ME, Saudou F and Humbert S (2004). The serum- and glucocorticoid-induced kinase SGK inhibits mutant huntingtin induced toxicity by phosphorylating serine 421 of huntingtin. Eur J Neurosci 19:273-279.

Ravikumar B, Vacher C, Berger Z, Davies JE, Luo S, Oroz LG, Scaravilli F, Easton DF, Duden R, O'Kane CJ and Rubinsztein DC (2004). Inhibition of mTOR induces autophagy and reduces toxicity of polyglutamine expansions in fly and mouse models of Huntington disease. Nat Genet 36:585–595.

Reggiori F and Klionsky DJ (2005). Autophagosomes: biogenesis from scratch? Curr Opin Cell Biol. 17(4):415-422.

Reichardt LF (2006). Neurotrophin-regulated signalling pathways. Philos Trans R Soc Lond B Biol Sci 361:1545–1564.

Reiner A, Albin RL, Anderson KD, D'Amato CJ, Penney JB and Young AB (1988). Differential loss of striatal projection neurons in Huntington disease. Proc Natl Acad Sci U S A 85:5733-5737.

Rego AC, Ward MW and Nicholls DG (2001). Mitochondria Control AMPA/Kainate Receptor-Induced Cytoplasmic Calcium Deregulation in Rat Cerebellar Granule Cells. J. Neurosci. 21(6):1893-1901.

Reynolds BA, Tetzlaff W and Weiss S (1992). A multipotent EGF-responsive striatal embryonic progenitor cell produces neurons and astrocytes. J. Neurosci. 12:4565-4574.

Reynolds BA and Weiss S (1996). Clonal and population analyses demonstrate that an EGF-responsive mammalian embryonic CNS precursor is a stem cell. Dev. Biol. 175:1-13.

Rigamonti D, Bauer JH, De-Fraja C, Conti L, Sipione S, Sciorati C, Clementi E, Hackam A, Hayden MR, Li Y, Cooper JK, Ross CA, Govoni S, Vincenz C and Cattaneo E (2000). Wild-type huntingtin protects from apoptosis upstream of caspase-3. J Neurosci 20:3705-3713.

Rigamonti D, Sipione S, Goffredo D, Zuccato C, Fossale E and Cattaneo E (2001). Huntingtin's neuroprotective activity occurs via inhibition of procaspase-9 processing. J Biol Chem 276:14545-14548.

Robitaille Y, Lopes-Cendes I, Becher M, Rouleau G and Clark AW (1997). The neuropathology of CAG repeat diseases: review and update of genetic and molecular features. Brain Pathol 7:901-926.

Rokudai S., Fujita N., Hashimoto Y. and Tsuruo T. (2000) Cleavage and inactivation of antiapoptotic Akt/PKB by caspases during apoptosis. J. Cell Physiol. 182(2), 290-296.

Rosas HD, Koroshetz WJ, Chen YI, Skeuse C, Vangel M, Cudkowicz ME, Caplan K, Marek K, Seidman LJ, Makris N, Jenkins BG and Goldstein JM (2003). Evidence for more widespread cerebral pathology in early HD: an MRI-based morphometric analysis. Neurology 60:1615–1620.

Rosas HD, Hevelone ND, Zaleta AK, Greve DN, Salat DH and Fischl B (2005). Regional cortical thinning in preclinical Huntington disease and its relationship to cognition. Neurology 65:745–747.

Rosas HD, Tuch DS, Hevelone ND, Zaleta AK, Vangel M, Hersch SM and Salat DH (2006). Diffusion tensor imaging in presymptomatic and early Huntington's disease: selective white matter pathology and its relationship to clinical measures. Mov Disord 21:1317–1325.

Rosenstock T, Duarte AI and Rego AC (2010). Mitochondrial-Associated Metabolic Changes and Neurodegeneration in Huntington's Disease - from Clinical Features to the Bench. Current Drug Targets 11:1218-1236.

Rosenstock TR, de Brito OM, Lombardi V, Louros S, Ribeiro M, Almeida S, Ferreira IL, Oliveira CR and Rego AC (2011). FK506 ameliorates cell death features in Huntington's disease striatal cell models. Neurochem. Int. 59(5):600-609.

Ross CA (2002). Polyglutamine pathogenesis: emergence of unifying mechanisms for Huntington's disease and related disorders. Neuron 35:819-822.

Rubinsztein DC, Leggo J, Chiano M, Dodge A, Norbury G, Rosser E and Craufurd D (1997). Genotypes at the GluR6 kainate receptor locus are associated with variation in the age of onset of Huntington disease. Proc Natl Acad Sci U S A 94:3872-3876.

Rubinsztein DC, Wyttenbach A and Rankin J (1999). Intracellular inclusions, pathological markers in diseases caused by expanded polyglutamine tracts? J Med Genet 36:265-270.

Rubio N (1997). Mouse astrocytes store and deliver brain-derived neurotrophic factor using the non-catalytic gp95trkB receptor. Eur. J. Neurosci. 9:1847–1853.

Sah DW, Ray J and Gage FH (1997). Regulation of voltage- and ligand-gated currents in rat hippocampal progenitor cells in vitro. J. Neurobiol. 32:95.110.

Sanchez I, Xu CJ, Juo P, Kakizaka A, Blenis J and Yuan J (1999). Caspase-8 is required for cell death induced by expanded polyglutamine repeats. Neuron 22:623-633.

Sanchez I, Mahlke C and Yuan J (2003). Pivotal role of oligomerization in expanded polyglutamine neurodegenerative disorders. Nature 421:373-379.

Santos DM, Xavier JM, Morgado AL, Solá S and Rodrigues CM (2012). Distinct regulatory functions of calpain 1 and 2 during neural stem cell self-renewal and differentiation. PLoS One 7(3):e33468.

Sapp E, Schwarz C, Chase K, Bhide PG, Young AB, Penney J, Vonsattel JP, Aronin N and DiFiglia M (1997). Huntingtin localization in brains of normal and Huntington's disease patients. Ann Neurol 42:604-612.

Sarkar S and Rubinsztein DC (2008). Huntington's disease: degradation of mutant huntingtin by autophagy. FEBS J. 275:4263–4270.

Saudou F, Finkbeiner S, Devys D and Greenberg ME (1998). Huntingtin acts in the nucleus to induce apoptosis but death does not correlate with the formation of intranuclear inclusions. Cell 95:55-66.

Sawa A, Wiegand GW, Cooper J, Margolis RL, Sharp AH, Lawler JF Jr, Greenamyre JT, Snyder SH and Ross CA (1999). Increased apoptosis of Huntington disease lymphoblasts associated with repeat length-dependent mitochondrial depolarization. Nat Med 5:1194-1198.

Schaffar G, Breuer P, Boteva R, Behrends C, Tzvetkov N, Strippel N, Sakahira H, Siegers K, Hayer-Hartl M and Hartl FU (2004). Cellular toxicity of polyglutamine expansion proteins; mechanism of transcription factor deactivation. Mol Cell 15:95-105.

Scherzinger E, Lurz R, Turmaine M, Mangiarini L, Hollenbach B, Hasenbank R, Bates GP, Davies SW, Lehrach H and Wanker EE (1997). Huntingtin-encoded polyglutamine expansions form amyloid-like protein aggregates in vitro and in vivo. Cell 90:549-558.

Schilling G, Becher MW, Sharp AH, Jinnah HA, Duan K, Kotzuk JA, Slunt HH, Ratovitski T, Cooper JK, Jenkins NA, Copeland NG, Price DL, Ross CA and Borchelt DR (1999). Intranuclear inclusions and neuritic aggregates in transgenic mice expressing a mutant N-terminal fragment of huntingtin. Hum. Mol. Genet. 8:397–407.

Schmitt I, Bachner D, Megow D, Henklein P, Hameister H, Epplen JT and Riess O (1995). Expression of the Huntington disease gene in rodents: cloning the rat homologue and evidence for downregulation in non-neuronal tissues during development. Hum Mol Genet 4:1173-1182.

Schneider SA, Walker RH and Bhatia KP (2007). The Huntington's disease-like syndromes: what to consider in patients with a negative Huntington's disease gene test. Nat Clin Pract Neurol. 3(9):517-25.

Sebastião AM, Assaife-Lopes N, Diógenes MJ, Vaz SH and Ribeiro JA (2011). Modulation of brain-derived neurotrophic factor (BDNF) actions in the nervous system by adenosine A(2A) receptors and the role of lipid rafts. Biochim Biophys Acta. 1808(5):1340-1349.

Sekiguchi A, Kanno H, Ozawa H, Yamaya S and Itoi E (2012). Rapamycin promotes autophagy and reduces neural tissue damage and locomotor impairment after spinal cord injury in mice. J. Neurotrauma 29(5):946-956.

Seneca S, Fagnart D, Keymolen K, Lissens W, Hasaerts D, Debulpaep S, Desprechins B, Liebaers I and De Meirleir L (2004). Early onset Huntington disease: a neuronal degeneration syndrome. Eur J Pediatr. 163(12):717-721.

Seo H, Sonntag K and Isacson O (2004). Generalized brain and skin proteasome inhibition in Huntington's disease. Ann Neurol 56(3):319-28.

Seo H, Kim W and Isacson O (2008). Compensatory changes in the ubiquitin– proteasome system, brain-derived neurotrophic factor and mitochondrial complex II/III in YAC72 and R6/2 transgenic mice partially model Huntington's disease patients. Human Molecular Genetics 17(20):3144-3153.

Shiwach RS and Norbury CG (1994). A controlled psychiatric study of individuals at risk for Huntington's disease. Br J Psychiatry 165:500-505.

Sieradzan KA and Mann DM (2001). The selective vulnerability of nerve cells in Huntington's disease. Neuropathol Appl Neurobiol 27:1-21.

Silva A, Pereira J, Relvas JB, Oliveira CR and Rego AC (2009). BDNF and Extracellular Matrix Regulate Differentiation of Mice Neurosphere-Derived Cells into a GABAergic Neuronal Phenotype. J. Neurosci. Res. 87(9):1986. 1996.

Simpson JM, Gil-Mohapel J, Pouladi M Ghilan M, Xie Y, Hayden M and Christie B (2011). Altered adult hippocampal neurogenesis in the YAC128 transgenic mouse model of Huntington disease. Neurobiol. Dis. 41(2):249-60.

Sipione S and Cattaneo E (2001). Modeling Huntington's disease in cells, flies, and mice. Mol Neurobiol 23:21-51.

Sipione S, Rigamonti D, Valenza M, Zuccato C, Conti L, Pritchard J, Kooperberg C, Olson JM and Cattaneo E (2002). Early transcriptional profiles in huntingtin-inducible striatal cells by microarray analyses. Hum Mol Genet 11:1953-1965.

Slow EJ, van Raamsdonk J, Rogers D, Coleman SH, Graham RK, Deng Y, Oh R, Bissada N, Hossain SM, Yang YZ, Li XJ, Simpson EM, Gutekunst CA, Leavitt BR and Hayden MR (2003). Selective striatal neuronal loss in a YAC128 mouse model of Huntington disease. Hum. Mol. Genet. 12(13):1555-67.

Slow EJ, Graham RK, Osmand AP, Devon RS, Lu G, Deng Y, Pearson J, Vaid K, Bissada N, Wetzel R, Leavitt BR and Hayden MR (2005). Absence of behavioral abnormalities and

neurodegeneration in vivo despite widespread neuronal huntingtin inclusions. Proc Natl Acad Sci U S A 102:11402–11407.

Smith DL, Portier R, Woodman B, Hockly E, Mahal A, Klunk WE, Li XJ, Wanker E, Murray KD ans Bates GP (2001). Inhibition of polyglutamine aggregation in R6/2 HD brain slices-complex dose-response profiles. Neurobiol Dis 8:1017-1026.

Soares S and Sotelo C (2004). Adult neural stem cells from the mouse subventricular zone are limited in migratory ability compared to progenitor cells from similar origin. Neuroscience 128:807.817.

Solá S, Morgado AL and Rodrigues CM. Death receptors and mitochondria: two prime triggers of neural apoptosis and differentiation (2013). Biochim Biophys Acta. 1830(1):2160-2166. Epub 2012 Oct 2.

Squitieri F, Gellera C, Cannella M, Mariotti C, Cislaghi G, Rubinsztein DC, Almqvist EW, Turner D, Bachoud-Levi AC, Simpson SA, Delatycki M, Maglione V, Hayden MR and Donato SD (2003). Homozygosity for CAG mutation in Huntington disease is associated with a more severe clinical course. Brain 126:946-955.

Steffan JS, Kazantsev A, Spasic-Boskovic O, Greenwald M, Zhu YZ, Gohler H, Wanker EE, Bates GP, Housman DE and Thompson LM (2000). The Huntington's disease protein interacts with p53 and CREB-binding protein and represses transcription. Proc Natl 124 Acad Sci U S A 97:6763-6768.

Steffan JS, Bodai L, Pallos J, Poelman M, McCampbell A, Apostol BL, Kazantsev A, Schmidt E, Zhu YZ, Greenwald M, Kurokawa R, Housman DE, Jackson GR, Marsh JL and Thompson LM (2001). Histone deacetylase inhibitors arrest polyglutamine dependent neurodegeneration in Drosophila. Nature 413:739-743.

Stocchi V, Cucchiarini L, Magnani M, Chiarantini L, Palma P and Crescentini G. (1985). Simultaneous extraction and reverse-phase high-performance liquid chromatographic determination of adenine and pyridine nucleotides in human red blood cells. *Anal. Biochem.* 146:118-124.

Stoilov P., Castren E. and Stamm S. (2002). Analysis of the Human TrkB Gene Genomic Organization Reveals Novel TrkB Isoforms, Unusual Gene Length, and Splicing Mechanism. Biochem. Biophys. Res. Commun. 290:1054–1065.

Strand AD, Baquet ZC, Aragaki AK, Holmans P, Yang L, Cleren C, Beal MF, Jones L, Kooperberg C, Olson JM and Jones KR (2007). Expression profiling of Huntington's disease models suggests that brain-derived neurotrophic factor depletion plays a major role in striatal degeneration. J Neurosci 27: 11758–11768.

Sue CM and Schon EA (2000). Mitochondrial respiratory chain diseases and mutations in nuclear DNA: a promising start? Brain Pathol. 10(3):442-50.

Sun Y, Savanenin A, Reddy PH and Liu YF (2001). Polyglutamine-expanded huntingtin promotes sensitization of N-methyl-D-aspartate receptors via post-synaptic density 95. J Biol Chem 276:24713-24718.

Suter, M. Riek U, TuERK R, Schlattner U, Wallimann T and Neumann D (2006). Dissecting the role of 5'-AMP for allosteric stimulation, activation, and deactivation of AMP-activated protein kinase. J. Biol. Chem. 281, 32207–32216.

Swerdlow RH, Parks JK, Cassarino DS, Shilling AT, Bennett Jr. JP, Harrison MB and Parker Jr. WD (1999). Characterization of cybrid cell lines containing mtDNA from Huntington's disease patients. Biochem. Biophys. Res. Commun. 261:701-704.

Tabrizi SJ, Cleeter MW and Xuereb J, Taanman JW, Cooper JM and Schapira AH (1999). Biochemical abnormalities and excitotoxicity in Huntington's disease brain. Ann Neurol 45:25-32.

Takahashi J, Palmer TD and Gage FH. (1999). Retinoic acid and neurotrophins collaborate to regulate neurogenesis in adult-derived neural stem cell cultures. J. Neurobiol. 38:65-81.

Takahashi K and Yamanaka S (2006). Induction of pluripotent stem cells from mouse embryonic and adult fibroblast cultures by defined factors. Cell 126:663-676.

Takano H and Gusella JF (2002). The predominantly HEAT-like motif structure of huntingtin and its association and coincident nuclear entry with dorsal, an NF-kB/Rel/dorsal family transcription factor. BMC Neurosci 3:15.

Tanaka M, Machida Y, Niu S, Ikeda T, Jana NR, Doi H, Kurosawa M, Nekooki M and Nukina N (2004). Trehalose alleviates polyglutamine-mediated pathology in a mouse model of Huntington disease. Nat Med 10:148-154.

Tang TS, Tu H, Chan EY, Maximov A, Wang Z, Wellington CL, Hayden MR and Bezprozvanny I (2003). Huntingtin and huntingtin-associated protein 1 influence neuronal calcium signaling mediated by inositol-(1,4,5) triphosphate receptor type 1. Neuron 39:227-239.

Tao T and Tartakoff AM (2001). Nuclear relocation of normal huntingtin. Traffic 2:385-394.

Tate MC, Shear DA, Hoffman SW, Stein DG, Archer DR and LaPlaca MC. (2002). Fibronectin promotes survival and migration of primary neural stem cells transplanted into the traumatically injured mouse brain. Cell Transplant. 11:283-295.

Tarditi A, Camurri A, Varani K, Borea PA, Woodman B, Bates G, Cattaneo E and Abbracchio MP (2006). Early and transient alteration of adenosine A2A receptor signaling in a mouse model of Huntington disease. Neurobiol Dis 23: 44–53.

Tattersfield AS, Croon RJ, Liu YW, Kells AP, Faull RL and Connor B (2004). Neurogenesis in the striatum of the quinolinic acid lesion model of Huntington's disease. Neuroscience 127:319–332.

Teng HK, Lee R, Wright S, Tevar S, Almeida RD, Kermani P, Torkin R, Chen ZY, Lee FS, Kraemer RT, Nykjaer A and Hempstead BL (2005). ProBDNF induces neuronal apoptosis via activation of a receptor complex of p75NTR and sortilin. J. Neurosci. 25: 5455–5463.

Thakur AK, Jayaraman M, Mishra R, Thakur M, Chellgren VM, Byeon IJ, Anjum DH, Kodali R, Creamer TP, Conway JF, Gronenborn AM and Wetzel R (2009). Polyglutamine disruption of the huntingtin exon 1 N terminus triggers a complex aggregation mechanism. Nat Struct Mol Biol 16:380–389.

The Huntington's Disease Collaborative Research Group. (1993). A novel gene containing a trinucleotide repeat that is expanded and unstable on Huntington's disease chromosomes. Cell 72:971-983.

Tran PB, Ren D, Veldhouse TJ and Miller RJ (2004). Chemokine receptors are expressed widely by embryonic and adult neural progenitor cells. J. Neurosci. Res. 76:20-34.

Trettel F, Rigamonti D, Hilditch-Maguire P, Wheeler VC, Sharp AH, Persichetti F, Cattaneo E and MacDonald ME (2000). Dominant phenotypes produced by the HD mutation in STHdh(Q111) striatal cells. Hum Mol Genet 9:2799-2809.

Trushina E, Dyer RB, Badger JD 2nd, Ure D, Eide L, Tran DD, Vrieze BT, Legendre-Guillemin V, McPherson PS, Mandavilli BS, Van Houten B, Zeitlin S, McNiven M, Aebersold R, Hayden M, Parisi JE, Seeberg E, Dragatsis I, Doyle K, Bender A, Chacko C and McMurray CT (2004). Mutant huntingtin impairs axonal trafficking in mammalian neurons in vivo and in vitro. Mol Cell Biol. 24(18):8195-8209.

Turner C, Cooper JM and Schapira AH (2007). Clinical correlates of mitochondrial function in Huntington's disease muscle. Mov. Disord. 22:1715-1721.

van der Burg JM, Bacos K, Wood NI, Lindqvist A, Wierup N, Woodman B, Wamsteeker JI, Smith R, Deierborg T, Kuhar MJ, Bates GP, Mulder H, Erlanson-Albertsson C, Morton AJ, Brundin P, Petersén A and Björkqvist M (2008). Increased metabolism in the R6/2 mouse model of Huntington's disease. Neurobiol. Dis. 29:41–51.

van Raamsdonk JM, Murphy Z, Slow EJ, Leavitt BR and Hayden MR (2005). Selective degeneration and nuclear localization of mutant huntingtin in the YAC128 mouse model of Huntington disease. Hum. Mol. Genet. 14(24):3823-3835.

van Raamsdonk JM, Gibson WT, Pearson J, Murphy Z, Lu G, Leavitt BR and Hayden MR (2006). Body weight is modulated by levels of full-length huntingtin. Hum. Mol. Genet. 15:1513–1523.

van Raamsdonk JM, Murphy Z, Selva DM, Hamidizadeh R, Pearson J, Petersen A, Björkqvist M, Muir C, Mackenzie IR, Hammond GL, Vogl AW, Hayden MR and Leavitt BR (2007). Testicular degeneration in Huntington disease. Neurobiol. Dis. 26:512–520.

Varani K, Rigamonti D, Sipione S, Camurri A, Borea PA, Cattabeni F, Abbracchio MP and Cattaneo E (2001). Aberrant amplification of A2A receptor signaling in striatal cells expressing mutant huntingtin. FASEB J 15:1245–1247.

Velier J, Kim M, Schwarz C, Kim TW, Sapp E, Chase K, Aronin N and DiFiglia M (1998). Wild-type and mutant huntingtins function in vesicle trafficking in the secretory and endocytic pathways. Exp Neurol 152:34–40.

Ventimiglia R, Mather PE, Jones BE and Lindsay RM (1995). The neurotrophins BDNF, NT-3 and NT-4/5 promote survival and morphological and biochemical differentiation of striatal neurons in vitro. Eur J Neurosci 7:213-222.

Ventruti A and Cuervo AM (2007). Autophagy and neurodegeneration. Curr Neurol Neurosci Rep 7: 443–451.

Vescovi AL, Reynolds BA, Fraser DD and Weiss S (1993). bFGF regulates the proliferative fate of unipotent (neuronal) and bipotent (neuronal/astroglial) EGF-generated CNS progenitor cells. Neuron 11:951-966.

von HÖrsten S, Schmitt I, Nguyen HP, Holzmann C, Schmidt T, Walther T, Bader M, Pabst R, Kobbe P, Krotova J, Stiller D, Kask A, Vaarmann A, Rathke-Hartlieb S, Schulz JB, Grasshoff U, Bauer I, Vieira-Saecker AM, Paul M, Jones L, Lindenberg KS, Landwehrmeyer B, Bauer A, Li XJ, Riess O (2003). Transgenic rat model of Huntington's disease. Hum Mol Genet 12:617-624.

Vonsattel JP, Myers RH, Stevens TJ, Ferrante RJ, Bird ED and Richardson EP, Jr. (1985). Neuropathological classification of Huntington's disease. J Neuropathol Exp Neurol 44:559-577.

Vonsattel JP and DiFiglia M (1998). Huntington disease. J Neuropathol Exp Neurol 57:369-384.

Waelter S, Scherzinger E, Hasenbank R, Nordhoff E, Lurz R, Goehler H, Gauss C, Sathasivam K, Bates GP, Lehrach H and Wanker EE (2001). The huntingtin interacting protein HIP1 is a clathrin and alpha-adaptin-binding protein involved in receptor mediated endocytosis. Hum Mol Genet 10:1807-1817.

Warby SC, Chan EY, Metzler M, Gan L, Singaraja RR, Crocker SF, Robertson HA and Hayden MR (2005). Huntingtin phosphorylation on serine 421 is significantly reduced in the striatum and by polyglutamine expansion in vivo. Hum Mol Genet 14:1569–1577, 2005.

Ward MW, Rego AC, Frenguelli BG and Nicholls DG (2000). Mitochondrial membrane potential and glutamate excitotoxicity in cultured cerebellar granule cells. J. Neurosci. 20:7208-7219.

Watson FL, Heerssen HM, Moheban DB, Lin MZ, Sauvageot CM, Bhattacharyya A, Pomeroy SL and Segal RA (1999). Rapid nuclear responses to target-derived neurotrophins require retrograde transport of ligand-receptor complex. J Neurosci 19:7889-7900.

Wellington CL, Singaraja R, Ellerby L, Savill J, Roy S, Leavitt B, Cattaneo E, Hackam A, Sharp A, Thornberry N, Nicholson DW, Bredesen DE and Hayden MR (2000). Inhibiting caspase cleavage of huntingtin reduces toxicity and aggregate formation in neuronal and nonneuronal cells. J Biol Chem 275:19831-19838.

Wellington CL, Ellerby LM, Gutekunst CA, Rogers D, Warby S, Graham RK, Loubser O, van Raamsdonk J, Singaraja R, Yang YZ, Gafni J, Bredesen D, Hersch SM, Leavitt BR, Roy S,

Nicholson DW and Hayden MR (2002). Caspase cleavage of mutant huntingtin precedes neurodegeneration in Huntington's disease. J. Neurosci. 22:7862-7872.

Weydt P, Pineda VV, Torrence AE, Libby RT, Satterfield TF, Lazarowski ER, Gilbert ML, Morton GJ, Bammler TK, Strand AD, Cui L, Beyer RP, Easley CN, Smith AC, Krainc D, Luquet S, Sweet IR, Schwartz MW and La Spada AR (2006). Thermoregulatory and metabolic defects in Huntington's disease transgenic mice implicate PGC-1alpha in Huntington's disease neurodegeneration. Cell Metab. 4(5):349-62.

Wexler NS, Lorimer J, Porter J, Gomez F, Moskowitz C, Shackell E, Marder K, Penchaszadeh G, Roberts SA, Gayan J, Brocklebank D, Cherny SS, Cardon LR, Gray J, Dlouhy SR, Wiktorski S, Hodes ME, Conneally PM, Penney JB, Gusella J, Cha JH, Irizarry M, Rosas D, Hersch S, Hollingsworth Z, MacDonald M, Young AB, Andresen JM, Housman DE, De Young MM, Bonilla E, Stillings T, Negrette A, Snodgrass SR, Martinez-Jaurrieta MD, Ramos-Arroyo MA, Bickham J, Ramos JS, Marshall F, Shoulson I, Rey GJ, Feigin A, Arnheim N, Acevedo-Cruz A, Acosta L, Alvir J, Fischbeck K, Thompson LM, Young A, Dure L, O'Brien CJ, Paulsen J, Brickman A, Krch D, Peery S, Hogarth P, Higgins DS, Jr. and Landwehrmeyer B (2004). Venezuelan kindreds reveal that genetic and environmental factors modulate Huntington's disease age of onset. Proc Natl Acad Sci U S A 101:3498-3503.

Wharton DC and Tzagotoff A (1967). Cytochrome oxidase from beef heart mitochondria. Methods Enzymol. 10:245–250.

Wheeler VC, Auerbach W, White JK, Srinidhi J, Auerbach A, Ryan A, Duyao MP, Vrbanac V, Weaver M, Gusella JF, Joyner AL and MacDonald ME (1999). Length-dependent gametic CAG repeat instability in the Huntington's disease knock-in mouse. Hum Mol Genet 8:115-122.

Wheeler VC, White JK, Gutekunst CA, Vrbanac V, Weaver M, Li XJ, Li SH, Yi H, Vonsattel JP, Gusella JF, Hersch S, Auerbach W, Joyner AL and MacDonald ME (2000). Long glutamine tracts cause nuclear localization of a novel form of huntingtin in medium spiny striatal neurons in HdhQ92 and HdhQ111 knock-in mice. Hum Mol Genet 9:503-513.

Wheeler VC, Gutekunst CA, Vrbanac V, Lebel LA, Schilling G, Hersch S, Friedlander RM, Gusella JF, Vonsattel JP, Borchelt DR and MacDonald ME (2002). Early phenotypes that presage late-onset neurodegenerative disease allow testing of modifiers in Hdh CAG knock-in mice. Hum. Mol. Genet. 11:633–640.

Winner B, Kohl Z and Gage FH (2011). Neurodegenerative disease and adult neurogenesis. Eur J Neurosci. 33(6):1139-51.

Wong E and Cuervo AM (2010). Autophagy gone awry in neurodegenerative diseases. Nat Neurosci. 13(7):805-811.

Wu ZL, O'Kane TM, Scott RW, Savage MJ and Bozyczko-Coyne D (2002). Protein tyrosine phosphatases are up-regulated and participate in cell death induced by polyglutamine expansion. J Biol Chem. 277(46):44208-13.

Wyttenbach A, Swartz J, Kita H, Thykjaer T, Carmichael J, Bradley J, Brown R, Maxwell M, Schapira A, Orntoft TF, Kato K and Rubinsztein DC (2001). Polyglutamine expansions cause decreased CRE-mediated transcription and early gene expression changes prior to cell death in an inducible cell model of Huntington's disease. Hum Mol Genet 10:1829-1845.

Xia J, Lee DH, Taylor J, Vandelft M and Truant R (2003). Huntingtin contains a highly conserved nuclear export signal. Hum Mol Genet 12: 1393–1403.

Xie Y, Hayden MR and Xu B (2010). BDNF overexpression in the forebrain rescues Huntington's disease phenotypes in YAC128 mice. J Neurosci. 30(44):14708-18.

Yang W, Dunlap JR, Andrews RB and Wetzel R (2002). Aggregated polyglutamine peptides delivered to nuclei are toxic to mammalian cells. Hum Mol Genet 11:2905-2917.

Yang P, Arnold SA, Habas A, Hetman M and Hagg T (2008). Ciliary neurotrophic factor mediates dopamine D2 receptor-induced CNS neurogenesis in adult mice. J Neurosci 28:2231–2241.

Yi CH and Yuan J (2009). The jekyll and hyde functions of caspases. Dev Cell 16:21–34

Young KM, Merson TD, Sotthibundhu A, Coulson EJ and Bartlett PF (2007). p75 neurotrophin receptor expression defines a population of BDNF-responsive neurogenic precursor cells. J Neurosci 27:5146–5155.

Yu ZX, Li SH, Evans J, Pillarisetti A, Li H and Li XJ (2003). Mutant huntingtin causes context dependent neurodegeneration in mice with Huntington’s disease. J Neurosci 23:2193-202.

Zeron MM, Hansson O, Chen N, Wellington CL, Leavitt BR, Brundin P, Hayden MR and Raymond LA (2002). Increased sensitivity to N-methyl-D-aspartate receptor-mediated excitotoxicity in a mouse model of Huntington's disease. Neuron 33:849-860.

Zeron MM, Fernandes HB, Krebs C, Shehadeh J, Wellington CL, Leavitt BR, Baimbridge KG, Hayden MR and Raymond LA (2004). Potentiation of NMDA receptor-mediated excitotoxicity linked with intrinsic apoptotic pathway in YAC transgenic mouse model of Huntington's disease. Mol Cell Neurosci 25:469-479.

Zhang Y, Leavitt BR, van Raamsdonk JM, Dragatsis I, Goldowitz D, MacDonald ME, Hayden MR and Friedlander RM (2006). Huntingtin inhibits caspase-3 activation. EMBO J 25: 5896–5906, 2006.

Zigova T, Pencea V, Wiegand SJ, Luskin MB (1998). Intraventricular administration of BDNF increases the number of newly generated neurons in the adult olfactory bulb. Mol. Cell Neurosci. 11:234-45.

Zoghbi HY and Orr HT (2000). Glutamine repeats and neurodegeneration. Annu Rev Neurosci 23:217-247.

Zuccato C, Ciammola A, Rigamonti D, Leavitt BR, Goffredo D, Conti L, MacDonald ME, Friedlander RM, Silani V, Hayden MR, Timmusk T, Sipione S and Cattaneo E (2001). Loss of huntingtin-mediated BDNF gene transcription in Huntington's disease. Science 293:493-498.

Zuccato C, Tartari M, Crotti A, Goffredo D, Valenza M, Conti L, Cataudella T, Leavitt BR, Hayden MR, Timmusk T, Rigamonti D and Cattaneo E (2003). Huntingtin interacts with REST/NRSF to modulate the transcription of NRSE-controlled neuronal genes. Nat. Genet. 35:76-83.

Zuccato C and Cattaneo E (2007). Role of brain-derived neurotrophic factor in Huntington's disease. Prog Neurobiol. 81(5-6):294-330.

Zuccato C, Belyaev N, Conforti P, Ooi L, Tartari M, Papadimou E, MacDonald M, Fossale E, Zeitlin S, Buckley N and Cattaneo E (2007). Widespread disruption of repressor element-1 silencing transcription factor/neuron-restrictive silencer factor occupancy at its target genes in Huntington's disease. J Neurosci 27:6972–6983.

Zuccato C, Marullo M, Conforti P, MacDonald ME, Tartari M and Cattaneo E (2008). Systematic assessment of BDNF and its receptor levels in human cortices affected by Huntington's disease. Brain. Pathol. 18(2):225-38.

Zuccato C, Valenza M and Cattaneo E (2010). Molecular Mechanisms and Potential Therapeutical Targets in Huntington's Disease. Physiol Rev. 90(3):905-81.